



EDITE - ED 130

Dissertation ParisTech

T H E S I S

In partial fulfillment of the requirements for the degree of
doctor of philosophy from

TELECOM ParisTech

Specialization « Electronics and Communications »

presented and publicly defended by

Wassim TABIKH

the 26th of February 2018

Massive MIMO in 5G networks for intercell interference cancellation and capacity boost

Thesis Supervisor : **Dirk SLOCK**
Thesis Co-supervisor : **Yi YUAN-WU**

Committee

Mme Maryline HELARD, Professor, INSA de Rennes
M. Constantinos PAPADIAS, Professor, Athens Information Technology
Mme. Ghaya REKAYA, Professor, Télécom ParisTech
M. Pascal CHEVALIER, Professor, CNAM de Paris
M. Salah-Eddine EL AYOUBI, Assistant Professor, CentraleSupélec
M. Raphaël VISOZ, Research Engineer, Orange Labs

Reviewer
Reviewer
Examiner
Examiner
Examiner
Invited

TELECOM ParisTech

école de l'Institut Télécom - membre de ParisTech



EDITE - ED 130

Doctorat ParisTech

T H È S E

pour obtenir le grade de docteur délivré par

TELECOM ParisTech

Spécialité « Electronique et Communications »

présentée et soutenue publiquement par

Wassim TABIKH

le 26 Février 2018

**Utilisation du Massive MIMO dans les réseaux 5G pour
l'annulation d'interférence inter-cellule et pour l'augmentation
de la capacité**

Directeur de thèse : **Dirk SLOCK**
Co-encadrement de la thèse : **Yi YUAN-WU**

Jury

Mme Maryline HELARD, Professeur, INSA de Rennes
M. Constantinos PAPADIAS, Professeur, Athens Information Technology
Mme. Ghaya REKAYA, Professeur, Télécom ParisTech
M. Pascal CHEVALIER, Professeur, CNAM de Paris
M. Salah-Eddine EL AYOUBI, Maître de Conférences HDR, CentraleSupélec
M. Raphaël VISOZ, Ingénieur de Recherche, Orange Labs

Rapporteur
Rapporteur
Examineur
Examineur
Examineur
Invité

TELECOM ParisTech

école de l'Institut Télécom - membre de ParisTech

Abstract

The evolution of wireless communication must meet the increasingly high demand in mobile data. It is an important subject studied by Information Theorists in the last decade. A challenge has been launched by Qualcomm to increase the maximum rates of wireless by a factor of 1000 by 2020. It is clear that to reach this goal, a combination of different ingredients is necessary. The major limitation of wireless communication is the interference due to frequency reuse. For 2G networks, this interference was treated as noise and was limited by a moderate frequency reuse behavior. Spread spectrum in 3G created so much intracell interference that the frequency reuse issue became less problematic. The use of an orthogonal modulation which is orthogonal frequency-division multiplexing (OFDM) again in 4G led to an interference management by dynamic coordination of resource blocks. The use of multiple antennas started with multiple input multiple output (MIMO) in 3G and Multiuser (MU) MIMO (single cell) or Coordinated Multipoint (CoMP) for multiple cells in 4G. These techniques allowed only modest gains in rates. A new technique of interference management was born 5 years ago, the Interference Alignment (IA). IA permits to have a capacity which equals half of the capacity of an interference-free system. This technique supposes that each transmitter (Tx) knows the channels not only towards its receivers (Rxs), but the channels from all Txs to all receivers Rxs. A more recent interference management technique is Massive MIMO, where Txs use antennas at a very large scale. The idea is introduced in a single cell scenario for MU MIMO. Massive MIMO is motivated by many simplifications which appear in an asymptotic regime where base stations (BSs) are endowed with large numbers of antennas. MIMO allows simultaneous transmission of multiple streams (spatial multiplexing), which permits to increase the rates inevitably. Although MIMO makes use of multiple antennas at both Tx and Rx sides, it needs a very rich propagation environment (like in indoor); the MU MIMO allows the same spatial multiplexing with

single antenna users and any environment. However, for MU MIMO, all of the interference management must be done at the Tx side, which implies a good channel state information at trasmitter (CSIT) requirement. In this case, the optimal transmission technique becomes complex, which is the Dirty Paper Coding (DPC). If the number of transmit antennas increases a lot, a linear beamformer (BF) will be near optimal and even simple matched filters will be optimal asymptotically. Although such a large number of antennas looks freaky, we can argument that the RF circuits do not need to be very precise which allows to decrease the BS consumption. The goal of this thesis is to introduce complete and realistic solutions for interference management using Massive MIMO in a multicell (MC) scenario.

Acknowledgements

First, I would like to thank my supervisors, Prof. Dirk Slock and Dr. Yuan-Wu. I was extremely fortunate to be supervised by two acclaimed scientists and brilliant people, who helped me throughout my thesis. Prof. Slock, with his immense knowledge and constant motivation, was a valuable source of ideas. He helped me choose the right directions and overcome numerous obstacles I have been facing through my research. He posed hard questions which incited me to widen my research. Dr. Yuan-Wu, with her experience and infinite patience, followed meticulously the advancement of my project and was everyday here to support and guide me wisely. She was always available to answer my questions, with great attention to details.

My sincere thanks goes to my fellow colleagues both in Orange labs and in Eurecom, who provided me with an opportunity to join their team. It was great sharing the office with you all these years.

I am also grateful to the Orange and Eurecom staff for their assistance and Orange for funding my entire PhD research. The research of Orange Labs is partially supported by the EU H2020 projects Fantastic5G and ONE5G.

I am also grateful to the committee members of my jury, for their insightful comments and time spent reading my thesis.

And finally, I could not forget to express my gratitude to my family, girlfriend and friends for their continuous encouragement and emotional support.

Thank you.

Wassim Tabikh

Contents

| | |
|-------------------------|------------|
| Abstract | i |
| Acknowledgements | iii |
| List of Figures | vii |
| Abbreviations | ix |

| | |
|---|----------|
| 1 Motivation and Models | 1 |
| 1.1 Introduction | 1 |
| 1.2 Summary of Contributions | 5 |
| 1.3 Notation | 7 |
| 1.4 System Model | 7 |
| 1.4.1 The WSMSE algorithm | 10 |
| 1.4.2 The KG precoding algorithm | 12 |
| 1.5 Deterministic annealing (DA) and WSMSE-SR (Simple Receiver) | 14 |
| 1.5.1 DA | 14 |
| 1.5.2 The WSMSE-SR | 15 |
| 1.6 Channel estimation | 17 |
| 1.7 Conclusion | 19 |

| | |
|---|-----------|
| I Random Matrix Theory for large system analysis and Massive MIMO design | 21 |
|---|-----------|

| | |
|---|-----------|
| 2 The WSMSE algorithm: A Large System Analysis | 22 |
| 2.1 Introduction | 22 |
| 2.2 System model: The MISO IBC case | 23 |
| 2.3 Large system analysis | 25 |
| 2.3.1 Deterministic Equivalent of the SINR for the MF | 25 |
| 2.3.2 Deterministic equivalent of the SINR of proposed precoder for correlated channels | 26 |
| 2.3.3 Numerical results | 30 |
| 2.4 The MIMO single stream case | 32 |

| | | |
|------------|--|-----------|
| 2.4.1 | Applications of the deterministic equivalent of the SINR | 38 |
| 2.5 | Conclusion | 40 |
| 3 | Using the Complex Large System Analysis to Simplify Beamforming | 42 |
| 3.1 | Decentralized approach for large dimensions system | 42 |
| 3.2 | Signaling | 44 |
| 3.3 | Numerical results | 47 |
| 3.4 | Analytic solution | 47 |
| 3.5 | Conclusion | 53 |
| II | Further Random Matrix Theory exploitation with partial CSIT | 55 |
| 4 | Robust Beamformers for Partial CSIT | 56 |
| 4.1 | The naive approach : ENAIVEKG | 57 |
| 4.2 | The EWSMSE approach | 57 |
| 4.3 | The ESEI-WSR approach | 58 |
| 4.3.1 | Alternative expression of $\check{\mathbf{A}}_{c,k}$ | 60 |
| 4.4 | Numerical results and interpretation | 62 |
| 4.5 | Practical decentralized solution | 65 |
| 4.6 | The MISO case for large system analysis | 71 |
| 4.6.1 | Max EWSR BF (ESEI-WSR) in the MaMISO limit | 71 |
| 4.6.2 | EWSMSE and the naive approach | 72 |
| 4.7 | Large System Approximation of the EWSR | 73 |
| 4.7.1 | Large system analysis | 74 |
| 4.7.2 | Numerical results for MISO large system analysis | 75 |
| 4.8 | Alternative (sub-optimal) approach | 76 |
| 4.9 | Conclusion | 80 |
| 5 | Non-Linear Precoding Schemes | 82 |
| 5.1 | Introduction | 82 |
| 5.2 | The IBC signal model | 83 |
| 5.3 | The LA operation | 84 |
| 5.4 | Solving the EWSR problem | 87 |
| 5.4.1 | Max WSR with Perfect CSIT : DC approach | 87 |
| 5.4.2 | Solution with imperfect CSIT | 89 |
| 5.5 | Simulation results | 91 |
| 5.6 | Conclusion | 93 |
| III | Relaying with Random Matrix Theory | 94 |
| 6 | Beamformers Design with AF Relays | 95 |

| | | |
|----------|---|------------|
| 6.1 | Introduction | 95 |
| 6.2 | The IBRC signal model | 97 |
| 6.3 | The WSMSE precoder for IBRC | 99 |
| 6.4 | The KG precoder for IBRC | 101 |
| 6.5 | Numerical results and short discussion | 103 |
| 6.6 | Joint ZF-IN feasibility conditions | 105 |
| 6.7 | Conclusion | 108 |
| 7 | Conclusions and Future Works | 109 |
| 7.0.1 | Summary and conclusions | 109 |
| 7.0.2 | Future work | 113 |
| 8 | Résumé en Français | 114 |
| 8.1 | Introduction | 114 |
| 8.2 | Problème à résoudre | 116 |
| 8.2.1 | L'algorithme WSMSE | 118 |
| 8.2.2 | L'algorithme KG | 119 |
| 8.3 | Partie I: Random Matrix Theory for large system analysis and Massive MIMO design | 123 |
| 8.4 | Partie II: Further random matrix theory exploitation with partial CSIT | 124 |
| 8.5 | Partie III: Relaying with random matrix theory | 130 |
| 8.6 | Conclusions | 133 |
| A | Random Matrix Theory | 138 |
| B | Proof of an equivalent deterministic expression: Perfect CSIT | 140 |
| C | Proof of an equivalent deterministic expression: Imperfect CSIT | 142 |
| | Bibliography | 147 |

List of Figures

| | | |
|-----|---|----|
| 1.1 | The IBC or MC MU system model | 8 |
| 1.2 | Intercell interference at cell edges | 10 |
| 1.3 | Deterministic Annealing | 14 |
| 1.4 | WSR vs SNR for $C = 3$, $K = 2$, $M = 5$, $N = 3$ | 15 |
| 1.5 | WSR vs SNR for $C = 3$, $K = 2$, $M = 15$, $N = 1$ and $N = 2$ | 16 |
| 1.6 | WSR vs SNR for $C = 3$, $K = 2$, $M = 10$, $N = 2$ | 17 |
| 1.7 | Channel estimation in FDD | 18 |
| 2.1 | Sum rate comparisons between the IBC WSMSE and our proposed approximation for $C=2, K=15, M=30$ | 31 |
| 2.2 | Sum rate comparisons between the IBC WSMSE and our proposed approximation for $C=3, K=10, M=30$ | 32 |
| 2.3 | Sum rate comparisons between the IBC WSMSE and our proposed approximation for $C=3, K=9, M=30$ | 32 |
| 2.4 | Sum rate comparisons between the IBC WSMSE with MMSE filters and the IBC WSMSE with MF filters for $C=1$, $M=10$, $K=4$, $N=2$ | 37 |
| 2.5 | Sum rate comparisons between the IBC WSMSE and our proposed approximation for $C=1, K=20, M=30, N=\{1,2\}$ | 40 |
| 2.6 | Sum rate comparisons between the IBC WSMSE and our proposed approximation for $C=2, K=10, M=30, N=\{1,2\}$ | 41 |
| 3.1 | Sum rate comparisons for $C=3, K=2, M=15$ | 48 |
| 3.2 | Sum rate comparisons for $C=3, K=5, M=15$ | 49 |
| 3.3 | Figure corresponding to Assumption 3.1 | 49 |
| 3.4 | Figure corresponding to Assumption 3.2 | 50 |
| 4.1 | Sum rate comparisons for $C=2$, $M=8$, $K=4$, $N=1$ and uncorrelated channels, identity channel covariance matrices | 63 |
| 4.2 | Sum rate comparisons for $C=2$, $M=8$, $K=4$, $N=2$ and uncorrelated channels, identity channel covariance matrices | 63 |
| 4.3 | Sum rate comparisons for $C=2$, $M=8$, $K=4$, $N=4$ and uncorrelated channels, identity channel covariance matrices | 64 |
| 4.4 | Sum rate comparisons for $C=2$, $M=8$, $K=4$, $N=1$ and correlated low rank channels | 65 |

| | | |
|------|--|-----|
| 4.5 | Sum rate comparisons for $C=2, M=8, K=4, N=2$ and correlated low rank channels | 65 |
| 4.6 | Sum rate comparisons for $C=2, M=8, K=4, N=4$ and correlated low rank channels | 66 |
| 4.7 | Convergence behavior for $C=2, M=8, K=4, N=4$ and correlated low rank channels | 66 |
| 4.8 | Sum rate comparisons for $C=2, M=8, K=4, N=4$ and uncorrelated channels, identity channel covariance matrices | 70 |
| 4.9 | Sum rate comparisons for $C=2, M=8, K=3, N=4$ and uncorrelated channels, identity channel covariance matrices | 70 |
| 4.10 | Sum rate comparisons for $C=2, M=8, K=4, N=4$ and correlated low rank channels | 71 |
| 4.11 | Sum rate comparison for $C = 2, K = 6, M = 15, N = 1 \forall k$ and $rank(\mathbf{C}_{t,i,b_k}) = rank(\mathbf{C}_{p,i,b_k}) = 2 \forall i, \forall k$ and $\alpha^2 = \frac{1}{10}$ | 76 |
| 4.12 | Sum rate comparisons for $C=6, M=6$ and $N=6$ | 80 |
| 5.1 | Interference in DPC | 84 |
| 5.2 | Achievable sum rate for $C = 3, K = 9, M = 8, N = 2$ with 2-rank channel estimation error covariance matrices | 92 |
| 6.1 | The IBRC DL scenario | 97 |
| 6.2 | Sum rate Comparison for $C = 2, K = 4, M_{BS} = 4, N = 2, M_{RS} = 8$ | 104 |
| 6.3 | Relay and direct links | 105 |
| 8.1 | Communications multicellulaires | 116 |
| 8.2 | Interférence intercellulaire aux bords des cellules | 118 |
| 8.3 | Estimation du canal en FDD | 124 |
| 8.4 | Scénario avec relais | 130 |

Abbreviations

| | |
|-----------------|---|
| AF | Amplify and Forward |
| BF | Beamformer |
| BRC | Broadcast Relay Channels |
| BS | Base Station |
| CF | Compress and Forward |
| CoBF | Coordinated Beamforming |
| CoMP | Coordinated MultiPoint |
| CSIT | Channel State Information at the Transmitter |
| CSIR | Channel State Information at the Receiver |
| DA | Deterministic Annealing |
| DC | Difference of Concave functions |
| DF | Decode and Forward |
| DoF | Degrees of Freedom |
| DL | Downlink |
| DPC | Dirty Paper Coding |
| ESEI-WSR | Expected Signal covariance Expected Interference covariance based WSR |
| EWSMSE | Expected Weighted Sum Mean Squared Error |
| EWSR | Expected WSR |
| FD | Full Duplex |
| FDD | Frequency Division Duplexing |
| HD | Half Duplex |
| IA | Interference Alignment |
| iaRZF | interference-aware RZF |

| | |
|----------------|---|
| IBC | Interference Broadcast Channels |
| IBRC | Interference Broadcast Relay Channels |
| IoT | Internet of Things |
| IMAC | Interfering Multiple Access Channel |
| IN | Interference Neutralization |
| KG | Kim Giannakis |
| LA | Linear assignment |
| LoS | Line of Sight |
| LS | Large Scale |
| MAC | Medium Access Control / Multiple Access Channel |
| MC | Multicell |
| MF | Matched Filter |
| MMSE | Minimum Mean Squared Error |
| MIMO | Multiple-Input Multiple-Output |
| MISO | Multiple-Input Single-Output |
| MRC | Maximum Ratio Combining |
| MRT | Maximum Ratio Transmission |
| MSE | Mean Squared Error |
| MU | Multiusers |
| MmWaves | Millimeter Waves |
| OFDM | Orthogonal Frequency-Division Multiplexing |
| PAPR | Peak-to-Average Power Ratio |
| RF | Radio Frequency |
| RS | Relay Station |
| Rx | Receiver |
| SIC | Successive Interference Cancellation |
| SINR | Signal to Interference plus Noise Ratio |
| SNR | Signal to Noise Ratio |
| SR | Simple Receiver |
| SS | Single Stream |
| TDD | Time Division Duplexing |

| | |
|---------------|---|
| TSTINR | Total Signal to Total Interference plus Noise Ratio |
| Tx | Transmitter |
| UL | Uplink |
| WSMSE | Weighted Sum Mean Squared Error |
| WSR | Weighted Sum Rate |
| ZF | Zero-Forcing |

Chapter 1

Motivation and Models

1.1 Introduction

Demand for high data rates is growing heavily over the next years. In order to meet this demand in the next generation networks or 5G, a combination of ingredients are crucial:

- Densifying the network: putting the access points closer one to another.
- Adding more spectrum: the introduction of new high frequency bands in $5G \geq 6Ghz$ allows the introduction of millimeter-waves (mmWaves) communications.
- Adding more antennas at the BSs: Massive MIMO. We mean by 'Massive MIMO', systems having antenna arrays with a few hundred antennas serving tens of terminals in the same time-frequency resource. Massive MIMO is a serious enabler for 5G.

However, densifying the network will create more intercell interference in the system, which is already contaminated by intercell interference and mmWaves suffer from severe pathloss and penetration loss.

The main focus of this work is the Massive MIMO technology, which presents numerous advantages. [1–8] Massive MIMO **increases spectral efficiency** because tens of terminals are served simultaneously. It **increases energy efficiency**; the energy can be focused with extreme sharpness into small regions in space. Moreover, it **enables reduction of latency** by relying on the law of

large numbers and beamforming to avoid fading dips, so that fading no longer limits latency. It also **simplifies the Medium Access Control (MAC) layer**: The channel hardens and frequency domain scheduling no longer pays off. All subcarriers have the same gain so with OFDM the whole frequency band per resource block can be allocated to each user.

Massive MIMO **uses low-cost low-power Radio Frequency (RF) hardware**, e.g. the ultra linear 50 Watt amplifiers used in conventional amplifiers are replaced by low cost ones with output power in the milli-Watt range. This causes quality degradation in the RF. Although Massive MIMO reduces the constraints on accuracy RF, it relies on law of large number, so that hardware imperfections average out when signals from a large number of antennas are combined together.

Cheap hardware components are particularly prone to the following impairments:

- Amplifiers non-linearities: OFDM-based wireless communications systems suffer from high Peak-to-Average Power Ratio (PAPR), which necessitates the use of linear power amplifiers to avoid out-of-band radiation and signal distortions. Linear RF are more costly and less power efficient than their nonlinear counterparts, which induces high costs for large scale BSs.
- I/Q imbalance: It is one of the most severe RF impairments. On the one hand, non-ideal mixers cause phase imbalance between the I and Q branches. On the other hand, imperfect responses of amplifiers, filters, analog-to-digital and digital-to-analog converters result in gain imbalance between the I and Q branches. The resulting signal distortion is well known to cause inter-carrier interference in multi-rate systems.
- Phase noise: Phase noise is introduced during the up conversion of the baseband signal to passband and vice versa due to imperfections in the circuitry of local oscillators.

However, the influence of hardware impairments is mitigated by compensation algorithms which can be implemented by analog and digital processing and which benefit from the excess of degrees of freedom (DoF) by the Massive MIMO antennas configuration and the averaging effect in Massive MIMO

resulting.

Although Massive MIMO has numerous advantages [4, 9–12], scaling up the number of antennas faces several challenges that prevent the corresponding scaling of the gains. So, what are the challenges that Massive MIMO is facing? In a conventional Frequency Division Duplexing (FDD) system, the amount of time-free resources for Downlink (DL) pilots scales as the number of antennas. So, a massive MIMO system would require up to a 100 times more resources than a conventional system. The BS sends out pilots based on which the terminals estimate the channel responses, quantify the obtained estimates and feed them back to the BS. In the uplink (UL), the number of pilots is proportional to the number of users, which is acceptable. However, in a coherence interval (UL + DL) transmission, training and feedback have high overhead and hence the number of users servable would be limited.

To overcome the above, Time Division Duplexing (TDD) is used where the DL channel can be simply obtained from the UL channels due to channel reciprocity. We should not spend too much resources on pilots in TDD mode. Nevertheless, the max number of orthogonal pilot sequences that can exist is upper-bounded by the duration of the coherence interval divided by the delay-spread. The effect of reusing pilots from one cell to another is 'pilot contamination'.

This problem is not specific to Massive MIMO, but effect on Massive MIMO appears to be more profound. Pilot contamination causes channel estimation errors which in turn leads to DL intercell interference. Recent ideas based on the exploitation of side-information lying in the second-order statistics of the user channels, both for desired and interfering users, lead to a complete removal of pilot contamination effects in large number of antennas limit. Covariance-aware pilot assignment strategies within the channel estimation phase itself are used as well to combat the pilot contamination.

Therefore, even though pilot contamination is a tough problem, many practical solutions exist to eliminate its effects so that the system performance grows unboundedly to infinity with the number of antennas.

A crucial question is on what frequencies Massive MIMO will work. In 5G, we identify 3 groups of frequency bands:

- low-range frequencies (around 700 Mhz): it offers great penetration and

coverage and would be used for Internet of Things (IoT) which requires wide range coverage and good penetration especially when sensors are indoor. These frequencies will not be used for Massive MIMO, because, at these frequencies, the carrier wavelength λ is high. This would result to the antenna spacing $\frac{\lambda}{2}$ being larger, so the antenna array would in turn become very large. This is not practical. FDD mode is applicable in this range.

- mid-range frequencies around 2.6 Ghz: Massive MIMO will be used in this band, where it would be beneficial for its advantages discussed above. TDD mode is applicable in this range.
- high-range frequencies ≥ 6 Ghz (mmWaves): Massive MIMO is essential in this band. More details are given below.

Wireless industries face spectrum crunch at microwave frequencies (up to 6Ghz)[13]. Due to this fact, there is interest to exploit underutilized mmWaves. However, mmWaves face severe path loss, penetration loss and rain fading and are easily absorbed or scattered by gases. As a result, they require very high gain antenna systems, which can be provided by Massive MIMO. For that reason, there is a marriage between Massive MIMO and mmWaves.

Massive MIMO increases spectral efficiency by serving tens of terminals simultaneously. However, in order to do so, signals transmitted by the BSs must be precoded by some precoders/ BFs. What are the best precoders for Massive MIMO BSs?

With Massive MIMO, the effect of small fading, intracell interference and intercell interference vanish if and only if pilot contamination is dealt with [14–21]. It is shown that, with linear precoders in single cell scenario, the achievable sum rates are up to 98 percent of those achieved by DPC, for BS to user antenna ratios as low as 10.

For FDD systems, two-stage precoding schemes are used to reduce pilot resources and CSI feedback in FDD systems. The users are put into groups which have similar second-order channel statistics, i.e. transmit correlation. The first stage precoding is then used for each group of users semi-statistically. With reduced dimensions on the effective channel, simple channel feedback can be realized, thus the second-stage dynamic precoding can be applied. However, we stress the fact that Massive MIMO will mainly be deployed with TDD.

For high-range frequencies, the RF chains operating at such high frequencies

are so expensive that installing a RF chain per antenna is unlikely to happen. Hybrid analog digital architectures have been proposed in the literature. They utilize discrete phase shifters or switches, which move some of the signal processing from the digital baseband domain to the analog RF domain, so as to decrease the number of RF chains.

Massive MIMO can also be beneficial when combined with technologies such as full duplex (FD) relaying. FD has received a lot of research interest for its ability to recover the bandwidth loss induced by conventional half-duplex relaying. The benefit of improved spectral efficiency in the FD mode comes at the price of loop interference, due to signal leakage from the relay's output to input. Nevertheless, Relay station (RS) equipped with massive arrays loop can canceled out interference.

In this work, we focus on linear precoders for MC MU Massive MIMO scenarios for massive MIMO. For classical multicell MIMO networks, two algorithms are known to be the best. The first algorithm is the weighted sum minimum squared error (WSMSE) approach, which transforms the weighted sum rate (WSR) maximization problem into an equivalent WSMSE minimization problem with some special chosen weighted matrices that depend on the beamforming matrices as in [22], [23] and [24]. The other algorithm is the KG algorithm, which transforms the WSR maximization problem into a difference of concave function problems as in [25].

1.2 Summary of Contributions

In this thesis, we reconsider the WSMSE and KG algorithms and apply/ adapt them for Massive MIMO scenarios. The work is divided into three sub-parts. The first one concerns the Random Matrix Theory for large system analysis and Massive MIMO design and is discussed in Chapters 2 and 3. The second one is about the further Random Matrix Theory exploitation with partial CSIT. Details can be found in Chapters 4 and 5. Finally, Relaying with Random Matrix Theory is the main subject of Chapter 6.

As far as the first part is concerned, in Chapter 2, we perform a large system analysis on the WSMSE algorithm for MC MU massive MIMO scenarios in order to study its performance. The results are published in:

- Tabikh, Wassim; Slock, Dirk TM; Yuan-Wu, Yi, Weighted sum rate maximization of correlated MISO interference broadcast channels under linear precoding: a large system analysis, VTC 2016-Spring, IEEE 83rd Vehicular Technology Conference, 15-18 May 2016, Nanjing, China
- Tabikh, Wassim; Slock, Dirk TM; Yuan-Wu, Yi, A Large system analysis of weighted sum rate maximization of single stream MIMO interference broadcast channels under linear precoding, ISWCS 2016, Poznan, Poland

In Chapter 3, we inspire from the derivations in Chapter 2, and we propose a new fast-convergent precoder suitable for MC MU massive MIMO with perfect CSIT scenarios.

- Tabikh, Wassim; Yuan-Wu, Yi; Slock, Dirk TM, Decentralizing multi-cell maximum weighted sum rate precoding via large system analysis, EUSIPCO 2016, 24th European Signal Processing Conference, 28 August-2 September 2016, Budapest, Hungary

As far as the second part is concerned, in Chapter 4, we deal with scenarios where the Tx do not have anymore a good knowledge of the channels towards the users. A robust precoder is proposed for that case, and a study of its performance is provided using large system approach. The results are patented and then published in:

- Tabikh, Wassim; Yuan-Wu, Yi; Slock, Dirk, Beamforming design with combined channel estimate and covariance CSIT via random matrix theory, ICC 2017, IEEE International Conference on Communications, IEEE ICC 2017 Wireless Communications Symposium, May 21-25, Paris, France
- Tabikh, Wassim; Slock, Dirk TM; Yuan-Wu, Yi, MaMISO IBC beamforming design with combined channel estimate and covariance CSIT: a large system analysis, ICC 2017, WS08-3rd International Workshop on Advanced PHY and MAC Technology for Super Dense Wireless Networks (CROWD-NET), May 21-25, Paris, France
- Tabikh, Wassim; Slock, Dirk TM; Yuan-Wu, Yi, MIMO IBC beamforming with combined channel estimate and covariance CSIT, ISIT 2017,

IEEE International Symposium on Information Theory June 25-30, 2017,
Aachen, Germany

In Chapter 5, we deal with nonlinear robust transmit precoders design for the case of partial CSIT. The results are published in:

- Tabikh, Wassim; Slock, Dirk TM; Yuan-Wu, Yi, Robust Non-Linear Precoders for the MIMO Interference Broadcast Channels with Imperfect CSIT, submitted to EUSIPCO 2018, September 2018, Rome, Italy.

Finally, in Chapter 6, we extend our system model and we suppose the existence of relays. DoFs and new beamforming algorithms for MC MU scenarios are derived. The results are published in:

- Tabikh, Wassim; Slock, Dirk TM; Yuan-Wu, Yi, Relay aided coordinated beamforming and interference neutralization, ITA 2017, Information Theory and Applications Workshop, February 12-17 2017, San Diego, USA

Chapter 7 concludes and gives insights into possible extensions of the current work in the future.

1.3 Notation

The following notation is adopted throughout the thesis: Scalars are denoted in lower case, vectors are denoted in bold-face and lower case, matrices are denoted in bold-face and upper case. The subscripts $(\cdot)^T$ and $(\cdot)^H$ denote the matrix transpose and conjugate transpose respectively. $\det(\cdot)$, $\text{tr}(\cdot)$ and $(\cdot)^{-1}$ denote the matrix determinant, trace and inverse respectively. $\mathbb{E}(\cdot)$ denotes the expectation of a random variable. $\log(\cdot)$ denotes the binary logarithm. \mathbf{I}_M denotes the identity matrix of dimension M, $x \sim \mathcal{NC}(0, \sigma^2)$ denotes that x follows a complex Gaussian distribution with zero mean and σ^2 variance.

1.4 System Model

We analyse a cellular DL MC MU MIMO scenario where C cells are presented, $c=1\dots C$, each of the C cells consists of one BS with M antennas which transmits

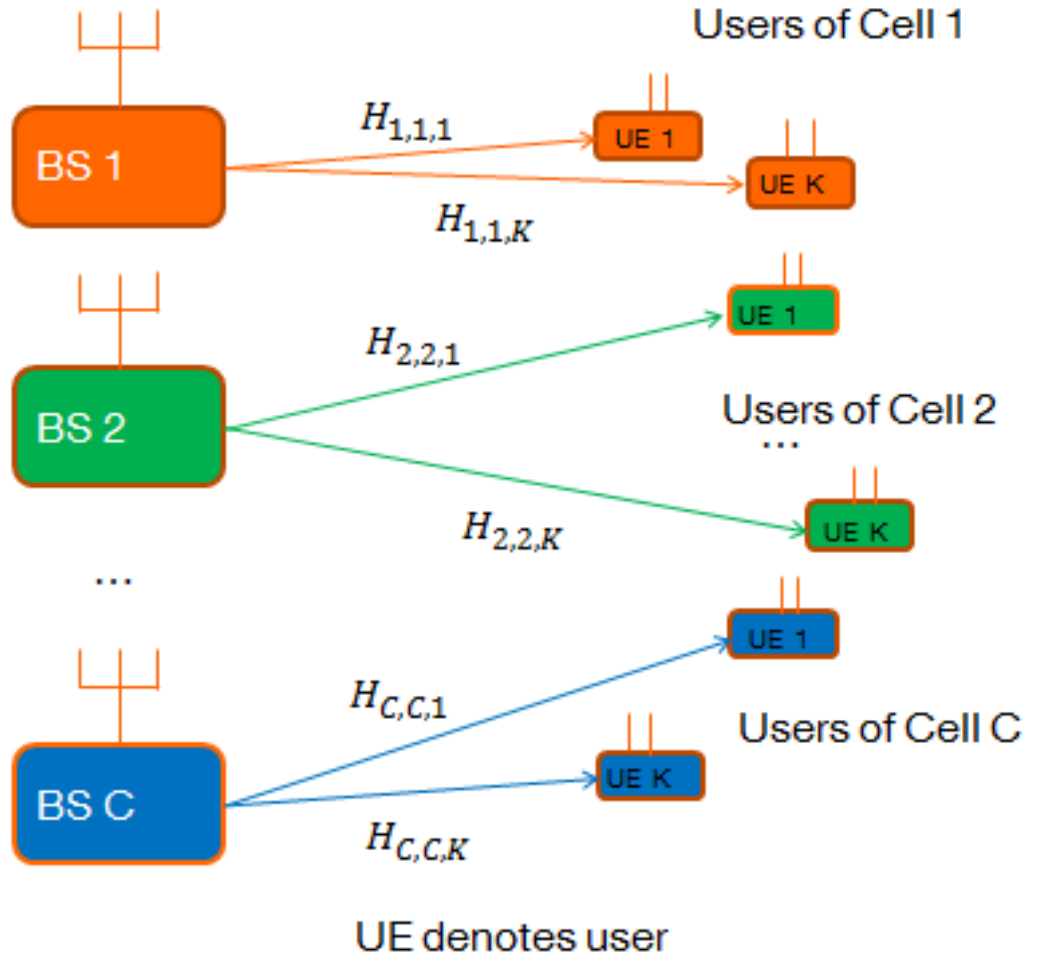


FIGURE 1.1: The IBC or MC MU system model

data to K users equipped with N -antennas RxS (See Figure 1.1). We assume transmission on a single narrow-band carrier. The received signal $\mathbf{y}_{c,k} \in \mathbb{C}^{N \times 1}$ at the k th user in cell c reads

$$\mathbf{y}_{c,k} = \sum_{m=1}^C \sum_{l=1}^K \mathbf{H}_{m,c,k} \mathbf{G}_{m,l} \mathbf{s}_{m,l} + \mathbf{n}_{c,k} \quad (1.1)$$

where the user symbols are chosen from a Gaussian codebook, i.e, $\mathbf{s}_{m,l} \in \mathbb{C}^{d_{m,l,1}}$,

where each one of its elements $\sim \mathcal{NC}(0, 1)$, are linearly precoded and form the transmit signal; $d_{m,l}$ is the number of streams allowed by the user l of cell m ; $\mathbf{G}_{m,l} \in \mathbb{C}^{M \times d_{m,l}}$ is the precoding vector of user l of cell m , $\mathbf{H}_{m,c,k} \in \mathbb{C}^{N \times M}$ is the channel matrix from the m th transmitter to the k th user of cell c , and the $\mathbf{n}_{c,k}$ is a $\mathbb{C}^{N \times 1}$ vector independent complex Gaussian noise terms with zero mean and variance σ^2 . Moreover, the channel $\mathbf{H}_{i,c,k}$ has as covariance matrix $\mathbb{E}[\mathbf{H}_{i,c,k}^H \mathbf{H}_{i,c,k}] = \mathbf{\Theta}_{i,c,k}$ and the precoders are subject to an average power constraint due to power budget limitation at each Tx, thus

$$\text{tr} \mathbf{G}_c \mathbf{G}_c^H \preceq P_c \text{ for } c \in \mathcal{C} \quad (1.2)$$

where \mathcal{C} is the set of all BSs.

$\mathbf{G}_c = [\mathbf{G}_{c,1}, \mathbf{G}_{c,2}, \dots, \mathbf{G}_{c,K}] \in \mathbb{C}^{M \times K}$ is the precoding matrix and P_c is the total available transmit power of cell c .

Under the assumption of optimal single-user decoding and perfect CSIT and CSI at the receivers (CSIR), the achievable rate $r_{c,k}$ of the k th user of cell c is given by

$$r_{c,k} = \log \det(\mathbf{I}_N + \mathbf{\Gamma}_{c,k}) \quad (1.3)$$

$$\mathbf{\Gamma}_{c,k} = \mathbf{R}_{c,k}^{-1} \mathbf{H}_{c,c,k} \mathbf{Q}_{c,k} \mathbf{H}_{c,c,k}^H \quad (1.4)$$

where $\mathbf{Q}_{c,k} = \mathbf{G}_{c,k} \mathbf{G}_{c,k}^H$ is the transmit covariance matrix, $\mathbf{\Gamma}_{c,k}$ is the signal to interference plus noise ratio (SINR) of the k th user of cell c and $\mathbf{R}_{c,k}$ is the received interference plus noise covariance matrix at the k th user of cell c , given by

$$\begin{aligned} \mathbf{R}_{c,k} &= \mathbf{H}_{c,c,k} \mathbf{Q}_{c,k} \mathbf{H}_{c,c,k}^H + \mathbf{R}_{c,k}^- \\ \mathbf{R}_{c,k}^- &= \sum_{(j,i) \neq (c,k)} \mathbf{H}_{j,c,k} \mathbf{Q}_{j,i} \mathbf{H}_{j,c,k}^H + \sigma^2 \mathbf{I}_N. \end{aligned} \quad (1.5)$$

The rate, especially when the RxS are located at the cell edges, is greatly influenced by the intercell interferences (Figure 1.2).

For instance, for a cell edge user, the received interference signal in the DL can be severe and even of a comparable strength to the useful signal, which degrades the achieved rate significantly. To enhance the performance in cellular systems and maximize the WSR of all users, smart spatial signal processing techniques at the BSs and the RxS are needed. Furthermore, we assume a coordinated beamforming (CoBF) scheme in which each BS sends data to its

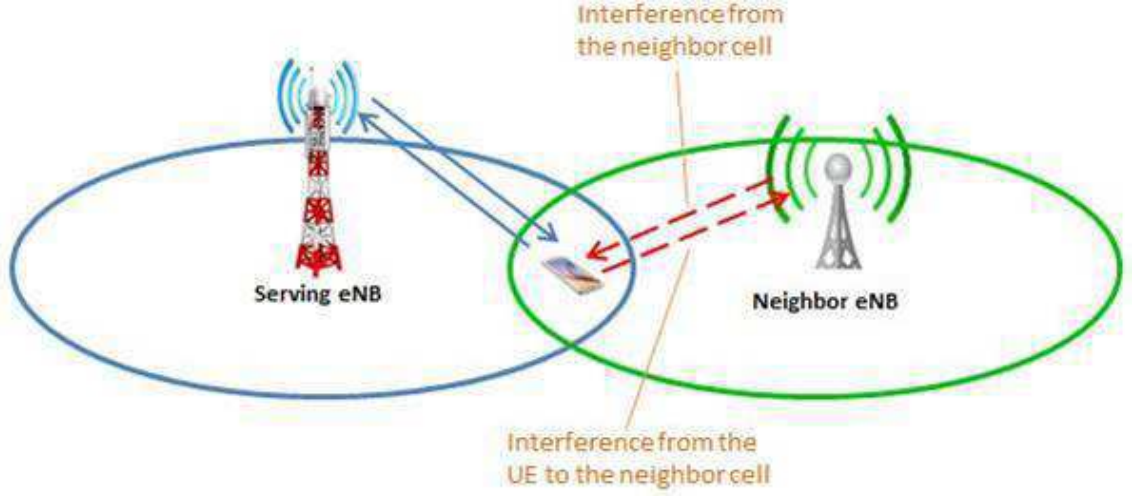


FIGURE 1.2: Intercell interference at cell edges

own users only but CSI is shared between the BSs so that each BS can exploit its excess number of spatial dimensions to mitigate the interference generated in other cells. Thus, we are facing an optimization problem which is the following

$$\begin{aligned} \mathbf{G} = \arg \max_{\mathbf{G}} & \sum_{c=1}^C \sum_{k=1}^K u_{c,k} r_{c,k} \\ \text{s.t. } & \text{tr} \mathbf{G}_c \mathbf{G}_c^H \leq P_c \text{ for } c \in \mathcal{C} \end{aligned} \quad (1.6)$$

where \mathbf{G} is the short notation for $\{\mathbf{G}_c\}_{c \in \mathcal{C}}$ and where $u_{c,k} \geq 0$ is the weight of the k^{th} user of cell c .

Two algorithms exist that solve this problem: the WSMSE and the KG algorithms which we will discuss below.

1.4.1 The WSMSE algorithm

The optimization problem in (1.6) is hard to be solved directly, since it is highly non concave in the precoding matrix \mathbf{G} . To solve it, we consider the linear receive filters $\mathbf{F}_{c,k} \in \mathbb{C}^{N \times d_{c,k}}$, the error variance $\mathbf{E}_{c,k} \in \mathbb{C}^{d_{c,k} \times d_{c,k}}$ after the linear receive filtering, given in (1.8), and we introduce additional weighting matrices $\mathbf{W}_{c,k} \in \mathbb{C}^{d_{c,k} \times d_{c,k}}$, so that the utility function (1.6) can be modified

and an equivalent optimization problem can be formulated as [22]:

$$\begin{aligned} \{\mathbf{G}, \mathbf{F}, \mathbf{W}\} = \\ \arg \min_{\mathbf{G}, \mathbf{F}, \mathbf{W}} \sum_{(c,k)} u_{c,k} (\text{tr}(\mathbf{W}_{c,k} \mathbf{E}_{c,k}) - \log \det(\mathbf{W}_{c,k})) \\ \text{s.t. } \text{tr} \mathbf{G}_c \mathbf{G}_c \leq P_c \text{ for } c \in \mathcal{C} \end{aligned} \quad (1.7)$$

with

$$\mathbf{E}_{c,k} = \mathbb{E}[(\mathbf{F}_{c,k}^H \mathbf{y}_{c,k} - \mathbf{s}_{c,k})(\mathbf{F}_{c,k}^H \mathbf{y}_{c,k} - \mathbf{s}_{c,k})^H]. \quad (1.8)$$

is the mean squared error (MSE), i.e. the error variance at the Rx. The advantage of this formulation is that the objective function is now convex and quadratic in \mathbf{G} . Denote $\rho_c = \frac{P_c}{\sigma^2}$, the signal-to-noise ratio (SNR) in cell c . From (1.7), and after applying alternating optimization techniques, the precoders are obtained as the following

$$\mathbf{F}_{c,k} = (\sigma^2 \mathbf{I}_N + \sum_{m=1}^C \sum_{l=1}^K \mathbf{H}_{m,c,k} \mathbf{G}_{m,l} \mathbf{G}_{m,l}^H \mathbf{H}_{m,c,k}^H)^{-1} \mathbf{H}_{c,c,k} \mathbf{G}_{c,k} \quad (1.9)$$

$$\mathbf{W}_{c,k} = (\mathbf{I}_{d_{c,k}} - \mathbf{F}_{c,k}^H \mathbf{H}_{c,c,k} \mathbf{G}_{c,k})^{-1} \quad (1.10)$$

$$\mathbf{G}_{c,k} = (\sum_j^C \sum_i^K u_{j,i} \mathbf{H}_{c,j,i}^H \mathbf{D}_{j,i} \mathbf{H}_{c,j,i} + \lambda_c \mathbf{I}_M)^{-1} \mathbf{H}_{c,c,k}^H \mathbf{F}_{c,k} \mathbf{W}_{c,k} \quad (1.11)$$

where $\mathbf{D}_{i,j} = \mathbf{F}_{i,j} \mathbf{W}_{i,j} \mathbf{F}_{i,j}^H$. Subsequently $\mathbf{F}_{c,k}$ and $\mathbf{W}_{c,k}$ are computed, which then constitute the new precoder $\mathbf{G}_{c,k}$. The Lagrangian λ_c must be adjusted by bisection in order to satisfy the power constraints. However, if we would like to not do any bisection, [24] has proposed a closed-form expression for the Lagrangian, thus the precoder is reformulated as follows:

$$\mathbf{G}_{c,k} = \xi_c (\sum_j^C \sum_i^K u_{j,i} \mathbf{H}_{c,j,i}^H \mathbf{D}_{j,i} \mathbf{H}_{c,j,i} + \frac{\text{tr} \mathbf{D}_c}{M \rho_c} \mathbf{I}_M)^{-1} \mathbf{H}_{c,c,k}^H \mathbf{F}_{c,k} \mathbf{W}_{c,k} \quad (1.12)$$

$\mathbf{W}_c = \text{diag}(w_{c,1}, \dots, w_{c,K})$, $\mathbf{A}_c = \text{diag}(a_{c,1}, \dots, a_{c,K})$, $\mathbf{D}_c = \mathbf{A}_c^H \mathbf{W}_c \mathbf{A}_c$ and $\mathbf{A} = \text{diag}(\mathbf{A}_1, \mathbf{A}_2, \dots, \mathbf{A}_C)$, $\mathbf{D} = \text{diag}(\mathbf{D}_1, \mathbf{D}_2, \dots, \mathbf{D}_C)$, ξ_c is the normalization term and given by

$$\xi_c^{(j)} = \sqrt{\frac{P_c}{\mathbf{G}_{c,k} \mathbf{G}_{c,k}^H}} = \sqrt{\frac{P_c}{\Psi_c^{(j)}}}. \quad (1.13)$$

This process is repeated until convergence to a local optimum.

1.4.2 The KG precoding algorithm

Another way to solve the problem in (1.6) is to use a classical difference of concave functions (DC) programming approach as in [25] and [26]. Moreover, all of this section stem from [25]. This problem in (1.6) is non concave because of interference, the KG algorithm proposes to isolate the signal of interest from the sum rate of the rest of the signals which renders the problem non concave. The rest is then linearized using Taylor's expansion method, since a linear function is simultaneously convex and concave. More specifically, consider the dependence of WSR on $\mathbf{Q}_{c,k}$ alone. Then, the objective function in (1.6) can be rewritten as:

$$\begin{aligned} WSR &= u_{c,k} \log \det(\mathbf{R}_{c,k}^{-1} \mathbf{R}_{c,k}) + WSR_{\overline{c,k}}, \\ WSR_{\overline{c,k}} &= \sum_{(j,i) \neq (c,k)} u_{j,i} \log \det(\mathbf{R}_{j,i}^{-1} \mathbf{R}_{j,i}) \end{aligned} \quad (1.14)$$

Consider the first order Taylor series expansion in $\mathbf{Q}_{c,k}$ around $\hat{\mathbf{Q}}$ (i.e. all $\hat{\mathbf{Q}}_{j,i}$) with e.g. $\hat{\mathbf{R}}_{j,i} = \mathbf{R}_{j,i}(\hat{\mathbf{Q}})$, then

$$\begin{aligned} WSR_{\overline{c,k}}(\mathbf{Q}_{c,k}, \hat{\mathbf{Q}}) &\approx WSR_{\overline{c,k}}(\hat{\mathbf{Q}}_{c,k}, \hat{\mathbf{Q}}) - \text{tr}\{(\mathbf{Q}_{c,k} - \hat{\mathbf{Q}}_{c,k}) \hat{\mathbf{A}}_{c,k}\} \\ \text{With } \hat{\mathbf{A}}_{c,k} &= - \left. \frac{\partial WSR_{\overline{c,k}}(\mathbf{Q}_{c,k}, \hat{\mathbf{Q}})}{\partial \mathbf{Q}_{c,k}} \right|_{\hat{\mathbf{Q}}_{c,k}, \hat{\mathbf{Q}}} \\ &= \sum_{(j,i) \neq (c,k)} u_{j,i} \mathbf{H}_{c,j,i}^H (\hat{\mathbf{R}}_{j,i}^{-1} - \hat{\mathbf{R}}_{j,i}^{-1}) \mathbf{H}_{c,j,i} \end{aligned} \quad (1.15)$$

Note that the linearised (tangent) expression for $WSR_{\overline{c,k}}$ constitutes a lower bound for it. Now, dropping constant terms, reparameterizing the $\mathbf{Q}_{c,k} = \mathbf{G}_{c,k} \mathbf{G}_{c,k}^H$, performing this linearisation for all users, and augmenting the WSR cost function with the constraints, we get the Lagrangian

$$\begin{aligned} WSR(\mathbf{G}, \hat{\mathbf{G}}, \lambda) &= \\ \sum_{j=1}^C \lambda_c P_c &+ \sum_{c=1}^C \sum_{k=1}^K u_{c,k} \log \det(\mathbf{I}_{d_{c,k}} + \mathbf{G}_{c,k}^H \hat{\mathbf{B}}_k \mathbf{G}_{c,k}) - \text{tr}\{\mathbf{G}_{c,k}^H (\hat{\mathbf{A}}_{c,k} + \lambda_c \mathbf{I}_M) \mathbf{G}_{c,k}\} \end{aligned} \quad (1.16)$$

where

$$\hat{\mathbf{B}}_{c,k} = \mathbf{H}_{c,c,k}^H \hat{\mathbf{R}}_{c,k}^{-1} \mathbf{H}_{c,c,k} . \quad (1.17)$$

The gradient (w.r.t. $\mathbf{G}_{c,k}$) of this concave WSR lower bound is actually still the same as that of the original WSR criterion. And it allows an interpretation as a generalized eigenmatrix condition, thus $\mathbf{G}'_{c,k} = \text{eigenmatrix}(\hat{\mathbf{B}}_{c,k}, \hat{\mathbf{A}}_{c,k} + \lambda_c \mathbf{I}_M)$ is the (normalized) generalized eigenmatrix of the two indicated matrices, with eigenvalues $\boldsymbol{\Sigma}_{c,k} = \text{eigenvalues}(\hat{\mathbf{B}}_{c,k}, \hat{\mathbf{A}}_{c,k} + \lambda_c \mathbf{I}_M)$. The Lagrange multipliers λ_c , for all c , are adjusted to satisfy the power constraints $\sum_{k,l} \mathbf{P}_{c,k}(l,l) = P_c$. This can be done by bisection and gets executed per BS. Note that some Lagrange multipliers could be zero. Let $\boldsymbol{\Sigma}_{c,k}^{(1)} = \mathbf{G}'_{c,k} \hat{\mathbf{B}}_{c,k} \mathbf{G}'_{c,k}$, $\boldsymbol{\Sigma}_{c,k}^{(2)} = \mathbf{G}'_{c,k} \hat{\mathbf{A}}_{c,k} \mathbf{G}'_{c,k}$. The advantage of formulation (1.16) is that it allows straightforward power adaptation: introducing powers $\mathbf{P}_{c,k} \geq 0$ and substituting $\mathbf{G}_{c,k} = \mathbf{P}_{c,k}^{\frac{1}{2}} \mathbf{G}'_{c,k}$ in (1.16) yields

$$WSR = \sum_c \lambda_c P_c + \sum_{c,k}^K \{u_{c,k} \log \det(\mathbf{I}_{d_{c,k}} + \mathbf{P}_{c,k} \boldsymbol{\Sigma}_{c,k}^{(1)}) - \text{tr}(\mathbf{P}_{c,k} (\boldsymbol{\Sigma}_{c,k}^{(2)} + \lambda_c \mathbf{I}))\} \quad (1.18)$$

which leads to the following interference leakage aware water filling

$$\mathbf{P}_{c,k}(l,l) = \left(\frac{1}{\boldsymbol{\Sigma}_{c,k}^{(1)}(l,l)} \left(\frac{u_k \boldsymbol{\Sigma}_{c,k}^{(1)}(l,l)}{\boldsymbol{\Sigma}_{c,k}^{(2)}(l,l) + \lambda_c} - 1 \right) \right)^+ \quad (1.19)$$

for all l s.t. $\boldsymbol{\Sigma}_{c,k}^{(1)} > 0$ where $z^+ = \max(0, z)$. Note also that as with any alternating optimization procedure, there are many updating schedules possible, with different impact on convergence speed. The quantities to be updated are the $\mathbf{G}'_{c,k}$, the $\mathbf{P}_{c,k}$ and the λ_c . The advantage of the DC approach is that it works for any number of streams/user $d_{c,k}$, by simply taking more or less eigenvectors. In other words, we can take the $d_{c,k}^{max}$ max eigenvectors of the eigenmatrix $\mathbf{G}'_{c,k}$. We mean by the max eigenvectors, the eigenvectors corresponding to the highest eigenvalues. The waterfilling then automatically determines (at each iteration) how many streams can be sustained.

1.5 Deterministic annealing (DA) and WSMSE-SR (Simple Receiver)

1.5.1 DA

From [23], we recall that the maximization problem in (1.6) is highly non concave. At low SNR (high noise variance), any interference is negligible compared to the noise. Hence, all links can be considered decoupled, and, like in single-user MIMO, rate maximization becomes SNR maximization for a single stream to which all transmit power is devoted. The optimal Tx and Rx filters are the left and right singular vectors corresponding to the largest singular value of the channel between the Tx and Rx. This implies that, for $SNR = 0$, a convergence to the global optimum is guaranteed.

Meanwhile, as soon as the SNR increases, many further local optima get introduced due to the appearance of the additional streams. Then, as the SNR increases further, more streams and local optima appear. The idea of DA (Figure 1.3) is to initialize the WSMSE (KG) with the solution of the WSMSE (KG) algorithm at lower SNR, starting from very low SNR, which guarantees a convergence to a global optimum. This process goes on until a stream distribution is reached, at some higher SNR, corresponding to a maximal stream distribution for which interference alignment is feasible. Indeed, at very high SNR, the Tx and Rx filters converge to the global solution.

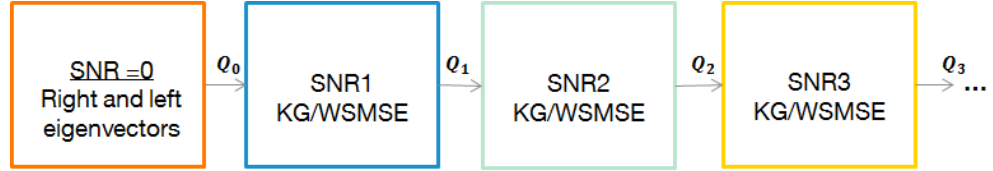


FIGURE 1.3: Deterministic Annealing

In order to prove the efficiency of the DA approach, we plot the sum rate versus SNR corresponding to an IBC system where the signals are precoded by the WSMSE (KG) precoder and by the WSMSE (KG) precoder with DA. This latter means that precoders at lower SNR will serve as initializations for the precoding algorithm at higher SNR. The classical WSMSE precoder is initialized by the right eigenvectors of user's channel. The classical KG is initialized by zero matrices. The overall number of iterations will remain the

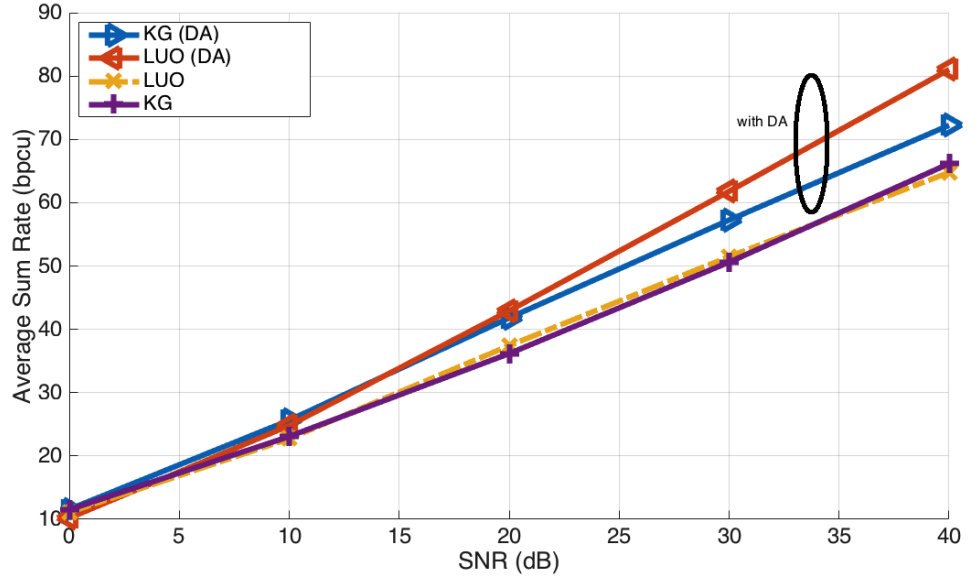


FIGURE 1.4: WSR vs SNR for $C = 3$, $K = 2$, $M = 5$, $N = 3$

same.

In other words, with DA the number of iterations will be the sum of the number of iterations needed to converge at each of the SNR used before achieving our goal SNR. However, using the classical algorithms we do not need to iterate over lower SNRs, but we run our algorithm immediately at the goal SNR; a number of iterations, which equals the total number of iterations in the case of DA is herein needed. We can observe in Figure 1.4 that DA enhances a lot the performance of the WSMSE (or LUO) and KG algorithms.

1.5.2 The WSMSE-SR

We propose a variant of the WSMSE, which consists in using a Matched filter (MF) Rx as the user's Rx instead of the minimum mean squared error (MMSE) Rx (1.9), when the number of antennas is very large compared to the number of users. So now, we are no more obliged to exchange the interference received at each user. The Rx expression (1.9) becomes:

$$\mathbf{F}_{c,k} = (\sigma^2 \mathbf{I}_N + \mathbf{H}_{c,c,k} \mathbf{G}_{c,k} \mathbf{G}_{c,k}^H \mathbf{H}_{c,c,k}^H)^{-1} \mathbf{H}_{c,c,k} \mathbf{G}_{c,k} \quad (1.20)$$

The new precoder is denoted as WSMSE-SR. The explanation is as follows: The Tx and Rx cooperate to cancel the interference received because of transmission to other users. If the number of Tx antennas is very high, the Tx can cancel the interference by itself and there is no need to use complicated Rx. So, simple Rx techniques are optimal herein.

Surprisingly, the WSMSE precoder with a large number of Tx and simple Rx, i.e. the WSMSE-SR precoder, converges almost always to better local optima compared to the classical WSMSE precoder. The explanation is simple. When we dispose of simple Rx, the Tx and Rx are no more coupled via the interference, which eases the convergence. This procedure does not affect the performance, since we have enough antennas at the Tx to cancel the interference, as discussed earlier.

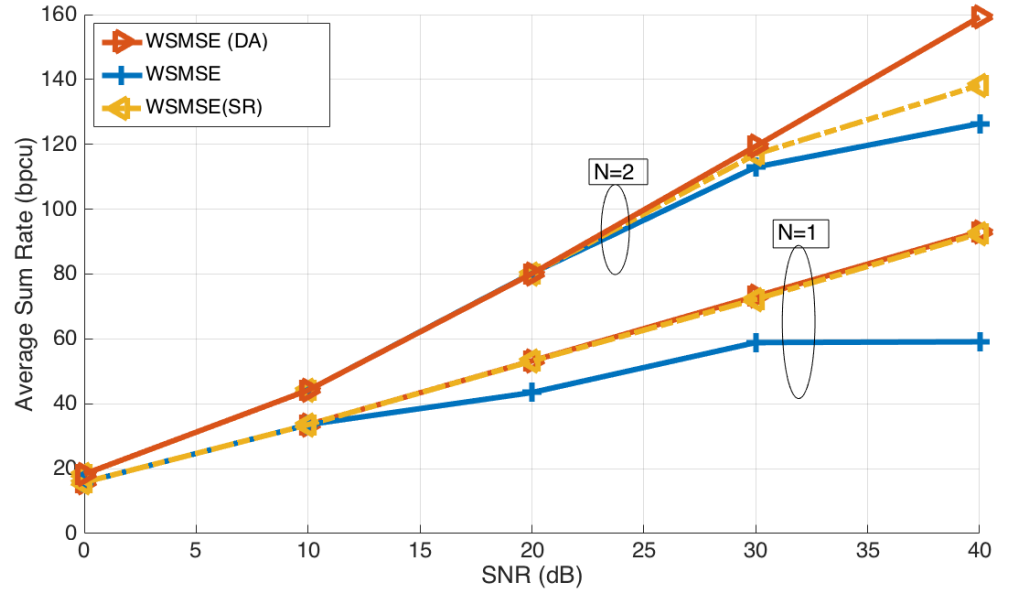


FIGURE 1.5: WSR vs SNR for $C = 3$, $K = 2$, $M = 15$, $N = 1$ and $N = 2$

Figures 1.5 and 1.6 show that the WSMSE-SR is a compromise between the WSMSE and the WSMSE with DA, since it has the advantage of requiring less information to exchange, it reaches better local optimum than the WSMSE but still does not reach the global optimum as the WSMSE-DA does. We would like to recall that this approach is only applicable when the number of Tx antennas is not less than the sum of the receive antennas of all users, as highlighted in Figures 1.5 and 1.6.

To summarize,

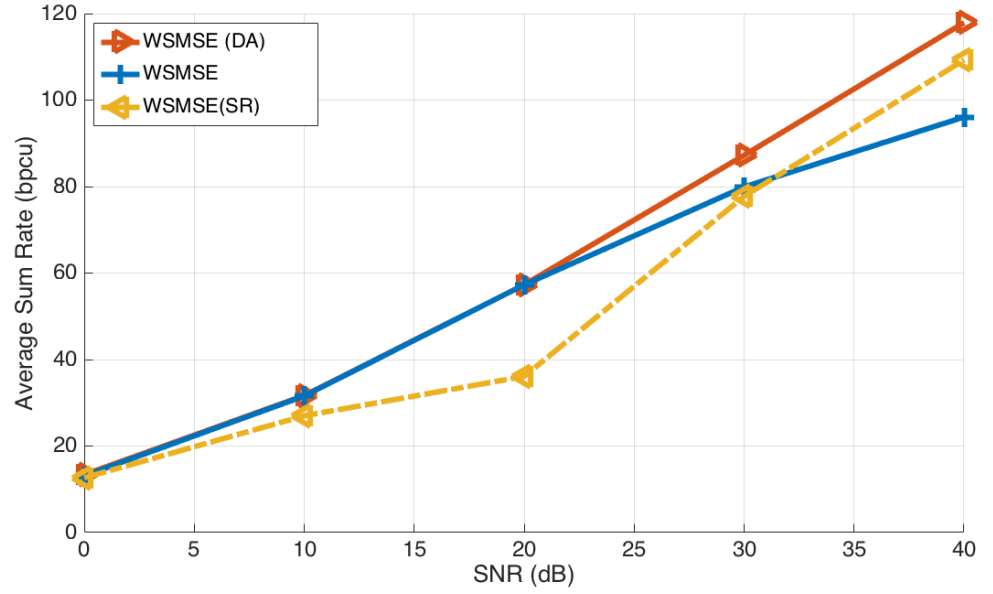


FIGURE 1.6: WSR vs SNR for $C = 3$, $K = 2$, $M = 10$, $N = 2$

- the WSMSE with DA is an extension of the WSMSE, which consists in applying the DA approach on the WSMSE precoder. It reaches the global optimum, instead of local optimum in the case of WSMSE.
- the WSMSE-SR is a variant of the WSMSE, which consists in replacing the MMSE Rx by an MF Rx. It reaches better optima compared to the WSMSE with the advantage of having simpler Rx, which implies less information exchange. However, this method is applicable only for very large numbers of transmit antennas.
- the WSMSE-SR approach is useful in the case of large system analysis for MIMO single stream scenarios, as we will show later on in Chapter 2.

1.6 Channel estimation

In a MIMO system, the CSI can be acquired in FDD mode as depicted in Figure 1.7, i.e. each user estimates the channels based on a DL training and then feeds back the channel estimates to the BS through the reverse link. This is not spectrally efficient in Massive MIMO since in that case, the BS is equipped with a very large number of antennas; hence the channel estimation, which uses downlink resources proportional to the number of antennas of the

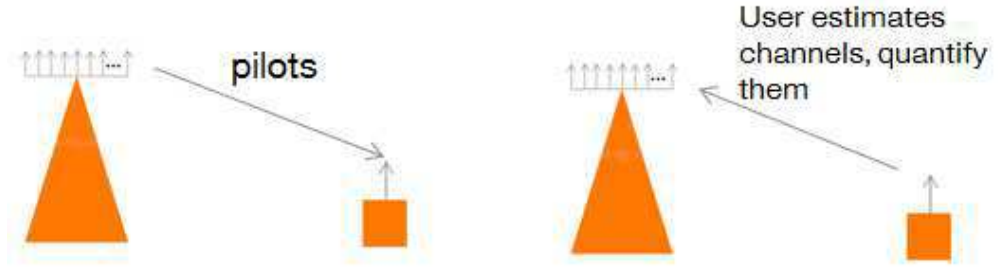


FIGURE 1.7: Channel estimation in FDD

BS in FDD, becomes challenging and the feedback consumption in UL becomes also challenging.

However, in TDD the BS can estimate CSI directly from the uplink training due to channel reciprocity. Then, in the DL, the BS uses the channel estimates to precode the transmit signals. As a consequence, TDD is considered for Massive MIMO studies and deployment. Moreover, the estimation process in TDD can generate some errors, i.e. the estimate and the real channel are not exactly the same. In that case we say that we have partial CSIT. Beamformers for that case will be studied later on in this work. So, we assume that the real channels \mathbf{H} , the estimate $\bar{\mathbf{H}}$ and the error $\tilde{\mathbf{H}}$ are related as follows:

$$\mathbf{H} = \bar{\mathbf{H}} + \tilde{\mathbf{H}} \quad (1.21)$$

We also assume Kronecker model for the channels, hence (1.21) can be written as:

$$\mathbf{H} = \bar{\mathbf{H}} + \mathbf{C}_r^{1/2} \tilde{\mathbf{H}}^{(2)} \boldsymbol{\Theta}_p^{1/2} = \mathbf{C}_r^{1/2} \tilde{\mathbf{H}}^{(1)} \boldsymbol{\Theta}_t^{1/2} + \mathbf{C}_r^{1/2} \tilde{\mathbf{H}}^{(2)} \boldsymbol{\Theta}_p^{1/2} \quad (1.22)$$

$\tilde{\mathbf{H}}^{(1)}$ and $\tilde{\mathbf{H}}^{(2)}$ have i.i.d. complex entries of zero mean and variance $\frac{1}{MN}$. The channel estimate covariance matrix at the Tx $\boldsymbol{\Theta}_t$ and the error covariance matrix $\boldsymbol{\Theta}_p$ are non-negative Hermitian and of uniformly bounded spectral norm w.r.t. to the number of transmit antennas M . The channel covariance matrix at the Rx \mathbf{C}_r is non-negative hermitian. It is considered as an identity matrix in this chapter and in this thesis in general.

Each Tx knows $\bar{\mathbf{H}}$ and $\boldsymbol{\Theta}_p$ only. In order to design precoders for the partial CSIT case, we must, from now on, solve the Expected WSR (EWSR) problem instead of the WSR maximization problem in (1.6). The objective function is $EWSR(\mathbf{Q})$.

The constraint is however the same as in (1.6). We recall it:

$$s.t. \text{tr} \mathbf{Q}_c \leq P_c \text{ for } c \in \mathcal{C} \quad (1.23)$$

where

$$EWSR(\mathbf{Q}) = E_{\mathbf{H}} WSR = E_{\mathbf{H}} \sum_c \sum_k u_{c,k} \log \det(\mathbf{I}_M + \mathbf{H}_{c,c,k}^H \mathbf{R}_{c,k}^{-1} \mathbf{H}_{c,c,k} \mathbf{Q}_{c,k}) \quad (1.24)$$

We explore many approaches to solve this problem in Chapter 4.

1.7 Conclusion

In this chapter, we have introduced the main problem of interest which is to design precoders that maximize the weighted sum rate for MC scenarios under a power budget constraint per cell. The rate is very influenced by intercell interference. We propose to use CoBF, where all BSs exchange their knowledge of the channels to design jointly all the BFs in the network. The problem is formulated as the WSR maximization problem. If the ratio number of served users per cell to number of transmit antennas is small enough (around $\frac{1}{10}$), simple linear beamformers such as MF achieve very good performance. For general cases, two algorithms are known to be the best in terms of achievable sum rates, WSMSE and KG. WSMSE solves the sum rate maximization problem by reformulating it as a minimization of a function of the MSE. A solution is given by an iterative algorithm where at each iteration we alternate between the calculation of \mathbf{F} , \mathbf{W} and \mathbf{G} which represent respectively the filter at Rx side, a weight and the beamformer. KG proposes to decompose the sum rate objective function into two functions, one corresponding to the rate of the user (c, k) of interest and the second one corresponding to the the sum rate of the rest of the users. These two functions are concave in $\mathbf{Q}_{c,k}$ (transmit covariance) and non concave in $\mathbf{Q}_{c,k}$ respectively. It is proposed to linearize the non concave part, so that we get a new objective function which is the difference of a concave function and a linear function (concave and convex at the sum time). The solution of the new problem is given by the eigenmatrix of two matrices. It is a normalized solution so power must be adjusted. It is proposed to be done using waterfilling. WSMSE and KG both converge to local optima. To force them to converge to global optima, we propose a DA

approach. Moreover, we propose the WSMSE-SR beamformer which is variant of the WSMSE algorithm by replacing the MMSE expression of \mathbf{F} by a MF expression. The proposed beamformer has lower complexity than WSMSE.

Part I

Random Matrix Theory for large system analysis and Massive MIMO design

Chapter 2

The WSMSE algorithm: A Large System Analysis

2.1 Introduction

We consider the Multiple-input Single-Output (MISO) MC MU scenario, which is a special case of the general system model detailed in Chapter 1. In this case, the Rxs are equipped with a single receive antenna: $N = 1$.

In this Chapter, we are interested in studying the performance of linear precoders, extended from the originally proposed MC MU MIMO (or IBC MIMO) to MC MU massive MISO scenarios. We carry out a large system analysis of the performance of the WSMSE precoding algorithm applied to the MISO MC MU case, for large number of transmit antennas and large number of users served per BS.

Herein, we extend the work in [27], which presents the deterministic equivalent expressions of the SINR of the WSMSE iterative algorithm for MU (or broadcast channels (BC)). We also inspire from the works in [28] and [29], which present Massive MISO deterministic equivalents of the SINR, corresponding to the sub-optimal zero-forcing (ZF) and regularized zero-forcing (RZF) precoders. Although our study could be considered an extension of the work in [28], [29] and [27], this extension is not straightforward and needs careful attention as concerning the impact of inter-cell interference.

Other works on large systems exist, e.g. [30], [31], [32], [33] and [34]. A multi cell RZF denoted interference-aware RZF (iaRZF) is presented in [31]. This

latter maximizes the sum rate as our precoder does, but it is not good for all existing scenarios, e.g. the scenario where many users are located on the cell edges, in fact, corresponds to a good BF only in the case of identical intra-cell channel attenuation and identical inter-cell channel attenuation.

Algorithms that minimize the total transmit power for large systems are presented in [32], [33] and [34]. However, they are different from the WSMSE approach, which maximizes the total sum rate instead of minimizing the total power. Furthermore, the deterministic limit of the SINR corresponding to the iterative IBC WSMSE process is presented, which makes it possible to evaluate its performance more easily and compare to other algorithms and precoders.

2.2 System model: The MISO IBC case

We reconsider the section 1.4 and adapt it to MISO scenario. The advantage of using MISO over MIMO is the possibility to perform large system analysis on the SINR expression for the MISO case. We assume transmission on a single narrow-band carrier, the received signal $y_{c,k}$ at the k th user in cell c reads

$$y_{c,k} = \sum_{m=1}^C \sum_{l=1}^K \mathbf{h}_{m,c,k}^H \mathbf{g}_{m,l} s_{m,l} + n_{c,k} \quad (2.1)$$

where $s_{m,l} \sim \mathcal{NC}(0, 1)$; $\mathbf{g}_{m,l} \in \mathbb{C}^M$ is the precoding vector of user l of cell m , $\mathbf{h}_{m,c,k}^H \in \mathbb{C}^{1 \times M}$ is the channel vector from the m th transmitter to the k th user of cell c , and the $n_{c,k}$ is the noise. Moreover, the channel $\mathbf{h}_{i,c,k}^H$ is correlated as $\mathbb{E}[\mathbf{h}_{i,c,k} \mathbf{h}_{i,c,k}^H] = \mathbf{\Theta}_{i,c,k}$ thus

$$\mathbf{h}_{i,c,k} = \sqrt{M} \mathbf{\Theta}_{i,c,k}^{1/2} \mathbf{z}_{i,c,k} \quad (2.2)$$

where $\mathbf{z}_{i,c,k}$ has i.i.d. complex entries of zero mean and variance $\frac{1}{M}$ and the $\mathbf{\Theta}_{i,c,k}^{1/2}$ is the Hermitian square-root of $\mathbf{\Theta}_{i,c,k}$. The correlation matrix $\mathbf{\Theta}_{i,c,k}$ is non-negative Hermitian and of uniformly bounded spectral norm w.r.t. to M . For notational convenience, we denote $\mathbf{\Theta}_{c,c,k}$ as $\mathbf{\Theta}_{c,k}$.

Under the assumption of optimal single-user decoding and perfect CSIT and CSIR, the achievable rate of the k th user of cell c is given by

$$r_{c,k} = \log(1 + \gamma_{c,k}) \quad (2.3)$$

$$\gamma_{c,k} = \frac{|\mathbf{h}_{c,c,k}^H \mathbf{g}_{c,k}|^2}{\sum_{(m,l) \neq (c,k)} \mathbf{h}_{m,c,k}^H \mathbf{g}_{m,l} \mathbf{g}_{m,l}^H \mathbf{h}_{m,c,k} + \sigma^2} \quad (2.4)$$

where $\gamma_{c,k}$ is the SINR of the k th of cell c .

As previously, the precoders maximize the WSR of all users so we are facing an optimization problem which is the following

$$\begin{aligned} \mathbf{G} = \arg \max_{\mathbf{G}} & \sum_{c=1}^C \sum_{k=1}^K u_{c,k} r_{c,k} \\ \text{s.t. } & \text{tr} \mathbf{G}_c \mathbf{G}_c^H \leq P_c \text{ for } c \in \mathcal{C} \end{aligned} \quad (2.5)$$

where \mathbf{G} is the short notation for $\{\mathbf{G}_c\}_{c \in \mathcal{C}}$, $\mathbf{G}_c = [\mathbf{g}_{c,1}, \mathbf{g}_{c,2}, \dots, \mathbf{g}_{c,K}] \in \mathbb{C}^{M \times K}$ and where $u_{c,k} \geq 0$ is the weight of the k^{th} user of cell c . Using the WSMSE algorithm from section 1.4.1, the precoders are obtained as follows

$$a_{c,k} = \mathbf{g}_{c,k}^H \mathbf{h}_{c,c,k} (\sigma^2 + \sum_{m=1}^C \sum_{l=1}^K \mathbf{h}_{m,c,k}^H \mathbf{g}_{m,l} \mathbf{g}_{m,l}^H \mathbf{h}_{m,c,k})^{-1} \quad (2.6)$$

$$e_{c,k} = (1 + \gamma_{c,k})^{-1} \quad (2.7)$$

$$w_{c,k} = u_{c,k} (e_{c,k})^{-1} \quad (2.8)$$

$$\tilde{\mathbf{g}}_{c,k} = (\mathbf{H}_c^H \mathbf{D} \mathbf{H}_c + \frac{\text{tr} \mathbf{D}_c}{\rho_c} \mathbf{I}_M)^{-1} \mathbf{h}_{c,c,k} a_{c,k}^H w_{c,k} \quad (2.9)$$

where $\mathbf{g}_{c,k} = \xi_c \tilde{\mathbf{g}}_{c,k}$ with $\xi_c = \sqrt{\frac{P_c}{\text{tr} \tilde{\mathbf{G}}_c \tilde{\mathbf{G}}_c^H}}$.

We recall $\mathbf{W}_c = \text{diag}(w_{c,1}, \dots, w_{c,K})$, $\mathbf{A}_c = \text{diag}(a_{c,1}, \dots, a_{c,K})$, $\mathbf{D}_c = \mathbf{A}_c^H \mathbf{W}_c \mathbf{A}_c$ and $\mathbf{A} = \text{diag}(\mathbf{A}_1, \mathbf{A}_2, \dots, \mathbf{A}_C)$, $\mathbf{D} = \text{diag}(\mathbf{D}_1, \mathbf{D}_2, \dots, \mathbf{D}_C)$,

$\mathbf{H}_c = [\mathbf{h}_{c,1,1}, \dots, \mathbf{h}_{c,1,K}, \mathbf{h}_{c,2,1}, \dots, \mathbf{h}_{c,2,K}, \dots, \mathbf{h}_{c,C,K}]^H \in \mathbb{C}^{KC \times M}$ is the compound channel. Subsequently $a_{c,k}$ and $w_{c,k}$ are computed, which then constitute the new precoder $\mathbf{g}_{c,k}$. This process is repeated until convergence to a local optimum. *UL/DL duality*: the Tx filter $\mathbf{g}_{c,k}$ is of the form of a MMSE linear Rx for the dual UL in which $\frac{\text{tr} \mathbf{D}_c}{\rho_c}$ plays the role of Rx noise variance and $u_{c,k} w_{c,k}$ plays the role of stream variance.

2.3 Large system analysis

In this section, performance analysis is conducted for the precoder of the previous section. The large-system limit is considered, where the number of transmit antennas M and the numbers of users served per BS K go to infinity while keeping the ratio K/M finite such that $\limsup_M K/M < \infty$ and $\liminf_M K/M > 0$.

The results should be understood in the way that, for each set of system dimension parameters M and K we provide an approximate expression for the SINR and the achieved sum rate, and the expression is tight as M and K grow large.

Before we continue with our performance analysis of the above precoder, a deterministic equivalent of the SINR of the MF precoder is required.

All vectors and matrices should be understood as sequences of vectors and matrices of growing dimensions.

2.3.1 Deterministic Equivalent of the SINR for the MF

Our precoder must be initialized so we have chosen the MF precoder to do the job.

Theorem 2.1: Let $\gamma_{c,k}^{MF}$ be the SINR of user k under MF precoding, i.e., $\mathbf{G}_c = \frac{\xi_c}{M} \mathbf{H}_c^H$ then, $\gamma_{c,k}^{MF} - \bar{\gamma}_{c,k}^{MF} \xrightarrow{M \rightarrow \infty} 0$, almost surely, where $\mathbf{H}_c = [\mathbf{h}_{c,c,1}, \dots, \mathbf{h}_{c,c,K}]^H$ and

$$\bar{\gamma}_{c,k}^{MF} = \frac{1}{\frac{1}{\beta_c \rho_c} + \frac{1}{M^2} \sum_{(l,i) \neq (c,k)} \text{tr} \mathbf{\Theta}_{l,c,k} \mathbf{\Theta}_{l,i}} \quad (2.10)$$

Proof: The normalization parameter is $\xi_c = \sqrt{\frac{P_c}{\frac{1}{M^2} \text{tr} \mathbf{H}_c^H \mathbf{H}_c}}$, where and thus we have

$$\bar{\xi}_c = \sqrt{\frac{P_c}{\frac{1}{M^2} \sum_{k=1}^K \text{tr} \mathbf{\Theta}_{c,k}}} = \sqrt{\beta_c P_c} \quad (2.11)$$

Denote $P_{c,k} = \|\mathbf{g}_{c,k}^H \mathbf{h}_{c,c,k}\|^2$ the signal power of the k^{th} user of cell c . Applying [[35], Lemma 2.7] we have $\frac{1}{M} \mathbf{h}_{c,c,k}^H \mathbf{h}_{c,c,k} - 1 \xrightarrow{M \rightarrow \infty} 0$ and hence

$$\bar{P}_{c,k} = \bar{\xi}_c^2 = \beta_c P_c \quad (2.12)$$

The interference is:

$$\frac{\xi_c^2}{M} \sum_{m=1, m \neq c}^C \mathbf{z}_{m,c,k}^H \boldsymbol{\Theta}_{m,c,k}^{1/2} \mathbf{H}_{\hat{m}}^H \mathbf{H}_{\hat{m}} \boldsymbol{\Theta}_{m,c,k}^{1/2} \mathbf{z}_{m,c,k} + \frac{\xi_c^2}{M} \mathbf{z}_{c,c,k}^H \boldsymbol{\Theta}_{c,c,k}^{1/2} \mathbf{H}_{\hat{c},[k]}^H \mathbf{H}_{\hat{c},[k]} \boldsymbol{\Theta}_{c,c,k}^{1/2} z_{c,c,k},$$

where $\mathbf{H}_{\hat{m},[k]} = [\mathbf{h}_{m,m,1}, \dots, \mathbf{h}_{m,m,k-1}, \mathbf{h}_{m,m,k+1}, \dots, \mathbf{h}_{m,m,K}]^H$.

Now we apply again [[35], Lemma 2.7] since $\frac{1}{M} \boldsymbol{\Theta}_{m,c,k}^{1/2} \mathbf{H}_{\hat{m}}^H \mathbf{H}_{\hat{m}} \boldsymbol{\Theta}_{m,c,k}^{1/2}$ and $\frac{1}{M} \boldsymbol{\Theta}_{c,c,k}^{1/2} \mathbf{H}_{\hat{c},[k]}^H \mathbf{H}_{\hat{c},[k]} \boldsymbol{\Theta}_{c,c,k}^{1/2}$ have uniformly bounded spectral norm w.r.t M almost surely, and obtain

$$\begin{aligned} & \left[\frac{1}{M} \sum_{m=1, m \neq c}^C \mathbf{z}_{m,c,k}^H \boldsymbol{\Theta}_{m,c,k}^{1/2} \mathbf{H}_{\hat{m}}^H \mathbf{H}_{\hat{m}} \boldsymbol{\Theta}_{m,c,k}^{1/2} \mathbf{z}_{m,c,k} \right. \\ & \quad \left. + \frac{1}{M} \mathbf{z}_{c,c,k}^H \boldsymbol{\Theta}_{c,c,k}^{1/2} \mathbf{H}_{\hat{c},[k]}^H \mathbf{H}_{\hat{c},[k]} \boldsymbol{\Theta}_{c,c,k}^{1/2} \mathbf{z}_{c,c,k} \right] \\ & - \left[\frac{1}{M^2} \sum_{m \neq c} \sum_{i=1}^K \text{tr} \boldsymbol{\Theta}_{m,c,k} \boldsymbol{\Theta}_{m,i} + \frac{1}{M^2} \sum_{i \neq k} \text{tr} \boldsymbol{\Theta}_{c,k} \boldsymbol{\Theta}_{c,i} \right] \rightarrow 0 \end{aligned} \quad (2.13)$$

almost surely. Substituting the terms in (2.4) by their respective deterministic equivalents yields (2.10), which completes the proof.

2.3.2 Deterministic equivalent of the SINR of proposed precoder for correlated channels

For the precoder (2.9), a deterministic equivalent of the SINR is provided in the following theorem

Theorem 2.2: Let $\gamma_{c,k}$ be the SINR of the k th user of cell c with the precoder defined in (2.9). Then, a deterministic equivalent $\bar{\gamma}_{c,k}^{(j)}$ at iteration $j > 0$ and under MF initialization is given by

$$\bar{\gamma}_{c,k}^{(j)} = \frac{\bar{w}_{c,k}^{(j)} (\bar{m}_{c,k}^{(j)})^2}{\bar{\Upsilon}_{c,k}^{(j)} + \bar{\Upsilon}_{c,k}^{(j)} + \bar{d}_{c,k}^{(j)} \frac{\bar{\Psi}_c^{(j)}}{\rho_c} (1 + \bar{m}_{c,k}^{(j)})^2} \quad (2.14)$$

where

$$\bar{m}_{c,k}^{(j)} = \frac{1}{M} \text{tr} \bar{\Theta}_{c,k}^{(j)} \mathbf{V}_c \quad (2.15)$$

$$\bar{\Psi}_c^{(j)} = \frac{1}{M} \sum_{i=1}^K \frac{\bar{w}_{c,i}^{(j)} e'_{c,i}}{(1 + e_{c,i})^2} \quad (2.16)$$

$$\bar{\Upsilon}_{c,k}^{(j)} = \frac{1}{M} \sum_{l=1, l \neq k}^K \frac{\bar{w}_{c,l}^{(j)}}{(1 + \bar{m}_{c,l}^{(j)})^2} e'_{c,c,k,c,l} \quad (2.17)$$

$$\hat{\Upsilon}_{c,k}^{(j)} = \frac{1}{M} \sum_{m=1, m \neq c}^C \frac{(1 + \bar{m}_{c,k}^{(j)})^2}{(1 + \bar{m}_{m,c,k}^{(j)})^2} \sum_{l=1}^K \frac{\bar{w}_{m,l}^{(j)}}{(1 + \bar{m}_{m,l}^{(j)})^2} e'_{m,c,k,m,l} \quad (2.18)$$

with $\bar{\Theta}_{m,c,k} = d_{c,k} \Theta_{m,c,k}$, $\bar{m}_{m,c,k}^{(j)} = \frac{1}{M} \text{tr} \bar{\Theta}_{m,c,k}^{(j)} \mathbf{V}_m$ and $\bar{a}_{c,k}^{(j)}$, $\bar{w}_{c,k}^{(j)}$ and $\bar{d}_{c,k}^{(j)}$ are given by

$$\bar{a}_{c,k}^{(j)} = \frac{1}{\sqrt{\bar{P}_{c,k}^{(j-1)}}} \frac{\bar{\gamma}_{c,k}^{(j-1)}}{1 + \bar{\gamma}_{c,k}^{(j-1)}} \quad (2.19)$$

$$\sqrt{\bar{P}_{c,k}^{(j-1)}} = \frac{1}{\bar{a}_{c,k}^{(j-1)}} \sqrt{\frac{P}{\bar{\Psi}_c^{(j-1)}}} \frac{\bar{m}_{c,k}^{(j-1)}}{1 + \bar{m}_{c,k}^{(j-1)}} \quad (2.20)$$

$$\bar{w}_{c,k}^{(j)} = (1 + \bar{\gamma}_{c,k}^{(j-1)}) \quad (2.21)$$

$$\bar{d}_{c,k}^{(j)} = \bar{w}_{c,k}^{(j)} \bar{a}_{c,k}^{2(j)}. \quad (2.22)$$

Denoting

$$\mathbf{V}_c = (\mathbf{F}_c + \bar{\alpha}_c \mathbf{I}_M)^{-1} \quad (2.23)$$

with $\bar{\alpha}_c^{(j)} = \frac{\text{tr} \bar{\mathbf{D}}_c^{(j)}}{M \rho_c}$, three systems of coupled equations have to be solved. First, we need to introduce $e_{m,c,k} \forall \{m, c, k\} \in \{\mathcal{C}, \mathcal{C}, \mathcal{K}_c\}$, where \mathcal{K}_c is the set of all users of cell c , which form the unique positive solutions of

$$e_{m,c,k} = \frac{1}{M} \text{tr} \bar{\Theta}_{m,c,k} \mathbf{V}_m, \quad (2.24)$$

$$\mathbf{F}_m = \frac{1}{M} \sum_{j=1}^C \sum_{i=1}^K \frac{\bar{\Theta}_{m,j,i}}{1 + e_{m,j,i}}. \quad (2.25)$$

$e_{c,c,k}$ and $m_{c,c,k}$ denote $e_{c,k}$ and $m_{c,k}$ respectively.

Secondly, we give $e'_{m,c,k} \forall \{m, c, k\} \in \{\mathcal{C}, \mathcal{C}, \mathcal{K}_c\}$ which form the unique positive

solutions of

$$e'_{m,c,k} = \frac{1}{M} \text{tr} \bar{\Theta}_{m,c,k} \mathbf{V}_m (\mathbf{F}'_m + \mathbf{I}_M) \mathbf{V}_m, \quad (2.26)$$

$$\mathbf{F}'_m = \frac{1}{M} \sum_{j=1}^C \sum_{i=1}^K \frac{\bar{\Theta}_{m,j,i} e'_{m,j,i}}{(1 + e_{m,j,i})^2}. \quad (2.27)$$

And finally, we provide $e'_{m,c,k,m,l} \forall \{m, c, k, l\} \in \{\mathcal{C}, \mathcal{C}, \mathcal{K}_c, \mathcal{K}_c\}$ which form the unique positive solutions of

$$e'_{m,c,k,m,l} = \frac{1}{M} \text{tr} \bar{\Theta}_{m,c,k} \mathbf{V}_m (\mathbf{F}'_{m,m,l} + \bar{\Theta}_{m,l}) \mathbf{V}_m \quad (2.28)$$

$$\mathbf{F}'_{m,m,l} = \frac{1}{M} \sum_{j=1}^C \sum_{i=1}^K \frac{\bar{\Theta}_{m,j,i} e'_{m,j,i,m,l}}{(1 + e_{m,j,i})^2}. \quad (2.29)$$

For $j = 0$, $\bar{\gamma}_{c,k}^{(0)} = \bar{\gamma}_{c,k}^{MF}$, given by Theorem 2.1 and $\bar{P}_{c,k}^{(0)} = \beta_c P_c$, cf. (2.12).

Proof: For $j \geq 1$, define $\mathbf{\Gamma}_c^{(j)} = \frac{1}{M} \mathbf{H}_c^H \bar{\mathbf{D}}^{(j)} \mathbf{H}_c + \bar{\alpha}_c^{(j)} \mathbf{I}_M$, the precoder at the end of iteration j is given by

$$\bar{\mathbf{g}}_{c,k}^{(j)} = \frac{\xi_c^{(j)}}{M} (\mathbf{\Gamma}_c^{(j)})^{-1} \mathbf{h}_{c,c,k} \bar{a}_{c,k}^{H,(j)} \bar{w}_{c,k}^{(j)} \quad (2.30)$$

for each user k in the cell c ,

where $\xi_c^{(j)}$ is

$$\xi_c^{(j)} = \sqrt{\frac{P_c}{\frac{1}{M^2} \text{tr}(\mathbf{\Gamma}_c^{(j)})^{-2} \mathbf{H}_{\hat{c}}^H \bar{\mathbf{A}}_c^{H,(j)} \bar{\mathbf{W}}_c^{2,(j)} \bar{\mathbf{A}}_c^{(j)} \mathbf{H}_{\hat{c}}}} = \sqrt{\frac{P_c}{\Psi_c^{(j)}}}. \quad (2.31)$$

We derive the deterministic equivalents of the normalization term $\xi_c^{(j)}$, the signal power $|\bar{\mathbf{g}}_{c,k}^{H,(j)} \mathbf{h}_{c,c,k}|^2$ and the interference power

$\sum_{m=1}^C \sum_{l \neq k \text{ if } m=c}^K \mathbf{h}_{m,c,k}^H \bar{\mathbf{g}}_{m,l}^{(j)} \bar{\mathbf{g}}_{m,l}^{H,(j)} \mathbf{h}_{m,c,k}$. We will show that in the following.

a) *Power normalization:* The term $\Psi_c^{(j)}$ can be written as

$$\begin{aligned} \Psi_c^{(j)} &= \frac{1}{M^2} \sum_{k=1}^K \bar{w}_{c,k}^{(j)} \bar{d}_{c,k}^{(j)} \mathbf{z}_{c,c,k}^H \boldsymbol{\Theta}_{c,k}^{(1/2)} (\mathbf{\Gamma}_c^{(j)})^{-2} \boldsymbol{\Theta}_{c,k}^{(1/2)} \mathbf{z}_{c,c,k} \\ &= \frac{1}{M^2} \sum_{k=1}^K \bar{w}_{c,k}^{(j)} \mathbf{z}_{c,c,k}^H \bar{\boldsymbol{\Theta}}_{c,k}^{(1/2)} (\mathbf{\Gamma}_c^{(j)})^{-2} \bar{\boldsymbol{\Theta}}_{c,k}^{(1/2)} \mathbf{z}_{c,c,k}. \end{aligned} \quad (2.32)$$

Similarly to [28], [29] and [27] a deterministic equivalent $\bar{\Psi}_c$ such that $\Psi_c - \bar{\Psi}_c \xrightarrow{M \rightarrow \infty} 0$, almost surely, is given by

$$\begin{aligned}\bar{\Psi}_c^{(j)} &= \frac{1}{M} \sum_{k=1}^K \bar{w}_{c,k}^{(j)} \frac{\frac{1}{M} \text{tr} \bar{\Theta}_{c,k}^{(j)} (\Gamma_c^{(j)})^{-2}}{(1 + \frac{1}{M} \text{tr} \bar{\Theta}_{c,k}^{(j)} (\Gamma_c^{(j)})^{-1})^2} \\ &= \frac{1}{M} \sum_{k=1}^K \bar{w}_{c,k}^{(j)} \frac{\bar{m}_{c,k}'^{(j)}}{(1 + \bar{m}_{c,k}^{(j)})^2} = \frac{1}{M} \sum_{k=1}^K \bar{w}_{c,k}^{(j)} \frac{e_{c,k}'}{(1 + e_{c,k})^2},\end{aligned}\quad (2.33)$$

where we denote $\bar{m}_{c,k}^{(j)} = \frac{1}{M} \text{tr} \bar{\Theta}_{c,k}^{(j)} (\Gamma_c^{(j)})^{-1}$ and $\bar{m}_{c,k}'^{(j)}$ the derivative w.r.t z at $z = -\bar{\alpha}_c^{(j)}$.

b) Signal power: The square-root of the signal power $P_{c,k}^{(j)} = |\bar{\mathbf{g}}_{c,k}^{H,(j)} \mathbf{h}_{c,c,k}|^2$ is

$$\begin{aligned}\sqrt{P_{c,k}^{(j)}} &= \xi_c^{(j)} \bar{a}_{c,k}^{(j)} \bar{w}_{c,k}^{(j)} \mathbf{z}_{c,c,k}^H \Theta_{c,k}^{\frac{1}{2}} (\Gamma_c^{(j)})^{-1} \Theta_{c,k}^{\frac{1}{2}} \mathbf{z}_{c,c,k} \\ &= \frac{\xi_c^{(j)}}{\bar{a}_{c,k}^{(j)}} \mathbf{z}_{c,c,k}^H \bar{\Theta}_{c,k}^{1/2} (\Gamma_c^{(j)})^{-1} \bar{\Theta}_{c,k}^{\frac{1}{2},(j)} \mathbf{z}_{c,c,k}.\end{aligned}\quad (2.34)$$

Again, following [27], [28] and [29] a deterministic equivalent $\sqrt{\bar{P}_{c,k}^{(j)}}$ of (2.34) is given by

$$\sqrt{\bar{P}_{c,k}^{(j)}} = \frac{\bar{\xi}_c^{(j)}}{\bar{a}_{c,k}^{(j)}} \frac{\bar{m}_{c,k}^{(j)}}{1 + \bar{m}_{c,k}^{(j)}}, \quad (2.35)$$

where $\bar{\xi}_c^{(j)} = \sqrt{\frac{P_c}{\bar{\Psi}_c^{(j)}}}$.

c) Interference power: The interference power received by user k of cell c can be written as

$$\begin{aligned}& \sum_{m=1}^C \sum_{l=1, l \neq k \text{ if } m=c}^K \mathbf{h}_{m,c,k}^H \bar{\mathbf{g}}_{m,l}^{H,(j)} \bar{\mathbf{g}}_{m,l}^{H,(j)} \mathbf{h}_{m,c,k} \\ &= \frac{\xi_c^{2,(j)}}{M^2} \sum_{m=1}^C \mathbf{h}_{m,c,k}^H (\Gamma_m^{(j)})^{-1} \sum_{l=1, l \neq k \text{ if } m=c}^K \bar{a}_{m,l}^{2,(j)} \bar{w}_{m,l}^{2,(j)} \mathbf{h}_{m,m,l} \mathbf{h}_{m,m,l}^H (\Gamma_m^{(j)})^{-1} \mathbf{h}_{m,c,k} \\ &= \frac{\xi_c^{2,(j)}}{\bar{d}_{c,k}^{(j)}} \sum_{m=1}^C \mathbf{z}_{m,c,k}^H \bar{\Theta}_{m,c,k}^{\frac{1}{2},(j)} (\Gamma_m^{(j)})^{-1} \\ & \quad \times \sum_{l \neq k \text{ if } m=c}^K \bar{w}_{m,l}^{(j)} \bar{\Theta}_{m,l}^{\frac{1}{2},(j)} \mathbf{z}_{m,m,l} \mathbf{z}_{m,m,l}^H \bar{\Theta}_{m,l}^{\frac{1}{2},(j)} (\Gamma_m^{(j)})^{-1} \bar{\Theta}_{m,c,k}^{\frac{1}{2},(j)} \mathbf{z}_{m,c,k}\end{aligned}\quad (2.36)$$

Which can be approximated as the following

$$\begin{aligned} & \sum_{m=1}^C \sum_{l=1, (l,m) \neq (k,c)}^K \mathbf{h}_{m,c,k}^H \bar{\mathbf{g}}_{m,l}^{H,(j)} \bar{\mathbf{g}}_{m,l}^{H,(j)} \mathbf{h}_{m,c,k} \\ & - \frac{\bar{\xi}_c^{2,(j)} [\bar{\mathbf{\Upsilon}}_{c,k}^{(j)} + \bar{\mathbf{\Upsilon}}_{c,k}^{(j)}]}{\bar{d}_{c,k}^{(j)} (1 + \bar{m}_{c,k}^{(j)})^2} \xrightarrow{M \rightarrow \infty} 0, \end{aligned} \quad (2.37)$$

almost surely, where $\bar{\mathbf{\Upsilon}}_{c,k}^{(j)}$ and $\bar{\mathbf{\Upsilon}}_{c,k}^{(j)}$ are given by the expressions (2.17) and (2.18) which represent the large system limits of the intra-cell and inter-cell interference respectively, the proof is given in Appendix B.

2.3.3 Numerical results

In this section, results of simulations based on realistic settings with a finite number of transmit antennas corroborate the correctness of the proposed approximation. We use the IBC WSMSE algorithm with MF initialization and compare it to the large system approximation in Theorem 2.2. The channel correlation matrix is modeled as [27]

$$[\boldsymbol{\Theta}_{m,c,k}]_{ij} = \frac{1}{\boldsymbol{\Theta}_{m,c,k,max} - \boldsymbol{\Theta}_{m,c,k,min}} \int_{\boldsymbol{\Theta}_{m,c,k,min}}^{\boldsymbol{\Theta}_{m,c,k,max}} e^{\mathbf{j} \frac{2\pi}{\lambda} \delta_{ij} \cos(\Theta)} d\Theta \quad (2.38)$$

where $\mathbf{j} = \sqrt{-1}$, λ denotes the signal wavelength and δ_{ij} is the distance between antenna i and j . We choose the range of azimuth angle $\boldsymbol{\Theta}_{m,c,k}$ of user k as $\boldsymbol{\Theta}_{m,c,k,min} = -\pi$ and $\boldsymbol{\Theta}_{m,c,k,max} = \phi_{m,c,k} - \pi$, where $\phi_{m,c,k} = 2\pi \frac{c*k}{KC}$. The transmitter is endowed with a uniform linear array (ULA) of antennas. We assume that δ_{ij} is independent of M so that the spectral norm of $\boldsymbol{\Theta}_{m,c,k}$ remains bounded as M grows large, let $\delta_{ij} = \frac{\lambda}{2}|j - i|$.

Figures 2.1 and 2.2 show the WSMSE precoder and its approximation for correlated channels ($\boldsymbol{\Theta}_{m,c,k} \neq \mathbf{I}_M$) and i.i.d. channels ($\boldsymbol{\Theta}_{m,c,k} = \mathbf{I}_M$) for $C = 2$ and $C = 3$ respectively. For the simulations of the IBC WSMSE algorithm, we used 200 channel realizations. It can be observed that for i.i.d channels the approximation is accurate for low SNR, but less precise at high SNR.

As the Figures 2.1 and 2.2 suggest, this effect is diminished when the channel

is correlated resulting in an increased accuracy of the approximation for high SNR. Or for i.i.d channels the inaccuracy effect at high SNR diminishes when the system load ($\frac{C*K}{M}$) decreases as shown in the figure 2.3 for load = 0.9. The reason of imprecision for full load $\frac{C*K}{M} = 1$ is that the regularization term in (2.23) is going to be imprecise at high SNR.

Moreover, we observed that the sum rate of our system stays unmodified for the same total number of users (Fig. 2.1 and Fig. 2.2) while keeping in mind the fact that we have more total power budget as the number of transmitters increases.

Finally, we demonstrated that our asymptotic sum rate follows the simulated one, which validates our asymptotic approach. Although the sum rate expression for the approximation approach (2.14) seems to be complex, we need to calculate it only once per a given SNR, while we need to run the IBC WSMSE simulations as many times as the number of channel realizations, i.e. 200 times.

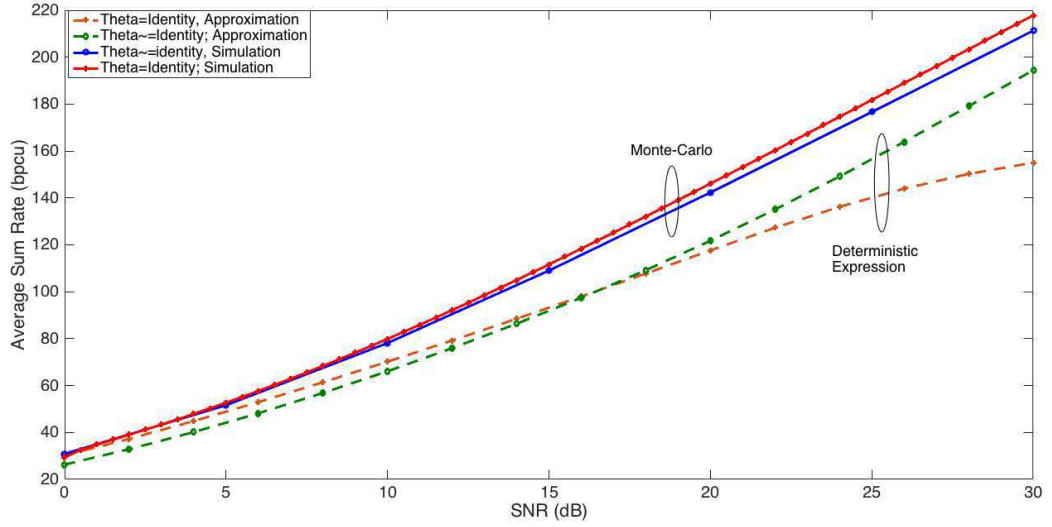


FIGURE 2.1: Sum rate comparisons between the IBC WSMSE and our proposed approximation for $C=2, K=15, M=30$.

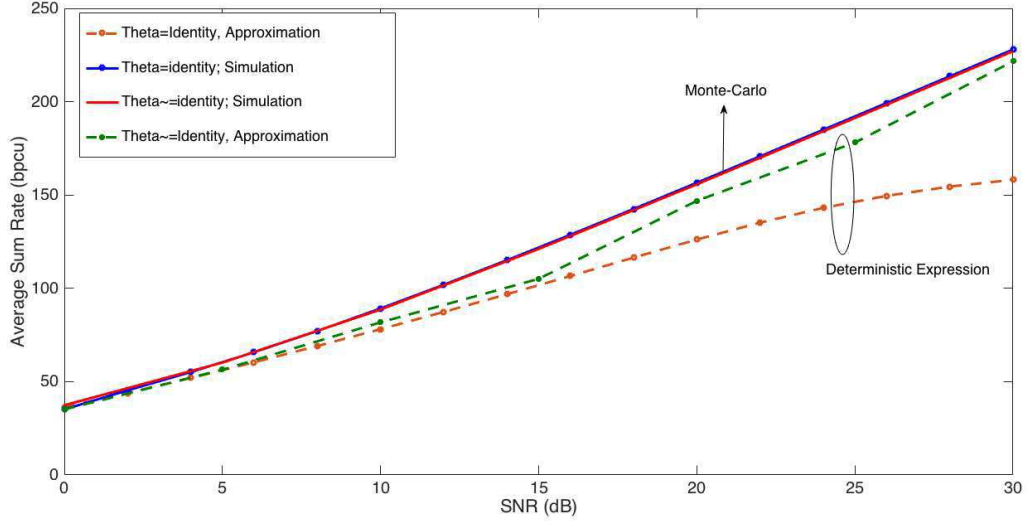


FIGURE 2.2: Sum rate comparisons between the IBC WSMSE and our proposed approximation for $C=3, K=10, M=30$.

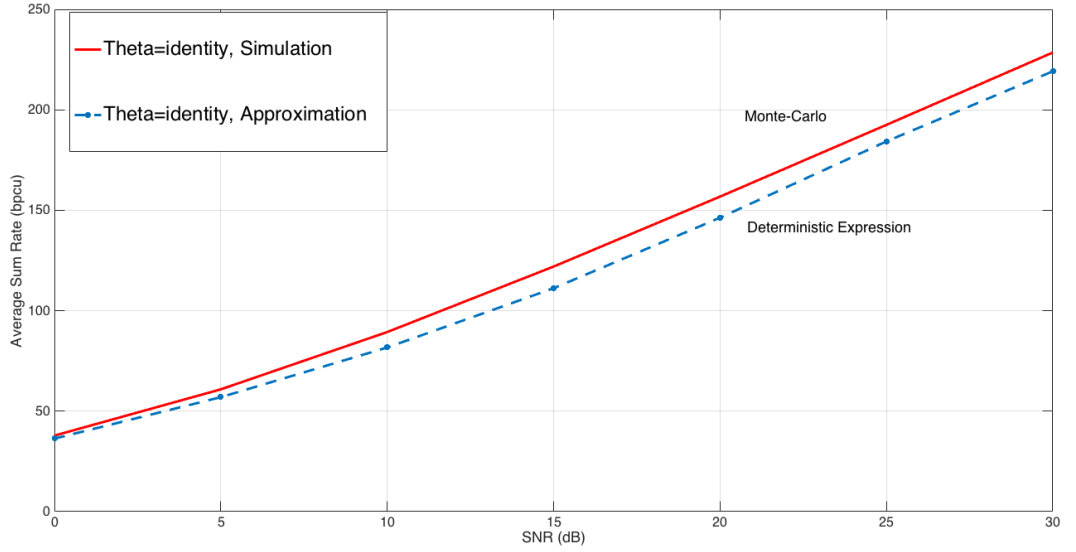


FIGURE 2.3: Sum rate comparisons between the IBC WSMSE and our proposed approximation for $C=3, K=9, M=30$.

2.4 The MIMO single stream case

In the section, we will switch to the MIMO single stream case and we will show that the SINR in that case is amenable as well to large system analysis. We provide a large system analysis of the performance of the WSMSE algorithm for MIMO IBC single stream scenario. The received signal $\mathbf{y}_{c,k}$ at the k th user

in cell c reads

$$\mathbf{y}_{c,k} = \sum_{m=1}^C \sum_{l=1}^K \mathbf{H}_{m,c,k} \mathbf{g}_{m,l} s_{m,l} + \mathbf{n}_{c,k} \quad (2.39)$$

where

$$\mathbf{H}_{i,c,k}^H = \sqrt{NM} \boldsymbol{\Theta}_{i,c,k}^{1/2} \mathbf{X}_{i,c,k} \boldsymbol{\Theta}_{r,i,c,k}^{1/2} \quad (2.40)$$

$\mathbf{X}_{i,c,k}^H$ is an $N \times M$ matrix with i.i.d. complex entries of zero mean and variance $\frac{1}{NM}$ and the $\boldsymbol{\Theta}_{i,c,k}^{1/2}$ and $\boldsymbol{\Theta}_{r,i,c,k}^{1/2}$ are the Hermitian square-root of $\boldsymbol{\Theta}_{i,c,k}$ and $\boldsymbol{\Theta}_{r,i,c,k}$ respectively. Treating interference as noise, user k of cell c will apply a linear receive filter $\mathbf{f}_{c,k}$ of dimensions $N \times 1$ to maximize the signal power (diversity) while reducing any residual interference that would not have been (sufficiently) suppressed by the precoder. The achievable rate of the k th user of cell c is given by

$$R_{c,k} = \log(1 + \gamma_{c,k}) \quad (2.41)$$

$$\gamma_{c,k} = \frac{|\mathbf{f}_{c,k}^H \mathbf{H}_{c,c,k} \mathbf{g}_{c,k}|^2}{\sum_{(m,l) \neq (c,k)} \mathbf{f}_{c,k}^H \mathbf{H}_{m,c,k} \mathbf{g}_{m,l} \mathbf{g}_{m,l}^H \mathbf{H}_{m,c,k} \mathbf{f}_{c,k} + \mathbf{f}_{c,k}^H \mathbf{f}_{c,k} \sigma^2} \quad (2.42)$$

where $\gamma_{c,k}$ is the SINR of the k th user of cell c .

The WSMSE solution for the MIMO single stream case is as follows:

$$\mathbf{f}_{c,k} = \mathbf{g}_{c,k}^H \mathbf{H}_{c,c,k}^H (\sigma^2 \mathbf{I}_N + \sum_{m=1}^C \sum_{l=1}^K \mathbf{H}_{m,c,k} \mathbf{g}_{m,l} \mathbf{g}_{m,l}^H \mathbf{H}_{m,c,k}^H)^{-1} \quad (2.43)$$

$$e_{c,k} = (1 + \gamma_{c,k})^{-1} \quad (2.44)$$

$$w_{c,k} = u_{c,k} (e_{c,k})^{-1} \quad (2.45)$$

$$\tilde{\mathbf{g}}_{c,k} = \left(\sum_{i,j} \mathbf{H}_{c,i,j}^H \mathbf{f}_{i,j} d_{i,j} \mathbf{f}_{i,j}^H \mathbf{H}_{c,i,j} + \frac{\text{tr} \mathbf{D}_c}{\rho_c} \mathbf{I}_M \right)^{-1} \mathbf{H}_{c,c,k}^H \mathbf{f}_{c,k} w_{c,k} \quad (2.46)$$

Where $\mathbf{W}_c = \text{diag}(w_{c,1}, \dots, w_{c,K})$, $\mathbf{F}_c = \text{blockdiag}(\mathbf{f}_{c,1}, \dots, \mathbf{f}_{c,K})$, $\mathbf{D}_c = \mathbf{F}_c \mathbf{W}_c \mathbf{F}_c^H$.

Performance analysis is conducted for the proposed precoder. A deterministic equivalent of the SINR is provided in the following theorem.

Theorem 2.3: Let $\gamma_{c,k}$ be the SINR of the k th user of cell c with the precoder defined in (2.46). Then, a deterministic equivalent $\bar{\gamma}_{c,k}^{(j)}$ at iteration $j > 0$ is given by

$$\bar{\gamma}_{c,k}^{(j)} = \frac{\bar{w}_{c,k}^{(j)} (\bar{m}_{c,k}^{(j)})^2}{\bar{\Upsilon}_{c,k}^{(j)} + \hat{\Upsilon}_{c,k}^{(j)} + \bar{d}_{c,k}^{(j)} \frac{\bar{\Psi}_c^{(j)}}{\rho_c} (1 + \bar{m}_{c,k}^{(j)})^2} \quad (2.47)$$

where

$$\bar{m}_{c,k}^{(j)} = \frac{1}{M} \text{tr} \bar{\Theta}_{c,k}^{(j)} \mathbf{V}_c \quad (2.48)$$

$$\bar{\Psi}_c^{(j)} = \frac{1}{NM} \sum_{i=1}^K \frac{\bar{w}_{c,i}^{(j)} e'_{c,i}}{(1 + e_{c,i})^2} \quad (2.49)$$

$$\bar{\Upsilon}_{c,k}^{(j)} = \frac{1}{M} \sum_{l=1, l \neq k}^K \frac{\bar{w}_{c,l}^{(j)}}{(1 + \bar{m}_{c,l}^{(j)})^2} e'_{c,c,k,l} \quad (2.50)$$

$$\hat{\Upsilon}_{c,k}^{(j)} = \frac{1}{M} \sum_{m=1, m \neq c}^C \frac{(1 + \bar{m}_{c,k}^{(j)})^2}{(1 + \bar{m}_{m,c,k}^{(j)})^2} \sum_{l=1}^K \frac{\bar{w}_{m,l}^{(j)}}{(1 + \bar{m}_{m,l}^{(j)})^2} e'_{m,c,k,m,l} \quad (2.51)$$

with $\bar{\Theta}_{m,c,k} = d_{c,k} \Theta_{m,c,k}$, $\bar{m}_{m,c,k}^{(j)} = \frac{1}{M} \text{tr} \bar{\Theta}_{m,c,k}^{(j)} \mathbf{V}_m$. Furthermore, we have

$$\bar{a}_{c,k}^{(j)} = \frac{1}{\sqrt{P_{c,k}^{(j-1)}}} \frac{\bar{\gamma}_{c,k}^{(j-1)}}{1 + \bar{\gamma}_{c,k}^{(j-1)}} \quad (2.52)$$

$$\sqrt{P_{c,k}^{(j-1)}} = \frac{1}{\bar{a}_{c,k}^{(j-1)}} \sqrt{\frac{P}{\bar{\Psi}_c^{(j-1)}}} \frac{\bar{m}_{c,k}^{(j-1)}}{1 + \bar{m}_{c,k}^{(j-1)}} \quad (2.53)$$

$$\bar{w}_{c,k}^{(j)} = (1 + \bar{\gamma}_{c,k}^{(j-1)}) \quad (2.54)$$

$$\bar{d}_{c,k}^{(j)} = \bar{w}_{c,k}^{(j)} \bar{a}_{c,k}^{2(j)} \quad (2.55)$$

where $\bar{a}_{c,k}$ denotes the module of the linear receive filter $\mathbf{f}_{c,k}$. Denoting

$$\mathbf{V}_c = (\mathbf{T}_c + \bar{\alpha}_c \mathbf{I}_M)^{-1} \quad (2.56)$$

with $\bar{\alpha}_c^{(j)} = \frac{\text{tr} \bar{\mathbf{D}}_c^{(j)}}{M \rho_c}$, three systems of coupled equations have to be solved. First, we need to introduce $e_{m,c,k} \forall \{m, c, k\} \in \{\mathcal{C}, \mathcal{C}, \mathcal{K}_c\}$, where \mathcal{K}_c is the set of all users of cell c , which form the unique positive solutions of

$$e_{m,c,k} = \frac{1}{M} \text{tr} \bar{\Theta}_{m,c,k} \mathbf{V}_m, \quad (2.57)$$

$$\mathbf{T}_m = \frac{1}{M} \sum_{j=1}^C \sum_{i=1}^K \frac{\bar{\Theta}_{m,j,i}}{1 + e_{m,j,i}}. \quad (2.58)$$

$e_{c,c,k}$ and $m_{c,c,k}$ denote $e_{c,k}$ and $m_{c,k}$ respectively.

Secondly, we give $e'_{1,1}, \dots, e'_{1,K}, \dots, e'_{C,1}, \dots, e'_{C,K}$ which form the unique positive

solutions of

$$e'_{c,k} = \frac{1}{M} \text{tr} \bar{\mathbf{\Theta}}_{c,k} \mathbf{V}_c (\mathbf{T}'_c + \mathbf{I}_M) \mathbf{V}_c, \quad (2.59)$$

$$\mathbf{T}'_c = \frac{1}{M} \sum_{j=1}^C \sum_{i=1}^K \frac{\bar{\mathbf{\Theta}}_{c,j,i} e'_{j,i}}{(1 + e_{c,j,i})^2}. \quad (2.60)$$

And finally, we provide $e'_{m,c,k,m,l} \forall \{m, c, k, l\} \in \{\mathcal{C}, \mathcal{C}, \mathcal{K}_c, \mathcal{K}_c\}$ which form the unique positive solutions of

$$e'_{m,c,k,m,l} = \frac{1}{M} \text{tr} \bar{\mathbf{\Theta}}_{m,c,k} \mathbf{V}_m (\mathbf{T}'_{m,m,l} + \bar{\mathbf{\Theta}}_{m,l}) \mathbf{V}_m \quad (2.61)$$

$$\mathbf{T}'_{m,m,l} = \frac{1}{M} \sum_{j=1}^C \sum_{i=1}^K \frac{\bar{\mathbf{\Theta}}_{m,j,i} e'_{m,j,i,m,l}}{(1 + e_{m,j,i})^2}. \quad (2.62)$$

For $j \geq 1$, define $\mathbf{\Gamma}_c^{(j)} = \frac{1}{NM} \mathbf{H}_c \bar{\mathbf{D}}^{(j)} \mathbf{H}_c^H + \bar{\alpha}_c^{(j)} \mathbf{I}_M$, with $\mathbf{D} = \text{diag}(\mathbf{D}_1, \mathbf{D}_2, \dots, \mathbf{D}_C)$ and $\mathbf{H}_c = [\mathbf{H}_{c,1,1}^H, \dots, \mathbf{H}_{c,1,K}^H, \mathbf{H}_{c,2,1}^H, \dots, \mathbf{H}_{c,2,K}^H, \dots, \mathbf{H}_{c,C,K}^H]$, the precoder at the end of iteration j is given by

$$\bar{\mathbf{g}}_{c,k}^{(j)} = \frac{\boldsymbol{\xi}_c^{(j)}}{M} (\mathbf{\Gamma}_c^{(j)})^{-1} \mathbf{H}_{c,c,k}^H \bar{a}_{c,k}^{(j)} \mathbf{f}_{0,k}^{(j)} \bar{w}_{c,k}^{(j)} \quad (2.63)$$

for each user k in the cell c ,

where $\mathbf{f}_{0,c,k}$ is the the normalized linear receive filter such that $\mathbf{f}_{c,k} = a_{c,k} \mathbf{f}_{0,c,k}$, and $\xi_c^{(j)}$ is given by

$$\xi_c^{(j)} = \sqrt{\frac{P_c}{\frac{1}{M^2} \text{tr}(\mathbf{\Gamma}_c^{(j)})^{-2} \mathbf{H}_{\hat{c}}^H \bar{\mathbf{F}}_c^{H,(j)} \bar{\mathbf{W}}_c^{2,(j)} \bar{\mathbf{F}}_c^{(j)} \mathbf{H}_{\hat{c}}^H}} = \sqrt{\frac{P_c}{\boldsymbol{\Psi}_c^{(j)}}}. \quad (2.64)$$

where $\mathbf{H}_{\hat{c}} = [\mathbf{H}_{c,c,1}^H, \dots, \mathbf{H}_{c,c,K}^H]$. We derive the deterministic equivalents of the normalization term $\xi_c^{(j)}$, the signal power $|\bar{\mathbf{g}}_{c,k}^{H,(j)} \mathbf{H}_{c,c,k}^H|^2$ and the interference power

$\sum_{m=1}^C \sum_{l \neq k}^K \mathbf{f}_{c,k}^H \mathbf{H}_{m,c,k} \bar{\mathbf{g}}_{m,l}^{(j)} \bar{\mathbf{g}}_{m,l}^{H,(j)} \mathbf{H}_{m,c,k}^H \mathbf{f}_{c,k}$ similarly to [27], [28] and [29] and , i.e., using the same logic and mathematical approach, but for a more complex problem. We will show that in the following.

Proof: We write $\mathbf{f}_{c,k}$ as $\mathbf{f}_{c,k} = a_{c,k} \mathbf{f}_{0,c,k}$ with $a_{c,k} = \sqrt{\mathbf{f}_{c,k}^H \mathbf{f}_{c,k}}$ and $|\mathbf{f}_{0,c,k}| = 1$.

Let $P_{c,k}^{(j)} = |\mathbf{f}_{0,c,k}^{H,(j)} \mathbf{H}_{c,c,k} \mathbf{g}_{c,k}^{(j)}|^2 = |\mathbf{H}_{c,c,k} \mathbf{g}_{c,k}^{(j)}|^2$. We have

$$\begin{aligned}
\mathbf{g}_{c,k}^{(j)} &= \frac{\xi_c^{(j)}}{NM} (\mathbf{\Gamma}_{c,[c,k]}^{(j)})^{-1} \mathbf{H}_{c,c,k}^H \mathbf{f}_{0,c,k}^{(j)} a_{c,k}^{(j)} w_{c,k}^{(j)} \\
&\quad - \frac{\xi_c^{(j)}}{NM} (\mathbf{\Gamma}_c^{(j)})^{-1} \frac{1}{NM} \mathbf{H}_{c,c,k}^H \mathbf{f}_{0,c,k}^{(j)} d_{c,k}^{(j)} \mathbf{f}_{0,c,k}^{H,(j)} \mathbf{H}_{c,c,k} (\mathbf{\Gamma}_{c,[c,k]}^{(j)})^{-1} \mathbf{H}_{c,c,k}^H \mathbf{f}_{0,c,k}^{(j)} a_{c,k}^{(j)} w_{c,k}^{(j)}; \\
&= \frac{\xi_c^{(j)}}{NM} (\mathbf{\Gamma}_{c,[c,k]}^{-1} \mathbf{H}_{c,c,k}^H \mathbf{f}_{0,c,k}^{(j)} a_{c,k}^{(j)} w_{c,k}^{(j)} - m_{c,k}^{(j)} \mathbf{g}_{c,k}^{(j)}); \\
&= \frac{\xi_c^{(j)}}{(1 + m_{c,k}^{(j)}) NM} (\mathbf{\Gamma}_{c,[c,k]}^{(j)})^{-1} \mathbf{H}_{c,c,k}^H \mathbf{f}_{0,c,k}^{(j)} a_{c,k}^{(j)} w_{c,k}^{(j)}. \tag{2.65}
\end{aligned}$$

Thus,

$$\begin{aligned}
\sqrt{P_{c,k}^{(j)}} &= \frac{\xi_c^{(j)} a_{c,k}^{(j)} w_{c,k}^{(j)}}{(1 + m_{c,k}^{(j)}) NM} |\mathbf{H}_{c,c,k} (\mathbf{\Gamma}_{c,[c,k]})^{-1} \mathbf{H}_{c,c,k}^H \mathbf{f}_{0,c,k}| \\
&= \frac{\xi_c^{(j)}}{a_{c,k}^{(j)} (1 + m_{c,k}^{(j)})} |\mathbf{\Theta}_{r,c,k}^{1/2} \mathbf{X}_{c,c,k} \bar{\mathbf{\Theta}}_{c,k}^{1/2} (\mathbf{\Gamma}_{c,[c,k]})^{-1} \bar{\mathbf{\Theta}}_{c,k}^{1/2} \mathbf{X}_{c,c,k}^H \mathbf{\Theta}_{r,c,k}^{1/2} \mathbf{f}_{0,c,k}^{(j)}| \\
&= \frac{\xi_c^{(j)}}{a_{c,k}^{(j)} (1 + m_{c,k}^{(j)})} |\mathbf{\Theta}_{r,c,k}^{1/2} \frac{1}{M} \text{tr}\{\bar{\mathbf{\Theta}}_{c,k} (\mathbf{\Gamma}_c^{(j)})^{-1}\} \mathbf{I}_N \mathbf{\Theta}_{r,c,k}^{1/2} \mathbf{f}_{0,c,k}^{(j)}| \\
&= \frac{\xi_c^{(j)} m_{c,k}}{a_{c,k}^{(j)} (1 + m_{c,k}^{(j)})} |\mathbf{\Theta}_{r,c,k}^{1/2} \mathbf{f}_{0,c,k}^{(j)}| = \frac{\xi_c^{(j)} m_{c,k}}{a_{c,k}^{(j)} (1 + m_{c,k}^{(j)})}. \tag{2.66}
\end{aligned}$$

Where $\mathbf{\Gamma}_{c,[c,k]} = \mathbf{\Gamma}_c - \mathbf{H}_{c,c,k} d_{c,k} \mathbf{H}_{c,c,k}$.

From (2.66) we see that if $\mathbf{\Theta}_{r,c,k} = \mathbf{I}_N$ the filters will have no effect on the signal power which motivates our choice for the channel correlation matrix at the receiver side as an identity matrix for the rest of the proof. Then,

$$\begin{aligned}
\Psi_c^{(j)} &= \frac{1}{(NM)^2} \text{tr} \left(\sum_k (\mathbf{\Gamma}_c^{(j)})^{-2} \mathbf{H}_{c,c,k}^H \mathbf{f}_{0,c,k}^{(j)} a_{c,k}^2 w_{c,k}^2 \mathbf{f}_{0,c,k}^H \mathbf{H}_{c,c,k} \right) \\
&= \frac{1}{NM} \text{tr} \left(\sum_k w_{c,k}^{(j)} d_{c,k}^{(j)} \mathbf{z}_{c,c,k}^{H,(j)} \mathbf{\Theta}_{c,k}^{1/2} (\mathbf{\Gamma}_c^{(j)})^{-2} \mathbf{\Theta}_{c,k}^{1/2} \mathbf{z}_{c,c,k}^{(j)} \right) \\
&= \frac{1}{NM} \text{tr} \left(\sum_k w_{c,k}^{(j)} \mathbf{z}_{c,c,k}^{H,(j)} \bar{\mathbf{\Theta}}_{c,k}^{1/2} (\mathbf{\Gamma}_c^{(j)})^{-2} \bar{\mathbf{\Theta}}_{c,k}^{1/2} \mathbf{z}_{c,c,k}^{(j)} \right) \\
&\dots \rightarrow \bar{\Psi}_c^{(j)}. \tag{2.67}
\end{aligned}$$

the rest of the proof is as in 2.3.2. $\mathbf{z}_{c,c,k} = \mathbf{X}_{c,c,k}^H \mathbf{f}_{0,c,k}^{(j)}$ will have i.i.d entries of zero mean and $\frac{1}{NM}$ variance if $\mathbf{f}_{c,k}^{(j)}$ is a MF as in (2.68) instead of the MMSE filter in (2.43)

$$\mathbf{f}_{c,k}^{MF} = \mathbf{g}_{c,k}^H \mathbf{H}_{c,c,k}^H (\sigma^2 \mathbf{I}_N + \mathbf{H}_{c,c,k} \mathbf{g}_{c,k} \mathbf{g}_{c,k}^H \mathbf{H}_{c,c,k}^H)^{-1} \quad (2.68)$$

The good performance of the MF filters is demonstrated in Figure 2.4 and in Chapter 1 when we proposed the WSMSE-SR precoder. In fact, when $\mathbf{f}_{c,k}^{(j)}$ is a MF, the WSMSE precoder becomes the WSMSE-SR precoder introduced in 1.5.2. We have proved by simulations that using a MF Rx is correct especially when we have large system dimensions. Finally, the interference power can be

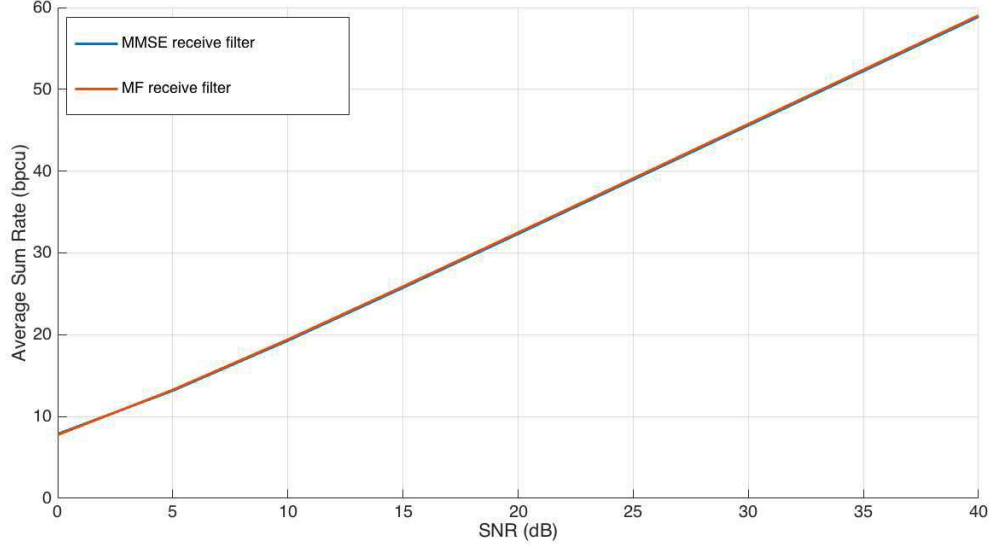


FIGURE 2.4: Sum rate comparisons between the IBC WSMSE with MMSE filters and the IBC WSMSE with MF filters for $C=1$, $M=10$, $K=4$, $N=2$

given by

$$\left(\frac{\bar{\xi}_c^{(j)}}{NM}\right)^2 \mathbf{f}_{0,c,k}^{H,(j)} \mathbf{H}_{m,c,k} \sum_{m,l;(m,l) \neq (c,k)} \mathbf{H}_{m,c,k} \bar{\mathbf{g}}_{m,l}^{(j)} \bar{\mathbf{g}}_{m,l}^{H,(j)} \mathbf{H}_{m,c,k}^H \quad (2.69)$$

$$\times \mathbf{H}_{m,c,k}^H \mathbf{f}_{0,c,k}^{(j)} \quad (2.70)$$

$$= (\bar{\xi}_c^{(j)})^2 \mathbf{z}_{m,c,k}^H \boldsymbol{\Theta}_{m,c,k}^{1/2} \quad (2.71)$$

$$\times \sum_{m,l;(m,l) \neq (c,k)} \mathbf{H}_{m,c,k} \bar{\mathbf{g}}_{m,l}^{(j)} \bar{\mathbf{g}}_{m,l}^{H,(j)} \mathbf{H}_{m,c,k}^H \boldsymbol{\Theta}_{m,c,k}^{1/2} \mathbf{z}_{m,c,k} \quad (2.72)$$

$$= \frac{\xi_c^{2,(j)}}{d_{c,k}^{(j)}} \mathbf{z}_{m,c,k}^H \bar{\boldsymbol{\Theta}}_{m,c,k}^{1/2} \sum_{m,l;(m,l) \neq (c,k)} \bar{w}_{m,l}^{(j)} (\bar{\boldsymbol{\Gamma}}_m^{(j)})^{-1} \quad (2.73)$$

$$\times \bar{\boldsymbol{\Theta}}_{m,l}^{1/2} \mathbf{z}_{m,l}^H \bar{\boldsymbol{\Theta}}_{m,l}^{1/2} (\bar{\boldsymbol{\Gamma}}_m^{(j)})^{-1} \bar{\boldsymbol{\Theta}}_{m,c,k}^{1/2} \mathbf{z}_{m,c,k} \quad (2.74)$$

$$\dots \rightarrow \frac{\xi_c^{2,(j)}}{d_{c,k}^{(j)}} \frac{\bar{\boldsymbol{\Upsilon}}_{c,k}^{(j)} + \bar{\hat{\boldsymbol{\Upsilon}}}_{c,k}^{(j)}}{(1 + \bar{m}_{c,c,k}^{(j)})^2}. \quad (2.75)$$

as in section 2.3.2. The filters are MF filters as denoted previously which completes the proof.

2.4.1 Applications of the deterministic equivalent of the SINR

In this subsection, the deterministic equivalent of the SINR in (2.47) is used in order to prove a property of the MU communications. We prove that for a BC system, the achievable SINR for a system with N -antennas receivers Rx and where only a single stream (SS) equals N times the SINR achieved in the case of MISO for identical channel covariance matrices. Thus,

$$\gamma_{BC,SS,NRx} = N \times \gamma_{BC,MISO} \quad (2.76)$$

Proof: For a BC system with K users where all channel covariances matrices $\boldsymbol{\Theta}_k$ are identical, the equations (2.59) and (2.61) can be written as:

$$e_{i,(j)}' = \frac{e_{i,(j)}'}{\bar{d}_i} = \frac{1}{\bar{\boldsymbol{\Xi}}^{(j)}} \frac{e_1^{(j)}}{1 - c^{(j)} e_2^{(j)}}, e_{k,(j)}' = \frac{e_{i,k,(j)}'}{\bar{d}_i} = \frac{\bar{d}_k^{(j)}}{\bar{\boldsymbol{\Xi}}^{(j)}} \frac{e_2^{(j)}}{1 - c^{(j)} e_2^{(j)}}, \quad (2.77)$$

where $c^{(j)} = \frac{\Delta^{(j)}}{(\Xi^{(j)})^2}$,

$$\Delta^{(j)} = \frac{1}{M} \sum_{k=1}^K \left(\frac{1}{\bar{d}_k^{(j)}} + e^{(j)} \right)^{-2}, \quad \Xi^{(j)} = \frac{1}{M} \sum_{k=1}^K \left(\frac{1}{\bar{d}_k^{(j)}} + e^{(j)} \right)^{-1}, \quad (2.78)$$

$$e^{(j)} = \frac{e_k^{(j)}}{\bar{d}_k^{(j)}} = \frac{1}{M} \text{tr} \Theta \mathbf{V}, \quad e_1^{(j)} = \Xi^{(j)} \frac{1}{M} \text{tr} \Theta \mathbf{V}^2, \quad (2.79)$$

and

$$e_2^{(j)} = \Xi^{(j)} \frac{1}{M} \text{tr} \Theta^2 \mathbf{V}^2. \quad (2.80)$$

Furthermore, the equations (2.49), (2.50) and (2.51) can be written as:

$$\overline{\Psi}^{(j)} = e'^{(j)} \Omega^{(j)}, \quad \overline{\Upsilon}_k^{(j)} = e_k'^{(j)} \Omega_k^{(j)} \quad (2.81)$$

where

$$\Omega^{(j)} = \frac{1}{MN} \sum_{i=1}^K \frac{\bar{w}_i^{(j)}}{\bar{d}_i^{(j)}} \left(\frac{1}{\bar{d}_i^{(j)}} + e^{(j)} \right)^{-2}, \quad (2.82)$$

and

$$\Omega_k^{(j)} = \frac{1}{M} \sum_{i=1, i \neq k}^K \frac{\bar{w}_i^{(j)}}{\bar{d}_i^{(j)}} \left(\frac{1}{\bar{d}_i^{(j)}} + e^{(j)} \right)^{-2} \quad (2.83)$$

Thus, the SINR in (2.47) will be equivalent to:

$$\gamma_k^{(j)} = e^{(j)} \bar{w}_k^{(j)} (\Xi^{(j)})^2 \frac{\bar{d}_k^{(j)} e^{(j)} [1 - c^{(j)} e_2^{(j)}]}{e_2^{(j)} \Omega_k^{(j)} + \frac{e_1^{(j)}}{\rho} \Omega^{(j)} (1 + \bar{d}_k^{(j)}) e^{(j)}} \quad (2.84)$$

For $\Theta_k = \Theta \forall k$, we have: $\bar{d}_k^{(j)} = d$, $\Omega_k^{(j)} = \Omega_k = N \times \Omega^{(j)} = N \times \Omega$, $c^{(j)} = \beta = \frac{K}{M}$. Let e be the unique positive solution of (2.79), then we can show that

$$ed = \beta(1 + e\bar{d})e_2 + \frac{\beta}{\rho}(1 + e\bar{d})^2 e_1 \quad (2.85)$$

The interference is diminished after the convergence of the WSMSE: $e_2^{(j)} \Omega_k^{(j)} \rightarrow 0$. Substituting (2.85) in (2.84), we get due to the presence of N in the denominator of (2.82):

$$\gamma_k^{(j)} = Ne = N \times \gamma_{k,SS}^{(j)} \quad (2.86)$$

Where $\gamma_{k,SS}^{(j)}$ is the SINR when $N = 1$. We can extend the result in (2.76) to IBC systems. Now, we will prove using numerical simulations the double findings of this section. We prove the correctness of the deterministic equivalent

of the SINR of MIMO SS system (2.47) as well as the validity of (2.76). We have seen that the SINR scales with N . Thus, the weighted sum rate function of SNR curve in the case of N antennas Rx must be parallel to the one obtained in the case of MISO. Figure 2.5 shows the simulation of WSMSE precoder for $C = 1, K = 15, M = 30$ and its approximation for the both cases of $N = 1$ and $N = 2$. For the simulations of the WSMSE algorithm, we have used 200 channel realizations. It can be observed that for i.i.d channels the approximation is accurate and that our asymptotic sum rate follows the simulated one; which validates our asymptotic approach. Although the sum rate expression for the approximation approach (2.47) seems to be complex, however we need to calculate it only once per a given SNR, while we need to run the IBC WSMSE simulations as many times as the number of channel realizations, i.e. 200 times. Moreover, we can observe that the curves of $N = 1$ and $N = 2$ are parallel which validates our proposition (2.76). Similarly, Figure 2.6 with $C = 1, K = 15, M = 30$ for both cases of $N = 1$ and $N = 2$ validates our results for IBC systems.

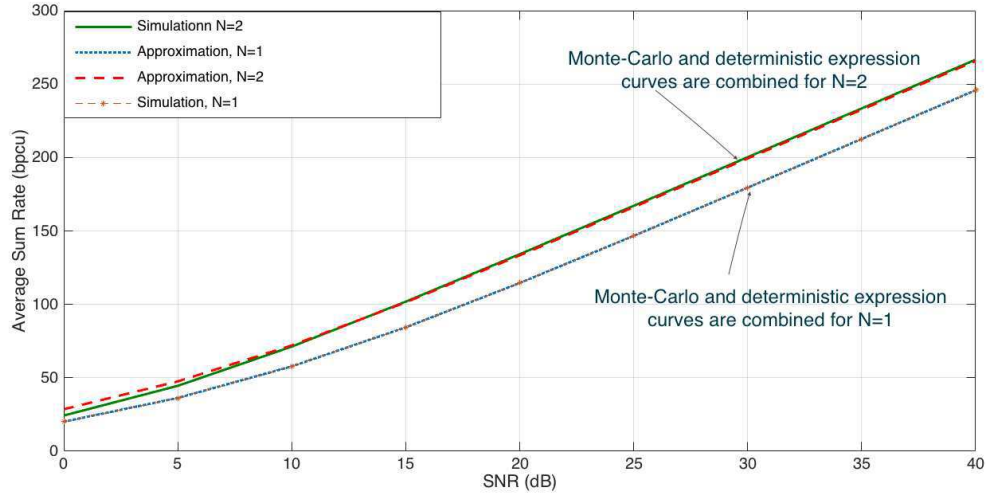


FIGURE 2.5: Sum rate comparisons between the IBC WSMSE and our proposed approximation for $C=1, K=20, M=30, N=\{1,2\}$

2.5 Conclusion

In order to assess the performance of algorithms like KG and WSMSE, Monte-Carlo simulation of the average rate versus SNR needs extensive averaging

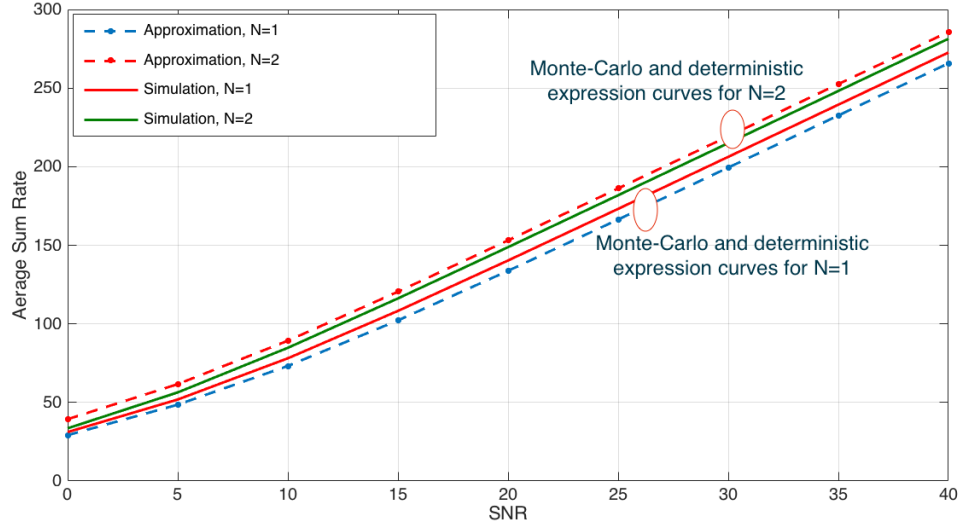


FIGURE 2.6: Sum rate comparisons between the IBC WSMSE and our proposed approximation for $C=2, K=10, M=30, N=\{1,2\}$

over many channel realizations. In order to ease this procedure of evaluation, in this chapter, we presented a consistent framework to study the WSMSE precoding for MISO based on the theory of large-dimensional random matrices. The tools from Random Matrix Theory allowed us to derive a deterministic expression of the rate for MISO. In MISO, the SINR is the ratio of scalar signal variance to scalar (interference + noise) variance. Hence, since we have a ratio of two scalars, Random Matrix Theory can be applied on each of these scalars apart resulting in a deterministic expression of the rate, which depends only on channels statistics and constant system parameters. The advantage of this proposition is that from now on, we do not need to do Monte-Carlo to evaluate performance. We have seen as well in this chapter that the deterministic expression represents well the true rate, especially when the total number of served users is inferior to the number of transmit antennas, which is true in general for Massive MIMO scenarios. Then, we proposed the same deterministic expression for MIMO single stream, i.e. MIMO but only a single stream is allowed to be transmitted. We used the resulting deterministic expression to show that the capacity scales with the number of receive antennas.

Chapter 3

Using the Complex Large System Analysis to Simplify Beamforming

The precoding schemes studied in Chapter 2 require a global knowledge of CSIT, which in turn requires a centralized controller to gather the information. If a centralized controller is not available, decentralized methods for optimal beamforming can be applied. In this chapter, we extend the works in [22], [23] and [24], in order to propose a decentralized beamforming approach that relies on the slow fading exchange of information between the BSs.

Our work is based on large system analysis. Other works on decentralization exist already in the literature, but they rather rely only on optimization techniques to decentralize, such as [36], [37] and [38], or on estimation tricks such as [30]. To the best of our knowledge, only one work considers decentralized coordinated beamforming using large system analysis [39], but it is sub-optimal. A work on decentralization techniques for decentralized minimum transmit power beamforming exists in [33], which is different from our WSMSE technique.

3.1 Decentralized approach for large dimensions system

The idea is to try to identify the quantities that require global knowledge of the channel vectors, the intercell interference $\Upsilon_{inter,c,k}$ and \mathbf{D} in our case, and

exchange them (or the quantities related to them) between the different BSs in such a way that the maximum WSR problem will decompose into parallel sub-problems (one per BS). However, it is necessary to limit as much as possible this exchange in order to be backhaul friendly (efficient). The solution in the last section can be reformulated as the following:

$$a_{c,k} = \mathbf{g}_{c,k}^H \mathbf{h}_{c,c,k} (\sigma^2 + \Upsilon_{intra,c,k} + \Upsilon_{inter,c,k})^{-1} \quad (3.1)$$

$$e_{c,k} = (1 + \gamma_{c,k})^{-1} \quad (3.2)$$

$$w_{c,k} = u_{c,k} (e_{c,k})^{-1} = u_{c,k} (1 - a_{c,k} \mathbf{h}_{c,c,k}^H \mathbf{g}_{c,k})^{-1} \quad (3.3)$$

$$\tilde{\mathbf{g}}_{c,k} = (\mathbf{H}_c^H \mathbf{D} \mathbf{H}_c + \frac{\text{tr} \mathbf{D}_c}{\rho_c} \mathbf{I}_M)^{-1} \mathbf{h}_{c,c,k} a_{c,k}^H w_{c,k} \quad (3.4)$$

with

$$\Upsilon_{intra,c,k} = \sum_n \mathbf{h}_{c,c,k}^H \mathbf{g}_{c,n} \mathbf{g}_{c,n}^H h_{c,c,k} \quad (3.5)$$

$$\Upsilon_{inter,c,k} = \sum_{m; m \neq c} \Upsilon_{inter,m,c,k} \quad (3.6)$$

and

$$\Upsilon_{inter,m,c,k} = \sum_n \mathbf{h}_{m,c,k}^H \mathbf{g}_{m,n} \mathbf{g}_{m,n}^H \mathbf{h}_{m,c,k} \quad (3.7)$$

This solution can be initialized by a random precoder, e.g., a matched filter (MF) precoder. In general, it needs a central processing node to be implemented because of (3.6) which depends on global channels knowledge as shown in (3.7). In the case of absence of this central node, (3.6) can be detected by each receiver and then fed back using an over-the-air link as in [22]. However, this approach is spectral inefficient.

Another way to decentralize consists in that each BS m calculates the quantities in (3.7), $\Upsilon_{inter,m,c,k}$ considered as the interference leakage from BS m to user k of cell $c \neq m$ for all the users and sends them to the BS c using a backhaul link. This procedure is a bit heavy, so it is beneficial to limit as much as possible the number of iterations. However, at high SNR, the solution above requires a lot of iterations to converge, hence, requires an extensive exchange of information using the backhaul link which burdens this latter and makes it practically infeasible. For a limited number of iterations, the solution becomes very sub-optimal.

Thus, in the following we present a new initialization method which accelerates the convergence, hence, few iterations are no more sub-optimal and the

backhaul-based decentralization becomes realistic. In this following, performance analysis is conducted for the proposed precoder. The large-system limit is considered, where M and K go to infinity while keeping the ratio K/M finite such that $\limsup_M K/M < \infty$ and $\liminf_M K/M > 0$.

Theorem 3.1: From 2.3.2, for a large MISO system, precoders $\tilde{\mathbf{g}}_{c,k}$ can be written as the following:

$$\tilde{\mathbf{g}}_{c,k} \tilde{\mathbf{g}}_{c,k}^H - \bar{\mathbf{g}}_{c,k} \bar{\mathbf{g}}_{c,k}^H \xrightarrow{M \rightarrow \infty} 0 \quad (3.8)$$

where

$$\bar{\mathbf{g}}_{c,k} = (\mathbf{H}_c^H \bar{\mathbf{D}} \mathbf{H}_c + \frac{\text{tr} \bar{\mathbf{D}}_c}{\rho_c} \mathbf{I}_M)^{-1} \mathbf{h}_{c,c,k} \bar{a}_{c,k}^H \bar{w}_{c,k} \quad (3.9)$$

We propose that (3.9) serves as an initialization for the iterative solution above. It also serves as a precoder itself, which is denoted as large system (LS)-precoder. Further details will be provided in the following sections. The fast-converging iterative algorithm behind (3.9) and the definitions of its terms are summarized in Algorithm 1. We give here the large system approximation of the intercell interference term as follows:

$$\bar{\mathbf{Y}}_{inter,c,k} = \lim_{j \rightarrow \infty} \frac{\bar{\xi}_c^{2,(j)} [\hat{\mathbf{Y}}_{c,k}^{(j)}]}{\bar{d}_{c,k}^{(j)} (1 + \bar{m}_{c,k}^{(j)})^2}. \quad (3.10)$$

3.2 Signaling

This section summarizes the iterative procedure to design transmit beamformers in a decentralized manner. The authors of [22] proposed a decentralized reasoning as well; so we will compare it to ours. They assumed that local channel information is available at each BS and for each user; we assume that as well. Moreover, they assume that each user has an additional channel to feedback information, which is $d_{i,k} = |a_{i,k}|^2 w_{i,k}$, to the BS; however we relax this assumption and we assume instead the existence of a backhaul link which is a way to save the wireless capacity consumption w.r.t an over-the-air link. It is used as explained in the previous section.

We would then propose three different strategies: a) The intercell interference-free strategy, where at each iteration of the precoders design each BS c calculates

Algorithm 1 Large System Computation of Dual UL Scalars

Step 1: Set $j = 0$ and calculate

$$\begin{aligned}\bar{\gamma}_{c,k}^{(0)} &= \frac{1}{\frac{1}{\beta_c \rho_c} + \frac{1}{M^2} \sum_{(l,i) \neq (c,k)} \text{tr} \Theta_{l,c,k} \Theta_{l,i}}. \\ \bar{a}_{c,k}^{(0)} &= \frac{1}{\sqrt{\bar{P}_{c,k}^{(0)}}} \frac{\bar{\gamma}_{c,k}^{(0)}}{1 + \bar{\gamma}_{c,k}^{(0)}}, \sqrt{\bar{P}_{c,k}^{(0)}} = \sqrt{\frac{P}{\frac{1}{M^2} \sum_{k=1}^K \Theta_{c,c,k}}}, \\ \bar{w}_{c,k}^{(0)} &= u_{c,k}(1 + \bar{\gamma}_{c,k}^{(0)}), \bar{d}_{c,k}^{(0)} = \bar{w}_{c,k}^{(0)} \bar{a}_{c,k}^{(0)}\end{aligned}$$

Step 2: Set $j = j + 1$ and calculate the following quantities:

$$\begin{aligned}\hat{\mathbf{Y}}_{c,k}^{(j)} &= \frac{1}{M} \sum_{m=1, m \neq c}^C \frac{(1 + \bar{m}_{c,k}^{(j)})^2}{(1 + \bar{m}_{m,c,k}^{(j)})^2} \sum_{l=1}^K \frac{\bar{w}_{m,l}^{(j)}}{(1 + \bar{m}_{m,l}^{(j)})^2} e_{m,c,k,m,l}'^{(j)}; \\ \bar{m}_{m,c,k}^{(j)} &= \frac{1}{M} \text{tr} \bar{\Theta}_{m,c,k}^{(j)} \mathbf{V}_m^{(j)}, \mathbf{V}_m^{(j)} = (\mathbf{F}_m^{(j)} + \bar{\alpha}_m^{(j)} \mathbf{I}_M)^{-1}, \\ \bar{m}_{c,k}^{(j)} &= \bar{m}_{c,c,k}^{(j)}, \\ \mathbf{F}_m^{(j)} &= \frac{1}{M} \sum_{j=1}^C \sum_{i=1}^K \frac{\bar{\Theta}_{m,j,i}^{(j)}}{1 + \bar{m}_{m,j,i}^{(j)}}, \text{ with } \bar{\Theta}_{m,c,k}^{(j)} = \bar{d}_{c,k}^{(j-1)} \Theta_{m,c,k}, \\ e_{m,c,k,m,l}'^{(j)} &= \frac{1}{M} \text{tr} \bar{\Theta}_{m,c,k}^{(j)} \mathbf{V}_m^{(j)} (\mathbf{F}_{m,m,l}'^{(j)} + \bar{\Theta}_{m,l}^{(j)}) \mathbf{V}_m^{(j)}, \\ \bar{\alpha}_m^{(j)} &= \frac{\sum_i \bar{d}_{m,i}^{(j-1)}}{M \rho_m}, \mathbf{F}_{m,m,l}'^{(j)} = \frac{1}{M} \sum_{j=1}^C \sum_{i=1}^K \frac{\bar{\Theta}_{m,j,i}^{(j)} e_{m,j,i,m,l}'^{(j)}}{(1 + \bar{m}_{m,j,i}^{(j)})^2}.\end{aligned}$$

$$\begin{aligned}\bar{\Psi}_c^{(j)} &= \frac{1}{M} \sum_{k=1}^K \bar{w}_{c,k}^{(j)} \frac{m_{c,k}'^{(j)}}{(1 + e_{c,k}^{(j)})^2}, \\ e_{c,k}'^{(j)} &= \frac{1}{M} \text{tr} \bar{\Theta}_{c,k}^{(j)} \mathbf{V}_c^{(j)} (\mathbf{F}_c'^{(j)} + \mathbf{I}_M) \mathbf{V}_c^{(j)}, \\ \bar{\Upsilon}_{c,k}^{(j)} &= \frac{1}{M} \sum_{l=1, l \neq k}^K \frac{\bar{w}_{c,l}^{(j)}}{(1 + \bar{m}_{c,l}^{(j)})^2} e_{c,c,k,c,l}'^{(j)}, \\ \mathbf{F}_c'^{(j)} &= \frac{1}{M} \sum_{j=1}^C \sum_{i=1}^K \frac{\bar{\Theta}_{c,j,i}^{(j)} e_{j,i}'^{(j)}}{(1 + \bar{m}_{c,j,i}^{(j)})^2}, \\ \bar{a}_{c,k}^{(j)} &= \frac{1}{\sqrt{\bar{P}_{c,k}^{(j-1)}}} \frac{\bar{\gamma}_{c,k}^{(j-1)}}{1 + \bar{\gamma}_{c,k}^{(j-1)}}, \\ \sqrt{\bar{P}_{c,k}^{(j-1)}} &= \frac{1}{\bar{a}_{c,k}^{(j-1)}} \sqrt{\frac{P}{\bar{\Psi}_c^{(j-1)}}} \frac{\bar{m}_{c,k}^{(j)}}{1 + \bar{m}_{c,k}^{(j)}}, \\ \bar{w}_{c,k}^{(j)} &= u_{c,k}(1 + \bar{\gamma}_{c,k}^{(j-1)}), \bar{d}_{c,k}^{(j)} = \bar{w}_{c,k}^{(j)} \bar{a}_{c,k}^{(j)}\end{aligned}$$

Step 3: $\bar{\gamma}_{c,k}^{(j)} = \frac{\bar{w}_{c,k}^{(j)} (\bar{m}_{c,k}^{(j)})^2}{\bar{\Upsilon}_{c,k}^{(j)} + \bar{\Upsilon}_{c,k}^{(j)} + \bar{d}_{c,k}^{(j)} \frac{\bar{\Psi}_c^{(j)}}{\rho_c} (1 + \bar{m}_{c,k}^{(j)})^2}$; $\rho_c = \frac{P_c}{\sigma^2}$.

Step 4: If converge stop and calculate $\bar{\mathbf{g}}_{c,k}^{(j)}$ as in Theorem 3.1, otherwise go to step 2.

*Note that all $e_{m,c,k} = \bar{m}_{m,c,k}$, $e_{c,k}'$ and $e_{m,c,k,m,l}'$ are obtained using the fixed-point iteration method as in Chapter 2.

only the quantities $\Upsilon_{intra,c,k}$ using the local channel information and supposes the $\Upsilon_{inter,c,k}$ is null. b) The constant intercell interference strategy, where for every iteration of the precoders design each BS c calculates the quantities $\Upsilon_{intra,c,k}$ using the local channel information but utilizes the intercell interference given by Algorithm 1 using (3.10). c) The up-to-date intercell interference strategy, where for every iteration of the precoders' design, each BS c calculates the quantities $\Upsilon_{intra,c,k}$ using the local channel information, then calculates the intercell interferences $\Upsilon_{inter,m,c,k}$ in (3.7) and sends them to the corresponding BS and finally this BS c collects the interference leakages corresponding to each user and sums them.

Clearly, the strategies (a) and (b) are sub-optimal but less demanding than (c) w.r.t to the backhaul capacity. Although the strategies (a) and (b) are sub-optimal, however they perform better than the approach in [22] by taking the MF initialization for a limited number of iterations. We recall that for each of the three strategies above, each BS calculates the $d_{c,k}$ for all served users and then send them to all the neighbouring BSs via the backhaul link. Furthermore, the fact that (c) requires that each BS m calculates the quantities in (3.7) for all users not served by m and then sends them to the concerned BS consumes more backhaul capacity than (a) and (b). The maximum number of iterations $iter_{max}$ is chosen to be very small, e.g., $iter_{max} = 2$ or $iter_{max} = 3$. The overall mechanism is described briefly in Algorithm 2.

Algorithm 2 The Decentralized Algorithm

Step 1: Set $iter = 0$. All BSs estimate local channel matrices (from BS to served users and to the users of the neighbouring cells). The BSs distribute the channel covariance matrices to neighbouring cells via the backhaul link only at slow fading rate. They apply Algorithm 1 and then calculate (3.9). They calculate (3.10) for strategy (b) and the intercell inteference $\Upsilon_{inter,m,c,k}$ with (3.9) for strategy (c) and exchange them with the concerned BS.

Step 2:

All the BSs calculate $\Upsilon_{intra,c,k}$, $a_{c,k}$, $w_{c,k}$ and $d_{c,k} = |a_{c,k}|^2 w_{c,k}$ using (3.5), (3.1) and (3.3) and send $d_{c,k}$ to the neighbouring BSs, at fast fading rate. Moreover, each BS calculates the interference leakages and collects the interference corresponding to its served users in strategy (c).

Step 3: All the BSs calculate their precoders using (3.4).

Step 4: $iter = iter + 1$, if $iter = iter_{max}$ stop, otherwise go to step 2.

3.3 Numerical results

In this section, results of simulations based on realistic settings with a finite number of transmit antennas show the correctness of the proposed approximation. We compare the three strategies of our decentralized algorithm to the WSMSE decentralized approach in [22], to the performance given by large system approximation in Chapter 2 which proposes an asymptotic approximation of the SINR of the WSMSE precoder at every iteration, and to the performance given directly by the precoder (3.9).

The channel correlation matrix $[\Theta_{m,c,k}]_{ij} \forall i, \forall j$ can be modeled as in [28]. In our case, we take them as identity matrices. For the simulations, we used 200 channel realizations, while the large system approximation in [11] needs only one channel realization. Furthermore, we used $iter_{max} = 3$ iterations for the simulation of strategies (a), (b) and (c), 1 iteration for (21) and 3, 30 and 100 iterations for [22].

In Fig. 3.1 and Figure 3.2, we can observe that the curves' performance corresponding to 'LS-precoder', 'strategy (a)', 'strategy (b)' and 'strategy (c)' are combined. We also notice that our precoders corresponding to LS-precoder, (a), (b) and (c) behave very efficiently in general, which means that they achieve higher rates than [22] with much less iterations (less information exchanged in the backhaul and smaller latencies). However, LS-precoder has a better performance in Figure 3.1 corresponding to a non fully loaded system ($load = \frac{KC}{M} < 1$) than in Figure 3.2 corresponding to a fully loaded system ($load = 1$).

Further explanations about the behavior of the large system approximations for fully loaded systems as in Figure 3.2 can be found in section 2.3.3.

3.4 Analytic solution

In practice, Massive MIMO BSs with hundreds of antennas serve tens of users, so $load = 0.1 < 1$. This description is more suitable for the configuration of Figure 3.1. Hence, we conclude that for practical Massive MIMO configuration the LS-precoder works very well.

In this section, we propose closed-form expressions for this LS-precoder for some special practical cases as explained below. The expressions for $\bar{a}_{c,k}^H$, $\bar{w}_{c,k}$, $\bar{\mathbf{D}}$ and $\bar{\xi}_c$ are given above. However, these expressions are a bit complex.

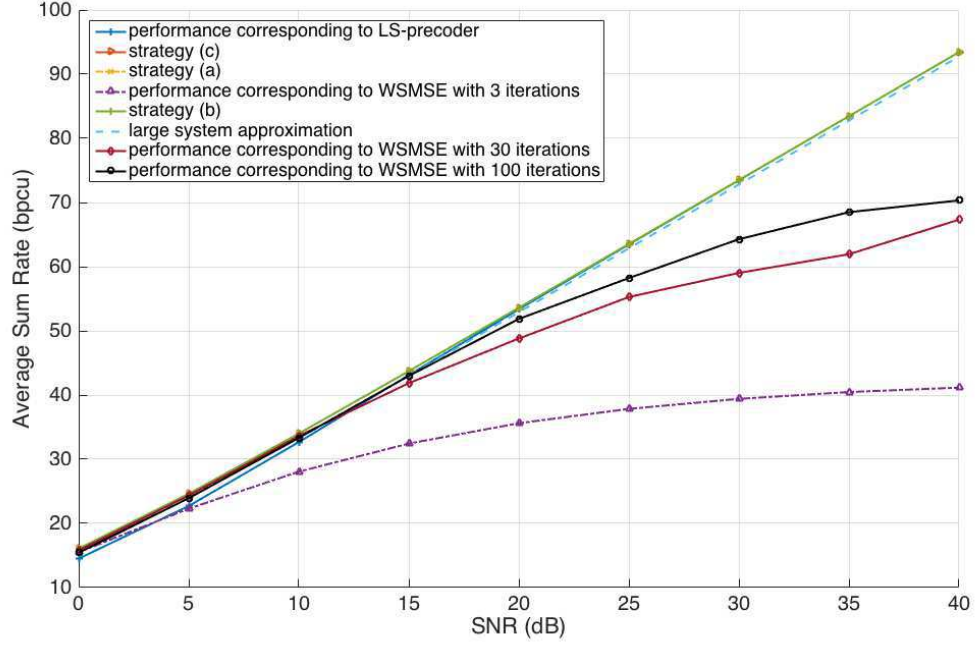


FIGURE 3.1: Sum rate comparisons for $C=3, K=2, M=15$.

Therefore, we propose closed-form expressions to determine $\bar{a}_{c,k}^H$, $\bar{w}_{c,k}$, $\bar{\mathbf{D}}$ and $\bar{\xi}_c$ for uncorrelated channels, identical $u_{c,k}$ for all c, k and at high SNR .

We now consider two simple case studies as depicted in Figures 3.3 and 3.4. Let α_{intra} and α_{inter} denote the path losses of the intracell and intercell channels respectively.

Assumption 3.1: $\Theta_{m,c,k} = \alpha_{intra} \mathbf{I}_M$ for all m, c and k such that $m = c$, $\Theta_{m,c,k} = \alpha_{inter} \mathbf{I}_M$ otherwise. The total available transmit power is the same for all cells, i.e. $P_i = P$ and $\rho_i = \rho$ for all i in \mathcal{C} . Non-negligible intercell interference: $\rho\alpha_{inter} \gg 1$. High SNR: $\rho\alpha_{intra} \gg 1$.

Theorem 3.1. *Let Assumption 3.1 hold, then for all c and k , $\bar{\gamma}_{c,k} = \bar{\gamma}$, $\bar{a}_{c,k} = \bar{a}$, $\bar{d}_{c,k} = \bar{d}$, $\bar{w}_{c,k} = \bar{w}$, $\bar{\xi}_c = \bar{\xi}$ and the intracell and intercell terms have closed-form expressions which are given by (3.11), (3.12), (3.13) and (3.14).*

$$\bar{\gamma} = \bar{m}_{intra} = \frac{\alpha_{intra}(1 - \beta^{-1})}{\beta_2^{-1}} \rho; \quad (3.11)$$

$$\bar{a} = (\bar{\gamma}\sigma^2)^{-\frac{1}{2}}; \bar{d} = \frac{1}{\sigma^2}; \bar{w} = \bar{\gamma}; \bar{\xi} = \frac{P}{\bar{d}}; \quad (3.12)$$

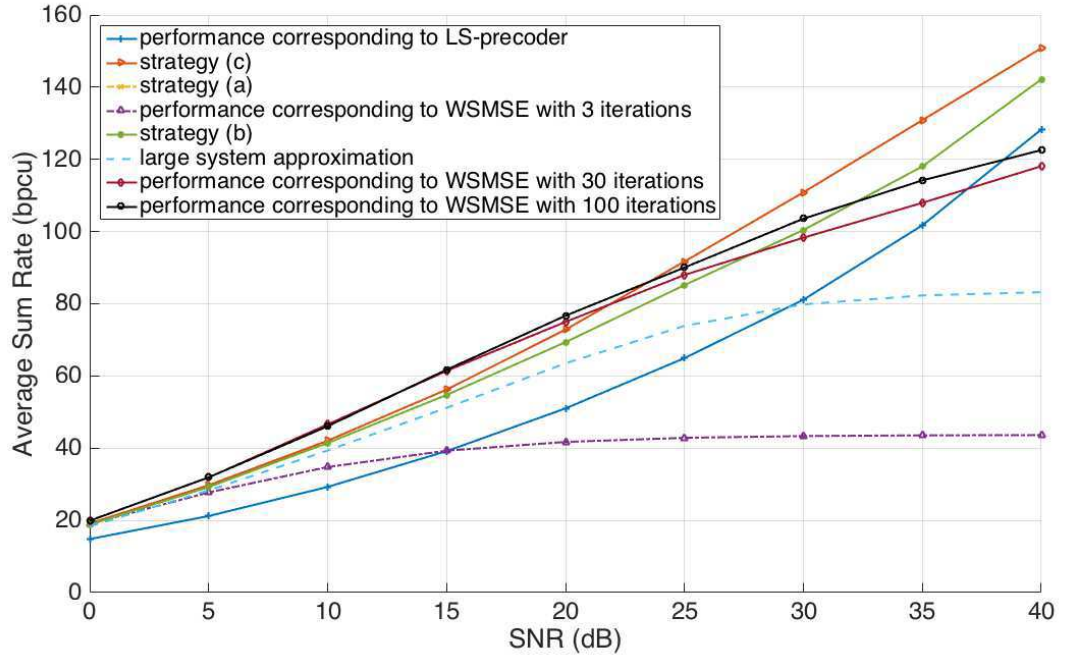


FIGURE 3.2: Sum rate comparisons for $C=3, K=5, M=15$.

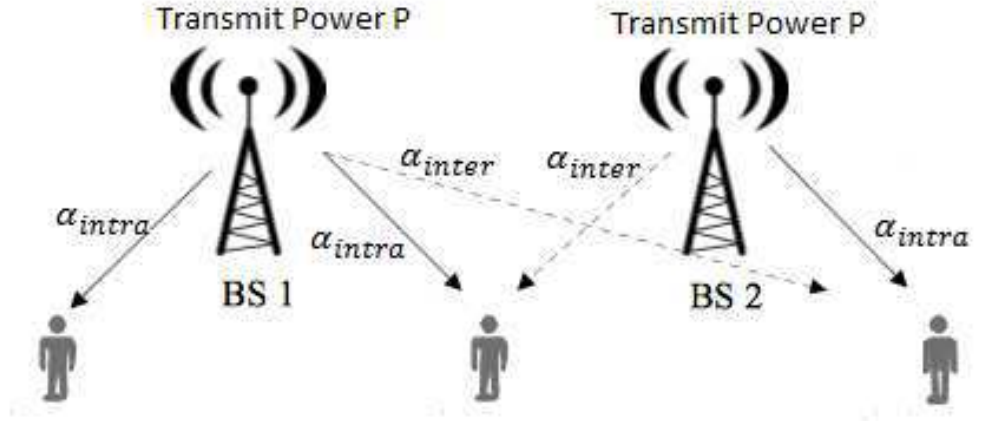


FIGURE 3.3: Figure corresponding to Assumption 3.1

$$intra = \sigma^2 \frac{\beta_2^{-1}}{1 - \beta^{-1}} \frac{1}{\bar{\gamma}}; \quad (3.13)$$

$$inter = \sigma^2 \frac{\frac{C-1}{M} K}{1 - \beta^{-1}} \frac{\alpha_{intra}}{\alpha_{inter}} \frac{1}{\bar{\gamma}}. \quad (3.14)$$

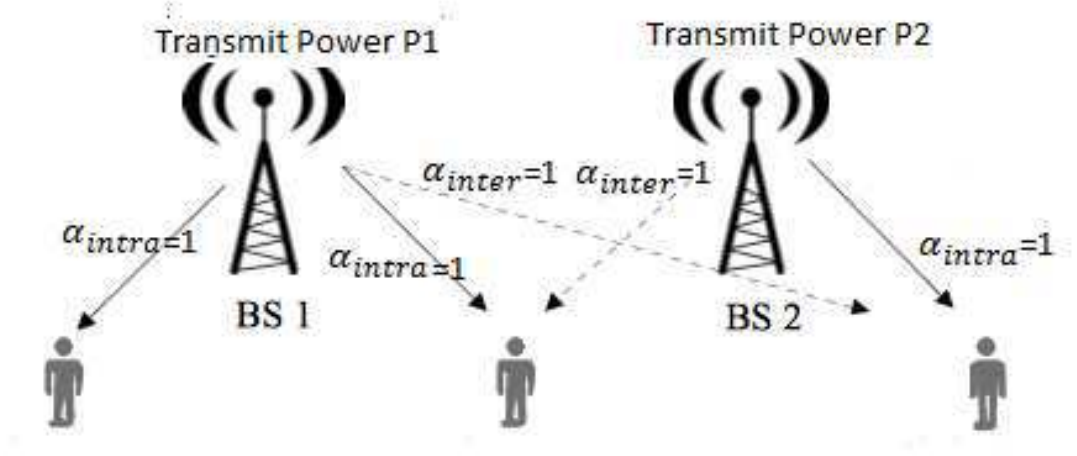


FIGURE 3.4: Figure corresponding to Assumption 3.2

where

$$\beta^{-1} = \frac{K \times C}{M}; \beta_2^{-1} = \frac{K}{M} \quad (3.15)$$

Note that interference is $\sim \frac{\sigma^2}{\rho}$. This means that the interference is completely reduced to the noise level by the WSMSE precoder.

Proof: If $\rho\alpha_{intra} \gg 1$ and $\rho\alpha_{inter} \gg 1$ we obtain from (2.15):

$$\bar{m}_{c,c,k} = \frac{1 - \beta^{-1}}{\beta_2^{-1}} \rho\alpha_{intra}; \bar{m}_{m,c,k} = \frac{1 - \beta^{-1}}{\beta_2^{-1}} \rho\alpha_{inter} \quad (3.16)$$

$$e = \frac{\bar{m}_{m,c,k}}{\alpha_{inter}} = \frac{\bar{m}_{c,c,k}}{\alpha_{intra}} \text{ with } m \neq c \quad (3.17)$$

In fact, from (2.15) we obtain

$$\bar{m}_{m,c,k} = \alpha_{inter} \times \bar{d} \times \frac{1}{M} \text{tr} \mathbf{V}_m = \bar{m}_{inter} \quad (3.18)$$

$$\bar{m}_{c,c,k} = \alpha_{intra} \times \bar{d} \times \frac{1}{M} \text{tr} \mathbf{V}_c = \bar{m}_{intra} \quad (3.19)$$

but $\mathbf{V}_c = \mathbf{V}_m$ (we suppose $\bar{m}_{intra} \sim 1 + \bar{m}_{intra}$ and $\bar{m}_{inter} \sim 1 + \bar{m}_{inter}$) because

$$\begin{aligned} \mathbf{V}_c^{-1} &= \frac{1}{M} \sum_{i,j} \frac{\bar{\Theta}_{c,i,j}}{\bar{m}_{c,i,j}} + \sum_{i=1}^K \frac{\bar{d}}{M\rho} \mathbf{I}_M \\ &= \frac{K}{M} \frac{\alpha_{intra} \bar{d}}{\bar{m}_{intra}} \mathbf{I}_M + (C-1)K \frac{\alpha_{inter} \bar{d}}{\bar{m}_{inter}} + \frac{K \bar{d}}{M\rho} \mathbf{I}_M = \mathbf{V}_m^{-1} = \mathbf{V}^{-1} \end{aligned} \quad (3.20)$$

Hereinafter,

$$\frac{\bar{m}_{intra}}{\alpha_{intra}\bar{d}} = \frac{\bar{m}_{inter}}{\alpha_{inter}\bar{d}} \quad (3.21)$$

(2.15) leads to:

$$\begin{aligned} \bar{m}_{intra} = \alpha_{intra}\bar{d}\mathbf{V} &= \alpha_{intra}\bar{d}\frac{1}{M}\text{tr}\left(\frac{K}{M}\frac{\alpha_{intra}\bar{d}}{\bar{m}_{intra}}\mathbf{I}_M\right. \\ &\quad \left.+ (C-1)K\frac{\alpha_{inter}\bar{d}}{\bar{m}_{inter}} + \frac{K}{M\rho}\mathbf{I}_M\right)^{-1} \end{aligned} \quad (3.22)$$

Using (3.21), we get:

$$\bar{m}_{intra} = \alpha_{intra}\bar{d}\mathbf{V} = \alpha_{intra}\bar{d}\frac{1}{M}\text{tr}\left(\frac{CK}{M}\frac{\alpha_{intra}\bar{d}}{\bar{m}_{intra}}\mathbf{I}_M + \frac{K\bar{d}}{M\rho}\mathbf{I}_M\right)^{-1} \quad (3.23)$$

We simplify by \bar{d} and use (3.15), we get:

$$\bar{m}_{intra} = \alpha_{intra}\bar{d}\mathbf{V} = \alpha_{intra}\left(\beta^{-1}\frac{\alpha_{intra}}{m_{intra}} + \beta_2^{-1}\frac{1}{\rho}\right)^{-1} \quad (3.24)$$

We solve this equation and get:

$$\bar{m}_{intra} = \frac{\alpha_{intra}(1 - \beta^{-1})}{\beta_2^{-1}}\rho \quad (3.25)$$

We do the same procedure for \bar{m}_{inter} .

From (2.26) we obtain:

$e'_{c,c,k} = e'_{intra} = e'\alpha_{intra}$ for all c and k . $e'_{m,c,k} = e'_{inter} = e'\alpha_{inter}$ for all m, c and k .

Thus,

$$e'_{intra} = \alpha_{intra}\bar{d}e^2\frac{1}{\bar{d}^2}\left(\frac{K}{M}\frac{\alpha_{intra}^2\bar{d}e'}{(\alpha_{intra}e)^2} + \frac{(C-1)K}{M}\frac{\bar{d}\alpha_{inter}^2e'}{(\alpha_{inter}e)^2} + 1\right) \quad (3.26)$$

$$= \alpha_{intra}\frac{1}{\bar{d}}e^2\left(\frac{1}{M}\frac{\bar{d}e'K}{e^2} + \frac{1}{M}\frac{(C-1)Ke'}{e^2} + 1\right) \quad (3.27)$$

$$= \frac{\alpha_{intra}\frac{1}{\bar{d}}e^2}{1 - \frac{1}{M}K - \frac{1}{M}(C-1)K} \quad (3.28)$$

From (2.28), $e'_{m,c,k,m,l} = e''_{intra} = \alpha_{intra} e''$ if $m = c$ else $e'_{m,c,k,m,l} = e''_{inter} = \alpha_{inter} e''$. Then,

$$e''_{intra} = \alpha_{intra} \bar{d} e^2 \frac{1}{\bar{d}^2} \left(\frac{1}{M} \frac{\alpha_{intra}^2 \bar{d} e'' K}{(\alpha_{intra} e)^2} + \frac{\frac{1}{M}(C-1)K \bar{d} \alpha_{inter}^2 e''}{(\alpha_{inter} e)^2} \right) \quad (3.29)$$

$$+ \alpha_{intra} \bar{d}) = \frac{\alpha_{intra}^2 e^2}{1 - \frac{K}{M} - \frac{(C-1)K}{M}}; \quad (3.30)$$

$$e''_{inter} = \alpha_{inter} \bar{d} e^2 \frac{1}{\bar{d}^2} \left(\frac{1}{M} \frac{\alpha_{intra}^2 \bar{d} e'' K}{(\alpha_{intra} e)^2} + \frac{\frac{1}{M}(C-1)K \bar{d} \alpha_{inter}^2 e''}{(\alpha_{inter} e)^2} \right) \quad (3.31)$$

$$+ \alpha_{intra} \bar{d}) = \frac{\alpha_{intra} \alpha_{inter} e^2}{1 - \frac{K}{M} - \frac{(C-1)K}{M}} \quad (3.32)$$

From (2.16), we get:

$$\bar{\Psi} = \frac{K}{M} w \frac{e'_{intra}}{\alpha_{intra}^2 e^2} = \frac{\beta_2^{-1}}{1 - \beta^{-1}} \bar{w} \frac{1}{\bar{d} \alpha_{intra}} \quad (3.33)$$

Similarly, we obtain:

$$\bar{\Upsilon} = \frac{\beta_2^{-1}}{1 - \beta^{-1}} \bar{w}; \hat{\Upsilon} = \frac{\frac{C-1}{K} M}{1 - \beta^{-1}} \frac{\alpha_{intra}}{\alpha_{inter}} \bar{w} \quad (3.34)$$

By simplifying by \bar{w} , (2.47) gives:

$$\bar{\gamma} = \frac{\bar{m}_{intra}^2}{\frac{\frac{C-1}{M} K}{1 - \beta^{-1}} \frac{\alpha_{intra}}{\alpha_{inter}} + \frac{\beta_2^{-1}}{1 - \beta^{-1}} + \frac{\beta_2^{-1}}{1 - \beta^{-1}} \frac{1}{\alpha_{intra}} \frac{1}{\rho} \bar{m}_{intra}^2} \quad (3.35)$$

Using (3.15), we get:

$$\bar{\gamma} = \frac{\bar{m}_{intra}^2}{\frac{\frac{C-1}{M} K}{1 - \beta^{-1}} \frac{\alpha_{intra}}{\alpha_{inter}} + \frac{\beta_2^{-1}}{1 - \beta^{-1}} + \bar{m}_{intra}} \quad (3.36)$$

However, $\bar{m}_{intra} \sim \rho$ so approximately $\bar{\gamma} = \bar{m}_{intra}$ at convergence and we have

:

$$\bar{\Psi} = \frac{\beta_2^{-1}}{\alpha_{intra}(1 - \beta^{-1})} \frac{1}{\bar{d}} \bar{\gamma} = \frac{\rho}{\bar{\gamma} \bar{d}} \bar{\gamma} = \frac{\rho}{\bar{d}} \quad (3.37)$$

From (2.20), (2.19) and (2.22) respectively we have:

$$\sqrt{\bar{P}} = \frac{1}{\bar{a}} \sqrt{\frac{P}{\bar{d} \sigma^2}} = \sqrt{\bar{d} \sigma^2} \frac{1}{\bar{a}} = (\bar{\gamma} \sigma^2)^{\frac{1}{2}}; \bar{a} = (\bar{\gamma} \sigma^2)^{-\frac{1}{2}}; \bar{d} = \frac{1}{\bar{\gamma} \sigma^2} \bar{\gamma} = \frac{1}{\sigma^2} \quad (3.38)$$

Finally, the intracell and intercell interferences are herein given by

$$intra = \frac{\xi^2 \bar{\mathbf{\Upsilon}}}{\bar{d} \bar{\gamma}^2} = \frac{P \mathbf{1} \bar{\mathbf{\Upsilon}}}{\bar{\Psi} \bar{d} \bar{\gamma}^2} = \frac{P \mathbf{1} \bar{\mathbf{\Upsilon}}}{\frac{P}{d} \bar{d} \bar{\gamma}^2} = \sigma^2 \frac{\bar{\mathbf{\Upsilon}}}{\bar{\gamma}^2} = \sigma^2 \frac{\beta_2^{-1}}{1 - \beta^{-1}} \frac{1}{\bar{\gamma}} \quad (3.39)$$

$$inter = \sigma^2 \frac{\hat{\mathbf{\Upsilon}}}{\bar{\gamma}^2} = \sigma^2 \frac{\frac{C-1}{K} M}{1 - \beta^{-1}} \frac{\alpha_{intra}}{\alpha_{inter}} \frac{1}{\bar{\gamma}} \quad (3.40)$$

Assumption 3.2: $\Theta_{m,c,k} = \mathbf{I}_M$ for all m, c, k . Different available total transmit power per cell.

Theorem 3.2. *Let Assumption 3.2 hold, then for all c and k $\bar{\gamma}_{c,k} = \bar{\gamma}_c$, $\bar{a}_{c,k} = \bar{a}_c$, $\bar{d}_{c,k} = \bar{d}_c$, $\bar{w}_{c,k} = \bar{w}_c$, $\bar{\xi}_c$ and the intracell and intercell terms have closed-form expressions which are given by (3.41), (3.42), (3.43), (3.44), (3.45) and (3.46).*

$$\bar{\gamma}_c \sim \bar{m}_c = \frac{1 - \beta^{-1}}{\beta_2^{-1}} \rho_c. \quad (3.41)$$

$$\bar{a}_c = (\bar{\gamma}_c \sigma^2)^{-\frac{1}{2}}; \quad (3.42)$$

$$\bar{d}_c = \frac{1}{\sigma^2}; \bar{w}_c = \bar{\gamma}_c; \quad (3.43)$$

$$\bar{\xi}_c = \frac{\bar{P}_c}{\frac{P_c}{d_c}}; \quad (3.44)$$

$$intra = \sigma^2 \frac{\beta_2^{-1}}{1 - \beta^{-1}} \frac{1}{\bar{\gamma}_c}; \quad (3.45)$$

$$inter = \frac{\sigma^2}{\bar{\gamma}_c^2} \frac{\beta_2^{-1}}{1 - \beta^{-1}} \sum_{m=1}^{C-1} \frac{\rho_c}{\rho_m} \bar{w}_m. \quad (3.46)$$

The proof is omitted because its is somehow similar to the one detailed above.

3.5 Conclusion

WSMSE and KG are hard to implemented in real systems. In this chapter, we considered the deterministic expressions for MISO derived in the previous chapter and deduced a new beamformer named 'LS-precoder'. It is based on deterministic values and has the advantage to converge in one iteration. Then, simple closed-form expressions for this precoder are given for some specific

scenarios. Moreover, signalling and practical implementation of WSMSE are treated in this chapter.

Part II

Further Random Matrix Theory exploitation with partial CSIT

Chapter 4

Robust Beamformers for Partial CSIT

In Part I, we investigated transmit precoding designs for the case of perfect CSIT. Two beamforming algorithms, WSMSE and KG, have been identified for MIMO DL as optimal solutions to solve the WSR problem under transmit power constraints and full knowledge of the CSIT. When the CSIT is partial, the WSR problem is denoted as the EWSR. Many precoders solve this latter, however they are sub-optimal.

Although solving the EWSR is difficult, in this chapter we show how to approach the optimal solution, leading to a novel precoder algorithm for the case of partial CSIT denoted as the Expected Signal Covariance Expected Interference Covariance based WSR (ESEI-WSR) BF. This BF takes advantage of the presence of both the error covariance matrices and channel estimates. We also apply the DA of section 1.5 to this BF, which boosts the convergence rate of our precoder and leads somehow the precoding algorithm to global optima.

In computer simulations using Matlab, the ESEI-WSR BF method shows a substantial gain in performance over the existing approaches, mainly the expected weighted sum mean squared error (EWSMSE) approach of [40], which does not benefit in a correct manner from the error covariance CSIT. We expect our precoder to be effective in practical communications systems. It reduces the consumption of backhaul capacity, especially in the practical special case presented in section 4.5 of this chapter, where it requires the exchange of scalars (traces of matrices) instead of square matrices of size the number of receive

antennas. We explore many approaches to solve the EWSR problem shown in (1.24).

4.1 The naive approach : ENAIVEKG

The naive approach ENAIVEKG, which uses the KG precoder introduced in section 1.4.2, but this time by replacing the real channels that we do not know by their estimates $\bar{\mathbf{H}}$. Please refer to 1.6 for further details on channel estimation. The disadvantage of this approach is that we do not use all the information that we know; we do not use the covariance CSIT (error covariance matrix), i.e. Θ_p . This approach is sub-optimal.

4.2 The EWSMSE approach

This EWSMSE approach is proposed in [40]. We rewrite in what follows the main results. The optimization problem in (1.24) as explained in [40] can be written as

$$\begin{aligned} \{\mathbf{G}, \mathbf{F}, \mathbf{W}\} = \\ \arg \min_{\mathbf{G}, \mathbf{F}, \mathbf{W}} \sum_{(c,k)} u_{c,k} (\text{tr}(\mathbf{W}_{c,k} \mathbf{E}_{c,k}) - \log \det(\mathbf{W}_{c,k})) \\ \text{s.t. } \text{tr} \mathbf{G}_c \mathbf{G}_c \leq P_c \text{ for } c \in \mathcal{C} \end{aligned} \quad (4.1)$$

with

$$\mathbf{E}_{c,k} = E_{\mathbf{H}|\bar{\mathbf{H}}}[(\mathbf{F}_{c,k}^H \mathbf{y}_{c,k} - \mathbf{s}_{c,k})(\mathbf{F}_{c,k}^H \mathbf{y}_{c,k} - \mathbf{s}_{c,k})^H]; \quad (4.2)$$

is the expected value of the MSE. The solution is given in [40] by an iterative procedure as follows:

$$\mathbf{F}_{c,k} = (\sigma^2 \mathbf{I}_N + \sum_{m=1}^C \sum_{l=1}^K (\bar{\mathbf{H}}_{m,c,k} \mathbf{G}_{m,l} \mathbf{G}_{m,l}^H \bar{\mathbf{H}}_{m,c,k}^H + \text{tr}(\boldsymbol{\Theta}_{p,m,c,k} \mathbf{G}_{m,l} \mathbf{G}_{m,l}^H)))^{-1} \bar{\mathbf{H}}_{c,c,k} \mathbf{G}_{c,k}; \quad (4.3)$$

$$\begin{aligned} \mathbf{W}_{c,k} = & (\mathbf{I}_{d_{c,k}} - \mathbf{F}_{c,k}^H \bar{\mathbf{H}}_{c,c,k} \mathbf{G}_{c,k} - \mathbf{G}_{c,k}^H \bar{\mathbf{H}}_{c,c,k}^H \mathbf{F}_{c,k} + \\ & \sum_l^C \sum_j^K \mathbf{F}_{c,k}^H \bar{\mathbf{H}}_{l,c,k} \mathbf{G}_{l,j} \mathbf{G}_{l,j}^H \bar{\mathbf{H}}_{l,c,k}^H \mathbf{F}_{c,k} + \\ & \mathbf{F}_{c,k}^H (\sum_l^K \sum_j^C \text{tr}(\boldsymbol{\Theta}_{p,l,c,k} \mathbf{G}_{l,j} \mathbf{G}_{l,j}^H) + \mathbf{I}_N) \mathbf{F}_{c,k})^{-1} \end{aligned} \quad (4.4)$$

$$\mathbf{G}_{c,k} = u_{c,k} (\sum_{j=1}^C \sum_{l=1}^K (\bar{\mathbf{H}}_{c,j,i}^H \mathbf{D}_{i,j} \bar{\mathbf{H}}_{c,j,i} + \text{tr}(\mathbf{D}_{i,j}) \boldsymbol{\Theta}_{p,c,i,j}) + \lambda_c \mathbf{I}_M)^{-1} \bar{\mathbf{H}}_{c,c,k}^H \mathbf{F}_{c,k} \mathbf{W}_{c,k} \quad (4.5)$$

Subsequently $\mathbf{F}_{c,k}$ and $\mathbf{W}_{c,k}$ are computed, which then constitute the new precoder $\mathbf{G}_{c,k}$. This process is repeated until convergence to a local optimum.

4.3 The ESEI-WSR approach

In the Massive MU MIMO limit where the number of transmit antennas M becomes very large, the WSR converges to a deterministic limit that depends on the distribution of the channels. The actual statistical distribution of the channel is one thing. The TxS have no choice but to design their BF's according to their partial CSIT. Then to get the actual resulting WSR, the BF's designed with the partial CSIT need to be evaluated with the actual channel distribution. Now, for the design with partial CSIT, the WSR will also converge to a deterministic limit in the Massive MU MIMO regime. We get a convergence for any term of the form

$$\mathbf{H} \mathbf{Q} \mathbf{H}^H \xrightarrow{M \rightarrow \infty} \mathbb{E}_{\mathbf{H}} \mathbf{H} \mathbf{Q} \mathbf{H}^H = \bar{\mathbf{H}} \mathbf{Q} \bar{\mathbf{H}}^H + \text{tr}\{\mathbf{Q} \boldsymbol{\Theta}_p\} \mathbf{C}_r. \quad (4.6)$$

We suppose $\mathbf{C}_r = \mathbf{I}_N$. $\bar{\mathbf{H}}$ is the estimate of the channel and $\boldsymbol{\Theta}_p$ is the covariance matrix of the error estimation. Using (4.6) we will extend the KG algorithm

in 1.4.2 to be more robust to partial channel knowledge . Let us define:

$$\begin{aligned} \mathbf{H}_{c,k} &= [\mathbf{H}_{1,c,k} \cdots \mathbf{H}_{C,c,k}] = \bar{\mathbf{H}}_{c,k} + \tilde{\mathbf{H}}_{c,k} \Theta_{p,c,k}^{1/2} \\ \mathbf{Q} &= \begin{bmatrix} \mathbf{Q}_1 & & \\ & \ddots & \\ & & \mathbf{Q}_C \end{bmatrix} = \begin{bmatrix} \sum_k \mathbf{Q}_{1,k} & & \\ & \ddots & \\ & & \sum_k \mathbf{Q}_{C,k} \end{bmatrix} = \\ & \sum_c \sum_k \mathbf{I}_c \mathbf{Q}_{c,k} \mathbf{I}_c^H; \end{aligned} \quad (4.7)$$

$$\mathbf{Q}_{c,k} = \mathbf{Q} - \mathbf{I}_c \mathbf{Q}_{c,k} \mathbf{I}_c^H.$$

where $\Theta_{p,c,k} = \text{blockdiag}\{\Theta_{p,1,c,k}, \dots, \Theta_{p,C,c,k}\}$, and \mathbf{I}_c is an all zero block vector except for an identity matrix in block c . Using (4.6), the interference plus noise covariance matrices of (1.5) give:

$$\begin{aligned} \check{\mathbf{R}}_{c,k} &= \sigma^2 \mathbf{I}_N + \bar{\mathbf{H}}_{c,k} \mathbf{Q} \bar{\mathbf{H}}_{c,k}^H + \text{tr}\{\mathbf{Q} \Theta_{p,c,k}\} \mathbf{I}_N \\ \check{\mathbf{R}}_{c,k} &= \sigma^2 \mathbf{I}_N + \bar{\mathbf{H}}_{c,k} \mathbf{Q}_{c,k} \bar{\mathbf{H}}_{c,k}^H + \text{tr}\{\mathbf{Q}_{c,k} \Theta_{p,c,k}\} \mathbf{I}_N \end{aligned} \quad (4.8)$$

which represent the total and the interference plus noise Rx covariance matrices in the Massive MU MIMO regime respectively.

This leads (1.14) to

$$\begin{aligned} WSR &= u_{c,k} \log \det(\check{\mathbf{R}}_{c,k}^{-1} \check{\mathbf{R}}_{c,k}) + WSR_{c,k} \\ WSR_{c,k} &= \sum_{(j,i) \neq (c,k)} u_{j,i} \log \det(\check{\mathbf{R}}_{j,i}^{-1} \check{\mathbf{R}}_{j,i}) \end{aligned} \quad (4.9)$$

where $\log \det(\check{\mathbf{R}}_{c,k}^{-1} \check{\mathbf{R}}_{c,k})$ is concave in $\mathbf{Q}_{c,k}$, $WSR_{c,k}$ is convex in $\mathbf{Q}_{c,k}$ and $\check{\mathbf{R}}_{c,k}$ and $\check{\mathbf{R}}_{c,k}$ are given by (4.8).

Consider the first order Taylor series expansion in $\mathbf{Q}_{c,k}$ around $\hat{\mathbf{Q}}$ of $WSR_{c,k}$ as explained in section 1.4.2 then

$$\hat{\mathbf{A}}'_{c,k} = \sum_{(j,i) \neq (c,k)} u_{j,i} \mathbf{H}_{c,j,i}^H (\check{\mathbf{R}}_{j,i}^{-1} - \check{\mathbf{R}}_{j,i}^{-1}) \mathbf{H}_{c,j,i} \quad (4.10)$$

And the term $\hat{\mathbf{B}}'_{c,k}$ corresponding to $\mathbf{B}_{c,k}$ can then be given by:

$$\hat{\mathbf{B}}'_{c,k} = \mathbf{H}_{c,c,k}^H \check{\mathbf{R}}_{c,k}^{-1} \mathbf{H}_{c,c,k} \quad (4.11)$$

Then, we calculate the expected values $\check{\mathbf{A}}_{c,k}$ and $\check{\mathbf{B}}_{c,k}$ of $\hat{\mathbf{A}}'_{c,k}$ and $\hat{\mathbf{B}}'_{c,k}$ respectively:

$$\begin{aligned}\check{\mathbf{B}}_{c,k} &= \mathbb{E}_{\mathbf{H}|\bar{\mathbf{H}}} \mathbf{H}_{c,c,k}^H \check{\mathbf{R}}_{c,k}^{-1} \mathbf{H}_{c,c,k} \\ &= \bar{\mathbf{H}}_{c,c,k}^H \check{\mathbf{R}}_{c,k}^{-1} \bar{\mathbf{H}}_{c,c,k} + \text{tr}\{\check{\mathbf{R}}_{c,k}^{-1}\} \Theta_{p,c,c,k}\end{aligned}\quad (4.12)$$

$$\begin{aligned}\check{\mathbf{A}}_{c,k} &= \mathbb{E}_{\mathbf{H}|\bar{\mathbf{H}}} \mathbf{A}'_{c,k} = \sum_{(j,i) \neq (c,k)} u_{j,i} [\check{\mathbf{A}}_{j,i,c,k}^C (\mathbf{I}_M + \mathbf{Q}_{c,k} \check{\mathbf{A}}_{j,i,c,k}^C)^{-1} \\ &\quad - \check{\mathbf{A}}_{j,i,c,k}^D (\mathbf{I}_M + \mathbf{Q}_{c,k} \check{\mathbf{A}}_{j,i,c,k}^D)^{-1}];\end{aligned}\quad (4.13)$$

with

$$\begin{aligned}\check{\mathbf{A}}_{j,i,c,k}^C &= \bar{\mathbf{H}}_{c,j,i}^H \check{\mathbf{R}}_{j,i,c,k}^{-1} \bar{\mathbf{H}}_{c,j,i} + \text{tr}\{\check{\mathbf{R}}_{j,i,c,k}^{-1}\} \Theta_{p,c,j,i} \\ \check{\mathbf{A}}_{j,i,c,k}^D &= \bar{\mathbf{H}}_{c,j,i}^H \check{\mathbf{R}}_{j,i,c,k}^{-1} \bar{\mathbf{H}}_{c,j,i} + \text{tr}\{\check{\mathbf{R}}_{j,i,c,k}^{-1}\} \Theta_{p,c,j,i}; \\ \check{\mathbf{R}}_{j,i,c,k} &= \sigma^2 \mathbf{I}_N + \bar{\mathbf{H}}_{j,i} \mathbf{Q}_{j,i,c,k} \bar{\mathbf{H}}_{j,i}^H + \text{tr}\{\mathbf{Q}_{j,i,c,k} \Theta_{p,j,i}\} \mathbf{I}_N; \\ \check{\mathbf{R}}_{j,i,c,k} &= \sigma^2 \mathbf{I}_N + \bar{\mathbf{H}}_{j,i} \mathbf{Q}_{c,k} \bar{\mathbf{H}}_{j,i}^H + \text{tr}\{\mathbf{Q}_{c,k} \Theta_{p,j,i}\} \mathbf{I}_N\end{aligned}\quad (4.14)$$

where $\mathbf{Q}_{j,i,c,k} = \mathbf{Q} - \mathbf{I}_c \mathbf{Q}_{c,k} \mathbf{I}_c^H - \mathbf{I}_j \mathbf{Q}_{j,i} \mathbf{I}_j^H$. The proof is given in Appendix C. As in section 1.4.2, to get the normalized precoder we use

$$\mathbf{G}'_{c,k} = \text{eigenmatrix}(\check{\mathbf{B}}_{c,k}, \check{\mathbf{A}}_{c,k} + \lambda_c \mathbf{I}_M) \quad (4.15)$$

with eigenvalues $\Sigma_{c,k} = \text{eigenvalues}(\check{\mathbf{B}}_{c,k}, \check{\mathbf{A}}_{c,k} + \lambda_c \mathbf{I}_M)$.

Let $\Sigma_{c,k}^{(1)} = \mathbf{G}'_{c,k} \check{\mathbf{B}}_{c,k} \mathbf{G}'_{c,k}$, $\Sigma_{c,k}^{(2)} = \mathbf{G}'_{c,k} \check{\mathbf{A}}_{c,k} \mathbf{G}'_{c,k}$. Powers $\mathbf{P}_{c,k} \geq 0$ are defined as in (1.19). λ_c is determined also as described in section 1.4.2. And we can take also only $d_{c,k}^{max}$ max eigenvectors as described in section 1.4.2. The algorithm can be then summarized as in Table 4.1. The more intuitive expression for $\check{\mathbf{A}}_{c,k}$ is given next. It provides more or less the same performance as (4.13) does.

4.3.1 Alternative expression of $\check{\mathbf{A}}_{c,k}$

Another expression of $\check{\mathbf{A}}_{c,k}$ can be derived using (4.6).

$$\begin{aligned}\check{\mathbf{A}}_{c,k} &= \mathbb{E}_{\mathbf{H}|\bar{\mathbf{H}}} \hat{\mathbf{A}}'_{c,k} = \sum_{(j,i) \neq (c,k)} u_{j,i} \bar{\mathbf{H}}_{c,j,i}^H (\check{\mathbf{R}}_{j,i}^{-1} - \check{\mathbf{R}}_{j,i}^{-1}) \bar{\mathbf{H}}_{c,j,i} \\ &\quad + \text{tr}\{\check{\mathbf{R}}_{j,i}^{-1} - \check{\mathbf{R}}_{j,i}^{-1}\} \Theta_{p,c,j,i}\end{aligned}\quad (4.16)$$

TABLE 4.1: The Iterative Algorithm

```

For  $(c, k) = (1, 1) \dots (C, K)$ , initialize  $\mathbf{Q}_{c,k}$ 
Repeat until convergence
  For  $c = 1 \dots C$ 
    Set  $\underline{\lambda}_c = 0, \bar{\lambda}_c = \lambda_{max}$ 
    For  $k$ 
      Compute  $\check{\mathbf{A}}_{c,k}$  using (4.13)
    Next  $k$ 
    Repeat until convergence
       $\lambda_c = \frac{1}{2}(\underline{\lambda}_c + \bar{\lambda}_c)$ 
      For  $k$ 
        Compute  $\check{\mathbf{B}}_{c,k}$  using (4.12)
        Compute the generalized eigenmatrix  $\mathbf{G}_{c,k}$  of  $\check{\mathbf{B}}_{c,k}$ 
          and  $\check{\mathbf{A}}_{c,k} + \lambda_c \mathbf{I}_M$ 
        Normalize the generalized eigenmatrix so as to have  $\mathbf{G}'_{c,k}$ 
        Compute  $\boldsymbol{\Sigma}_{c,k}^{(1)} = \mathbf{G}'_{c,k} \check{\mathbf{B}}_{c,k} \mathbf{G}'_{c,k}$ ,  $\boldsymbol{\Sigma}_{c,k}^{(2)} = \mathbf{G}'_{c,k} \check{\mathbf{A}}_{c,k} \mathbf{G}'_{c,k}$ 
        Compute  $\mathbf{P}_{c,k}$  as in (1.19)
      Next  $k$ 
      Compute  $\mathbf{P} = \sum_k \mathbf{P}_{c,k}$ 
      if  $\text{tr}(\mathbf{P}) \geq P_c$ , set  $\underline{\lambda}_c = \lambda$ , otherwise set  $\bar{\lambda}_c = \lambda$ 
    For all  $k$ , set  $\mathbf{Q}_{c,k} = \mathbf{G}'_{c,k} \mathbf{P}_{c,k} \mathbf{G}'_{c,k}$ 
  Next  $j$ 

```

Using simulations, it can be shown that (4.13) and (4.16) achieve the same performance. We didn't include these simulations in this manuscript.

Another way to solve the EWSR is to apply (4.6) directly on the EWSR in (1.24). We divide this latter into two parts. One corresponding to the rate of the user of interest (c,k) , concave in $\mathbf{Q}_{c,k}$, and the other part corresponding to the sum rate of the other users.

$$\begin{aligned}
EWSR = & u_{c,k} \log \det \{ \mathbf{I}_N + \check{\mathbf{R}}_{c,k} (\mathbf{H}_{c,c,k} \mathbf{Q}_{c,k} \mathbf{H}_{c,c,k}^H + \text{tr} \{ \mathbf{Q}_{c,k} \mathbf{C}_{p,c,c,k} \}) \} \\
& + \sum_{(j,i) \neq (c,k)} u_{j,i} \log \det \{ \mathbf{I}_N + \check{\mathbf{R}}_{j,i} (\mathbf{H}_{j,j,i} \mathbf{Q}_{j,i} \mathbf{H}_{j,j,i}^H + \text{tr} \{ \mathbf{Q}_{j,i} \mathbf{C}_{p,j,j,i} \}) \}
\end{aligned} \tag{4.17}$$

Consider the first order Taylor series expansion in $\mathbf{Q}_{c,k}$, we get

$$\check{\mathbf{A}}_{c,k} = \sum_{(j,i) \neq (c,k)} u_{j,i} \bar{\mathbf{H}}_{c,j,i}^H (\check{\mathbf{R}}_{j,i}^{-1} - \check{\mathbf{R}}_{j,i}^{-1}) \bar{\mathbf{H}}_{c,j,i} + \text{tr} \{ \check{\mathbf{R}}_{j,i}^{-1} - \check{\mathbf{R}}_{j,i}^{-1} \} \boldsymbol{\Theta}_{p,c,j,i} \tag{4.18}$$

which is the same as (4.16). And $\check{\mathbf{B}}_{c,k}$ can then be given by:

$$\check{\mathbf{B}}_{c,k} = \overline{\mathbf{H}}_{c,c,k}^H \check{\mathbf{R}}_{c,k}^{-1} \overline{\mathbf{H}}_{c,c,k} + \text{tr}\{\check{\mathbf{R}}_{c,k}^{-1}\} \boldsymbol{\Theta}_{p,c,c,k} \quad (4.19)$$

4.4 Numerical results and interpretation

In this section, we evaluate the different approaches ENAIVEKG, EWSMSE and ESEI-WSR through numerical simulations and show the achievable sum rate versus SNR for a MIMO system with $M = 8$. The Transmit covariance matrices $\boldsymbol{\Theta}_{p,i,c,k}$ are considered as uncorrelated identity matrices in Fig. 4.1, Fig. 4.2 and Fig. 4.3 and as correlated low rank matrices (rank = 4) in Fig. 4.4, Fig. 4.5 and Fig. 4.6. The low rank property of the correlation matrices is demonstrated in the work [41].

In our study, we apply the DA approach. We suppose that the error part of the signal has 25 percent of the total gain. From (1.22), we construct the channels $\mathbf{H}_{i,c,k}$ and the channel estimates $\overline{\mathbf{H}}_{i,c,k}$, for all i , c and k :

$$\mathbf{H}_{i,c,k} = \tilde{\mathbf{H}}_{i,c,k}^{(1)} \boldsymbol{\Theta}_{t,i,c,k}^{1/2} + \tilde{\mathbf{H}}_{i,c,k}^{(2)} \boldsymbol{\Theta}_{p,i,c,k}^{1/2} \quad (4.20)$$

$$\overline{\mathbf{H}}_{i,c,k} = \tilde{\mathbf{H}}_{i,c,k}^{(1)} \boldsymbol{\Theta}_{t,i,c,k}^{1/2} \quad (4.21)$$

Moreover, for the uncorrelated identity matrices of Fig. 4.1, Fig. 4.2 and Fig. 4.3, we have :

$$\boldsymbol{\Theta}_{p,i,c,k} = \alpha^2 \mathbf{I}_M \quad (4.22)$$

and

$$\boldsymbol{\Theta}_{t,i,c,k} = (1 - \alpha^2) \mathbf{I}_M \quad (4.23)$$

with α^2 accounting for the percentage of the gain residing in the error part. We take $\alpha^2 = \frac{1}{4}$. We note that in order to do the simulations correctly, we must consider that all of the real channel, the estimate and the error have the same rank, i.e. 4. In other words, for the correlated channel estimate covariance matrices, we take:

$$\boldsymbol{\Theta}_{p,i,c,k} = \alpha^2 \frac{\mathbf{S}\mathbf{S}^H}{\text{tr}(\mathbf{S}\mathbf{S}^H)} \times M \quad (4.24)$$

and

$$\boldsymbol{\Theta}_{t,i,c,k} = (1 - \alpha^2) \frac{\mathbf{T}\mathbf{T}^H}{\text{tr}(\mathbf{T}\mathbf{T}^H)} \times M \quad (4.25)$$

where \mathbf{S} and \mathbf{T} are matrices of dimension 8×4 whose elements are i.i.d. Furthermore, we apply DA on the different approaches. The simulations' parameters for all the figures are summarized in Table 4.2. As the figures

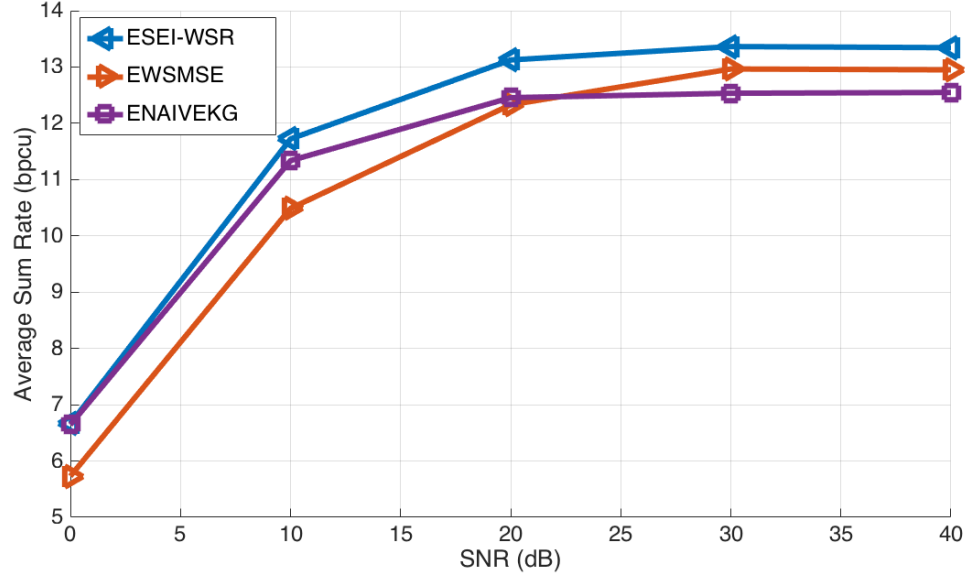


FIGURE 4.1: Sum rate comparisons for $C=2$, $M=8$, $K=4$, $N=1$ and uncorrelated channels, identity channel covariance matrices

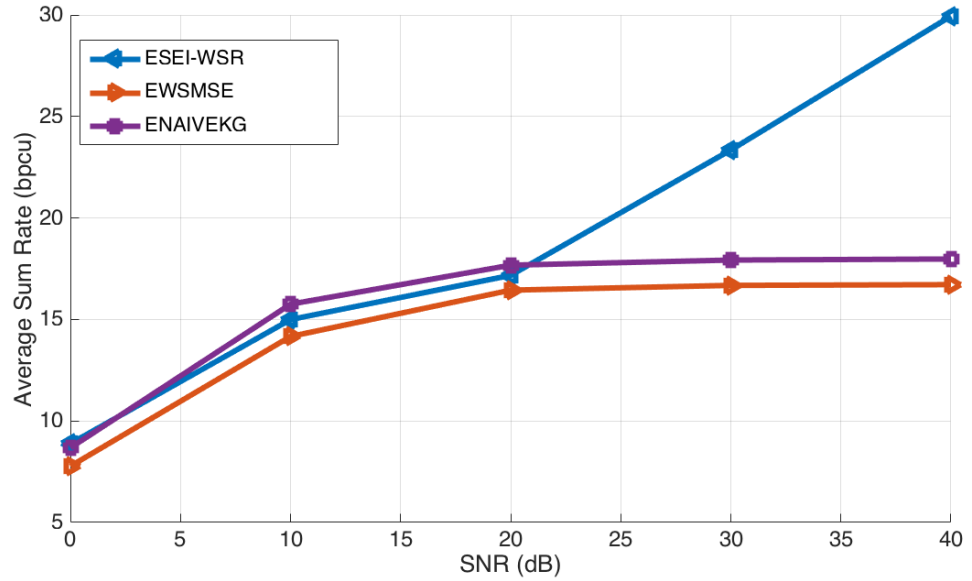


FIGURE 4.2: Sum rate comparisons for $C=2$, $M=8$, $K=4$, $N=2$ and uncorrelated channels, identity channel covariance matrices

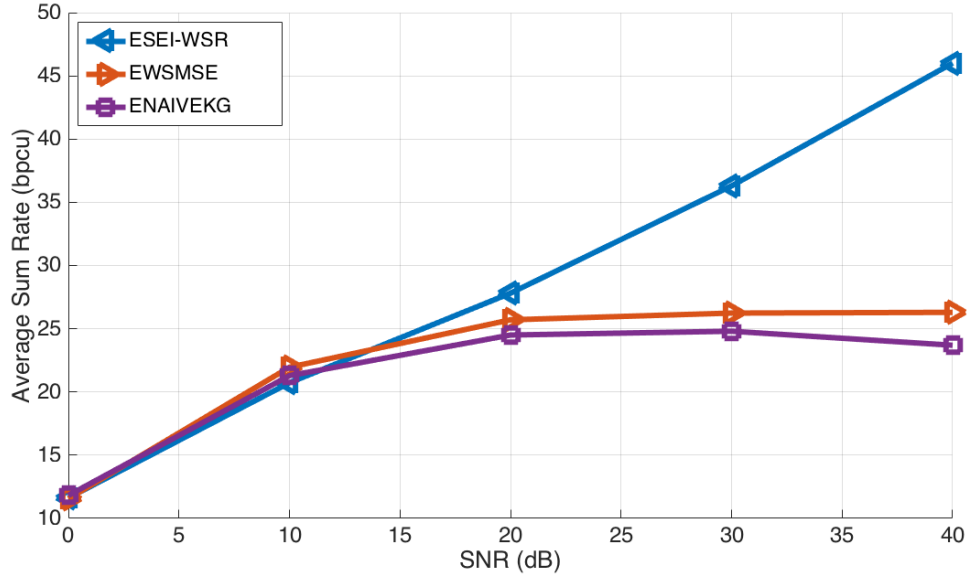


FIGURE 4.3: Sum rate comparisons for $C=2$, $M=8$, $K=4$, $N=4$ and uncorrelated channels, identity channel covariance matrices

suggest, the ESEI-WSR is, in general, the best precoder. The EWSMSE approach improves over ENAIVEKG by accounting for covariance CSIT in the interference. The improvement can be significant if the instantaneous channel CSIT quality does not scale with SNR. However, we note from (4.5) that EWSMSE also moves the channel estimation error in the signal term to the interference plus noise.

A further improvement is proposed here in the ESEI-WSR approach which represents a better approximation of the EWSR. In this approach, the channel uncertainty in the signal term is accounted for in the signal power. In fact, in the Massive MU MIMO setting, ESEI-WSR represents an EWSR upper bound due to the concavity of $\log(\cdot)$.

Furthermore, Fig. 4.7 shows the convergence of the ESEI-WSR with DA at 0 and 20 dB. We observe that the algorithm converges on average in few steps. Note that we must add on some more steps, e.g. for the case of 20 dB we must add some iterations which are necessary for the convergence of the precoder at SNRs = 0 and 10 dB according to the DA principle. So, the total number of iterations required is on average 3 – 4 times the number shown in this figure for 20 dB. The algorithm converges monotonically.

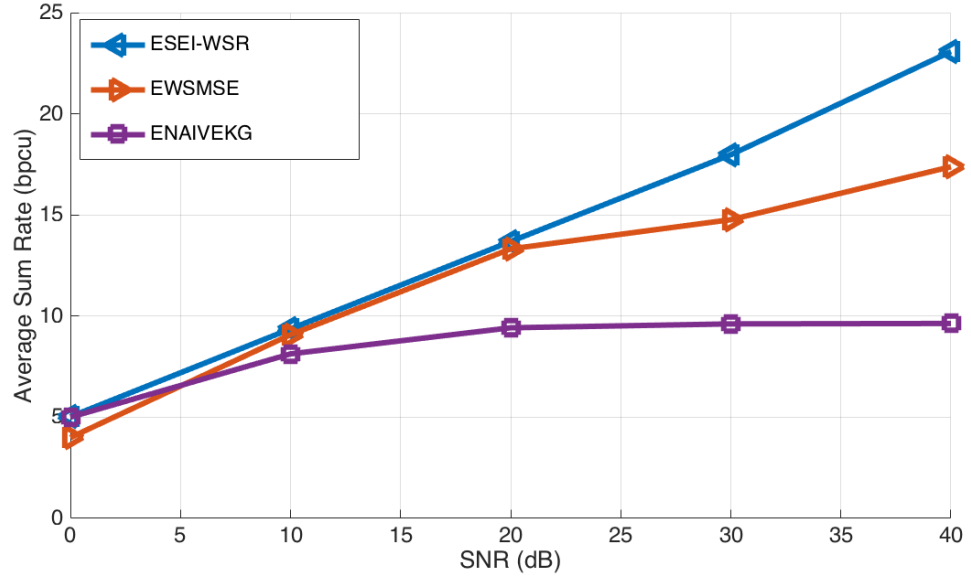


FIGURE 4.4: Sum rate comparisons for $C=2$, $M=8$, $K=4$, $N=1$ and correlated low rank channels

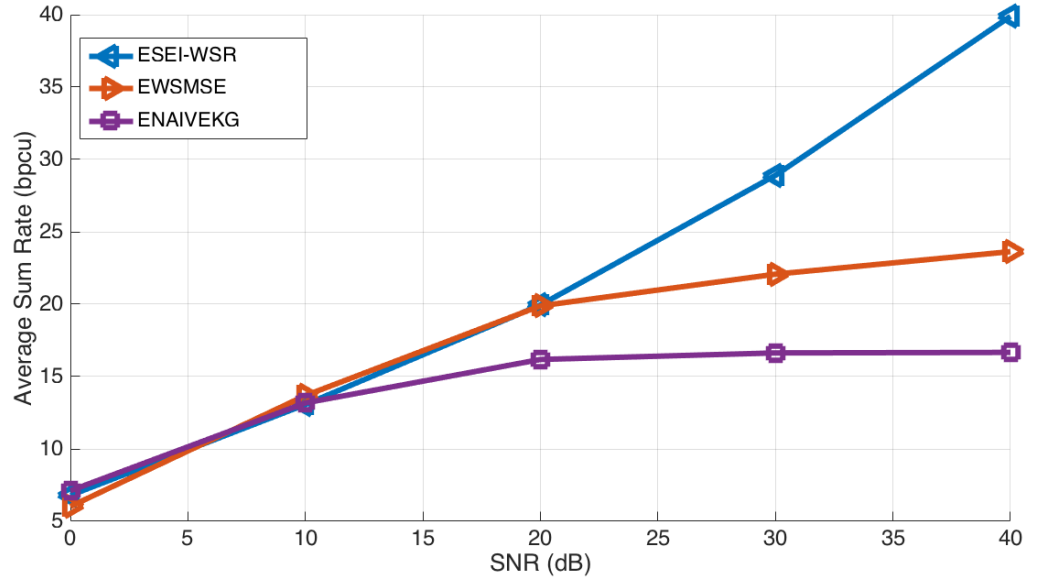


FIGURE 4.5: Sum rate comparisons for $C=2$, $M=8$, $K=4$, $N=2$ and correlated low rank channels

4.5 Practical decentralized solution

Our algorithm is difficult to be applied in practical systems because of the extensive exchange of information between the different base stations. To cope

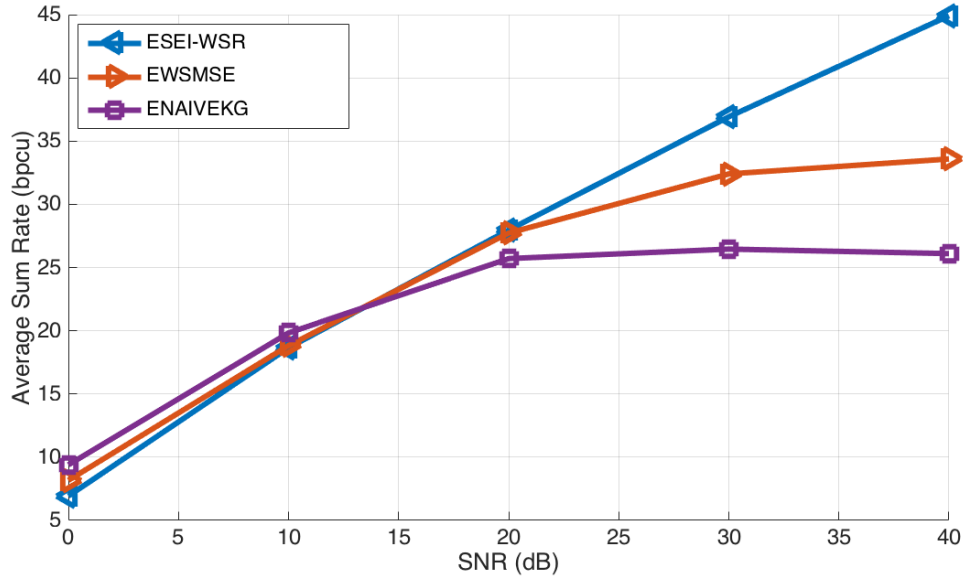


FIGURE 4.6: Sum rate comparisons for $C=2$, $M=8$, $K=4$, $N=4$ and correlated low rank channels

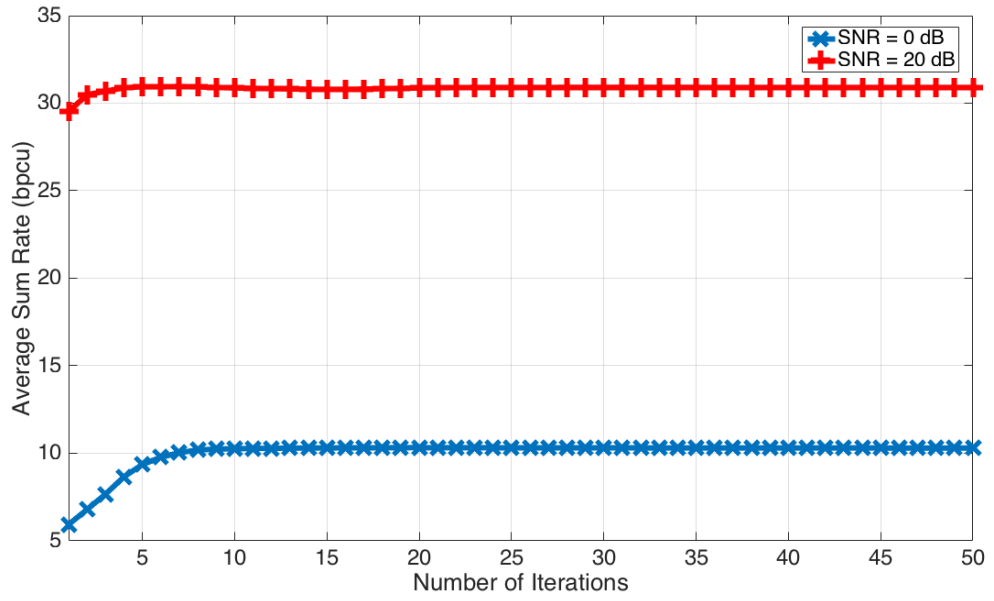


FIGURE 4.7: Convergence behavior for $C=2$, $M=8$, $K=4$, $N=4$ and correlated low rank channels

with this issue, we extend our ESEI-WSR algorithm in a way that it requires only instantaneous CSIT towards the desired receiver and statistics of the users of the others cells. Thus, we suppose that, always in the TDD case, a BS does not have any estimate for the intercell channels and that the intracell channels

are perfect, namely, for all c and k , $\mathbf{H}_{c,c,k} = \overline{\mathbf{H}}_{c,c,k}$; $\mathbf{H}_{j,c,k} = \boldsymbol{\Theta}_{p,j,c,k}^{1/2} \tilde{\mathbf{H}}_{j,c,k}^{(1)}$ for $j \neq c$. We suppose that BS j knows $\boldsymbol{\Theta}_{p,j,c,k}$ by reciprocity; in real systems, $\boldsymbol{\Theta}_{p,j,c,k}$ vary very slowly over time¹. The resultant algorithm is suitable for distributed implementation and has a low complexity with fast realization. In this case, we have:

$$\check{\mathbf{R}}_{c,k} = \sigma^2 \mathbf{I}_N + \mathbf{H}_{c,c,k} \mathbf{Q}_c \mathbf{H}_{c,c,k}^H + \text{tr}\{\mathbf{Q}_{\bar{c}} \boldsymbol{\Theta}_{p,c,k}\} \mathbf{I}_N \quad (4.26)$$

where $\mathbf{Q}_{\bar{c}} = \mathbf{Q} - \mathbf{I}_c \mathbf{Q}_c \mathbf{I}_c^H$.

$$\check{\mathbf{R}}_{\overline{c,k}} = \sigma^2 \mathbf{I}_N + \mathbf{H}_{c,c,k} \mathbf{Q}'_{c,k} \mathbf{H}_{c,c,k}^H + \text{tr}\{\mathbf{Q}_{\bar{c}} \boldsymbol{\Theta}_{p,c,k}\} \mathbf{I}_N \quad (4.27)$$

where $\mathbf{Q}'_{c,k} = \mathbf{Q}_c - \mathbf{Q}_{c,k}$.

$$\check{\mathbf{B}}_{c,k} = \mathbf{H}_{c,c,k}^H \check{\mathbf{R}}_{c,k}^{-1} \mathbf{H}_{c,c,k}. \quad (4.28)$$

$$\begin{aligned} \check{\mathbf{A}}_{c,k} = & \sum_{j \neq c} \sum_i u_{j,i} [\check{\mathbf{A}}_{j,i,c,k}^C (\mathbf{I}_M + \mathbf{Q}_{c,k} \check{\mathbf{A}}_{j,i,c,k}^C)^{-1} \\ & - \check{\mathbf{A}}_{j,i,c,k}^D (\mathbf{I}_M + \mathbf{Q}_{c,k} \check{\mathbf{A}}_{j,i,c,k}^D)^{-1}] \\ & + \sum_{i \neq k} u_{c,i} [\check{\mathbf{A}}_{c,i,c,k}^C (\mathbf{I}_M + \mathbf{Q}_{c,k} \check{\mathbf{A}}_{c,i,c,k}^C)^{-1} \\ & - \check{\mathbf{A}}_{c,i,c,k}^D (\mathbf{I}_M + \mathbf{Q}_{c,k} \check{\mathbf{A}}_{c,i,c,k}^D)^{-1}]; \end{aligned} \quad (4.29)$$

with, for $j \neq c$,

$$\check{\mathbf{A}}_{j,i,c,k}^C = \text{tr}\{\check{\mathbf{R}}_{j,i,c,k}^{-1}\} \boldsymbol{\Theta}_{p,c,j,i}; \quad (4.30)$$

$$\check{\mathbf{A}}_{j,i,c,k}^D = \text{tr}\{\check{\mathbf{R}}_{j,i,c,k}^{-1}\} \boldsymbol{\Theta}_{p,c,j,i}; \quad (4.31)$$

$$\check{\mathbf{R}}_{\overline{j,i,c,k}} = \sigma^2 \mathbf{I}_N + \mathbf{H}_{j,j,i} \mathbf{Q}'_{j,i} \mathbf{H}_{j,j,i}^H + \text{tr}\{\mathbf{Q}_{\bar{j,c,k}} \boldsymbol{\Theta}_{p,j,i}\} \mathbf{I}_N; \quad (4.32)$$

where $\mathbf{Q}_{\bar{j,c,k}} = \mathbf{Q} - \mathbf{I}_j \mathbf{Q}_j \mathbf{I}_j^H - \mathbf{I}_c \mathbf{Q}_{c,k} \mathbf{I}_c^H$.

$$\check{\mathbf{R}}_{j,i,c,k} = \sigma^2 \mathbf{I}_N + \mathbf{H}_{j,j,i} \mathbf{Q}_j \mathbf{H}_{j,j,i}^H + \text{tr}\{\mathbf{Q}_{\bar{j,c,k}} \boldsymbol{\Theta}_{p,j,i}\} \mathbf{I}_N; \quad (4.33)$$

and with, for $j = c$,

$$\check{\mathbf{A}}_{c,i,c,k}^C = \mathbf{H}_{c,c,i}^H \check{\mathbf{R}}_{c,i,c,k}^{-1} \mathbf{H}_{c,c,i}; \quad (4.34)$$

¹Although we operate in TDD but this slow variation of $\boldsymbol{\Theta}_{p,j,c,k}$ can be profitable for FDD mode as the mobile feedbacks over-the-air and the backhaul capacity consumption can be suitable with low exchange rhythm

$$\check{\mathbf{A}}_{c,i,c,k}^D = \mathbf{H}_{c,c,i}^H \check{\mathbf{R}}_{c,i,c,k}^{-1} \mathbf{H}_{c,c,i}; \quad (4.35)$$

$$\check{\mathbf{R}}_{c,i,c,k} = \sigma^2 \mathbf{I}_N + \mathbf{H}_{c,c,i} \mathbf{Q}_{c,i,c,k}' \mathbf{H}_{c,c,i}^H + \text{tr}\{\mathbf{Q}_{\bar{c}} \boldsymbol{\Theta}_{p,c,i}\} \mathbf{I}_N; \quad (4.36)$$

where $\mathbf{Q}_{c,i,c,k}' = \mathbf{Q}_c - \mathbf{Q}_{c,i} - \mathbf{Q}_{c,k}$.

$$\check{\mathbf{R}}_{c,i,c,k} = \sigma^2 \mathbf{I}_N + \mathbf{H}_{c,c,i} \mathbf{Q}_{c,k}' \mathbf{H}_{c,c,i}^H + \text{tr}\{\mathbf{Q}_{\bar{c}} \boldsymbol{\Theta}_{p,c,i}\} \mathbf{I}_N; \quad (4.37)$$

In order to build the precoder, each BS must know $\check{\mathbf{B}}_{c,k}$ and $\check{\mathbf{A}}_{c,k}$ for each of its users. To obtain $\check{\mathbf{A}}_{c,k}$ from (4.29), we need $\check{\mathbf{A}}_{j,i,c,k}^C$ and $\check{\mathbf{A}}_{j,i,c,k}^D$. To obtain $\check{\mathbf{A}}_{j,i,c,k}^D$ of (4.31), BS c just needs to know the trace of $\check{\mathbf{R}}_{j,i,c,k}^{-1}$ which will be given by BS j . From (4.33), j possesses the second matrix term and still needs the third term which is the product of a scalar and an identity matrix. This scalar is the trace of $\mathbf{Q}_{\bar{j},c,k} \boldsymbol{\Theta}_{p,j,i}$, which is a block diagonal matrix.

Next, exchange (E1) takes place. Then, BS j possesses all the necessary traces to obtain the third term, since the trace of a sum of matrices equals the sum of the traces of each matrix.

Exchange (E1) denotes that each BS l calculates the trace of $\mathbf{Q}_{l,m} \boldsymbol{\Theta}_{p,l,j,i}$ and sends it to BS j where $l = 1 \dots C$, $j = 1 \dots C$, $l \neq j$, $m = 1 \dots K$, $i = 1 \dots K$.

To obtain $\check{\mathbf{A}}_{c,i,c,k}^D$ of (4.35), the BS c needs $\check{\mathbf{R}}_{c,i,c,k}$ of (4.37). BS c possesses its second term, while for the third term, it can be obtained from the exchange (E1). Following a similar analysis, we can obtain $\check{\mathbf{A}}_{j,i,c,k}^C$ for all j . To obtain $\check{\mathbf{B}}_{c,k}$ of (4.28), BS c requires $\check{\mathbf{R}}_{c,k}$ as given in (4.27) where the second term is known by the BS itself and the third term, which is the same as the third term in (4.37) known above, can be gathered once (E1) is done. Herein, our solution is very suitable for practical distributed implementations because only scalars must be exchanged as in (E1).

The algorithm in Table 4.1 can still be applied by simply replacing the equations (4.13) and (4.12) by (4.29) and (4.28) respectively. We suppose as well for the EWSME null intercell channel estimates and perfect intracell channels and we compare both algorithms in Figures 4.8, 4.9 and 4.10. Although the authors in [42] studied our practical scenario for uncorrelated channels, $\Theta_{i,j,k} = \eta_{i,j,k} I_M$ for all i, j, k , and proposed a precoder in their paper, the authors attempted to provide a low-complexity closed-form precoder. Therefore, it cannot be compared to our precoder which results from an iterative algorithm.

Let us start with Fig. 4.8 corresponding to uncorrelated channels. We can observe that the ESEI-WSR is slightly better than the EWSMSE at low SNR

TABLE 4.2: Simulation Parameters : 'Y' denotes 'yes' and 'N' denotes 'no'

| Figure 4. | 4 | 5 | 6 | 7 |
|---------------------------------|----|----|----|----|
| Number of Cells C | 2 | 2 | 2 | 2 |
| Number of Transmit antennas M | 8 | 8 | 8 | 8 |
| Number of users per Cell K | 4 | 4 | 4 | 4 |
| Number of Receive Antennas N | 1 | 2 | 4 | 1 |
| Number of Channel Realizations | 50 | 50 | 50 | 50 |
| Low Rank Correlated Channels | N | N | N | Y |
| Rank | 8 | 8 | 8 | 4 |
| Uncorrelated Identity Matrices | Y | Y | Y | N |

| Figure 4. | 8 | 9 | 10 | 11 | 12 |
|---------------------------------|----|----|----|----|----|
| Number of Cells C | 2 | 2 | 2 | 2 | 2 |
| Number of Transmit antennas M | 8 | 8 | 8 | 8 | 8 |
| Number of users per Cell K | 4 | 4 | 4 | 3 | 4 |
| Number of Receive Antennas N | 2 | 4 | 4 | 4 | 4 |
| Number of Channel Realizations | 50 | 50 | 50 | 50 | 50 |
| Low Rank Correlated Channels | Y | Y | N | N | Y |
| Rank | 4 | 4 | 8 | 8 | 4 |
| Uncorrelated Identity Matrices | N | N | Y | Y | N |

but worse than the EWSMSE at high SNR. This result is contradictory to the result obtained in Fig. 4.3. This is due to the fact that the system is fully loaded. We recall that the load is given by:

$$load = \frac{CK}{M} \quad (4.38)$$

For Fig.4.8, $load = 1$ and hence the system is fully loaded. So as to avoid this problem, we propose a slight decrease of the load, as shown in Fig. 4.9. As expected, the ESEI-WSR returns to its normal behavior and outperforms the EWSMSE algorithm. Finally, in Fig.4.10 corresponding to correlated low rank channels, we remark that our ESEI-WSR outperforms the EWSMSE almost every time.

From now on we will consider the IBC MISO system model explained in Chapter 2. The goal is to perform a large system analysis of the beamforming algorithms in the case of partial CSIT as done in 2.3.2 but the case of perfect CSIT.

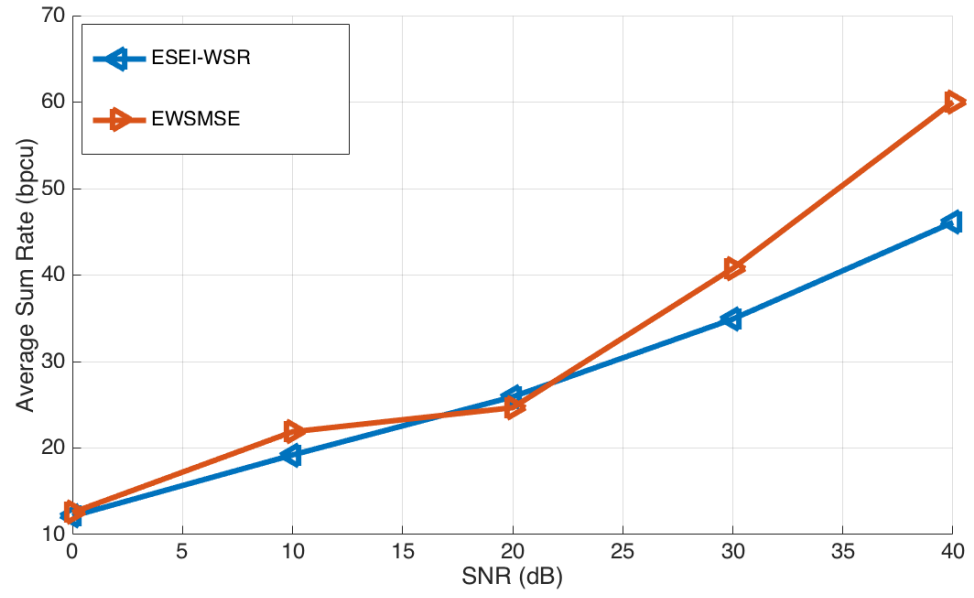


FIGURE 4.8: Sum rate comparisons for $C=2$, $M=8$, $K=4$, $N=4$ and uncorrelated channels, identity channel covariance matrices

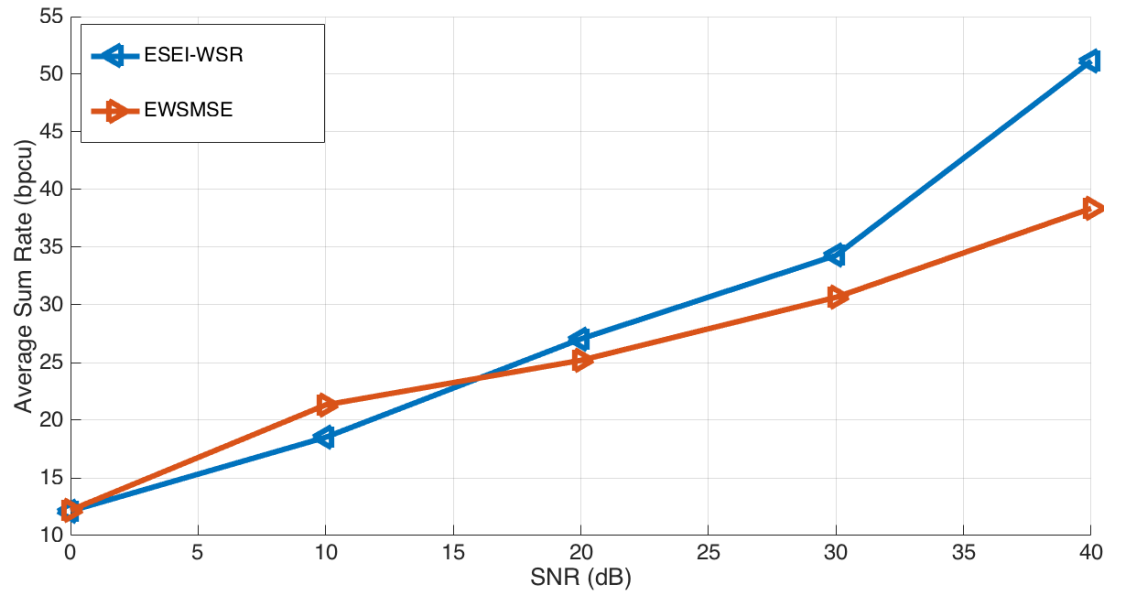


FIGURE 4.9: Sum rate comparisons for $C=2$, $M=8$, $K=3$, $N=4$ and uncorrelated channels, identity channel covariance matrices

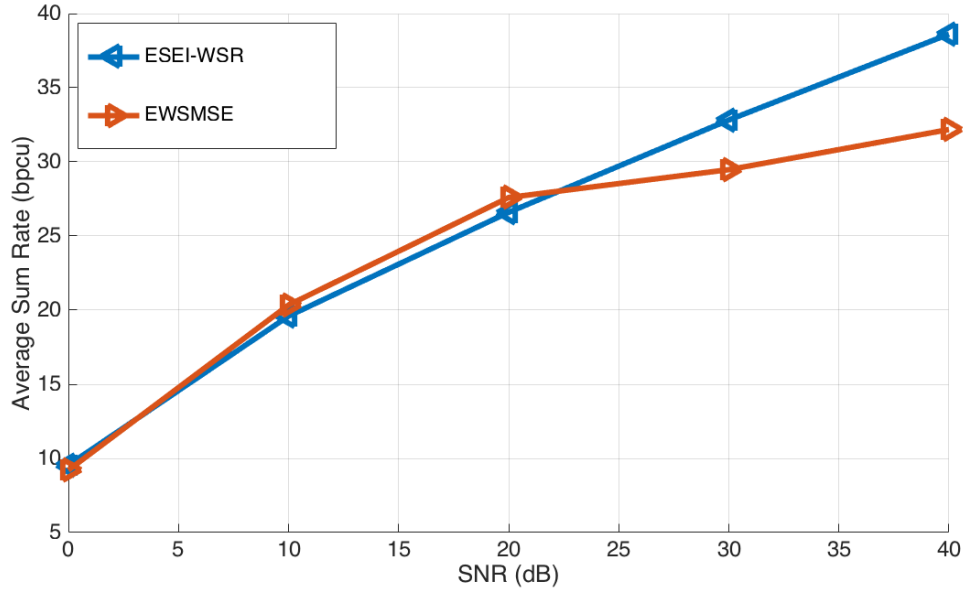


FIGURE 4.10: Sum rate comparisons for $C=2$, $M=8$, $K=4$, $N=4$ and correlated low rank channels

4.6 The MISO case for large system analysis

In this case we shall denote the matrices \mathbf{R} , \mathbf{H}^H as the scalar r and the vector \mathbf{h} . $\mathbf{S} = \mathbb{E}_{\mathbf{h}|\bar{\mathbf{h}}} \mathbf{h}\mathbf{h}^H = \bar{\mathbf{h}}\bar{\mathbf{h}}^H + \mathbf{\Theta}_p$. We consider a system-wide numbering of the users for this section and the next one.

4.6.1 Max EWSR BF (ESEI-WSR) in the MaMISO limit

The EWSR represents two rounds of averaging over the partial CSIT

$$\begin{aligned}
 EWSR &= \mathbb{E}_{\bar{\mathbf{h}}} \max_{\mathbf{g}} EWSR(\mathbf{g}) \\
 EWSR(\mathbf{g}) &= \mathbb{E}_{\mathbf{h}|\bar{\mathbf{h}}} WSR(g) = \sum_{k=1}^K u_k \mathbb{E}_{\mathbf{h}|\bar{\mathbf{h}}} \log(r_k/\bar{r}_k) \\
 &\stackrel{(a)}{=} \sum_{k=1}^K u_k [\log(\bar{r}_k) - \log(\bar{r}_k)]
 \end{aligned} \tag{4.39}$$

where transition (a) represents the MaMISO limit and

$$\begin{aligned}
 \bar{r}_k &= 1 + \sum_{i \neq k} \mathbb{E}_{\mathbf{h}|\bar{\mathbf{h}}} |\mathbf{h}_{k,b_i}^H \mathbf{g}_i|^2 = 1 + \sum_{i \neq k} \mathbf{g}_i^H \mathbf{S}_{k,b_i} \mathbf{g}_i \\
 \bar{r}_k &= \bar{r}_k + \mathbf{g}_k^H \mathbf{S}_{k,b_k} \mathbf{g}_k.
 \end{aligned} \tag{4.40}$$

By adding the Lagrange terms for the BS power constraints, $\sum_{c=1}^C \lambda_c (P_c - \sum_{k:b_k=c} \|\mathbf{g}_k\|^2)$, to the EWSR in (4.39), we get the gradient

$$\begin{aligned} \frac{\partial EWSR}{\partial \mathbf{g}_k^*} &= \alpha_k \mathbf{S}_{k,b_k} \mathbf{g}_k - \left[\sum_{i \neq k} \beta_i \mathbf{S}_{i,b_k} + \lambda_{b_k} \mathbf{I} \right] \mathbf{g}_k = 0 \\ \alpha_k &= \frac{u_k}{\bar{r}_k}, \quad \beta_k = u_k \left(\frac{1}{\bar{r}_k} - \frac{1}{\bar{r}_k} \right). \end{aligned} \quad (4.41)$$

This leads to the iterative (power method like) solution

$$\begin{aligned} \mathbf{g}'_k(\lambda_{b_k}) &= \left[\sum_{i \neq k} \beta_i \bar{\mathbf{h}}_{i,b_k} \bar{\mathbf{h}}_{i,b_k}^H + \Theta_{p,k} + \lambda_{b_k} \mathbf{I} \right]^{-1} \bar{\mathbf{h}}_{k,b_k} \alpha_k \hat{\mathbf{h}}_{k,b_k}^H \mathbf{g}_k \\ \mathbf{g}_k &= \xi_c \mathbf{g}'_k, \quad \xi_c = \sqrt{P_c / \sum_{k:b_k=c} \|\mathbf{g}'_k(\lambda_{b_k})\|^2} \\ \Theta_{p,k} &= \sum_{i \neq k} \beta_i \Theta_{p,i,b_k} - \alpha_k \Theta_{p,k,b_k}. \end{aligned} \quad (4.42)$$

The BF scale factors ξ_c are introduced because instead of a bisection method to force satisfaction of the power constraints, the Lagrange multipliers (if non-zero) can be adapted analytically as in [40] by exploiting $\sum_{k:b_k=c} \mathbf{g}_k^H \frac{\partial EWSR}{\partial \mathbf{g}_k^*} = 0$ and $\sum_{k:b_k=c} \|\mathbf{g}_k\|^2 = P_c$. Then from (4.41) we get

$$\lambda_c = \begin{cases} \lambda'_c & , \quad \zeta_c > P_c \\ 0 & , \quad \zeta_c \leq P_c \end{cases} \quad (4.43)$$

where

$$\begin{aligned} \lambda'_c &= \frac{1}{P_c} \sum_{k:b_k=c} [\alpha_k \mathbf{g}_k^H \mathbf{S}_{k,c} \mathbf{g}_k - \sum_{i \neq k} \beta_i \mathbf{g}_k^H \mathbf{S}_{i,c} \mathbf{g}_k] \\ \zeta_c &= \sum_{k:b_k=c} \|\mathbf{g}'_k(0)\|^2 \end{aligned} \quad (4.44)$$

Indeed, in the case of multiple power constraints, not all constraints are necessarily satisfied with equality.

4.6.2 EWSMSE and the naive approach

On one hand, the EWSMSE BF design of 4.2 can be obtained from the EWSR design above by setting $\tilde{\Theta}_{p,k,b_k} = 0$ in (4.40)-(4.44) hence $\mathbf{S}_{k,b_k} = \bar{\mathbf{h}}_{k,b_k} \bar{\mathbf{h}}_{k,b_k}^H$. On the other hand, the naive EWSR approach, which ignores the covariance of in any occurrence, is obtained from the EWSR design above by setting $\tilde{\Theta}_{p,k} = 0$ in (4.40)-(4.44) and setting $\mathbf{S}_{i,c} = \bar{\mathbf{h}}_{i,c} \bar{\mathbf{h}}_{i,c}^H$ for any (i, c) . Of course, these simplifications should be carried out in the BF design from (4.40)-(4.44), but not in the EWSR evaluation in (4.39)-(4.40).

4.7 Large System Approximation of the EWSR

Due to the law of large numbers, the scalars r_k , r_k^- , $a_k = \bar{\mathbf{h}}_{k,b_k}^H \mathbf{g}'_k$, $\|\mathbf{g}'_k(\lambda_{b_k})\|^2$, $\mathbf{g}_k^H \mathbf{S}_{k,c} \mathbf{g}_k$, $\mathbf{g}_k^H \mathbf{S}_{i,c} \mathbf{g}_k$ and hence α_k , β_k , ξ_c , λ'_c and ζ_c converge to deterministic limits as $M, K \rightarrow \infty$ at fixed ratio $\beta = M/K$. We shall perform a large system analysis to determine these deterministic limits, which will also provide the limiting value for

$$EWSR = \sum_{k=1}^K u_k \log(\bar{r}_k / \bar{r}_k^-) = \sum_{k=1}^K u_k \log(1 + \bar{\gamma}_k) \quad (4.45)$$

where the $\bar{\gamma}_k$ are the limiting SINRs. The deterministic limits will follow the same iterations as the BF design algorithm for which we can rewrite iteration j as

$$\begin{aligned} \mu_{k,i}^{(j)} &= \check{\mathbf{g}}_k^{(j-1)H} \mathbf{S}_{i,b_k} \check{\mathbf{g}}_k^{(j-1)}, \quad \forall i, k \\ \bar{r}_k^{(j)} &= 1 + \sum_{i \neq k} \xi_{b_i}^{2,(j-1)} \mu_{i,k}^{(j)}, \quad \bar{r}_k^{(j)} = \bar{r}_k^{(j)} + \xi_{b_k}^{2,(j-1)} \mu_{k,k}^{(j)} \\ \alpha_k^{(j)} &= \frac{u_k}{\bar{r}_k^{(j)}}, \quad \beta_k^{(j)} = u_k \left(\frac{1}{\bar{r}_k^{(j)}} - \frac{1}{\bar{r}_k^{(j)}} \right) \\ a_k^{(j-1)} &= \bar{\mathbf{h}}_{k,b_k}^H \check{\mathbf{g}}_k^{(j-1)} \\ \Theta_{p,k}^{(j)} &= \sum_{i \neq k} \beta_i^{(j)} \Theta_{p,i,b_k} - \alpha_k^{(j)} \Theta_{p,k,b_k} \\ \psi_k^{(j)}(0) &= \bar{\mathbf{h}}_{k,b_k}^H \left[\sum_{i \neq k} \beta_i^{(j)} \bar{\mathbf{h}}_{i,b_k} \bar{\mathbf{h}}_{i,b_k}^H + \Theta_{p,k}^{(j)} \right]^{-2} \bar{\mathbf{h}}_{k,b_k} \\ \nu_k^{(j)} &= \alpha_k^{(j)} \xi_{b_k}^{(j-1)} a_k^{(j-1)} \\ \zeta_c^{(j)} &= \xi_c^{2,(j-1)} \sum_{k:b_k=c} \psi_k^{(j)}(0) \nu_k^{2,(j)} \\ \check{\lambda}_c^{(j)} &= \frac{1}{P_c} \sum_{k:b_k=c} [\alpha_k^{(j)} \xi_{b_k}^{2,(j-1)} \mu_{k,k}^{(j)} - \sum_{i \neq k} \beta_i^{(j)} \xi_{b_k}^{2,(j-1)} \mu_{k,i}^{(j)}] \\ \lambda_c^{(j)} &= \begin{cases} \check{\lambda}_c^{(j)}, & \zeta_c^{(j)} > P_c \\ 0, & \zeta_c^{(j)} \leq P_c \end{cases} \end{aligned} \quad (4.46)$$

$$\begin{aligned} \check{\mathbf{g}}_k^{(j)} &= \left[\sum_{i \neq k} \beta_i^{(j)} \bar{\mathbf{h}}_{i,b_k} \bar{\mathbf{h}}_{i,b_k}^H + \Theta_{p,k}^{(j)} + \lambda_{b_k}^{(j)} \mathbf{I} \right]^{-1} \bar{\mathbf{h}}_{k,b_k} \nu_k^{(j)} \\ \psi_k^{(j)}(\lambda_{b_k}^{(j)}) &= \bar{\mathbf{h}}_{k,b_k}^H \left[\sum_{i \neq k} \beta_i^{(j)} \bar{\mathbf{h}}_{i,b_k} \bar{\mathbf{h}}_{i,b_k}^H + \Theta_{p,k}^{(j)} + \lambda_{b_k}^{(j)} \mathbf{I} \right]^{-2} \bar{\mathbf{h}}_{k,b_k} \\ \xi_c^{(j)} &= \sqrt{P_c / \sum_{k:b_k=c} \psi_k^{(j)}(\lambda_{b_k}^{(j)}) \nu_k^{2,(j)}} \\ \mathbf{g}_k^{(j)} &= \xi_c^{(j)} \check{\mathbf{g}}_k^{(j)} \end{aligned} \quad (4.47)$$

where we used the short-hand notation for e.g. $\nu_k^{2,(j)} = (\nu_k^{(j)})^2$. Note that $a_k^{(j)}$ can be computed recursively by introducing

$$\begin{aligned} \phi_k^{(j)} &= \bar{\mathbf{h}}_{k,b_k}^H \left[\sum_{i \neq k} \beta_i^{(j)} \bar{\mathbf{h}}_{i,b_k} \bar{\mathbf{h}}_{i,b_k}^H + \boldsymbol{\Theta}_k^{(j)} + \lambda_{b_k}^{(j)} \mathbf{I} \right]^{-1} \bar{\mathbf{h}}_{k,b_k}, \\ \Rightarrow a_k^{(j)} &= \phi_k^{(j)} \nu_k^{(j)} = \phi_k^{(j)} \alpha_k^{(j)} \xi_{b_k}^{(j-1)} a_k^{(j-1)}. \end{aligned} \quad (4.48)$$

4.7.1 Large system analysis

In the large system analysis, we do not compute the BFs \mathbf{g}_k . Instead, deterministic limits are determined for the following quantities: $\phi_k^{(j)}$, $\mu_{k,i}^{(j)}$, $\psi_k^{(j)}(0)$, $\psi_k^{(j)}(\lambda_{b_k}^{(j)})$.

The following results can now be obtained by applying the principles applied in section 2.3.2 For (with asymptotic equalities)

$$\begin{aligned} \phi_k &= \bar{\mathbf{h}}_{k,b_k}^H [\sum_{i \neq k} \beta_i \bar{\mathbf{h}}_{i,b_k} \bar{\mathbf{h}}_{i,b_k}^H + \boldsymbol{\Theta}_{p,k} + \lambda_{b_k} \mathbf{I}]^{-1} \bar{\mathbf{h}}_{k,b_k} \\ &= \text{tr}\{\boldsymbol{\Theta}_{p,k,b_k} [\sum_{i \neq k} \beta_i \bar{\mathbf{h}}_{i,b_k} \bar{\mathbf{h}}_{i,b_k}^H + \boldsymbol{\Theta}_{p,k} + \lambda_{b_k} \mathbf{I}]^{-1}\}, \end{aligned} \quad (4.49)$$

the deterministic limit $\phi_k = e_{k,b_k}(\lambda_{b_k})$ can be computed from the C sets of implicit equations

$$e_{k,c}(\lambda_c) = \text{tr}\{\underbrace{\boldsymbol{\Theta}_{t,k,b_k} \left(\sum_{i \neq k} \frac{\beta_i}{1 + \beta_i e_{i,c}(\lambda_c)} \boldsymbol{\Theta}_{t,i,c} + \tilde{\boldsymbol{\Theta}}_{k,c} + \lambda_c \mathbf{I} \right)^{-1}}_{\mathbf{T}_{k,c}(\lambda_c)}\} \quad (4.50)$$

where $\tilde{\boldsymbol{\Theta}}_{k,c} = \sum_{i \neq k} \beta_i \boldsymbol{\Theta}_{p,i,c} - \alpha_k \boldsymbol{\Theta}_{p,k,c}$, hence $\boldsymbol{\Theta}_{p,k} = \tilde{\boldsymbol{\Theta}}_{k,b_k}$. For $\psi_k(\lambda) = \psi_{k,b_k}(\lambda)$, we get

$$\begin{aligned} \psi_{k,b_k}(\lambda) &= \hat{\mathbf{h}}_{k,b_k}^H [\sum_{i \neq k} \beta_i \hat{\mathbf{h}}_{i,b_k} \hat{\mathbf{h}}_{i,b_k}^H + \boldsymbol{\Theta}_{p,k} + \lambda \mathbf{I}]^{-2} \hat{\mathbf{h}}_{k,b_k} \\ &= \text{tr}\{\boldsymbol{\Theta}_{i,k,b_k} [\sum_{i \neq k} \beta_i \hat{\mathbf{h}}_{i,b_k} \hat{\mathbf{h}}_{i,b_k}^H + \boldsymbol{\Theta}_{p,k} + \lambda \mathbf{I}]^{-2}\} \\ &= -\frac{d}{d\lambda} \text{tr}\{\boldsymbol{\Theta}_{t,k,b_k} \mathbf{T}_{k,b_k}^{-1}(\lambda)\} = -e'_{k,b_k}(\lambda) \end{aligned} \quad (4.51)$$

The $\psi_{k,b_k}(\lambda_{b_k})$ can be solved from the linear equations

$$\begin{aligned} \psi_{k,c}(\lambda_c) &= \text{tr}\{\boldsymbol{\Theta}_{t,k,b_k} \mathbf{T}_{k,c}^{-1}(\lambda_c) \mathbf{T}'_{k,c}(\lambda_c) \mathbf{T}_{k,c}^{-1}(\lambda_c)\} \\ \text{with } \mathbf{T}'_{k,c}(\lambda_c) &= \sum_{i \neq k} \frac{\beta_i \psi_{i,c}(\lambda_c)}{(1 + \beta_i e_{i,c}(\lambda_c))^2} \boldsymbol{\Theta}_{t,i,c} + \mathbf{I}. \end{aligned} \quad (4.52)$$

The C sets of equations (4.49) for the C values λ_c have to be augmented with a set $C+1$ for the $e_k(0)$. And also (4.52) has to be considered for $\psi_k(0)$.

For $\mu_{k,i}$ we introduce $\mu_{k,i} = \nu_k^2 \hat{\mu}_{k,i} + \nu_k^2 \tilde{\mu}_{k,i}$ with $\hat{\mu}_{k,i} = \check{\mathbf{g}}_k^H \hat{\mathbf{h}}_{i,b_k} \hat{\mathbf{h}}_{i,b_k}^H \check{\mathbf{g}}_k / \nu_k^2$ and $\tilde{\mu}_{k,i} = \check{\mathbf{g}}_k^H \boldsymbol{\Theta}_{p,i,b_k} \check{\mathbf{g}}_k / \nu_k^2$. We shall obtain $\tilde{\mu}_{k,i}$ as $\tilde{\mu}_{k,i} = e'_{k,b_k,i,b_k} = \frac{\partial}{\partial z} e_{k,b_k,i,b_k}(\lambda_{b_k}, 0)$ where

$$\begin{aligned} e_{k,c,i,d}(\lambda_c, z) &= \text{tr}\{\boldsymbol{\Theta}_{t,k,c} \mathbf{T}_{k,c,i,d}^{-1}(\lambda_c, z)\} \text{ with} \\ \mathbf{T}_{k,c,i,d}(\lambda_c, z) &= \sum_{j \neq k} \frac{\beta_j \boldsymbol{\Theta}_{t,j,c}}{1 + \beta_j e_{j,c,i,d}(\lambda_c, z)} +_{k,c} + \lambda_c \mathbf{I} - z \boldsymbol{\Theta}_{p,i,d} \end{aligned} \quad (4.53)$$

We can then obtain the $e'_{k,c,i,d}$ as the solution of the linear equations

$$\begin{aligned} e'_{k,c,i,d} &= \text{tr}\{\boldsymbol{\Theta}_{t,k,c} \mathbf{T}_{k,c,i,d}^{-1}(\lambda_c, 0) \mathbf{T}'_{k,c,i,d}(\lambda_c, 0) \mathbf{T}_{k,c,i,d}^{-1}(\lambda_c, 0)\} \\ \mathbf{T}'_{k,c,i,d}(\lambda_c, 0) &= \sum_{j \neq k} \frac{\beta_j e'_{j,c,i,d}(\lambda_c)}{(1 + \beta_j e_{j,c,i,d}(\lambda_c))^2} \boldsymbol{\Theta}_{t,j,c} + \boldsymbol{\Theta}_{p,i,d} \end{aligned} \quad (4.54)$$

On the other hand, we get $\hat{\mu}_{k,k} = a_k^2$. For $i \neq k$,

$$\begin{aligned} \hat{\mu}_{k,i} &= |\bar{\mathbf{h}}_{i,b_k}^H [\sum_{j \neq k} \beta_j \bar{\mathbf{h}}_{j,b_k} \bar{\mathbf{h}}_{j,b_k}^H + \boldsymbol{\Theta}_{p,k} + \lambda_{b_k} \mathbf{I}]^{-1} \bar{\mathbf{h}}_{k,b_k}|^2 \\ &= \frac{|\bar{\mathbf{h}}_{i,b_k}^H [\sum_{j \neq k,i} \beta_j \bar{\mathbf{h}}_{j,b_k} \bar{\mathbf{h}}_{j,b_k}^H + \boldsymbol{\Theta}_{p,k} + \lambda_{b_k} \mathbf{I}]^{-1} \bar{\mathbf{h}}_{k,b_k}|^2}{(1 + \beta_i \bar{\mathbf{h}}_{i,b_k}^H [\sum_{j \neq k,i} \beta_j \bar{\mathbf{h}}_{j,b_k} \bar{\mathbf{h}}_{j,b_k}^H + \boldsymbol{\Theta}_{p,k} + \lambda_{b_k} \mathbf{I}]^{-1} \bar{\mathbf{h}}_{i,b_k})^2} \end{aligned} \quad (4.55)$$

Hence $\hat{\mu}_{k,i} = \hat{\mu}_{k,i} / (1 + \beta_i e_{i,b_k}(\lambda_{b_k}))^2$ where the $\hat{\mu}_{k,i}$ are obtained from a system of equations similar to that for $\tilde{\mu}_{k,i}$ (as in (4.53), (4.54)), by replacing the $\boldsymbol{\Theta}_{p,i,b_k}$ by $\boldsymbol{\Theta}_{t,i,b_k}$.

4.7.2 Numerical results for MISO large system analysis

We plot the performance of the proposed ESEI-WSR with MF initialization and compare it to the proposed large system approximation. Figure 4.11 shows the performance of the precoder and its approximation for rank 2 correlated channels. Monte Carlo simulations are averaged over 1000 channel realizations. It can be observed that the approximation is very accurate which validates our asymptotic approach. Although the large system analysis for the sum rate seems complex, we need to calculate it only once per given SNR (independent of channel realization).

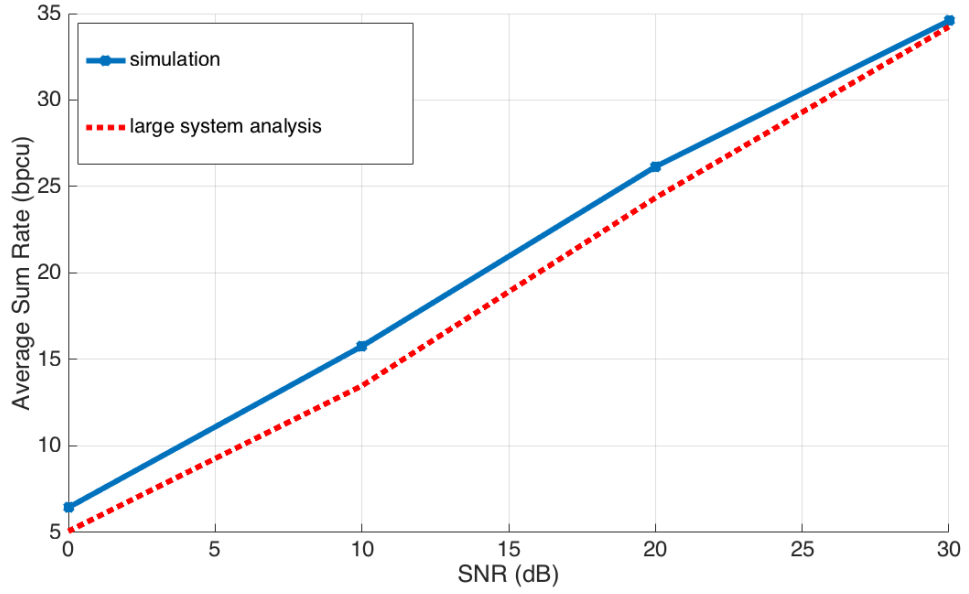


FIGURE 4.11: Sum rate comparison for $C = 2, K = 6, M = 15, N = 1 \forall k$ and $\text{rank}(\mathbf{C}_{t,i,b_k}) = \text{rank}(\mathbf{C}_{p,i,b_k}) = 2 \forall i, \forall k$ and $\alpha^2 = \frac{1}{10}$

4.8 Alternative (sub-optimal) approach

We propose another precoder to optimize the EWSR under partial CSIT. We reconsider as the KG algorithm in 1.4.2 but this time we apply results from a slightly different type of large system analysis which considers that the number of transmit antennas at the Tx and the number of receive antennas at the users are jointly going to infinity with bounded ratio whereas until now we have supposed that the number of transmit antennas and the number of users go jointly to infinity. Indeed, this particular regime of large systems is not in line with what future network will look like. In sub-6 GHz bands receivers will be merely equipped with 2 or 4 antennas. However, our study would still be very beneficial, since all the results that we obtain are accurate even when the number of users' antennas is finite or small. A recent paper in [43] used this assumption (regime), however, the authors used the large system to provide accurate estimates of the average achievable rates using some precoder and did not use the large system approach to design precoders as we do.

In what follows we shall go one step further in the separable channel correlation model and assume $\mathbf{C}_{r,k,b_i} = \mathbf{C}_{r,k}, \forall b_i$. From (1.5) and using the notation in

(4.7), $\mathbf{R}_{c,k}$ and $\mathbf{R}_{c,k}^-$ are given respectively by

$$\mathbf{R}_{c,k} = \mathbf{I} + \mathbf{H}_{c,k} \mathbf{Q} \mathbf{H}_{c,k}^H \quad (4.56)$$

and

$$\mathbf{R}_{c,k}^- = \mathbf{I} + \mathbf{H}_{c,k} \mathbf{Q}_{c,k}^- \mathbf{H}_{c,k}^H \quad (4.57)$$

The large MIMO asymptotics from [44],[45], in which both $M, N \rightarrow \infty$ at constant ratio, tend to give more precise approximations when M is not so large. For the general case of Gaussian CSIT with separable (Kronecker) covariance structure, [44],[45] lead to asymptotic expressions of the form

$$\begin{aligned} & \mathbb{E}_{\mathbf{H}} \log \det(\mathbf{I} + \mathbf{H} \mathbf{Q} \mathbf{H}^H) \\ &= \max_{z \geq 0, w \geq 0} \left\{ \log \det \begin{bmatrix} \mathbf{I} + w & \bar{\mathbf{H}} \\ -\mathbf{Q} \bar{\mathbf{H}}^H & \mathbf{I} + z \mathbf{Q} \Theta_p \end{bmatrix} - zw \right\}. \end{aligned} \quad (4.58)$$

where the maximization over z and w should be carried out alternately (and not jointly: the joint optimization may correspond to a global maximum or a saddle point; the cost function is concave however in z or w separately). We shall assume the same fully separable correlation Gaussian channel model. The EWSR of (1.24) can be written as

$$EWSR = \mathbb{E}_{\mathbf{H}} \sum_k \sum_c \left(\log \det \mathbf{R}_{c,k} - \log \det \mathbf{R}_{c,k}^- \right) \quad (4.59)$$

using (4.58), the EWSR now becomes

$$\begin{aligned} EWSR &= \sum_{k=1}^K \sum_{c=1}^C u_{c,k} \left(\max_{z_{c,k}, w_{c,k}} \{ \log \det \mathbf{S}_{c,k}(\mathbf{Q}, z_{c,k}, w_{c,k}) - \right. \\ &\quad \left. z_{c,k} w_{c,k} \right. \\ &\quad \left. - \max_{\overline{z}_{c,k}, \overline{w}_{c,k}} \left\{ \log \det \mathbf{S}_{c,k}(\mathbf{Q}_{c,k}^-, \overline{z}_{c,k}, \overline{w}_{c,k}) - \overline{z}_{c,k} \overline{w}_{c,k} \right\} \right) \end{aligned} \quad (4.60)$$

where

$$\mathbf{S}_k(\mathbf{Q}, z, w) = \begin{bmatrix} \mathbf{I} + w \mathbf{I} & \bar{\mathbf{H}}_{c,k} \\ -\mathbf{Q} \bar{\mathbf{H}}_{c,k}^H & \mathbf{I} + z \mathbf{Q} \Theta_{p,c,k} \end{bmatrix}. \quad (4.61)$$

Note that

$$\begin{aligned} \log \det \mathbf{S}_{c,k}(\mathbf{Q}, z, w) &= \log \det(\mathbf{I} + w \mathbf{I}) + \log \det(\mathbf{I} + \mathbf{Q} \mathbf{T}_{c,k}(z, w)) \\ &\text{with } \mathbf{T}_{c,k}(z, w) = z \Theta_{p,c,k} + \bar{\mathbf{H}}_{c,k}^H (\mathbf{I} + w \mathbf{I})^{-1} \bar{\mathbf{H}}_{c,k} \end{aligned} \quad (4.62)$$

where $\mathbf{T}_{c,k}$ plays the role of some kind of total Tx side channel correlation matrix. Note that the weighting coefficients z, w depend on the BFs also though. The EWSR expression in (4.60) can be maximized alternately over the $\{\mathbf{g}_k\}$, the $\{z_{c,k}, w_{c,k}\}$ and the $\{\overline{z_{c,k}}, \overline{w_{c,k}}\}$. For the optimization of the BFs $\mathbf{g}_{c,k}$, for given z, w , introduce

$$\begin{aligned}\widehat{\mathbf{R}}_{c,k,c,k} &= \mathbf{I} + \widehat{\mathbf{Q}}_{c,k} \mathbf{T}_k(z_{c,k}, w_{c,k}) \\ \widehat{\mathbf{R}}_{c,k} &= \mathbf{I} + \widehat{\mathbf{Q}}_{c,k} \mathbf{T}_{c,k}(\overline{z_{c,k}}, \overline{w_{c,k}}) \\ \widehat{\mathbf{R}}_{c,k} &= \mathbf{I} + \widehat{\mathbf{Q}}_{c,k} \mathbf{T}_k(z_{c,k}, w_{c,k}).\end{aligned}\quad (4.63)$$

Inspired by section 1.4.2, we get

$$\begin{aligned}\check{\mathbf{B}}_{c,k} &= \mathbf{I}_c^H \mathbf{T}_k(z_{c,k}, w_{c,k}) \widehat{\mathbf{R}}_{c,k,c,k}^{-1} \mathbf{I}_c \\ \check{\mathbf{A}}_{c,k} &= \sum_{(j,i) \neq (c,k)} u_i \mathbf{I}_j^H \left[\mathbf{T}_{j,i}(z_{j,i}, w_{j,i}) \widehat{\mathbf{R}}_{j,i}^{-1} - \mathbf{T}_{j,i}(\overline{z_{j,i}}, \overline{w_{j,i}}) \widehat{\mathbf{R}}_{j,i}^{-1} \right] \mathbf{I}_j.\end{aligned}\quad (4.64)$$

Note that in spite of their appearance, matrices of the form \mathbf{TR}^{-1} are symmetric. Indeed, if e.g. \mathbf{T} is invertible then $\mathbf{T}(\mathbf{I} + \mathbf{QT})^{-1} = (\mathbf{T}^{-1} + \mathbf{Q})^{-1}$. For the optimization $\max_{z \geq 0, w \geq 0} \{\log \det \mathbf{S}(\mathbf{Q}, z, w) - zw\}$, we get from the extremum conditions

$$\begin{aligned}w &= f(\mathbf{Q}, z, w) = \text{tr}\{\mathbf{Q}\mathbf{C}_t[\mathbf{I} + \mathbf{Q}\mathbf{T}(z, w)]^{-1}\} \\ z &= g(\mathbf{Q}, z, w) = \text{tr}\{\mathbf{C}_r[\mathbf{I} + w\mathbf{C}_r\overline{\mathbf{H}}(\mathbf{I} + z\mathbf{Q}\mathbf{C}_t)^{-1}\mathbf{Q}\overline{\mathbf{H}}^H]^{-1}\}\end{aligned}\quad (4.65)$$

which can be iterated until a fixed point. To get the normalized precoder we use

$$\mathbf{G}'_{c,k} = \text{eigenmatrix}(\check{\mathbf{B}}_{c,k}, \check{\mathbf{A}}_{c,k} + \lambda_c \mathbf{I}_M) \quad (4.66)$$

with eigenvalues $\Sigma_{c,k} = \text{eigenvalues}(\check{\mathbf{B}}_{c,k}, \check{\mathbf{A}}_{c,k} + \lambda_c \mathbf{I}_M)$.

Let $\Sigma_{c,k}^{(1)} = \mathbf{G}_{c,k}'^H \check{\mathbf{B}}_{c,k} \mathbf{G}_{c,k}'$, $\Sigma_{c,k}^{(2)} = \mathbf{G}_{c,k}'^H \check{\mathbf{A}}_{c,k} \mathbf{G}_{c,k}'$. Powers $\mathbf{P}_{c,k} \geq 0$ are defined as in (1.19). λ_c is determined also as described in section 1.4.2. The algorithm can then be summarized as in Table 4.3. The performance of the proposed precoder is evaluated through numerical simulations. The algorithm in Table 4.3 is repeated and averaged for 100 realizations of the channels $\mathbf{H}_{c,k}$ for all c, k and their estimates $\overline{\mathbf{H}}_{c,k}$.

Figure 4.12 shows the EWSR versus transmit SNR for a cellular network having $C = 6$ cells and one BS at the center of each cell. Then, we assume that each

TABLE 4.3: The Iterative Algorithm

```

For  $(c, k) = (1, 1) \dots (C, K)$ , initialize  $\mathbf{Q}_{c,k}$ ,  $z_{c,k}$ ,  $\overline{z_{c,k}}$ ,  $w_{c,k}$ ,  $\overline{w_{c,k}}$ ,
 $\mathbf{T}_k(z_{c,k}, w_{c,k})$ ,  $\mathbf{T}_k(\overline{z_{c,k}}, \overline{w_{c,k}})$ 
Repeat until convergence
  For  $j = 1 \dots C$ 
    Set  $\underline{\lambda}_c = 0$ ,  $\overline{\lambda}_c = \lambda_{max}$ 
    For  $k$ 
      Compute  $\check{\mathbf{A}}_{c,k}$  using (4.64)
    Next  $k$ 
    Repeat until convergence
       $\lambda_c = \frac{1}{2}(\underline{\lambda}_c + \overline{\lambda}_c)$ 
      For  $k$ 
        Compute  $\check{\mathbf{B}}_{c,k}$  using (4.64)
        Compute the generalized eigenmatrix  $\mathbf{G}_{c,k}$  of  $\check{\mathbf{B}}_{c,k}$ 
          and  $\hat{\mathbf{A}}_{c,k} + \lambda_c \mathbf{I}_M$ 
        Normalize the generalized eigenmatrix so as to have  $\mathbf{G}'_{c,k}$ 
        Compute  $\boldsymbol{\Sigma}_{c,k}^{(1)} = \mathbf{G}_{c,k}'^H \check{\mathbf{B}}_{c,k} \mathbf{G}_{c,k}'$ ,  $\boldsymbol{\Sigma}_{c,k}^{(2)} = \mathbf{G}_{c,k}'^H \check{\mathbf{A}}_{c,k} \mathbf{G}_{c,k}'$ 
        Compute  $\mathbf{P}_{c,k}$  as in (1.19)
      Next  $k$ 
      Compute  $\mathbf{P} = \sum_k \mathbf{P}_{c,k}$ 
      if  $\text{tr}(\mathbf{P}) \leq P_c$ , set  $\underline{\lambda}_c = \lambda_c$ , otherwise set  $\overline{\lambda}_c = \lambda_c$ 
    For all  $k$ , set  $\mathbf{Q}_{c,k} = \mathbf{G}_{c,k}'^H \mathbf{P}_{c,k} \mathbf{G}_{c,k}'^H$ 
    For all  $k$ , compute  $z_{c,k}$ ,  $\overline{z_{c,k}}$ ,  $w_{c,k}$ ,  $\overline{w_{c,k}}$ 
      and then compute  $\mathbf{T}_{c,k}(z_{c,k}, w_{c,k})$  and  $\mathbf{T}_{c,k}(\overline{z_{c,k}}, \overline{w_{c,k}})$ 
    Next  $j$ 

```

BS is endowed with a number $M = 6$ Transmit antennas and serving one Rx equipped with $N = 6$ Receive antennas. We assume $\mathbf{C}_r = \mathbf{I}_N$ and we compare the performance of the algorithm explained in Table 4.3 to the performance of the naive approach ENAIVEKG of 4.1. The TxS design their BF's according to their partial CSIT. Then, the BF's designed with the partial CSIT need to be evaluated with the real channel in order to get the actual resulting WSR. We suppose that the error covariances matrices $\Theta_{p,i,c,k}$ for all i , c and k are identity matrices multiplied by a scalar α^2 ; $\alpha^2 = \frac{1}{10}$ in Figure 4.12. From (1.22), we construct the channels $\mathbf{H}_{i,c,k}$ and the channel estimates $\overline{\mathbf{H}}_{i,c,k}$, for

all i , c and k :

$$\mathbf{H}_{i,c,k} = \tilde{\mathbf{H}}_{i,c,k}^{(1)} \mathbf{\Theta}_{t,i,c,k}^{1/2} + \tilde{\mathbf{H}}_{i,c,k}^{(2)} \mathbf{\Theta}_{p,i,c,k}^{1/2} \quad (4.67)$$

$$\bar{\mathbf{H}}_{k,b_k} = \tilde{\mathbf{H}}_{i,c,k}^{(1)} \mathbf{\Theta}_{t,i,c,k}^{1/2} . \quad (4.68)$$

Moreover, we have:

$$\mathbf{\Theta}_{p,i,c,k} = \alpha^2 \mathbf{I}_M \quad (4.69)$$

and

$$\mathbf{\Theta}_{t,i,c,k} = (1 - \alpha^2) \mathbf{I}_M \quad (4.70)$$

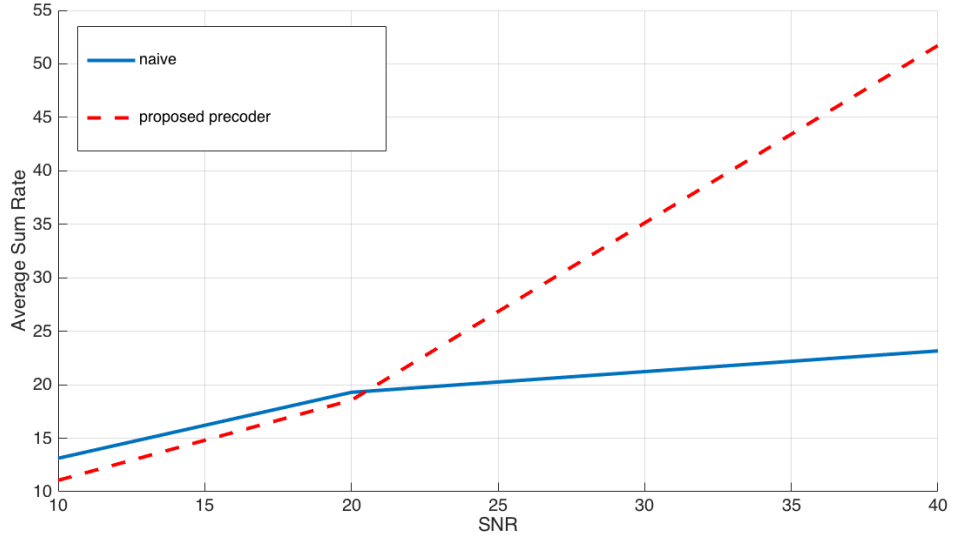


FIGURE 4.12: Sum rate comparisons for $C=6$, $M=6$ and $N=6$

We do not show simulations that compare the approach proposed in this section to the ESEI-WSR; however we can assure that the ESEI-WSR outperforms easily this approach.

4.9 Conclusion

In the previous chapters, we have talked about BFs. But a requirement to practically design the BFs is to know perfectly the channels. As explained in Chapter 1, the procedure to acquire the channels differ from FDD to TDD. We have concluded as well that TDD is more suitable to Massive MIMO. Then

we have said that in TDD, DL channels which are estimated from UL training suffer from estimation noise. In order to design beamformers robust to that, a new optimization problem must be dealt with, the EWSR maximization problem. The objective function is the expected value of the weighted sum rate. The constraints are always the same, a power budget limit per cell. The new problem of interest is a stochastic problem. Two solutions exist already, this first one is ENAIVEKG, which is the same as KG but it is proposed to replace the true channels but their estimates without considering the knowledge of channel estimation error covariance. The second one is EWSMSE, it proposes to reformulate the EWSR maximization problem into a minimization of the expected value of the MSE. Then comes our proposal. We propose to solve the EWSR as a DC approach. We divide the objective function into two parts corresponding to the expected value of the rate of the user of interest and to the expected sum rate of the others. A new objective function appears. The solution is given by the eigenmatrix of some matrices. Then, we propose to calculate the expected values of these matrices as shown in Appendix. Simulations show for different configurations that our approach is the best one. The gain over the other approaches comes from exploiting the channel covariance information not only in the interference terms, but also in the signal power. As in Chapter 2, we have derived deterministic expression for the rate for MISO. Moreover, we proposed another robust precoder for partial CSIT. However, this proposed precoder is less beneficial and achieve less gains than its counterpart, the ESEI-WSR precoder.

Chapter 5

Non-Linear Precoding Schemes

5.1 Introduction

In this chapter, we consider the DL of a MC MU MIMO known as the IBC MIMO scenario where we have many cells having each a BS equipped with many antennas serving many multi-antenna users. We use CoBF. In other words, at each cell, each BS sends signals to its connected users only and does not serve users from other cells. The main goal of this work is to jointly design the BF's transmitted by each BS in order to maximize the achievable sum rate of the cellular network. In the case of single cell multiuser MIMO the capacity is achieved using the famous DPC technique [46]. In the case of IBC MIMO, it is possible to use the DPC approach by cell, in other words, each BS applies the DPC as if it is the only cell in the network. This approach is suboptimal due to the interference created by each BS on the neighbouring cells. Herein Nguyen and Le-Ngoc in [47] proposed coordinated CoBF solution where the maximization of the WSR problem in the presence of DPC is done using techniques such as WSMSE or DC. In [47] perfect CSIT is considered which implies that the DPC conditions are fulfilled and DPC can be employed. To design the precoding matrices, CSIT must be known at the BSs. We suppose a TDD configuration. We recall that the main concept of DPC is that users in each cell will receive only a part of the intracell interference because the other part is meant to be encoded by the serving BS in such way that the user

will not see it as interference. However, this scenario will not hold if the CSIT is partial and the BS would not be able to encode the data [48]. Therefore, we present the Linear Assignment (LA) operation which is to the best of our knowledge the best way to practically design DPC in the case of partial CSIT [49]. If we want to design BC MIMO precoders, the LA precoders design explained in [50] will be enough. Meanwhile, as discussed above, in the MC case, intercell interference will be a major limitation and a new implementation is needed. We follow the example of [47] and use a CoBF technique where the maximization of the EWSR in the presence of LA using an approach similar to the ESEI-WSR approach of section 4.3 which combines DC and asymptotic limits of some expressions. ESEI-WSR is used to design linear robust BF's for partial CSIT. This approach consists in isolating and linearizing the sum-rate function at all other cells except a particular cell under consideration into a linear interference penalty. Then, maximizing the EWSR is like maximizing the BC EWSR with LA at the given cell minus a penalty-term corresponding to the intercell interference generated by the cell under consideration. The LA and DPC are difficult to be implemented in practice, however the Tomlinson-Harashima precoding [51] and Vector Precoding [52] allow the implementation of nonlinear precoders which achieve rates close to the ones achieved by the LA and DPC. In this chapter, we make the following key contribution: We provide a joint design of the linear assignment matrices of the LA operation as well as an robust design of transmit covariance matrices corresponding to the BF matrices for the MC MU cellular communications scenarios with partial CSIT.

5.2 The IBC signal model

Let us consider an IBC system with C cells and a total amount of K users. We shall consider a system-wide numbering of the users. User k is served by BS b_k . The $N \times 1$ received signal at user k in cell b_k is

$$\mathbf{y}_k = \underbrace{\mathbf{H}_{k,b_k} \mathbf{G}_k \mathbf{x}_k}_{\text{signal}} + \underbrace{\sum_{\substack{i \neq k \\ b_i = b_k}} \mathbf{H}_{k,b_k} \mathbf{G}_i \mathbf{x}_i}_{\text{intracell interf.}} + \underbrace{\sum_{j \neq b_k} \sum_{i: b_i = j} \mathbf{H}_{k,j} \mathbf{G}_i \mathbf{x}_i}_{\text{intercell interf.}} + \mathbf{v}_k \quad (5.1)$$

where \mathbf{x}_k are the intended $d_k \times 1$ signals (each white and unit variance), d_k is the number of intended streams, \mathbf{H}_{k,b_k} is the $N \times M$ channel from BS b_k

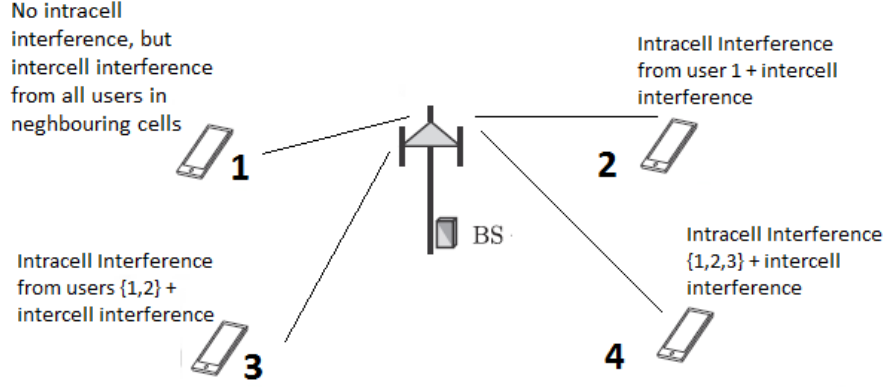


FIGURE 5.1: Interference in DPC

to user k . BS b_k serves $K_{b_k} = \sum_{i:b_i=b_k} 1$ users. We consider the noise as $\mathbf{v}_k \sim \mathcal{CN}(0, \sigma^2 \mathbf{I}_N)$. The $M \times d_k$ spatial Tx filter or BF is \mathbf{G}_k . We suppose that users $1, \dots, K_1$ belong to cell-1; users $K_1 + 1, \dots, K_1 + K_2$ belong to cell-2; \dots ; users $\sum_{c=1}^{C-1} K_c + 1, \dots, K$ belong to cell- C . At each cell b_k , the LA operation is used such that the intended codeword for user k does not see intracell interference from users $i > k : b_i = b_k$ (See Figure 5.1).

5.3 The LA operation

The LA operation is characterized by an auxiliary M -dimensional random variable \mathbf{u} with a particular linear structure given by:

$$\mathbf{u} = \mathbf{F}\mathbf{s} + \mathbf{x} \quad (5.2)$$

where \mathbf{F} is the LA assignment matrix and \mathbf{s} is the intracell interference which is known to the Tx. As concerning the design of \mathbf{u} , it was proved in [49] that the maximum rate is achieved by choosing \mathbf{x} and \mathbf{s} to be Gaussian and independent which have many implications on \mathbf{u} . For further details, please refer to [49]. Hence, when the transmit signal is generated as $\mathbf{x} = \mathbf{u} - \mathbf{F}\mathbf{s}$, the rate r_k of user k can be achievable, where:

$$r_k = \log \det(\mathbf{Q}_k) - E_H \{ \log \det [\mathbf{C}_k - \mathbf{Y}_k \mathbf{H}_{k,b_k}^H (\mathbf{H}_{k,b_k} \mathbf{B}_k \mathbf{H}_{k,b_k}^H + \mathbf{R}_k^{-1})^{-1} \mathbf{H}_{k,b_k} \mathbf{Y}_k^H] \} \quad (5.3)$$

where

$$\mathbf{Q}_k = \mathbf{G}_k \mathbf{G}_k^H \quad (5.4)$$

$$\mathbf{Y}_k = \mathbf{F}_k \mathbf{S}_k + \mathbf{Q}_k \quad (5.5)$$

$$\mathbf{B}_k = \mathbf{S}_k + \mathbf{Q}_k \quad (5.6)$$

$$\mathbf{C}_k = \mathbf{F}_k \mathbf{S}_k \mathbf{F}_k^H + \mathbf{Q}_k$$

$$\mathbf{S}_k = \sum_{j: b_j = b_k; j > k+1} \mathbf{Q}_j. \quad (5.8)$$

$$\begin{aligned} \mathbf{R}_k &= \mathbf{H}_{k,b_k} \mathbf{Q}_k \mathbf{H}_{k,b_k}^H + \mathbf{R}_{\bar{k}}, \\ \mathbf{R}_{\bar{k}} &= \sum_{i: b_i = b_k; i < k} \mathbf{H}_{k,b_i} \mathbf{Q}_i \mathbf{H}_{k,b_i}^H + \sigma^2 \mathbf{I}_N. \end{aligned} \quad (5.9)$$

\mathbf{R}_k , $\mathbf{R}_{\bar{k}}$ are the total and the interference plus noise Rx covariance matrices respectively.

We investigate the transmit side design of the LA assignment matrix \mathbf{F}_k and beamforming covariance matrix \mathbf{Q}_k that optimize the rate. There are some conditions that characterize the optimal design of \mathbf{F}_k and \mathbf{Q}_k . The two variables depend on each other. A valid approach is to iteratively design one variable at time while the others considered as fixed. This approach requires an exhaustive averaging in each iteration which might cause long execution time. To avoid this issue, the authors of [50] used the second-order statistics of the CSI and an upper-bound of the LA achievable rate to derive a closed-form solution for \mathbf{F}_k . The simulations in [50] show that this suboptimal approach provide almost the same performance as the optimal approach mentioned above but with reduced complexity. While the derivation stems from [50], however, there is a slight difference due to the fact that this latter deals only with single cell design and

no intercell interference to deal with. (5.3) can be rewritten as:

$$\begin{aligned}
r_k &= \log_2 \det(\mathbf{Q}_k) - \log_2 \det(\mathbf{C}_k) \\
&- \log_2 \det[(\bar{\mathbf{H}}_{k,b_k} \bar{\mathbf{H}}_{k,b_k}^H + \mathbf{C}_{p,k,b_k})(\mathcal{D}_k + \sum_{i < k: b_i = b_k} \mathbf{Q}_i) \\
&+ \sigma^2 \mathbf{I}_M + \tilde{\mathbf{R}}_{inter,k}] \\
&- \log_2 \det[(\bar{\mathbf{H}}_{k,b_k} \bar{\mathbf{H}}_{k,b_k}^H + \mathbf{C}_{p,k,b_k})(\mathbf{B}_k + \sum_{i < k: b_i = b_k} \mathbf{Q}_i) \\
&+ \sigma^2 \mathbf{I}_M + \tilde{\mathbf{R}}_{inter,k}]]
\end{aligned} \tag{5.10}$$

where

$$\mathcal{D}_k = \mathbf{B}_k - \mathbf{Y}_k^H \mathbf{C}_k^{-1} \mathbf{Y}_k \tag{5.11}$$

and

$$\tilde{\mathbf{R}}_{inter,k} = \sum_{j: b_j \neq b_k} \mathbf{H}_{i,b_j}^H \mathbf{H}_{i,b_j} \mathbf{Q}_j \tag{5.12}$$

We inspire from [50] and propose a closed-form expression for the assignment matrix \mathbf{F}_k such as:

$$\begin{aligned}
\mathbf{F}_k &= \mathbf{Q}_k \{ \mathbf{Q}_k + \sum_{j: b_j = b_k; j < k} \mathbf{Q}_j + [\bar{\mathbf{H}}_{k,b_k}^H (\mathbf{R}_{inter,k} + \sigma^2 \mathbf{I}_N)^{-1} \bar{\mathbf{H}}_{k,b_k} \\
&+ \boldsymbol{\Theta}_{p,k,b_k} \text{tr}((\mathbf{R}_{inter,k} + \sigma^2 \mathbf{I}_N)^{-1})]^{-1} \}
\end{aligned} \tag{5.13}$$

where

$$\mathbf{R}_{inter,k} = \sum_{j: b_j \neq b_k} \mathbf{H}_{k,b_j} \mathbf{Q}_j \mathbf{H}_{k,b_j}^H \tag{5.14}$$

We note that this matrix depends only on the second order statistics of the channels.

Now, it remains to calculate \mathbf{Q}_k . In (5.10), we replace \mathbf{F}_k by its closed-form expression (5.13), the obtained expression can be upper bounded, as shown in ([50], Appendix C), by the new objective function::

$$EWSR(\mathbf{Q}) = \mathbb{E}_{\mathbf{H}} \sum_k u_k \log_2 \det(\mathbf{I}_M + \mathbf{H}_{k,b_k}^H \mathbf{R}_k^{-1} \mathbf{H}_{k,b_k} \mathbf{Q}_k) \tag{5.15}$$

with u_k being the rate weights.

5.4 Solving the EWSR problem

For the case of perfect CSIT, DC approach is used where the 1st order Taylor series expansion of the covariance matrix, combined with successive interference cancellation (SIC) for the dual Multiple Access Channel (MAC) problem, leads to a separable convex optimization problem that provides successively the solutions of the optimal decoders. The effect of imperfect CSIT is then captured by considering the asymptotic expressions of channel covariances which in the infinite antenna limit equal the corresponding deterministic values. The precoding matrices are given by an iterative algorithm.

5.4.1 Max WSR with Perfect CSIT : DC approach

This section stems entirely from [47]. We assume that each BS implements the LA operation. It is utilized such that the intended codeword for a certain user k does not see the intracell interference from user- $i > k : b_i = b_k$. Consider as a starting point for the optimization of WSR which is equivalent to the EWSR in the perfect CSIT case.

$$\max_{\mathbf{Q}} WSR = WSR(\mathbf{Q}) \quad (5.16)$$

$$= \sum_{k=1}^K u_k \log_2 \det(\mathbf{I}_N + \mathbf{R}_{\bar{k}}^{-1} \mathbf{H}_{k,b_k} \mathbf{Q}_k \mathbf{H}_{k,b_k}^H) \quad (5.17)$$

where \mathbf{Q} represents the collection of transmit covariance matrices \mathbf{Q}_k . The WSR cost function needs to be augmented with the power constraints

$$\sum_{k:b_k=j} \text{tr}\{\mathbf{Q}_k\} \leq P_j^{BS}. \quad (5.18)$$

So our optimization problem can be expressed as the following:

$$\begin{aligned} & \max_{\mathbf{Q}} WSR(\mathbf{Q}) \\ & s.t. \sum_{k:b_k=j} \text{tr}\{\mathbf{Q}_k\} \leq P_j^{BS} \end{aligned} \quad (5.19)$$

where $WSR(\mathbf{Q})$ is given in (5.17). In a classical DC programming approach, Kim and Giannakis proposed to keep the concave signal terms and to replace the convex interference terms by the linear (and hence concave) tangent

approximation. Here, we consider the WSR of all the other cells except cell b_k , as this latter is not concave in \mathbf{Q}_k , we take their Taylor expansion around \mathbf{Q}_k and retain only the first linear term. Then, we get a set of C optimization problems corresponding to each cell. At cell b_k it can be written as:

$$\begin{aligned} & \max_{\mathbf{Q}} \sum_{i:b_i=b_k} u_i \log_2 \det(\mathbf{I}_N + \mathbf{R}_{\bar{i}}^{-1} \mathbf{H}_{i,b_k} \mathbf{Q}_i \mathbf{H}_{i,b_k}^H) \\ & \quad - \text{tr}\{(\hat{\mathbf{A}}_{b_k} + \lambda_{b_k} \mathbf{I}) \mathbf{Q}_i\} \\ & \text{subject to } \mathbf{Q}_i \geq 0 \ \forall i \end{aligned} \quad (5.20)$$

or

$$\begin{aligned} & \max_{\mathbf{Q}} \sum_{i:b_i=b_k} u_i \log_2 \det \left(\frac{\mathbf{R}_{inter,i} + \sum_{j:b_j=b_k;j \leq i} \mathbf{H}_{i,b_k} \mathbf{Q}_j \mathbf{H}_{i,b_k}^H}{\mathbf{R}_{inter,i} + \sum_{j:b_j=b_k;j < i} \mathbf{H}_{i,b_k} \mathbf{Q}_j \mathbf{H}_{i,b_k}^H} \right) \\ & \quad - \text{tr}\{(\hat{\mathbf{A}}_{b_k} + \lambda_{b_k} \mathbf{I}) \mathbf{Q}_i\} \\ & \text{subject to } \mathbf{Q}_i \geq 0 \ \forall i \end{aligned} \quad (5.21)$$

where

$$\begin{aligned} \hat{\mathbf{A}}_{b_k} &= - \left. \frac{\partial WSR_{\bar{k}}(\mathbf{Q}_k, \hat{\mathbf{Q}})}{\partial \mathbf{Q}_k} \right|_{\hat{\mathbf{Q}}_k, \hat{\mathbf{Q}}} \\ &= \sum_{\substack{K \\ b_i \neq b_k}} u_i \mathbf{H}_{i,b_k}^H (\mathbf{R}_{\bar{i}}^{-1} - \mathbf{R}_i^{-1}) \mathbf{H}_{i,b_k} \end{aligned} \quad (5.22)$$

As explained in [47], we change the variables as follows:

$$\tilde{\mathbf{Q}}_j = (\hat{\mathbf{A}}_{b_k} + \lambda_{b_k} \mathbf{I}_M)^{1/2} \mathbf{Q}_j (\hat{\mathbf{A}}_{b_k} + \lambda_{b_k} \mathbf{I}_M)^{1/2} \quad (5.23)$$

and

$$\tilde{\mathbf{H}}_{i,b_k} = \mathbf{R}_{inter,i}^{-1/2} \mathbf{H}_{i,b_k} (\hat{\mathbf{A}}_{b_k} + \lambda_{b_k} \mathbf{I}_M)^{-1/2} \quad (5.24)$$

Then (5.21) can be rewritten as:

$$\begin{aligned} & \max_{\mathbf{Q}} \sum_{i:b_i=b_k} u_i \log_2 \det \left(\frac{\mathbf{I}_N + \sum_{j:b_j=b_k;j \leq i} \tilde{\mathbf{H}}_{i,b_k} \tilde{\mathbf{Q}}_j \tilde{\mathbf{H}}_{i,b_k}^H}{\mathbf{I}_N + \sum_{j:b_j=b_k;j < i} \tilde{\mathbf{H}}_{i,b_k} \tilde{\mathbf{Q}}_j \tilde{\mathbf{H}}_{i,b_k}^H} \right) \\ & \quad - \text{tr}\{\hat{\mathbf{A}}_{b_k} \tilde{\mathbf{Q}}_i\} \\ & \text{subject to } \mathbf{Q}_i \geq 0 \ \forall i \end{aligned} \quad (5.25)$$

Using the MAC-BC duality, we can instead of maximizing the objective function in (5.25), optimize its dual function corresponding to MAC scenario where K N antennas users are transmitting to an M -antenna BS. The uplink channel from user i will be \mathbf{H}_{i,b_i}^H . The BS employs SIC to decode the signals from the K users. Therefore, our new problem will be:

$$\begin{aligned}
& \max_{\mathbf{D}} \sum_{i:b_i=b_k} \log_2 \det \left(\frac{\mathbf{I}_N + \sum_{j:b_j=b_k:j \geq i} \tilde{\mathbf{H}}_{i,b_k}^H \mathbf{D}_j \tilde{\mathbf{H}}_{i,b_k}}{\mathbf{I}_N + \sum_{j:b_j=b_k:j > i} \tilde{\mathbf{H}}_{i,b_k}^H \mathbf{D}_j \tilde{\mathbf{H}}_{i,b_k}} \right) \\
& \quad - \text{tr}\{\mathbf{D}_i\} \\
& \text{subject to } \mathbf{D}_i \geq 0 \quad \forall i
\end{aligned} \tag{5.26}$$

where \mathbf{D}_i is the precoding covariance matrix at user i . This is a convex optimization problem, which leads to optimal $\mathbf{D}_i \forall i : b_i = b_k$. Therefore, from \mathbf{D}_i we can re-obtain $\tilde{\mathbf{Q}}_i \forall i : b_i = b_k$ using MAC-BC transformation as detailed in [53]. It is easy to show that the problem in (5.26) is optimal as shown in [47]. The constraints are decoupled for each variable which allows a sequential maximization. Since the objective function is a subtraction of a log function to a linear function, the sequential optimization of $\mathbf{D}_1 \dots \mathbf{D}_k$ is guaranteed to converge to the optimal solution. The optimal solution of \mathbf{D}_i can be given as:

$$\mathbf{D}_i = u_i \mathbf{U}_i [\mathbf{I} - \boldsymbol{\Sigma}_i^{-1}]^+ \mathbf{U}_i^H \tag{5.27}$$

where $z^+ = \max(0, z)$ and \mathbf{U}_i and $\boldsymbol{\Sigma}_i$ come from the following eigen-decomposition operation:

$$\tilde{\mathbf{H}}_{i,b_k} (\mathbf{I}_N + \sum_{j:b_j=b_k,j > i}^K \tilde{\mathbf{H}}_{j,b_k}^H \mathbf{D}_j \tilde{\mathbf{H}}_{j,b_k})^{-1} \tilde{\mathbf{H}}_{i,b_k}^H = \mathbf{U}_i \boldsymbol{\Sigma}_i \mathbf{U}_i^H \tag{5.28}$$

5.4.2 Solution with imperfect CSIT

In order to solve the EWSR problem, we first solve the problem with the perfect CSI assumption, we get the expressions of the beamformers, and then, in order to apply these beamformers to the imperfect CSIT case, we have to use the expected values of many expressions instead of the deterministic values, as explained in this section and in (4.3). Furthermore, in the Massive MIMO limit, where the number of Tx antennas M becomes very large, we get a convergence for any term of the form

$$\mathbf{H} \mathbf{Q} \mathbf{H}^H \xrightarrow{M \rightarrow \infty} \mathbb{E}_{\mathbf{H}} \mathbf{H} \mathbf{Q} \mathbf{H}^H = \overline{\mathbf{H}} \mathbf{Q} \overline{\mathbf{H}}^H + \text{tr}\{\mathbf{Q} \boldsymbol{\Theta}_p\} \mathbf{C}_r. \tag{5.29}$$

In what follows we shall go one step further in the separable channel correlation model and assume $\mathbf{C}_{r,k,b_i} = \mathbf{C}_{r,k}, \forall b_i$. We get a new expression for $\hat{\mathbf{A}}_{b_k}$ as

follows:

$$\begin{aligned}\check{\mathbf{A}}_{b_k} &= \mathbf{E}_{\mathbf{H}} \hat{\mathbf{A}}_{b_k} = \sum_{b_i \neq b_k}^K u_i [\check{\mathbf{A}}_{i,k}^C (\mathbf{I}_M + \mathbf{Q}_k \check{\mathbf{A}}_{i,k}^C)^{-1} \\ &\quad - \check{\mathbf{A}}_{i,k}^D (\mathbf{I}_M + \mathbf{Q}_k \check{\mathbf{A}}_{i,k}^D)^{-1}] \end{aligned} \quad (5.30)$$

with

$$\begin{aligned}\check{\mathbf{A}}_{i,k}^C &= \bar{\mathbf{H}}_{i,b_k}^H \check{\mathbf{R}}_{i,k}^{-1} \bar{\mathbf{H}}_{i,b_k} + \text{tr}\{\check{\mathbf{R}}_{i,k}^{-1} \mathbf{C}_{r,i}\} \boldsymbol{\Theta}_{p,i,b_k}; \\ \check{\mathbf{A}}_{i,k}^D &= \bar{\mathbf{H}}_{i,b_k}^H \check{\mathbf{R}}_{i,k}^{-1} \bar{\mathbf{H}}_{i,b_k} + \text{tr}\{\check{\mathbf{R}}_{i,k}^{-1} \mathbf{C}_{r,i}\} \boldsymbol{\Theta}_{p,i,b_k}; \\ \check{\mathbf{R}}_{i,k} &= \sum_{j \neq k, j < i \text{ if } b_j = b_i}^K \bar{\mathbf{H}}_{i,b_j} \mathbf{Q}_j \bar{\mathbf{H}}_{i,b_j}^H + \text{tr}\{\mathbf{Q}_j \boldsymbol{\Theta}_{p,i,b_j}\} \mathbf{C}_{r,i} \\ &\quad + \sigma^2 \mathbf{I}_N; \\ \check{\mathbf{R}}_{i,k} &= \sum_{j \neq k, j \leq i \text{ if } b_j = b_i}^K \bar{\mathbf{H}}_{i,b_j} \mathbf{Q}_j \bar{\mathbf{H}}_{i,b_j}^H + \text{tr}\{\mathbf{Q}_j \boldsymbol{\Theta}_{p,i,b_j}\} \mathbf{C}_{r,i} \\ &\quad + \sigma^2 \mathbf{I}_N.\end{aligned}$$

The proof is similar to the proof of (4.3) so it is omitted. New expressions for the total and interference plus noise receive covariance matrices in (5.9) are given here according to (5.29):

$$\begin{aligned}\check{\mathbf{R}}_k &= \mathbf{H}_{k,b_k} \mathbf{Q}_k \mathbf{H}_{k,b_k}^H + \text{tr}\{\boldsymbol{\Theta}_{p,k,b_k} \mathbf{Q}_k\} \mathbf{C}_{r,k} + \check{\mathbf{R}}_{\bar{k}}, \\ \check{\mathbf{R}}_{\bar{k}} &= \sum_{i < k \text{ if } b_i = b_k} \mathbf{H}_{k,b_i} \mathbf{Q}_i \mathbf{H}_{k,b_i}^H + \text{tr}\{\boldsymbol{\Theta}_{p,k,b_i} \mathbf{Q}_i\} \mathbf{C}_{r,k} + \sigma^2 \mathbf{I}_N.\end{aligned} \quad (5.31)$$

$\mathbf{R}_{inter,k}$ given by (5.14) becomes:

$$\check{\mathbf{R}}_{inter,k} = \sum_{j: b_j \neq b_k} \mathbf{H}_{k,b_j} \mathbf{Q}_j \mathbf{H}_{k,b_j}^H + \text{tr}\{\boldsymbol{\Theta}_{p,k,b_j} \mathbf{Q}_j\} \mathbf{C}_{r,k} + \sigma^2 \mathbf{I}_N \quad (5.32)$$

Hence, we change the variables as follows:

$$\tilde{\mathbf{Q}}_j = (\check{\mathbf{A}}_{b_k} + \lambda_{b_k} \mathbf{I}_M)^{1/2} \mathbf{Q}_j (\check{\mathbf{A}}_{b_k} + \lambda_{b_k} \mathbf{I}_M)^{1/2} \quad (5.33)$$

and

$$\tilde{\mathbf{H}}_{i,b_k} = \check{\mathbf{R}}_{inter,i}^{-1/2} \mathbf{H}_{i,b_k} (\check{\mathbf{A}}_{b_k} + \lambda_{b_k} \mathbf{I}_M)^{-1/2} \quad (5.34)$$

Furthermore, the LA assignment matrix \mathbf{F}_k in (5.13) can be expressed as:

$$\check{\mathbf{F}}_k = \mathbf{Q}_k (\mathbf{Q}_k + \sum_{j: b_j = b_k; j < k} \mathbf{Q}_j + (\bar{\mathbf{H}}_{k,b_k} \check{\mathbf{R}}_{inter,k}^{-1} \bar{\mathbf{H}}_{k,b_k}^H + \boldsymbol{\Theta}_{p,k,b_k} \text{tr}\{\check{\mathbf{R}}_{inter,k}^{-1}\})^{-1})^{-1} \quad (5.35)$$

TABLE 5.1: The Iterative EWSR Algorithm

```

For  $k = 1 \dots K$ , initialize  $\mathbf{Q}_k$ 
Repeat until convergence
  For  $j = 1 \dots C$ 
    Set  $\underline{\lambda}_j = 0, \bar{\lambda}_j = \lambda_{max}$ 
    Compute  $\check{\mathbf{A}}_k$  using (5.31)
    Repeat until convergence
       $\lambda_j = \frac{1}{2}(\underline{\lambda}_j + \bar{\lambda}_j)$ 
      For  $k$  such that  $b_k = j$ 
        Change the variables as in (5.33) and (5.34)
        Repeat until convergence
          For  $k$  such that  $b_k = j$ 
            Update  $\mathbf{D}_i = u_i \mathbf{U}_i [\mathbf{I} - \boldsymbol{\Sigma}_i^{-1}] + \mathbf{U}_i^H$ 
          Next  $k$ 
        Compute optimal matrices  $\tilde{\mathbf{Q}}_1 \dots \tilde{\mathbf{Q}}_k$ 
        from  $\mathbf{D}_1 \dots \mathbf{D}_k$  by the MAC-BC transformation
        Recompute  $\mathbf{Q}_1 \dots \mathbf{Q}_k$  from  $\tilde{\mathbf{Q}}_1 \dots \tilde{\mathbf{Q}}_k$ 
        using the relation in (5.33)
      Next  $k$ 
      Compute  $P = \sum_{k:b_k=j} \text{tr}(\mathbf{Q}_k)$ 
      if  $P \geq P_j^{BS}$ , set  $\underline{\lambda}_j = \lambda_j$ , otherwise set  $\bar{\lambda}_j = \lambda_j$ 
    Next  $j$ 
  Next  $k$ 

```

5.5 Simulation results

This section simulates the achievable rate in the DL for different transmit schemes. We compare the following:

- A robust transmit design as described in Table 5.1, the sum rate is evaluated using (5.3)
- An upper bound of this latter where the evaluation is done this time using the classical $\log_2(\mathbf{I}_N + \mathbf{R}_k^{-1} \mathbf{H}_{k,b_k} \mathbf{Q}_k \mathbf{H}_{k,b_k}^H)$ expression.

- A naive approach, where the our robust design is used, nevertheless the channel estimation error covariance matrices are considered as unknown ($\Theta_p = 0$) when applying the algorithm in Table 1, here as well the evaluation of the performance is based on (5.3).
- The robust linear approach from section 4.3.

In order to proceed to the comparison of the algorithms mentioned above, we consider a MC MU scenario where we have 3 cells, a BS in the center of each cell and 3 users per cell. We assume 8 antennas at the BS and 2 receive antennas at each user. We assume that the channels are imperfectly known at the BS, the channel estimation error covariances Θ_p are considered as low rank matrices of rank 2 precisely. The low rank property of the covariance matrices is motivated in the work in [41]. The intercell channels are considered as attenuated by a factor of $\frac{1}{\sqrt{2}}$. We consider 50 realizations of the couple of $(\mathbf{H}, \bar{\mathbf{H}})$. We have $\bar{\mathbf{H}} = \mathbf{H} + \underbrace{\mathbf{C}_r^{1/2} \tilde{\mathbf{H}}_p \Theta_p^{1/2}}_{\text{error term}}$ from section 1.6 and we assume that the error term has a power gain which equals $\frac{1}{4}$ the power gain of \mathbf{H} . Figure

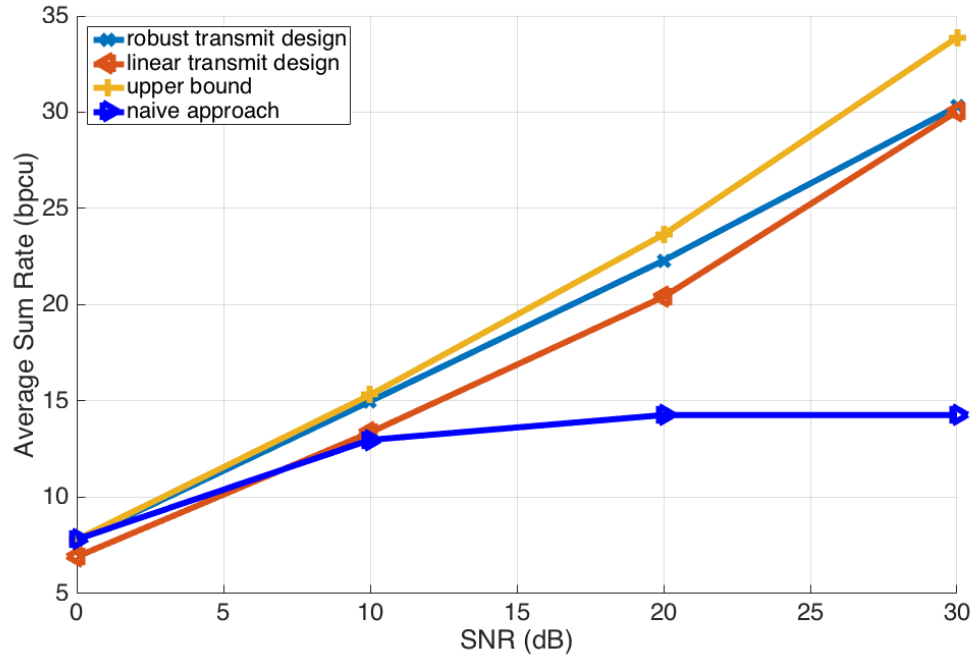


FIGURE 5.2: Achievable sum rate for $C = 3, K = 9, M = 8, N = 2$ with 2-rank channel estimation error covariance matrices

5.2 shows that the robust nonlinear BF has gain over the robust linear one.

To avoid joint design of \mathbf{F} and \mathbf{Q} , we justified our single variable \mathbf{Q} design by the upper bound of the achievable rate; and then we designed the \mathbf{F} with the closed-form solution (5.35). From the results of Figure 5.2, we can state that at high SNR we may need the joint \mathbf{F} and \mathbf{Q} design to get better performance.

5.6 Conclusion

The contributions in this chapter are based on the fact that we want to explore non linear robust BF's for partial CSIT. The most famous one is DPC. However, DPC works only with perfect CSIT and single cell scenario. We propose a variant of DPC which is LA that works with partial CSIT. With LA, we have a certain expression of the rate. There are two parameters: \mathbf{F} (LA matrix) and \mathbf{G} (beamforming matrix). We optimize w.r.t \mathbf{F} , we get a closed-form expression. We put this expression in the rate expression. We get a new objective function. The new objective is similar to EWSR of (1.24) but with difference at intracell interference. To solve this problem w.r.t \mathbf{Q} , a DC approach is used, where we decompose the objective function into two functions corresponding respectively to the rate of the cell of interest (the cell serving the user of interest) and to the sum rate of the other cells. We get a new objective function which is difference of concave functions, where the first function is the rate of the cell of interest and the second function is the penalty corresponding to the intercell interference generated by the cell of interest. We solve first the dual problem and the primal solution is then deduced by MAC-BC duality. Finally, the expected values of some expressions are calculated in order to be robust for partial CSIT.

Part III

Relaying with Random Matrix Theory

Chapter 6

Beamformers Design with AF Relays

6.1 Introduction

In Part I, We explained two beamforming algorithms from the state of the art: KG and WSMSE. We proposed DA. We introduced determinsitic equivalent of SINR for WSMSE. We proposed a beamformer that converges in one iteration. In Part II, Practical scenarios with imperfect channel knowledge are studied. We want beamformers that maximize sum rate with partial CSIT. This problem is denoted as EWSR. We solved the EWSR and proposed a new robust linear beamformer; then we performed large system analysis. We explained the linear assignment approach and proposed a new robust nonlinear beamformer.

In this part, we focus on relaying, which is a promising technology to improve the reliability and coverage of wireless systems. There are many types of relays that differ depending on the way the received signals are processed by the relays. We distinguish between the decode-and-forward (DF), the Amplify and forward (AF), the compress-and-forward (CF), mixed-forward and so forth.

In this chapter, we deal with the AF RSs where relays are used to linearly process the signal they receive and then re-transmit it to the final user. The advantage of this processing protocol is that it is transparent to the modulation and coding schemes and thus offers a flexible implementation. Again, the goal is to optimize the WSR via CoBF for Interference Broadcast Relay Channels (IBRC), as the papers in [54], [55] and [56] do. The first two papers extend

the WSMSE algorithm discussed extensively in the previous chapters to the broadcast relay channels (BRC) scenario for the two cases of absence and presence of direct links respectively. Meanwhile, the third paper uses a gradient descent suboptimal approach such as in [57].

Non-linear approaches such as DPC and so forth are presented in [58], [59] and [60], however non-linear approaches are out of the scope of this chapter.

As an extension to the conventional AF or the one-way relaying scheme, the two-way AF is proposed in [61], [62], [63], [64] [65] and [66]. It has the advantage of reducing the number of time-slots required to finish one round (UL and DL) of information exchange between the nodes, i.e. the BS and the users, using techniques based on network coding. With the two-way AF only two time slots are required compared to four time slots using the one-way AF. In this chapter, we are concerned only at a first point by the more challenging DL of cellular systems, so we do not consider the two-way AF.

Other papers design the BFs based on the optimization of other utility functions such as minimizing the MSE in [64],[65], [67–73]; minimizing the total transmit power [67]; minimizing the total leakage in [71]; maximizing the total signal to total interference plus noise ratio (TSTINR) in [74].

Moreover, we assume FD RSs. Many efforts focused on improving the FD transmissions, which increases the capacity of conventional Half-Duplex (HD) systems. As for the two-way relays, the real benefits of FD are gained by allowing UL and DL communications at the same time, which is not the case in this chapter. Further work is expected to deal with the simultaneous UL and DL communications. Main papers on FD beamforming with and without relays are as follows: [75], [76], [77] and [78].

In this chapter, we first neglect the direct link between the BS and the users and we propose an alternating optimization technique where we alternate between the optimization of the BFs at the BSs and at the RS. For the design of the RS, we reconsider the work in [54] and extend it from the case of BRC to the case of IBRC. Furthermore, for the BFs at the BS side, we reconsider the KG approach of section 1.4.2. Apart from faster convergence, the main advantage of KG is that its partial CSIT version demonstrates higher performance than the WSMSE approach.

Second, we consider a non negligible direct link. A new form of interference management is hence possible. This form is interference neutralization (IN), in which artificial multipath is introduced to provoke destructive interference

superposition at Rx's. So, with non negligible direct links, interference management is done via beamforming (ZF) at the BS and RS sides and via interference neutralization as well. Our contribution consists in studying the joint ZF+IN feasibility conditions at the BS and RS respectively. This involves the full column rank of Khatri-Rao products.

6.2 The IBRC signal model

In this chapter, we consider the MIMO IBRC with MIMO FD relay scenario known as the Two-Hop Interference Broadcast Scenario. We also consider a DL cellular network consisting of C cells serving a total of K N -antennas users with the assistance of a AF RS. The direct links between the BSs and the users are neglected. We shall consider a system-wide numbering of the users for some sections. User k is served by BS b_k . The system's configurations is depicted in Figure 6.1. The transmitted signal at BS c is given by:

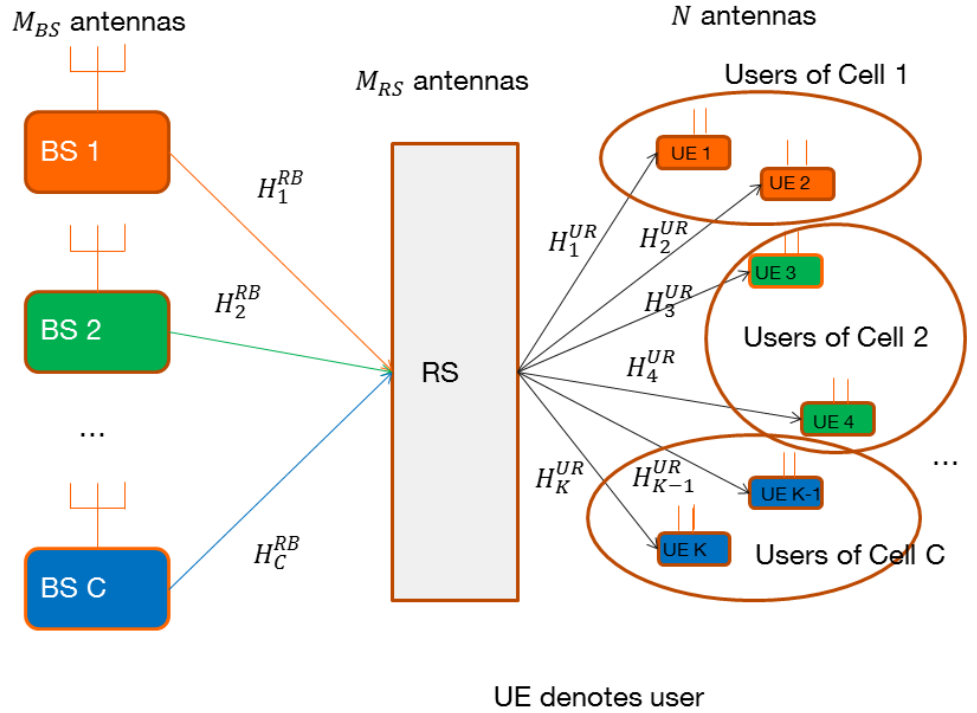


FIGURE 6.1: The IBRC DL scenario

$$\mathbf{x}_c = \sum_{i:b_i=c} \mathbf{G}_i \mathbf{s}_i \quad (6.1)$$

where $i : b_i = c$ denotes the users served by BS c . $\mathbf{s}_i \in \mathbb{C}^{d_k \times 1}$ represents the intended signal of user i and is chosen from a Gaussian codebook. \mathbf{G}_i is the BF of user i with dimensions $M_{BS} \times d_i$ with d_i being the number of streams designated to user i . At the RS, the received signal can be expressed as follows:

$$\mathbf{Y}_{RS} = \sum_c \mathbf{H}_c^{RB} \mathbf{x}_c + \mathbf{n}_{RS} \quad (6.2)$$

where $\mathbf{H}_c^{RB} \in \mathbb{C}^{M_{RS} \times M_{BS}}$ is the channel from BS c to the RS and $\mathbf{n}_{RS} \sim \mathcal{C}(0, \sigma_{RS}^2)$ follows a Gaussian additive noise of zero mean and σ_{RS}^2 variance. The covariance matrix \mathbf{R}_{RS} of the signal received \mathbf{Y}_{RS} at the RS is given as follows:

$$\mathbf{R}_{RS} = \sum_j \mathbf{H}_j^{RB} \left(\sum_{i:b_i=j} \mathbf{G}_i \mathbf{G}_i^H \right) \mathbf{H}_j^{RB,H} + \sigma_{RS}^2 \mathbf{I}_{M_{RS}} \quad (6.3)$$

The RS is an AF relay, hence it retransmits the signal after linearly preprocessing it with the relay matrix \mathbf{F} of dimensions $M_{RS} \times M_{RS}$. Then, the received signal at user k is given by:

$$\mathbf{Y}_k = \underbrace{\mathbf{H}_{k,b_k}^{UB} \mathbf{G}_k \mathbf{s}_k}_{\text{signal}} + \mathbf{Z}_k \quad (6.4)$$

with

$$\mathbf{Z}_k = \underbrace{\sum_{\substack{i \neq k \\ b_i = b_k}} \mathbf{H}_{k,b_k}^{UB} \mathbf{G}_i \mathbf{s}_i}_{\text{intracell interf.}} + \underbrace{\sum_{j \neq b_k} \sum_{i:b_i=j} \mathbf{H}_{k,j}^{UB} \mathbf{G}_i \mathbf{s}_i}_{\text{intercell interf.}} + \underbrace{\mathbf{H}_k^{UR} \mathbf{F} \mathbf{n}_{RS} + \mathbf{n}_k}_{\text{noise}}$$

where $\mathbf{H}_k^{UR} \in \mathbb{C}^{N \times M_{RS}}$ is the channel matrix from RS to user k and $\mathbf{n}_k \sim \mathcal{C}(0, \sigma^2)$ and $\mathbf{H}_{k,b_k}^{UB} = \mathbf{H}_k^{UR} \mathbf{F} \mathbf{H}_k^{RB} \in \mathbb{C}^{N \times M_{BS}}$ is the concatenation of BS-RS channel, relay matrix and RS-user channel

Since we wish to perform power control, the transmitted signals by the RS and by the BS are subject to the following constraints respectively:

$$\text{tr}(\mathbf{F} \mathbf{R}_{RS} \mathbf{F}^H) \leq P_{RS} \quad (6.5)$$

and

$$\text{tr} \mathbf{G}_c \mathbf{G}_c^H \leq P_c \text{ for } c \in \mathcal{C} \quad (6.6)$$

where P_{RS} and P_c are respectively the maximum transmit power of the RS and BS c and \mathcal{C} is the set of all BSs.

Our objective is to maximize the WSR, so the function becomes:

$$\begin{aligned} \mathbf{G} = \arg \max_{\mathbf{G}} & \sum_{c=1}^C \sum_k u_k r_k \\ \text{subject to} & \quad (6.5) \text{ and } (6.6) \end{aligned} \quad (6.7)$$

where u_k is the corresponding weight and r_k the achievable rate of user k . r_k is given by

$$r_k = \log \det(\mathbf{I}_N + \mathbf{\Gamma}_k) \quad (6.8)$$

$$\mathbf{\Gamma}_k = \mathbf{R}_{z_k}^{-1} \mathbf{H}_{k,b_k}^{\overline{UB}} \mathbf{Q}_k \mathbf{H}_{k,b_k}^{\overline{UB},H} \quad (6.9)$$

where $\mathbf{Q}_k = \mathbf{G}_k \mathbf{G}_k^H$ is the transmit covariance matrix at the BS, $\mathbf{\Gamma}_k$ is the SINR of the k th user and \mathbf{R}_{z_k} is the received interference plus noise covariance matrix at user k given by

$$\begin{aligned} \mathbf{R}_{z_k} = & \sum_{i \neq k: b_i = b_k} \mathbf{H}_{k,b_k}^{\overline{UB}} \mathbf{G}_i \mathbf{G}_i^H \mathbf{H}_{k,b_k}^{\overline{UB},H} + \\ & \sum_{j \neq b_k} \sum_{i: b_i = j} \mathbf{H}_{k,j}^{\overline{UB}} \mathbf{G}_i \mathbf{G}_i^H \mathbf{H}_{k,j}^{\overline{UB},H} + \sigma_{RS}^2 \mathbf{H}_k^{UR} \mathbf{F} \mathbf{F}^H \mathbf{H}_k^{UR,H} + \sigma^2 \mathbf{I}_N \end{aligned} \quad (6.10)$$

Moreover, we define the covariance matrix \mathbf{R}_k of the total received signal at user k as follows:

$$\begin{aligned} \mathbf{R}_k = & \sum_j \sum_{i: b_i = j} \mathbf{H}_{k,j}^{\overline{UB}} \mathbf{G}_i \mathbf{G}_i^H \mathbf{H}_{k,j}^{\overline{UB},H} + \sigma_{n_{RS}}^2 \mathbf{H}_k^{UR} \mathbf{F} \mathbf{F}^H \mathbf{H}_k^{UR,H} + \sigma^2 \mathbf{I}_N \\ = & \mathbf{R}_{z_k} + \mathbf{H}_{k,b_k}^{UR} \mathbf{G}_k \mathbf{G}_k^H \mathbf{H}_{k,b_k}^{UR,H} \end{aligned} \quad (6.11)$$

6.3 The WSMSE precoder for IBRC

The optimization problem in (6.7) is hard to solve directly, since it is highly non convex in the precoding matrix at the BS \mathbf{G} and at the RS \mathbf{F} , where \mathbf{G}

without any index represents the collection of BF at the BSs \mathbf{G}_k . Similarly, \mathbf{W} and \mathbf{D} , whose definitions are given in the following, represent the collection of \mathbf{W}_k and \mathbf{D}_k respectively. To solve it, we reformulate it as an equivalent WSMSE minimization problem as explained in 1.4.1. The new minimization problem is (the constraints are the same as above):

$$\min_{\mathbf{G}, \mathbf{F}, \mathbf{W}, \mathbf{D}} \sum_k (\text{tr}(\mathbf{W}_k \mathbf{\Psi}_k) - \log(\mathbf{W}_k)) \quad (6.12)$$

Where

$$\begin{aligned} \mathbf{\Psi}_k = & \mathbf{I}_{d_k} - \mathbf{G}_k^H \mathbf{H}_{k,b_k}^{\overline{UB},H} \mathbf{D}_k - \mathbf{D}_k^H \mathbf{H}_{k,b_k}^{\overline{UB}} \mathbf{G}_k + \sum_{i:b_i=b_k} \mathbf{D}_k^H \mathbf{H}_{k,b_k}^{\overline{UB}} \mathbf{G}_i \mathbf{G}_i^H \mathbf{H}_{k,b_k}^{\overline{UB},H} \mathbf{D}_k \\ & + \sum_{j \neq b_k} \sum_{i:b_i=j} \mathbf{D}_k^H \mathbf{H}_{k,j}^{\overline{UB}} \mathbf{G}_i \mathbf{G}_i^H \mathbf{H}_{k,j}^{\overline{UB},H} \mathbf{D}_k + \sigma_{RS}^2 \mathbf{D}_k^H \mathbf{H}_k^{UR} \mathbf{F} \mathbf{F}^H \mathbf{H}_k^{UR,H} \mathbf{D}_k + \sigma^2 \mathbf{D}_k^H \mathbf{D}_k \end{aligned} \quad (6.13)$$

where the $\mathbf{\Psi}_k$ is the MSE covariance matrix for general Tx and Rx filters, $\mathbf{W}_k \in \mathbb{C}^{d_k \times d_k}$ is an additional weighting matrix and $\mathbf{D}_k \in \mathbb{C}^{N \times d_k}$ is the Rx at user k . The new problem is quadratic in \mathbf{G} and (\mathbf{F}) if we suppose as \mathbf{F} and (\mathbf{G}) fixed respectively. Thus, it can be solved using alternating optimization. The optimal \mathbf{W}_k and \mathbf{D}_k for fixed $\mathbf{F}, \mathbf{G}, \mathbf{D}$ and \mathbf{F}, \mathbf{G} respectively are given by:

$$\mathbf{W}_k = \mathbf{\Psi}_k^{-1} \quad (6.14)$$

and

$$\mathbf{D}_k = \mathbf{G}_k^H \mathbf{H}_{k,b_k}^{\overline{UB},H} (\mathbf{R}_k)^{-1} \quad (6.15)$$

because the two objective functions (6.7) and (6.12) are equivalents only if $\mathbf{W}_k = \mathbf{\Psi}_k^{-1}$. To determine \mathbf{F} , we must consider all other variables as fixed and set the following Lagrangian as null, as follows:

$$\mathcal{L}_1 = \sum_k \text{tr}(\mathbf{W}_k \mathbf{\Psi}_k) + \lambda (\text{tr}(\mathbf{F} \mathbf{R} \mathbf{F}^H) - P_{RS}) \quad (6.16)$$

$$\begin{aligned}
\frac{d\mathcal{L}_1}{dF} = 0 &\implies \\
\mathbf{F} &= \left(\sum_i \mathbf{H}_i^{UR,H} \mathbf{D}_i^H \mathbf{W}_i \mathbf{D}_i \mathbf{H}_i^{UR} + \lambda \mathbf{I}_{M_{RS}} \right)^{-1} \\
&\times \left(\sum_j \sum_{l \neq b_k} \sum_{i:b_i=l} \mathbf{H}_j^{UR,H} \mathbf{D}_j \mathbf{W}_j \mathbf{D}_j^H \mathbf{H}_j^{UR} \mathbf{F} \mathbf{H}_l^{RB} \mathbf{G}_i \mathbf{G}_i^H \mathbf{H}_l^{RB,H} \right. \\
&\left. - \sum_i \mathbf{H}_i^{UR,H} \mathbf{D}_i \mathbf{W}_i \mathbf{G}_i^H \mathbf{H}_{b_i}^{RB,H} \right) \left(\sum_j \sum_{i:b_i=j} \mathbf{H}_j^{RB} \mathbf{G}_i \mathbf{G}_i^H \mathbf{H}_j^{RB,H} + \sigma_{RS}^2 \mathbf{I}_{M_{RS}} \right)^{-1}
\end{aligned} \tag{6.17}$$

$$\tag{6.18}$$

The Lagrangian λ must be adjusted by bisection. Now, we proceed to determine the BF \mathbf{G}_k while the other variables are considered as fixed. Two constraints are related to that problem. We reduce it to a problem with a single sum constraint as follows:

$$\mathcal{L}_2 = \sum_k \text{tr}(\mathbf{W}_k \mathbf{\Psi}_k) + \xi \left(\sum_j \sum_{i:b_i=j} \mu_j \text{tr}(\mathbf{Q}_i) + \lambda \text{tr}(\mathbf{F} \mathbf{R}_{RS} \mathbf{F}^H) - P_t \right)$$

where P_t is the total transmit power.

$$\begin{aligned}
\frac{d\mathcal{L}_2}{d\mathbf{G}_k} = 0 &\implies \\
\mathbf{G}_k &= \left(\sum_i \mathbf{H}_{i,b_k}^{\overline{UB},H} \mathbf{D}_i \mathbf{W}_i \mathbf{D}_i^H \mathbf{H}_{i,b_k}^{\overline{UB}} + \xi (\mu_{b_k} \mathbf{I}_{M_{BS}} \right. \\
&\left. + \lambda \mathbf{E}_{b_k}^{RB,H} \mathbf{F}^H \mathbf{F} \mathbf{E}_{b_k}^{RB}) \right)^{-1} \mathbf{H}_{k,b_k}^{\overline{UB},H} \mathbf{D}_k \mathbf{W}_k
\end{aligned} \tag{6.19}$$

The Lagrangian ξ and λ must be adjusted by bisection in order to satisfy the power constraints at the RS. To determine the maximum $\mu_{b_k} \forall b_k$ and λ a subgradient method is applied. For further details, please refer to [54].

6.4 The KG precoder for IBRC

In this section, we propose a variant for the calculation of the Tx BFs, which is the KG approach of 1.4.2. We assume fixed relay matrix, hence we are concerned by the Transmit BFs. The starting point is the objective function of (6.7).

$$\begin{aligned}
WSR &= u_k \log \det(\mathbf{R}_{z_k}^{-1} \mathbf{R}_k) + WSR_{z_k}, \\
WSR_{z_k} &= \sum_{i=1, \neq k}^K u_i \log \det(\mathbf{R}_{z_i}^{-1} \mathbf{R}_i)
\end{aligned} \tag{6.20}$$

where \mathbf{R}_{z_k} and \mathbf{R}_k are given by (6.7) and (6.12). $\log \det(\mathbf{R}_{z_k}^{-1} \mathbf{R}_k)$ is concave in \mathbf{Q}_k but WSR_{z_k} is not. We consider the first order Taylor series expansion of WSR_{z_k} in \mathbf{Q}_k around $\hat{\mathbf{Q}}$ (i.e. all $\hat{\mathbf{Q}}_i$) with e.g. $\hat{\mathbf{R}}_i = \mathbf{R}_i(\hat{\mathbf{Q}})$, then

$$\begin{aligned} WSR_{z_k}(\mathbf{Q}_k, \hat{\mathbf{Q}}) &\approx WSR_{z_k}(\hat{\mathbf{Q}}_k, \hat{\mathbf{Q}}) - \text{tr}\{(\mathbf{Q}_k - \hat{\mathbf{Q}}_k) \hat{\mathbf{A}}_k\} \\ \hat{\mathbf{A}}_k &= - \left. \frac{\partial WSR_{z_k}(\mathbf{Q}_k, \hat{\mathbf{Q}})}{\partial \mathbf{Q}_k} \right|_{\hat{\mathbf{Q}}_k, \hat{\mathbf{Q}}} = \sum_{i \neq k}^K u_i \mathbf{H}_{i,b_k}^{\overline{UB}, H} (\hat{\mathbf{R}}_{z_i}^{-1} - \hat{\mathbf{R}}_i^{-1}) \mathbf{H}_{i,b_k}^{\overline{UB}} \end{aligned} \quad (6.21)$$

We get the Lagrangian

$$\begin{aligned} WSR(\mathbf{G}, \hat{\mathbf{G}}, \lambda) &= \sum_{j=1}^C \mu_j P_c + \\ &\sum_{k=1}^K u_k \log \det(\mathbf{I}_{d_k} + \mathbf{G}_k^H \hat{\mathbf{B}}_k \mathbf{G}_k) - \text{tr}\{\mathbf{G}_k^H (\hat{\mathbf{A}}_k + \mu_{b_k} \mathbf{I}_M + \lambda \mathbf{H}_{b_k}^{RB, H} \mathbf{F}^H \mathbf{F} \mathbf{H}_{b_k}^{RB} \mathbf{G}_k)\} \end{aligned} \quad (6.22)$$

where

$$\hat{\mathbf{B}}_k = \mathbf{H}_{k,b_k}^{\overline{UB}, H} \hat{\mathbf{R}}_{z_k}^{-1} \mathbf{H}_{k,b_k}^{\overline{UB}}. \quad (6.23)$$

The gradient (w.r.t. \mathbf{G}_k) of this concave WSR allows an interpretation as a generalized eigenmatrix condition, thus $\mathbf{G}_k' = \text{eigenmatrix}(\hat{\mathbf{B}}_k, \hat{\mathbf{A}}_k + \mu_{b_k} \mathbf{I}_M + \lambda \mathbf{H}_{b_k}^{RB, H} \mathbf{F}^H \mathbf{F} \mathbf{H}_{b_k}^{RB})$ is the (normalized) generalized eigenmatrix of the two indicated matrices, with eigenvalues $\Sigma_k = \text{eigenvalues}(\hat{\mathbf{B}}_k, \hat{\mathbf{A}}_k + \mu_{b_k} \mathbf{I}_M + \lambda \mathbf{H}_{b_k}^{RB, H} \mathbf{F}^H \mathbf{F} \mathbf{H}_{b_k}^{RB})$. Let $\Sigma_k^{(1)} = \mathbf{G}_k'^H \hat{\mathbf{B}}_k \mathbf{G}_k'$, $\Sigma_k^{(2)} = \mathbf{G}_k'^H \hat{\mathbf{A}}_k \mathbf{G}_k'$. The advantage of formulation (6.22) is that it allows straightforward power adaptation: introducing diagonal power matrices $\mathbf{P}_k \geq 0$ and substituting $\mathbf{G}_k = \mathbf{G}_k' \mathbf{P}_k^{\frac{1}{2}}$ in (6.22) yields

$$\begin{aligned} WSR &= \sum_{j=1}^C \lambda_j P_j^{BS} + \sum_{k=1}^K [u_k \log \det(\mathbf{I}_{d_k} + \mathbf{P}_k \Sigma_k^{(1)}) \\ &\quad - \text{tr}\{\mathbf{P}_k (\Sigma_k^{(2)} + \mu_{b_k} \mathbf{I}_{d_k} + \lambda \mathbf{H}_{b_k}^{RB, H} \mathbf{F}^H \mathbf{F} \mathbf{H}_{b_k}^{RB})\}] \end{aligned} \quad (6.24)$$

which leads to the following interference leakage aware water filling

$$\mathbf{P}_k(l, l) = \quad (6.25)$$

$$\left(\frac{1}{\Sigma_k^{(1)}(l, l)} \left(\frac{u_k \Sigma_k^{(1)}(l, l)}{\Sigma_k^{(2)}(l, l) + \mu_{b_k} + \lambda (\mathbf{E}_{b_k}^H \mathbf{F}^H \mathbf{F} \mathbf{E}_{b_k})(l, l)} - 1 \right) \right)^+ \quad (6.26)$$

for all l s.t. $\Sigma_k^{(1)} > 0$ where $z^+ = \max(0, z)$.

We propose to use the optimization method exposed in this section in order to

TABLE 6.1: The Iterative WSR Algorithm

| |
|--|
| For $k = 1 \dots K$, initialize $\mathbf{G}_k^{(0)}$ |
| Initialize $\mathbf{F}^{(0)}$ |
| Repeat until convergence |
| 1. Compute $\mathbf{D}_k^{(j+1)}$ and $\mathbf{W}_k^{(j+1)}$ for $\forall k$ for fixed $\mathbf{G}^{(j)}$ and $\mathbf{F}^{(j)}$ using (6.15) and (6.14). |
| 2. Compute $\mathbf{F}^{(j+1)}$ for fixed $\mathbf{D}^{(j+1)}$, $\mathbf{W}^{(j+1)}$ and $\mathbf{G}^{(j)}$ using (6.18). |
| 3. Repeat Until Convergence |
| 3.1 Compute $\mathbf{G}_k'^{(i+1)}$ and $\mathbf{P}_k^{(i+1)}$ using $\mathbf{G}_k'^{(i+1)} =$ eigenmatrix($\widehat{\mathbf{B}}_k^{(j)}, \hat{\mathbf{A}}_k^{(j)} + \mu_{b_k}^{(i)} \mathbf{I}_M + \lambda \mathbf{H}_{b_k}^{RB,H} \mathbf{F}^{H,(j)} \mathbf{F}^{(j)} \mathbf{H}_{b_k}^{RB}$) and (6.26) respectively. |
| 3.2 Update $\mu_{b_k}^{(i+1)}$ for $\forall k$ and $\lambda^{(i+1)}$ as $\mu_{b_k}^{(i+1)} = \mu_{b_k}^{(i)} + \alpha \left(\sum_{i:b_i=b_k} \text{tr} \mathbf{Q}_i^{(i+1)} - P_{b_k} \right) \text{ for } \forall b_k$ $\lambda^{(i+1)} = \lambda^{(i)} + \alpha \left(\text{tr} (\mathbf{F}^{(j)} \mathbf{R}_{RS}^{(j)} \mathbf{F}^{H,(j)}) - P_{BS} \right)$ |

update the BFs at the BSs \mathbf{G} . Meanwhile, we use the approach of the previous section in order to update \mathbf{F} . The final algorithm is explained in Table 4.1, where α denotes the step size of the subgradient algorithm.

6.5 Numerical results and short discussion

In this section, we present some simulation results which prove that our algorithm is slightly better than the pure WSMSE algorithm.

We consider the DL of a cellular system consisting of $C = 2$ cells having BSs with $M_{BS} = 4$ antennas each and serving a total of $K = 4$ $N = 2$ -antennas users with the help of a RS endowed with $M_{RS} = 8$ antennas. The power of the different BSs and RS are normalized such that $P_i = 1 = P_{RS}$ for $i \in \mathcal{C}$. However, $\sigma^2 = \sigma_{RS}^2 = \frac{1}{SNR}$, where SNR ranges from 0 to 20 dB in the simulations. The channel coefficients are generated as i.i.d zero mean unit-variance complex Gaussian random variables. We average 50 different channel realizations to produce our results. The step size is chosen to be $\alpha = 0.01$. The convergence

criteria for the third step in Table 4.1 are as follows:

$$|\lambda \text{tr}(\mathbf{F}\mathbf{R}_{RS}\mathbf{F}^H) - P_{RS}| \leq \epsilon \quad (6.27)$$

$$|\mu_{b_k}(\sum_{i:b_i=b_k} \text{tr}\mathbf{Q}_i - P_{b_k})| \leq \epsilon \text{ for } \forall b_k \quad (6.28)$$

with $\epsilon = 0.001$.

Figure 6.2 shows that our proposed algorithm is slightly better than the pure WSMSE algorithm. A small difference can be explained by the fact that this study does not assume a direct link between the BSs and the users, hence all the work must be performed by the RS and some changes at the BS side would not affect a lot the final achievable sum rate.

Indeed, the value of this work does not reside only in this difference of sum rate. More than that, this work smooths the path for future studies where imperfect channel estimations would be assumed. In that particular case, our proposed method based on KG to design \mathbf{G} and on the WSMSE approach to design \mathbf{F} would be way more advantageous than the pure WSMSE, since, in general, KG-based BFs are more robust to channel imperfections as shown in Chapter 4.

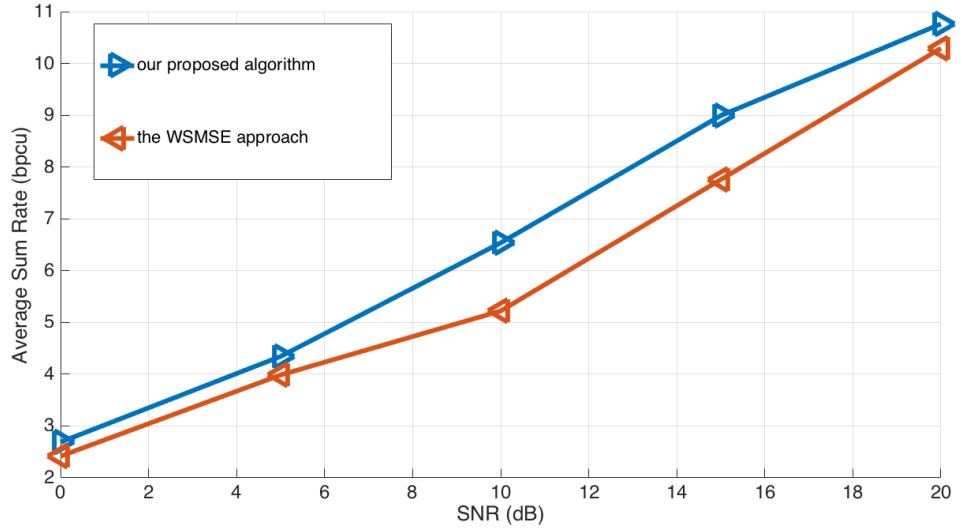


FIGURE 6.2: Sum rate Comparison for $C = 2, K = 4, M_{BS} = 4, N = 2, M_{RS} = 8$

6.6 Joint ZF-IN feasibility conditions

We consider MISO IBRC with MIMO FD relay with direct links (Figure 6.3). So, BS and users communicate both directly and via relay. $\mathbf{h}_{c,c,k}^{UB}$ and $\mathbf{h}_{c,k}^{UR}$ are

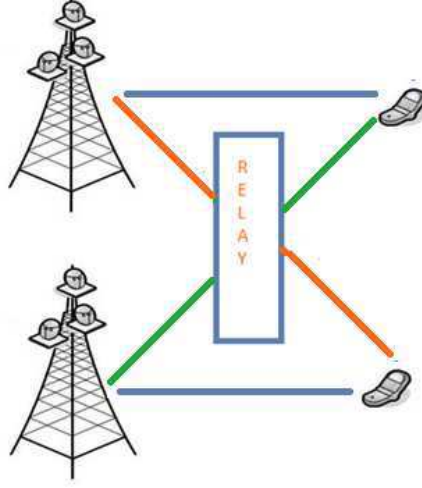


FIGURE 6.3: Relay and direct links

now vectors of dimensions $1 \times M_{BS}$ and $1 \times M_{RS}$ respectively. In this section we do not use system-wide numbering of the users. Let us suppose that we have K users per cell. The received signal can be written as:

$$\begin{aligned}
 y_{c,k} = & \underbrace{\mathbf{h}_{c,c,k}^{UB} \mathbf{g}_{c,k} x_{c,k} + \sum_{(j,i) \neq (c,k)}^{(C,K)} \mathbf{h}_{c,j,k}^{UB} \mathbf{g}_{j,i} x_{j,i}}_{\text{direct signal}} + v_{c,k} \\
 & + \underbrace{\mathbf{h}_{c,k}^{UR} \mathbf{F} \left\{ \sum_{(j,i)=(1,1)}^{(C,K)} \mathbf{H}_j^{RB} \mathbf{g}_{j,i} x_{j,i} + n_{c,k} \right\}}_{\text{link via relay}}
 \end{aligned} \tag{6.29}$$

where the conditions for joint ZF-IN on the BF vectors $\mathbf{g}_{j,i}$ and the AF matrix \mathbf{F} are indicated. The noise-free received signal can be rewritten as:

$$y_{c,k} = \underbrace{(\mathbf{h}_{c,c,k}^{UB} + \mathbf{h}_{c,k}^{UR} \mathbf{F} \mathbf{H}_c^{RB}) \mathbf{g}_{c,k}}_{\neq 0} x_{c,k} + \sum_{(j,i)=(1,1), \neq (c,k)}^{(C,K)} \underbrace{(\mathbf{h}_{c,j,k}^{UB} + \mathbf{h}_{c,k}^{UR} \mathbf{F} \mathbf{H}_j^{RB}) \mathbf{g}_{j,i}}_{=0} x_{j,i} \tag{6.30}$$

These conditions can perhaps be more easily interpreted in a dual UL in which we have an Interfering Multiple Access Channel (IMAC) plus Relay:

$$\mathbf{g}_{j,i}^H (\mathbf{h}_{c,j,k}^{UB,H} + \mathbf{H}_j^{RB,H} \mathbf{F}^H \mathbf{h}_{c,k}^{UR,H}) = 0 \quad \forall (j,i) \neq (c,k) \quad (6.31)$$

in which the BF $\mathbf{g}_{j,i}^H$ now plays the role of ZF Rx. Having M_{BS} antennas, the BS Rx can zero force $M_{BS} - 1$ interfering streams while still receiving the stream of interest. For user (j,i) , let $S_{j,i}$ denote the set of $M_{BS} - 1$ users that will be suppressed by $\mathbf{g}_{j,i}$. Then, the conditions (6.31) become IN conditions for the AF matrix \mathbf{F} for the interfering users $(c,k) \notin \{(j,i)\}, S_{j,i}\}$. The number of such conditions is $KC(KC - 1)(M_{BS} - 1)KC = KC(KC - M_{BS})$. Note that the ZF conditions for the $\mathbf{g}_{j,i}$ and the IN conditions for \mathbf{F} involve different (and hence independent) user channels $\mathbf{h}_{c,j,k}$. Hence, even though the ZF and IN conditions are coupled, the BF can be considered as independent of \mathbf{F} in the IN conditions. For the same reason also, the direct overall channel gains appearing in (6.30) (for $(c,j,k) = (c,c,k)$) will be non-zero, in spite of the conditions (6.31).

By introducing the $\text{vec}(\cdot)$ operator, which stacks consecutive columns of a matrix in a supervector, with the property $\text{vec}(\mathbf{AXB}) = (\mathbf{B}^T \otimes \mathbf{A})\text{vec}(\mathbf{X})$ where \otimes denotes the Kronecker product, and taking Hermitian transpose of the scalars in (6.31), we can rewrite the IN conditions from (6.31) as:

$$\text{vec}^H(\mathbf{F}^H)(\mathbf{h}_{c,k}^{UR,T} \otimes \mathbf{H}_j^{RB} \mathbf{g}_{j,i}) = -\mathbf{h}_{c,j,k}^{UB} \mathbf{g}_{j,i} \quad (6.32)$$

which need to hold for $\forall (c,k) \notin \{(j,i)\}, S_{j,i}\}$. There are many ways of selecting the sets $S_{j,i}$, leading to many solutions for joint ZF-IN. Each solution will correspond to a local optimum for utility optimization designs. Let us consider one specific choice for the $S_{j,i}$ in which the $M_{BS} - 1$ users to be ZF'd comprise in any case the $K - 1$ other users in cell j and such that $S_j = \{(j,i)\}, S_{j,i}\}$ is independent of i . Then let $\mathbf{H}_j^{UR} = [\mathbf{h}_{c,k}^{UR,T}, (c,k) \notin S_j]$ which is a matrix of size $M_{RS} \times (CK - M_{BS})$. Introduce $\mathbf{G}_j = [\mathbf{g}_{j,1} \cdots \mathbf{g}_{j,k}]$ of size $M_{BS} \times K$ and $\mathbf{h}_j^{UB} = [\mathbf{h}_{c,j,k}^{UB} \mathbf{g}_j, (c,k) \notin S_j]$, then we can rewrite (6.32) as

$$\text{vec}^H(\mathbf{F}^H)[\mathbf{H}_1^{UR} \otimes \mathbf{H}_1^{RB} \mathbf{G}_1 \cdots \mathbf{H}_C^{UR} \otimes \mathbf{H}_C^{RB} \mathbf{G}_C] = -[\mathbf{h}_1^{UB} \cdots \mathbf{h}_C^{UB}] \quad (6.33)$$

This system of equations can be solved for $\text{vec}^H(\mathbf{F}^H)$ if the matrix of coefficients has full column rank. To investigate this, we can use the following Lemma.

Lemma 4.1: Full column rank conditions of Khatri-Rao product. We consider the block matrices $\mathbf{A} = [\mathbf{A}_1 \cdots \mathbf{A}_n]$, $\mathbf{B} = [\mathbf{B}_1 \cdots \mathbf{B}_n]$ with compatible column block structure, their Khatri-Rao product $\mathbf{A} \cdot \mathbf{B} = [\mathbf{A}_1 \otimes \mathbf{B}_1 \cdots \mathbf{A}_n \otimes \mathbf{B}_n]$ has full column rank if and only if (iff)

1. all \mathbf{A}_i and \mathbf{B}_i have column rank
2. at least one of \mathbf{A} or \mathbf{B} has full column rank.

Proof. Sufficiency is fairly straightforward. For necessity, (1) is a result of $\text{rank}(\mathbf{A}_i \otimes \mathbf{B}_i) = \text{rank}(\mathbf{A}_i)\text{rank}(\mathbf{B}_i)$. (2) for the case $n=2$, by contradiction: given that the \mathbf{A}_i and \mathbf{B}_i have full column rank, but if both \mathbf{A} and \mathbf{B} didn't have full column rank, then vectors $\mathbf{a}_i, \mathbf{b}_i$ exist so that $\mathbf{A}_1 \mathbf{a}_1 = \mathbf{A}_2 \mathbf{a}_2$ and $\mathbf{B}_1 \mathbf{b}_1 = \mathbf{B}_2 \mathbf{b}_2$. Then $\mathbf{A}_1 \mathbf{a}_1 \mathbf{b}_1^T \mathbf{B}_1 = \mathbf{A}_2 \mathbf{a}_2 \mathbf{b}_2^T \mathbf{B}_2$ and

$$\text{vec}(\mathbf{B}_i \mathbf{b}_i \mathbf{a}_i^T \mathbf{A}_i^T) = (\mathbf{A}_i \otimes \mathbf{B}_i) \text{vec}(\mathbf{b}_i \mathbf{a}_i^T) = (\mathbf{A}_i \otimes \mathbf{B}_i)(\mathbf{a}_i \otimes \mathbf{b}_i) \quad (6.34)$$

Hence, $(\mathbf{A} \cdot \mathbf{B})[(\mathbf{a}_1 \otimes \mathbf{b}_1)^T - (\mathbf{a}_2 \otimes \mathbf{b}_2)^T]^T = 0$, which means that $\mathbf{A} \cdot \mathbf{B}$ would not have full column rank. Applying Lemma 4.1 to (6.33) leads to the following.

Theorem 4.1: Interference Neutralization Feasibility IN the MISO IRBC with MIMO relay with the dimensions considered above, IN is feasible iff

$$M_{RS} \geq \max(K, CK - M_{BS}, \min(K, CK - M_{BS})), K \leq M_{BS} \quad (6.35)$$

This leads to the following evolution for the number of relay antennas:

$$M_{RS} = \begin{cases} 0, & 1 \leq K \leq \frac{M_{BS}}{C} \\ C^2(K - \frac{M_{BS}}{C}), & \frac{M_{BS}}{C} \leq K \leq \frac{M_{BS}}{C-1} \text{ where in the first regime only} \\ CK, & \frac{M_{BS}}{C-1} \leq K \leq M_{BS} \end{cases}$$

ZF BF is needed. The following are two variations on the basic scenario.

Intracell BF. In this case, the BF is non-cooperative between cells and only considers the intracell users (the BF is multicell oblivious). All intercell interference needs to be canceled by IN. Hence, $N = C(CK - M_{BS})$ gets replaced by $M_{RS} = C(C - 1)K$.

BF-independent AF The IN equations will not depend on the BF \mathbf{G}_j (though the BF will still depend on the AF \mathbf{F}) if interference is not neutralized starting from the BF inputs but starting from the BS antennas. Then, the factors \mathbf{G}_j disappear from the equation in (6.33). This leads to IN conditions:

$M_{RS} \geq \max(M_{BS}, CK - M_{BS}, \min(M_{BS}, CK - M_{BS}))$. The ZF and IN conditions can be solved iteratively as follows. Start e.g. with $\mathbf{F} = 0$.

1. The BFs $\mathbf{g}_{j,i}$ can be solved by ZF the direct links in (6.30) w.r.t. the effective channels in (6.31) of the other users in S_j .
2. The AF matrix \mathbf{F} can then be determined from the equations (6.33).

Iterate (1) and (2) until convergence. Whereas joint ZF-IN can have many solutions, fixing the sets S_j forces convergence to one particular solution (apart from underdeterminacy issues of course if N is larger than necessary). For the case of $C = 2$ cells, $M_{RS} = 4(K - \frac{M_{BS}}{2})^+$ which evolves from 0 to $2M_{BS}$ as K evolves from $\frac{M_{BS}}{2}$ to M . For the Intracell BF case, we get $M_{RS} = 2K$, whereas the BF-independent AF case (typically) also leads to $M_{RS} = 4(K - \frac{M_{BS}}{2})^+$.

6.7 Conclusion

In this chapter, we treat the problem of communications with relays. In the first study, we treat the case where the BSs and the users can't communicate directly but via a relay. Again, the problem of interest is to design jointly all the BFs and the relay matrix. We suppose perfect CSIT. A WSMSE-type solution exists. We propose a WSMSE-DC based solution where the relay matrix is always given by the WSMSE approach, but the BFs at the Tx side are given by a DC approach. Briefly, the BFs are given by linearizing the objective function corresponding to the sum rate of all the users except for the one of interest. We show that this solution is better. In the second study, we suppose that the BSs and the users can communicate via two ways, directly or via the relay. Two interference management techniques are at stake: IA and IN. IA is the interference management technique highlighted in all of the chapters of this thesis. IN appears here for the first time, where artificial multipath is introduced to provoke destructive interference superposition at Rxs. We derive the DoFs of such scenario. The difficulty of IN is that the relay must know the channels from BSs to users which is hard to be achieved in practice.

Chapter 7

Conclusions and Future Works

7.0.1 Summary and conclusions

Some results of this thesis are presented in the deliverables of two European Projects H2020 Fantastic5G (<http://fantastic5g.com>) and One5G (<https://one5g.eu>). The thesis treats the problem of interference cancellation and capacity maximization in Massive MIMO 5G networks. The study focuses on the wireless access segment of 5G cellular communications and targets the key problem of interference that is due to frequency reuse. This has been a long standing impairment in cellular networks of all generations that will be further exacerbated in 5G networks, due to the expected dense cell deployment. In this context, the thesis proposes new interference management alternatives thanks to the Massive MIMO antenna regime, taking into account also the practical challenges of Massive antenna arrays. Chapter 1 provides the motivation and sets the context for the thesis studies. It also introduces the key notation and system model to be studied. The main drawbacks and challenges of antenna and system design when the number of antennas at the base station scales to large numbers (such as RF impairments and channel contamination) are first discussed, followed by a discussion on the important topic of pilot contamination and its elimination. This is followed by a presentation of the frequency bands for 5G and a motivation of the combined mmwave / Massive MIMO communication. After the notation and system setup, two precoding algorithms (WSMSE and KG) are presented in detail, since they constitute

the basis for the thesis' proposed techniques for the massive MIMO regime. This is followed by the presentation of deterministic annealing and channel estimation for this considered setup. A listing of the key contributions of the thesis is also included in this chapter. Chapter 2 contains a performance analysis of the WSMSE algorithm in the large system regime (antennas, users) of multi-cell / multi-user massive MISO networks based on Random Matrix Theory. The work can be seen as an extension of previous studies which rely on deterministic equivalent SINR expressions (since SINR is a key capacity parameter for MISO systems). This approach is adopted here as well and applied to the WSMSE precoders presented in Chapter 1, assuming perfect CSI and centralized precoding. The derived deterministic equivalent expressions are then validated numerically, showing good agreement with the actual sum rates for the case of 3 cells, 30 antennas and on the order of 10 users per cell. The results are then extended to the MIMO single stream cases, where the equivalent deterministic SINR approach is again shown to be valid. The derived deterministic equivalent SINR expressions are then used in order to prove a capacity scaling result for the case of multi-antenna receivers. Chapter 3 considers the case of decentralized coordinated beamforming that relies on slow fading information exchange between the base stations. The large system analysis approach is adopted again, focusing on the WSMSE technique and targeting optimal beamforming solutions in this sense. The approach relies on the exchange of interference leakage terms that are caused by every base station to all the users of every interfering base station via fixed (perfectly reliable) backhaul links. Since in general this information exchange may be heavy and take many iterations until it converges, the initialization of the precoders is key both in terms of convergence speed and of the attained solution. For this, the thesis proposes a new initialization which is shown theoretically to be asymptotically optimal in the large system (infinite antenna / infinite users, with fixed ratio between them) regime (Theorem 3.1), termed 'LS-precoder'. Three different variants of interference leakage calculation and exchange between base stations are considered, ranging from the calculation of only intracell interference based on local channel knowledge and complete disregard of intercell interference to the calculation of all up-to-date intra and inter cell interference and full sharing between all the cells via the fixed backhaul links. Interestingly, even the two sub-optimal variants that do not use the up-to-date intercell interference, perform better than previously proposed

techniques and in fact seem to have identical performance between them and offer minimal gain over the LS precoder initialization in the non-fully loaded case. They also converge very fast (in 2 to 3 iterations). The results also show that non-fully loaded networks ($KC/M < 1$) perform clearly better than fully loaded ones. The chapter concludes with some closed-form expressions of the LS precoder for some highly idealized assumptions of diagonal channel covariance matrices (which may relate to actual situations in asymptotic large scale regimes). Chapter 4 switches gears by assuming partial CSIT, (still assuming perfect CSIR) and targeting again optimal precoders for the large system regime. The problem is formulated as an optimization of the EWSR objective function. The proposed technique is termed ESEI-WSR and relies on the fact that in the large (Massive) system regime, the expected weighted sum rate (over the channels) will converge to the actual WSR and can be written as a function of the WSR corresponding to the estimated channel and an error term that relies on the channel error covariance matrix. The corresponding precoder is optimal in this sense (having assumed, as throughout the thesis, an identity channel covariance matrix at each receiver). DA is again adopted in order to drive the solution to avoid local optima. The ESEI-WSR thus obtained is then numerically evaluated for small / practical configurations (2 cells, 8 antennas and 4 users per cell) and shown to provide small gains over previous sub-optimal approaches for the case of single antenna receivers but clearly better performance for multi (2 or 4) antenna receivers, in which case the sub-optimal approaches show a flooring of their performance. While optimal in the above sense, the ESEI-WSR technique is heavy in terms of channel information exchange between base stations requirements. For this, a practical decentralized extension is derived, wherein instantaneous CSIT is only used for the intended receivers, while unintended receivers of other cells are only captured via the corresponding channel covariance matrices (intracell channels are assumed perfectly known via TDD, while intercell instantaneous channels are unknown). The algorithm is suitable for distributed implementation (due to the small required information exchange, i.e., only several scalars coming from the trace function need be exchanged) and has low complexity and fast convergence. Its performance is numerically evaluated for a number of cases (correlated low rank channels and uncorrelated channels with identity channel covariances). The ESEI-WSR is then further formulated and simplified for the case of Massive MISO channels by using the large system analysis

tools. An alternative suboptimal approach based on the KG algorithm is then proposed for the case of both transmit and receive antennas jointly growing to infinity with bounded ratio, showing numerically significant gains over the naïve approach. Chapter 5 departs from the realm of linear precoding and considers nonlinear schemes. The MIMO IBC setup is formulated and the pursued approach consists of a combination of per-cell nonlinear scheme and a cooperative management on the interference leaked by the precoders of all the cells in order to jointly optimize the ESEI-WSR criterion introduced in Chapter 4. In view of partial CSIT, the chosen per-cell nonlinear precoding is LA instead of DPC, which would be optimal in the case of perfect CSIT. After the formulation of the IBC problem, the linear assignment and beamforming matrices are formulated, setting the ground for the sought joint transmit design. As the two parameter sets (matrices) depend on one another, an alternative optimization approach would make sense, yet would require a high complexity. To avoid this, a closed form expression is derived for the LA matrix, based on an upper bound of the rate. This reduced the search of the optimal beamforming matrix to a single criterion (ESWR), similar to the one introduced in Chapter 1. For the case of perfect CSIT, a previously derived approach by Nguyen and Le-Ngoc is adopted, where the 1st order Taylor series expansion of the covariance matrix, combined with successive interference cancellation for the dual (MAC) problem, leads to a separable convex optimization problem that provides successively the solutions of the optimal decoders. For the case of partial CSIT, the same approach is followed, but the effect of partial CSIT is captured by considering the asymptotic expressions of channel covariances which in the infinite antenna limit equal the corresponding deterministic values (same approach as in Section 4.3). The precoding matrices are obtained in an iterative way by assuming a certain diagonalization property of the separable channel correlations. The obtained solutions are numerically evaluated for cases of 3 cells, 3 users per cell, 8 base station antennas and 2 antennas per receiver terminal and compared with (and shown to be superior to) the robust linear solutions, as well as other special cases and bounds. Finally, Chapter 6 considers the case of the interference broadcast channel with use of relays (termed IRBC). A two-hop relay configuration is considered and AF relaying is adopted, wherein the relaying nodes perform new linear combining to the received signals, subject to new power constraints. It is further assumed that relays are full-duplex (as opposed to conventional half-duplex relaying), in

order to further boost the spectral efficiency. After introducing the IBRC signal model, the maximization of the weighted sum rate metric is formulated, subject to the power constraints. Then, we explain the existing WSMSE solution. However, we propose an Alternate optimization, using WSME precoding for the base station precoders and KG filters for the relay stations. The chapter concludes by considering the case where direct links between the base stations and the end users exist as well and derives conditions and a solution that involve zero forcing precoding and interference neutrality.

7.0.2 Future work

Numerous extensions of this works are possible. Ranging from studying the practical implementation of the algorithms proposed in this thesis to extending the relays study in Chapter 6 to partial CSIT... Massive MIMO is beneficial for sub-6 Ghz, but essential for mmWaves. Concerning mmWaves, the beamformers developed in this thesis may not be feasible because we would need as many RF chains as the number of antennas which is very costly at high frequencies. It would be very useful to investigate hybrid design of beamformers that are suitable for mmWaves. It involves a two stage design one RF and another digital stage in baseband which are optimized jointly.

Chapter 8

Résumé en Français

8.1 Introduction

L'évolution des communications sans fil doit répondre à la demande toujours croissante de débits plus élevés. C'est l'un des sujets phares étudiés dans la théorie d'information pendant cette dernière décennie. Un défi a été lancé par Qualcomm pour augmenter les débits maximales des communications sans fil par un facteur 1000 pour l'horizon 2020. Il est déjà clair que pour atteindre cet objectif, une combinaison d'ingrédients est nécessaire. La caractéristique majeure des communications sans fil est l'interférence dû à la réutilisation des fréquences. Dans les systèmes 2G, cette interférence est subie comme du bruit et limitée par une réutilisation modérée des fréquences. L'étalement de spectre dans les systèmes 3G mène à trop d'interférence intracellulaire, ainsi une réutilisation des fréquences entre cellules est devenue moins problématique. L'utilisation du OFDM dans les systèmes 4G a mené à une gestion des interférences par coordination dynamique des blocs de ressources. Cependant, cela ne permet que des gains modestes en débit. Une nouvelle technique de gestion des interférences a vu le jour il y a 5 ans: l'alignement d'interférences (IA). La promesse de l'IA est qu'avec cette gestion des interférences la capacité d'un réseau sans fils est égale la moitié de la capacité en absence d'interférences (comme si tous les liens étaient filaires et ne transmettaient que la moitié du temps). Le hic est que cela suppose que chaque transmetteur connaisse les canaux, non seulement de lui vers tous les récepteurs, mais aussi ceux à partir de tous les autres transmetteurs (Tx)s vers tous les récepteurs (Rx)s. Finalement, une autre technique encore plus récente est l'IA avec du Massive

MIMO, l'utilisation des antennes multiples, mais à échelle massive. L'idée est d'abord introduite dans un contexte mono-cellulaire, pour le MU MIMO. L'idée est motivée par des simplifications qui apparaissent dans un régime asymptotique d'une station de base avec un nombre d'antennes massif. Le MIMO permet la transmission simultanée de flux multiples (le multiplexage spatial) ce qui permet d'augmenter les débits de manière évidente. Alors que le MIMO nécessite des antennes multiples aussi bien du côté du Tx que du côté du Rx, et nécessite un environnement de propagation très riche (comme en indoor), le MU MIMO permet le même multiplexage spatial avec des utilisateurs mono-antenne et un environnement de propagation quelconque. Dans le MU MIMO toute la gestion des interférences s'effectue par le Tx ce qui nécessite une très bonne connaissance du canal au Tx. Quand le nombre d'antennes du Tx augmente beaucoup, un transmetteur linéaire tel qu'un filtre adapté (qui ne nécessite pas de calculs) devient optimal asymptotiquement. Bien qu'un nombre super élevé (par exemple 100) d'antennes de transmission puisse sembler effrayant, on argumente qu'un autre effet du régime asymptotique est que les circuits RF des antennes n'ont pas besoin d'être très précis et qu'en dépit des premières impressions, tout cela permet de diminuer la consommation globale de la station de base. L'objectif de la thèse est d'introduire des solutions complètes et réalistes pour la gestion des interférences multi-utilisateur entre cellules en se servant du Massive MIMO dans un contexte multicellulaire. Le Massive MIMO a plusieurs avantages.

- Il augmente l'efficacité spectrale : parce que de nombreux utilisateurs sont servis en même temps
- Il augmente l'efficacité en énergie : parce que l'énergie peut-être bien focalisée sur une très petite région de l'espace
- Il permet de diminuer la latence : Le Massive MIMO repose sur la loi des grands nombres pour éviter l'évanouissement

Dans cette thèse, on s'intéresse à faire de l'IA avec du Massive MIMO afin de pouvoir réaliser des précodeurs qui maximisent la somme pondérée des débits des utilisateurs dans un scénario de communications multicellulaires.

Si le rapport nombre d'utilisateurs servis/ nombre d'atennes de transmission par station de base $\leq \frac{1}{10}$ est respecté, des précodeurs linéaires simples tel que MF seront capable d'atteindre de très bonnes performances. Dans le cas

contraire, deux solutions existent. Cependant, ces solutions souffrent d'une convergence à des optimums locaux, non résistance aux imperfections des canaux de transmission et nécessitent beaucoup d'itérations pour converger.

8.2 Problème à résoudre

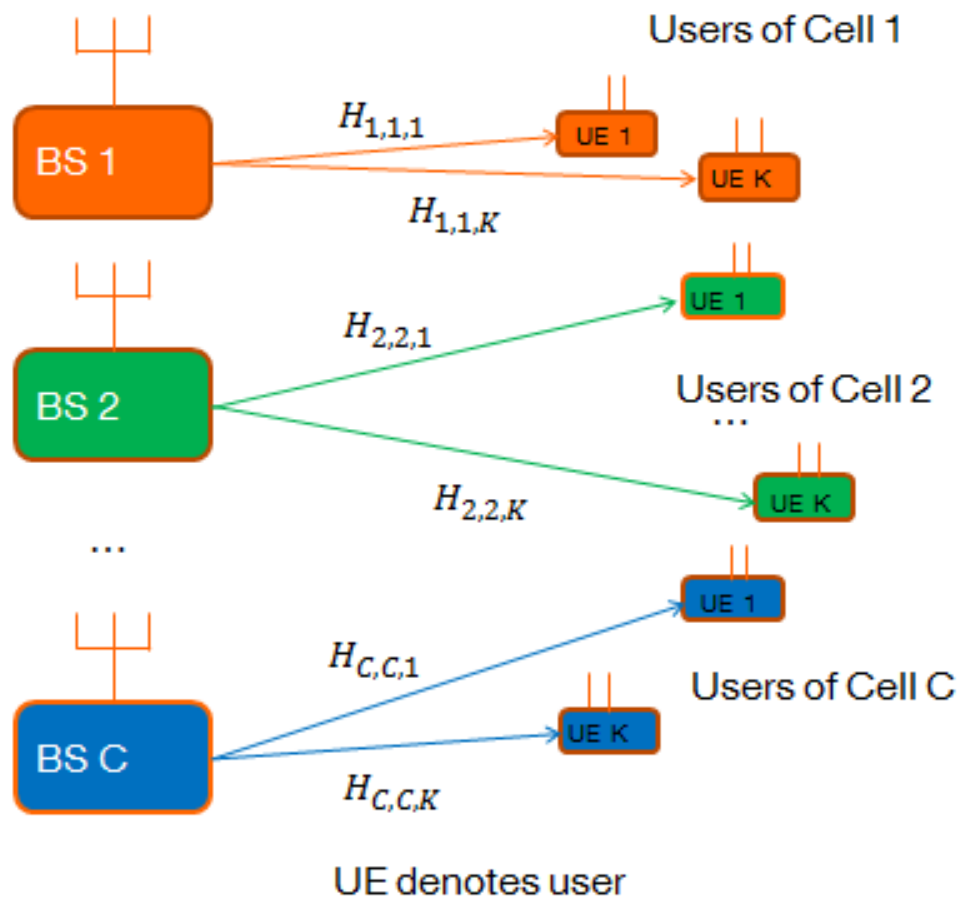


FIGURE 8.1: Communications multicellulaires

On considère un système de communications multicellulaires avec C cellules (Figure 8.1). une station de base par cellule équipée de M antennes de transmission et K utilisateurs par cellule avec N antennes chacun. On assume une transmission sur un seul resource bloc. Le signal reçu par l'utilisateur k

de la cellule c est donné par: $\mathbf{y}_{c,k} \in \mathbb{C}^{N \times 1}$

$$\mathbf{y}_{c,k} = \sum_{m=1}^C \sum_{l=1}^K \mathbf{H}_{m,c,k} \mathbf{G}_{m,l} \mathbf{s}_{m,l} + \mathbf{n}_{c,k} \quad (8.1)$$

où les symboles transmis sont Gaussiens, c.à.d, $\mathbf{s}_{m,l} \in \mathbb{C}^{d_{m,l},1}$, $d_{m,l}$ est le nombre de flux pour l'utilisateur l de la cellule m ; $\mathbf{G}_{m,l} \in \mathbb{C}^{M \times d_{m,l}}$ est le précodeur de l'utilisateur l de la cellule m , $\mathbf{H}_{m,c,k} \in \mathbb{C}^{N \times M}$ est le canal depuis le $m^{\text{ième}}$ transmetteur et vers l'utilisateur k de la cellule c , $\mathbf{n}_{c,k} \in \mathbb{C}^{N \times 1}$ est un bruit Gaussien de moyenne nulle et de variance égale à σ^2 .

Le débit $r_{c,k}$ de l'utilisateur k de la cellule c est:

$$r_{c,k} = \log \det(\mathbf{I}_N + \mathbf{\Gamma}_{c,k}) \quad (8.2)$$

$$\mathbf{\Gamma}_{c,k} = \mathbf{R}_{c,k}^{-1} \mathbf{H}_{c,c,k} \mathbf{Q}_{c,k} \mathbf{H}_{c,c,k}^H \quad (8.3)$$

où $\mathbf{Q}_{c,k} = \mathbf{G}_{c,k} \mathbf{G}_{c,k}^H$ est la matrice de covariance de transmission $\mathbf{\Gamma}_{c,k}$ est le rapport signal sur interférence plus bruit (SINR) de l'utilisateur k de la cellule c et $\mathbf{R}_{c,k}$ est la matrice de covariance de l'interférence plus bruit toujours de l'utilisateur k de la cellule c , donnée par

$$\begin{aligned} \mathbf{R}_{c,k} &= \mathbf{H}_{c,c,k} \mathbf{Q}_{c,k} \mathbf{H}_{c,c,k}^H + \mathbf{R}_{c,k}^- \\ \mathbf{R}_{c,k}^- &= \sum_{(j,i) \neq (c,k)} \mathbf{H}_{j,c,k} \mathbf{Q}_{j,i} \mathbf{H}_{j,c,k}^H + \sigma^2 \mathbf{I}_N. \end{aligned} \quad (8.4)$$

Le débit est très dégradé par les interférences intercellulaires surtout pour les utilisateurs aux bords des cellules (8.2). Pour y remédier on propose d'utiliser le CoBF où les BSs se partagent leur connaissance des canaux de transmission envers les différents utilisateurs du réseau afin de réaliser conjointement les différents précodeurs. Cela se reformule en un problème de maximisation de la somme pondérée des débits (WSR) avec une contrainte de puissance par cellule.

$$\begin{aligned} \mathbf{G} = \arg \max_{\mathbf{G}} & \sum_{c=1}^C \sum_{k=1}^K u_{c,k} r_{c,k} \\ \text{s.t. } & \text{tr} \mathbf{G}_c \mathbf{G}_c^H \leq P_c \text{ for } c \in \mathcal{C} \end{aligned} \quad (8.5)$$

En d'autres termes, on veut calculer conjointement tous les précodeurs de telle

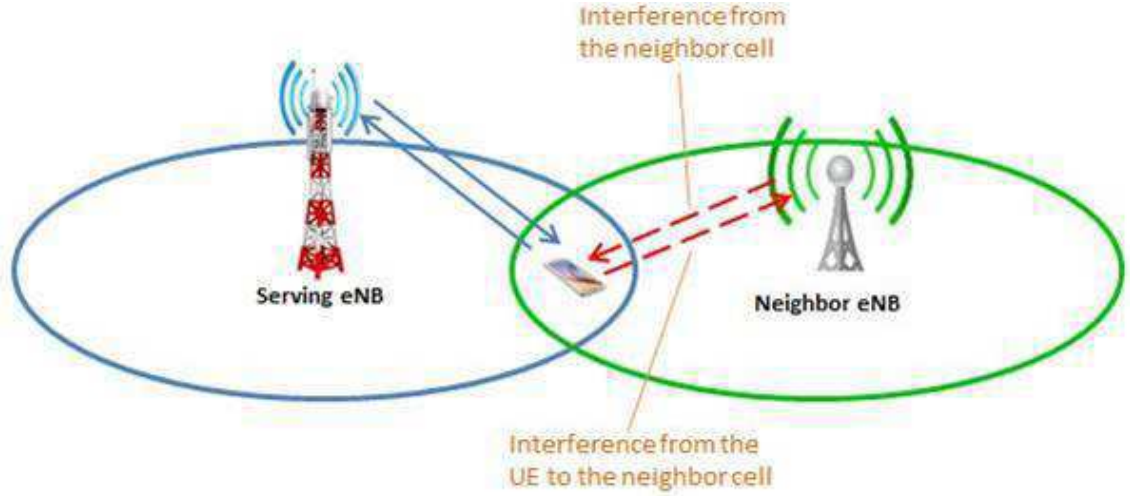


FIGURE 8.2: Interférence intercellulaire aux bords des cellules

manière à avoir une somme de débits maximale. Le problème d'optimisation est non concave, donc c'est difficile de le résoudre. Cependant, deux solutions existent: WSMSE et KG.

8.2.1 L'algorithme WSMSE

Le premier algorithme est WSMSE qui veut dire somme pondérée de l'erreur quadratique moyenne (WSMSE). Pour résoudre (8.5), il a été proposé de reformuler ce problème en un problème de minimisation d'une fonction de l'erreur quadratique moyenne (MSE):

$$\begin{aligned}
 \{\mathbf{G}, \mathbf{F}, \mathbf{W}\} = \\
 \arg \min_{\mathbf{G}, \mathbf{F}, \mathbf{W}} \sum_{(c,k)} u_{c,k} (\text{tr}(\mathbf{W}_{c,k} \mathbf{E}_{c,k}) - \log \det(\mathbf{W}_{c,k})) \quad (8.6) \\
 \text{s.t. } \text{tr} \mathbf{G}_c \mathbf{G}_c \leq P_c \text{ for } c \in \mathcal{C}
 \end{aligned}$$

avec

$$\mathbf{E}_{c,k} = \mathbb{E}[(\mathbf{F}_{c,k}^H \mathbf{y}_{c,k} - \mathbf{s}_{c,k})(\mathbf{F}_{c,k}^H \mathbf{y}_{c,k} - \mathbf{s}_{c,k})^H]. \quad (8.7)$$

étant la MSE. L'avantage de cette reformulation est que la nouvelle fonction de coût est convexe et quadratique en \mathbf{G} . Soit $\rho_c = \frac{P_c}{\sigma^2}$, le rapport signal sur bruit (SNR) dans la cellule c . La solution est un algorithme itératif, où à chaque itération on calcule \mathbf{F} , \mathbf{W} et \mathbf{G} et qui représentent pour l'utilisateur k de la cellule c respectivement le filtre au récepteur, un certain poids et le filtre

d'émission.

$$\mathbf{F}_{c,k} = (\sigma^2 \mathbf{I}_N + \sum_{m=1}^C \sum_{l=1}^K \mathbf{H}_{m,c,k} \mathbf{G}_{m,l} \mathbf{G}_{m,l}^H \mathbf{H}_{m,c,k}^H)^{-1} \mathbf{H}_{c,c,k} \mathbf{G}_{c,k} \quad (8.8)$$

$$\mathbf{W}_{c,k} = (\mathbf{I}_{d_{c,k}} - \mathbf{F}_{c,k}^H \mathbf{H}_{c,c,k} \mathbf{G}_{c,k})^{-1} \quad (8.9)$$

$$\mathbf{G}_{c,k} = (\sum_{j=1}^C \sum_{i=1}^K u_{j,i} \mathbf{H}_{c,j,i}^H \mathbf{D}_{j,i} \mathbf{H}_{c,j,i} + \lambda_c \mathbf{I}_M)^{-1} \mathbf{H}_{c,c,k}^H \mathbf{F}_{c,k} \mathbf{W}_{c,k} \quad (8.10)$$

avec $\mathbf{D}_{i,j} = \mathbf{F}_{i,j} \mathbf{W}_{i,j} \mathbf{F}_{i,j}$. Le Lagrangien λ_c doit être ajusté par bisection afin de satisfaire les contraintes de puissance. Cet algorithme converge vers un optimum local.

8.2.2 L'algorithme KG

Le deuxième algorithme pour résoudre (8.5) est KG pour Kim et Giannakis, les deux auteurs qui l'ont introduit. Cet algorithme propose de diviser la fonction d'utilité en deux parties. La première correspond au débit de l'utilisateur d'intérêt (k, c) et la seconde partie correspond à la somme des débits des autres utilisateurs. La première partie étant concave en \mathbf{Q}_k et la deuxième partie non concave en \mathbf{Q}_k , il a été proposé de linéariser la fonction d'utilité en utilisant les séries de Taylor. La fonction d'utilité peut être ainsi écrite sous la forme:

$$\begin{aligned} WSR &= u_{c,k} \log \det(\mathbf{R}_{c,k}^{-1} \mathbf{R}_{c,k}) + WSR_{\overline{c,k}}, \\ WSR_{\overline{c,k}} &= \sum_{(j,i) \neq (c,k)} u_{j,i} \log \det(\mathbf{R}_{j,i}^{-1} \mathbf{R}_{j,i}) \end{aligned} \quad (8.11)$$

Après linéarisation, on aura:

$$\begin{aligned} WSR_{\overline{c,k}}(\mathbf{Q}_{c,k}, \hat{\mathbf{Q}}) &\approx WSR_{\overline{c,k}}(\hat{\mathbf{Q}}_{c,k}, \hat{\mathbf{Q}}) - \text{tr}\{(\mathbf{Q}_{c,k} - \hat{\mathbf{Q}}_{c,k}) \hat{\mathbf{A}}_{c,k}\} \\ \text{With } \hat{\mathbf{A}}_{c,k} &= - \left. \frac{\partial WSR_{\overline{c,k}}(\mathbf{Q}_{c,k}, \hat{\mathbf{Q}})}{\partial \mathbf{Q}_{c,k}} \right|_{\hat{\mathbf{Q}}_{c,k}, \hat{\mathbf{Q}}} \\ &= \sum_{(j,i) \neq (c,k)} u_{j,i} \mathbf{H}_{c,j,i}^H (\hat{\mathbf{R}}_{j,i}^{-1} - \hat{\mathbf{R}}_{j,i}^{-1}) \mathbf{H}_{c,j,i} \end{aligned} \quad (8.12)$$

En d'autres termes, en utilisant $\mathbf{Q}_k = \mathbf{G}_k \mathbf{G}_k^H$, on a:

$$WSR(\mathbf{G}, \hat{\mathbf{G}}, \lambda) = \sum_{j=1}^C \lambda_c P_c + \sum_{c=1}^C \sum_{k=1}^K u_{c,k} \log \det(\mathbf{I}_{d_{c,k}} + \mathbf{G}_{c,k}^H \hat{\mathbf{B}}_k \mathbf{G}_{c,k}) - \text{tr}\{\mathbf{G}_{c,k}^H (\hat{\mathbf{A}}_{c,k} + \lambda_c \mathbf{I}_M) \mathbf{G}_{c,k}\} \quad (8.13)$$

where

$$\hat{\mathbf{B}}_{c,k} = \mathbf{H}_{c,c,k}^H \hat{\mathbf{R}}_{c,k}^{-1} \mathbf{H}_{c,c,k} . \quad (8.14)$$

Une fonction linéaire est à la fois concave et convexe alors cette dernière fonction correspond à une différence de fonctions concaves (DC). Le nouveau problème de maximisation a une solution donnée par une matrices généralisée de deux matrices $\mathbf{G}'_{c,k} = \text{eigenmatrix}(\hat{\mathbf{B}}_{c,k}, \hat{\mathbf{A}}_{c,k} + \lambda_c \mathbf{I}_M)$ Soient $\Sigma_{c,k}^{(1)} = \mathbf{G}_{c,k}'^H \hat{\mathbf{B}}_{c,k} \mathbf{G}_{c,k}'$, $\Sigma_{c,k}^{(2)} = \mathbf{G}_{c,k}'^H \hat{\mathbf{A}}_{c,k} \mathbf{G}_{c,k}'$. Il s'agit d'une solution normalisée, il nous faut donc ajuster les puissances, cela se fait par Waterfilling.

$$\mathbf{P}_{c,k}(l, l) = \left(\frac{1}{\Sigma_{c,k}^{(1)}(l, l)} \left(\frac{u_k \Sigma_{c,k}^{(1)}(l, l)}{\Sigma_{c,k}^{(2)}(l, l) + \lambda_c} - 1 \right) \right)^+ \quad (8.15)$$

L'avantage de cette approche c'est qu'elle marche pour n'importe quel nombre de flux $d_{c,k}$, en prenant simplement plus ou moins de vecteurs propres. En d'autres termes, on peut prendre les $d_{c,k}^{max}$ vecteurs propres correspondant aux vecteurs propres maximaux de la matrice généralisée.

KG et WSMSE convergent tous les deux vers des optimums locaux, pour y remédier, on propose l'approche 'deterministic annealing'. L'algorithme est initialisé avec les précodeurs obtenus à très bas SNR (interférence négligée par rapport au bruit) avant de prendre en compte de manière progressive l'alignement des interférences dès que le SNR le permet. Une variante du WSMSE est de remplacer le filtre de réception \mathbf{F} de WSMSE par du filtrage adapté (MF) conduisant à des performances similaires aux précédentes pour un grand nombre d'antennes d'émission mais offrant une convergence plus rapide avec moins de complexité.

Les contributions de cette thèse sont divisées en trois parties:

La partie I, intitulée *Random Matrix Theory for large system analysis and Massive MIMO design* est composée de 2 chapitres respectivement intitulés *The WSMSE algorithm: a large system analysis* et *Using the complex large system analysis to simplify beamforming*. Dans le second chapitre, on traite l'extension de l'algorithme WSMSE au cas multi-user massive MIMO où chaque utilisateur est équipé d'une seule antenne (MISO). Des expressions du SINR et du débit maximum sont fournies pour des petits rapports $\frac{K}{M}$. Dans le chapitre 3, une

simplification du précodeur WSMSE pour MISO, basée sur l'analyse de systèmes larges, est proposée pour une architecture décentralisée. Trois stratégies de mise en oeuvre sont ensuite déclinées selon que les interférences entre cellules sont négligées, estimées localement ou plus globalement, conduisant à des overheads différents.

Les publications correspondantes à cette partie sont les suivantes:

- Tabikh, Wassim; Slock, Dirk TM; Yuan-Wu, Yi, Weighted sum rate maximization of correlated MISO interference broadcast channels under linear precoding: a large system analysis, VTC 2016-Spring, IEEE 83rd Vehicular Technology Conference, 15-18 May 2016, Nanjing, China
- Tabikh, Wassim; Slock, Dirk TM; Yuan-Wu, Yi, A Large system analysis of weighted sum rate maximization of single stream MIMO interference broadcast channels under linear precoding, ISWCS 2016, Poznan, Poland
- Tabikh, Wassim; Yuan-Wu, Yi; Slock, Dirk TM, Decentralizing multi-cell maximum weighted sum rate precoding via large system analysis, EUSIPCO 2016, 24th European Signal Processing Conference, 28 August-2 September 2016, Budapest, Hungary

La partie II, intitulée *Further random matrix theory exploitation with partial CSIT* est composée des chapitres 4 et 5 respectivement intitulés *robust beamformers for partial CSIT* et *non-linear precoding schemes*. Dans le chapitre 4, on propose plusieurs précodeurs lorsque la connaissance des canaux aux transmetteurs (CSIT) n'est pas parfaite sur la base de l'analyse des systèmes larges. Les systèmes étudiés offrent des performances qui varient selon l'exploitation ou non d'information sur la covariance des canaux dans les calculs des termes interférents ou dans la puissance des signaux. La mise en oeuvre dans un système décentralisé est étudiée ; plusieurs solutions dont une basée sur la variation lente de certaines caractéristiques des canaux sont discutées.

Dans le chapitre 5, ce sont des solutions à base de précodeurs non-linéaires basés sur les techniques de type Dirty Paper Coding (DPC) et assignement linéaire qui sont étudiées toujours dans le cas d'une CSIT partielle.

Les résultats de cette partie sont publiés dans les suivants:

- Tabikh, Wassim; Yuan-Wu, Yi; Slock, Dirk, Beamforming design with combined channel estimate and covariance CSIT via random matrix

theory, ICC 2017, IEEE International Conference on Communications, IEEE ICC 2017 Wireless Communications Symposium, May 21-25, Paris, France

- Tabikh, Wassim; Slock, Dirk TM; Yuan-Wu, Yi, MaMISO IBC beamforming design with combined channel estimate and covariance CSIT: a large system analysis, ICC 2017, WS08-3rd International Workshop on Advanced PHY and MAC Technology for Super Dense Wireless Networks (CROWD-NET), May 21-25, Paris, France
- Tabikh, Wassim; Slock, Dirk TM; Yuan-Wu, Yi, MIMO IBC beamforming with combined channel estimate and covariance CSIT, ISIT 2017, IEEE International Symposium on Information Theory June 25-30, 2017, Aachen, Germany
- Tabikh, Wassim; Slock, Dirk TM; Yuan-Wu, Yi, Robust Non-Linear Precoders for the MIMO Interference Broadcast Channels with Imperfect CSIT, submitted to EUSIPCO 2018, September 2018, Rome, Italy.

La partie III *relaying with random matrix theory* est constituée du seul chapitre 6 lui même intitulé *Beamformers Design with AF relays*. Cette étude permet d'introduire les techniques à relais de type AF et de les considérer dans un contexte massive-MIMO avec ou sans lien direct entre la station de base (BS) et les utilisateurs. Les algorithmes présentés dans le chapitre 1 (WSMSE et KG) sont alors adaptés aux cas sans lien avec un traitement au niveau des relais. On étudie ensuite le cas avec un lien direct entre la BS et les utilisateurs, sans considérer un grand nombre d'utilisateurs; on étudie des transmissions en full duplex en proposant un précodeur de type ZF (Zero Forcing) au niveau de la station de base et une technique de neutralisation des interférence au niveau des relais. Le résultat de cette partie est publié dans un papier de conférence:

- Tabikh, Wassim; Slock, Dirk TM; Yuan-Wu, Yi, Relay aided coordinated beamforming and interference neutralization, ITA 2017, Information Theory and Applications Workshop, February 12-17 2017, San Diego, USA

Le chapitre 7 *Conclusions et future works* vient clore le document de thèse.

8.3 Partie I: Random Matrix Theory for large system analysis and Massive MIMO design

Pour évaluer les performances des algorithmes KG et WSMSE, il faut faire des simulations du débit atteignable en fonction du SNR pour des simulations Monte-Carlo. Or ce dernier nécessite un moyennage sur un nombre suffisant grand de tirages de canaux différents. Dans cette partie, on propose d'utiliser la théorie des matrices aléatoire afin d'en sortir des expressions déterministes du débit pour les systèmes MISO. Le débit est fonction du SINR qui est le rapport de la covariance signal sur la covariance (interférence + bruit). Pour MISO, ce rapport est un rapport de scalaires donc l'application des théories des matrices aléatoires est tout à fait possible. L'expression déterministe résultante ne dépend que des statistiques, comme par exemple la matrice de covariance du canal, et ne dépend donc pas de la valeur instantanée du canal. L'avantage c'est qu'on n'a plus besoin de faire de simulations type Monte-Carlo, mais il faudra juste tracer la courbe correspondante à l'expression déterministe pour des matrices de covariance du canal de notre choix.

Pour prouver que notre expression, donnée par l'équation (2.47), est correcte on trace le débit atteignable en fonction du SNR par les simulations Monte-Carlo ainsi que par l'expression déterministe pour trois cas de figure 2.1 and 2.2 et 2.3. D'après les figures on remarque qu'en général l'expression déterministe se comporte très bien et donne une approximation assez correcte. Cependant, on remarque un petit écart dans les deux premières figures qui se rétrécit dans la troisième figure. On peut en conclure que les expressions déterministes à base d'analyse de systèmes larges est plus précise quand le rapport nombre d'utilisateurs servis en total (=nombre de cellules \times nombre d'utilisateurs par cellule) sur nombre d'antennes de transmission par station de base (en suppose que les stations de base aillent le même nombre d'antennes) est plus petit.

Ensuite, on propose de faire la même procédure pour du MIMO mono-flux. De même, on aura un SINR qui est un rapport de scalaires, donc une analyse des systèmes larges est faisable. Des simulations (Figure 2.5 et Figure 2.6) montrent à nouveau que notre approche est correcte.

KG et WSMSE étant relativement lents à converger, on propose un nouveau précodeur basé sur les résultats de l'analyse des systèmes larges. L'avantage de cette nouvelle contribution c'est que ce précodeur converge en une seule

itération, ce qui réduit à fond les échanges entre les stations de base et réduit également la latence.

8.4 Partie II: Further random matrix theory exploitation with partial CSIT

Dans ce qui précède, on a parlé de précodeurs. Or, pour réaliser pratiquement un précodeur, une connaissance parfaite des canaux de transmission de toutes les BSs vers tous les utilisateurs de la même cellule et des cellules voisines est requise.

L'acquisition des canaux diffère selon qu'on est en TDD ou en FDD. En FDD, les BSs envoient des pilotes à partir desquels les utilisateurs estiment les canaux, les quantifient puis envoient un feedback aux BSs (Figure 8.3) Or, le nombre

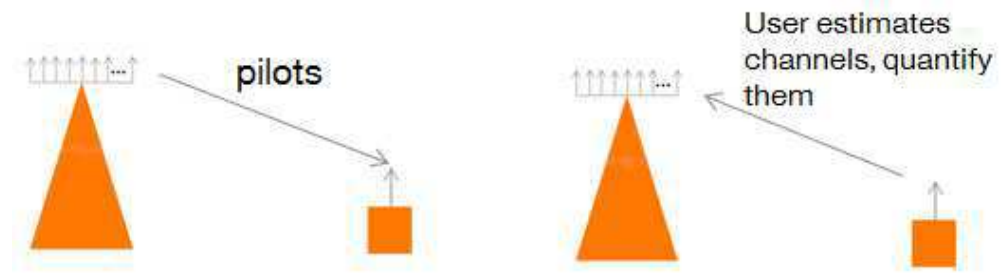


FIGURE 8.3: Estimation du canal en FDD

de pilotes y nécessaire est proportionnel au très grand nombre d'antennas de transmission. Donc le nombre de pilotes requis est lui-même très grand. C'est pour cela que le TDD sera utilisé au lieu du FDD.

Pour le TDD, les BSs obtiennent les canaux du lien descendant (DL) par réciprocité en se référant à une estimation des canaux à la base de pilotes envoyés sur le lien montant (UL). Cette procédure d'estimation du canal est en général accompagnée par un certain bruit d'estimation. Par conséquent, le canal réel \mathbf{H} et son estimé seront légèrement différents et seront reliés par la relation suivante:

$$\mathbf{H} = \bar{\mathbf{H}} + \tilde{\mathbf{H}} \quad (8.16)$$

Ou

$$\mathbf{H} = \bar{\mathbf{H}} + \mathbf{C}_r^{1/2} \tilde{\mathbf{H}}^{(2)} \boldsymbol{\Theta}_p^{1/2} = \mathbf{C}_r^{1/2} \tilde{\mathbf{H}}^{(1)} \boldsymbol{\Theta}_t^{1/2} + \mathbf{C}_r^{1/2} \tilde{\mathbf{H}}^{(2)} \boldsymbol{\Theta}_p^{1/2} \quad (8.17)$$

$\tilde{\mathbf{H}}^{(1)}$ et $\tilde{\mathbf{H}}^{(2)}$ sont complexes i.i.d. d'espérance nulle et de variance $\frac{1}{MN}$. La matrice de covariance de l'estimé $\mathbf{\Theta}_t$ et la matrice de covariance de l'erreur d'estimation $\mathbf{\Theta}_p$ sont Hermitiennes non-négatives. La matrice de covariance du côté du récepteur \mathbf{C}_r est une matrice Hermitienne non-négative également. Elle est considérée comme une matrice identité dans cette thèse.

Chaque Tx transmetteur ne connaît que $\bar{\mathbf{H}}$ et $\mathbf{\Theta}_p$. $\tilde{\mathbf{H}}$ est l'erreur d'estimation du canal. En prenant en compte cette connaissance partielle des canaux, notre problème d'intérêt sera toujours de réaliser conjointement les précodeurs mais cette fois en supposant une connaissance partielle des canaux. Cela se reformule comme suit:

$$EWSR(\mathbf{Q}) = E_{\mathbf{H}} WSR = E_{\mathbf{H}} \sum_c \sum_k u_{c,k} \log \det(\mathbf{I}_M + \mathbf{H}_{c,c,k}^H \mathbf{R}_{c,k}^{-1} \mathbf{H}_{c,c,k} \mathbf{Q}_{c,k}) \quad (8.18)$$

avec une contrainte sur les puissances par cellule

$$s.t. \text{tr} \mathbf{Q}_c \leq P_c \text{ for } c \in \mathcal{C} \quad (8.19)$$

En d'autres termes, il faut maximiser l'espérance de la somme pondérée des débits sachant qu'on a une puissance de transmission limitée par BS. Il s'agit d'un problème stochastique.

Deux solutions existent déjà pour résoudre ce problème: ENAIVEKG et EWSMSE. ENAIVEKG propose d'appliquer KG, mais en remplaçant le terme \mathbf{H} par $\bar{\mathbf{H}}$. Cette solution est sous-optimale parce qu'elle ne profite pas de la connaissance des covariances $\mathbf{\Theta}_p$. EWSMSE propose de reformuler le problème de maximisation en un autre problème de minimisation d'une fonction de l'espérance de MSE. On montre par simulations que cette approche est également sous-optimale.

Notre approche consiste à résoudre le problème EWSR en utilisant en une approche DC. Pour un système Massive MIMO, en utilisant la loi des grands nombres, on a:

$$\mathbf{H} \mathbf{Q} \mathbf{H}^H \xrightarrow{M \rightarrow \infty} E_{\mathbf{H}} \mathbf{H} \mathbf{Q} \mathbf{H}^H = \bar{\mathbf{H}} \mathbf{Q} \bar{\mathbf{H}}^H + \text{tr}\{\mathbf{Q} \mathbf{\Theta}_p\} \mathbf{C}_r. \quad (8.20)$$

On suppose $\mathbf{C}_r = \mathbf{I}_N$. $\bar{\mathbf{H}}$ est l'estimé du canal et Θ_p est la matrice de covariance de l'erreur d'estimation. Soient

$$\begin{aligned} \mathbf{H}_{c,k} &= [\mathbf{H}_{1,c,k} \cdots \mathbf{H}_{C,c,k}] = \bar{\mathbf{H}}_{c,k} + \tilde{\mathbf{H}}_{c,k} \Theta_{p,c,k}^{1/2} \\ \mathbf{Q} &= \begin{bmatrix} \mathbf{Q}_1 & & \\ & \ddots & \\ & & \mathbf{Q}_C \end{bmatrix} = \begin{bmatrix} \sum_k \mathbf{Q}_{1,k} & & \\ & \ddots & \\ & & \sum_k \mathbf{Q}_{C,k} \end{bmatrix} = \\ &\sum_c \sum_k \mathbf{I}_c \mathbf{Q}_{c,k} \mathbf{I}_c^H; \\ \mathbf{Q}_{c,\bar{k}} &= \mathbf{Q} - \mathbf{I}_c \mathbf{Q}_{c,k} \mathbf{I}_c^H. \end{aligned} \quad (8.21)$$

avec $\Theta_{p,c,k} = \text{blockdiag}\{\Theta_{p,1,c,k}, \dots, \Theta_{p,C,c,k}\}$, and \mathbf{I}_c est vecteur bloc nul sauf au bloc c où on a une matrice d'identité. En utilisant (8.20), on obtient:

$$\begin{aligned} \check{\mathbf{R}}_{c,k} &= \sigma^2 \mathbf{I}_N + \bar{\mathbf{H}}_{c,k} \mathbf{Q} \bar{\mathbf{H}}_{c,k}^H + \text{tr}\{\mathbf{Q} \Theta_{p,c,k}\} \mathbf{I}_N \\ \check{\mathbf{R}}_{c,\bar{k}} &= \sigma^2 \mathbf{I}_N + \bar{\mathbf{H}}_{c,k} \mathbf{Q}_{c,\bar{k}} \bar{\mathbf{H}}_{c,k}^H + \text{tr}\{\mathbf{Q}_{c,\bar{k}} \Theta_{p,c,k}\} \mathbf{I}_N \end{aligned} \quad (8.22)$$

Cela mène (8.11) à

$$\begin{aligned} WSR &= u_{c,k} \log \det(\check{\mathbf{R}}_{c,k}^{-1} \check{\mathbf{R}}_{c,k}) + WSR_{c,\bar{k}}, \\ WSR_{c,\bar{k}} &= \sum_{(j,i) \neq (c,k)} u_{j,i} \log \det(\check{\mathbf{R}}_{j,i}^{-1} \check{\mathbf{R}}_{j,i}) \end{aligned} \quad (8.23)$$

avec $\log \det(\check{\mathbf{R}}_{c,k}^{-1} \check{\mathbf{R}}_{c,k})$ étant concave en $\mathbf{Q}_{c,k}$, $WSR_{c,\bar{k}}$ est non-concave en $\mathbf{Q}_{c,k}$ et $\check{\mathbf{R}}_{c,k}$ et $\check{\mathbf{R}}_{c,\bar{k}}$ sont données par (8.22).

On linéarise la partie correspondante à la somme des débits de tous les utilisateurs sauf l'utilisateur d'intérêt, ce qui donne:

$$\hat{\mathbf{A}}'_{c,k} = \sum_{(j,i) \neq (c,k)} u_{j,i} \mathbf{H}_{c,j,i}^H (\check{\mathbf{R}}_{j,i}^{-1} - \check{\mathbf{R}}_{j,i}^{-1}) \mathbf{H}_{c,j,i} \quad (8.24)$$

Et le terme $\hat{\mathbf{B}}'_{c,k}$ correspondant à $\mathbf{B}_{c,k}$ est donné par:

$$\hat{\mathbf{B}}'_{c,k} = \mathbf{H}_{c,c,k}^H \check{\mathbf{R}}_{c,\bar{k}}^{-1} \mathbf{H}_{c,c,k} \quad (8.25)$$

On calcule ensuite les espérances $\check{\mathbf{A}}_{c,k}$ $\check{\mathbf{B}}_{c,k}$ de $\hat{\mathbf{A}}'_{c,k}$ et $\hat{\mathbf{B}}'_{c,k}$ respectivement:

$$\begin{aligned} \check{\mathbf{B}}_{c,k} &= \mathbb{E}_{\mathbf{H}|\bar{\mathbf{H}}} \mathbf{H}_{c,c,k}^H \check{\mathbf{R}}_{c,\bar{k}}^{-1} \mathbf{H}_{c,c,k} \\ &= \bar{\mathbf{H}}_{c,c,k}^H \check{\mathbf{R}}_{c,\bar{k}}^{-1} \bar{\mathbf{H}}_{c,c,k} + \text{tr}\{\check{\mathbf{R}}_{c,\bar{k}}^{-1}\} \Theta_{p,c,c,k} \end{aligned} \quad (8.26)$$

$$\check{\mathbf{A}}_{c,k} = \sum_{(j,i) \neq (c,k)} u_{j,i} [\check{\mathbf{A}}_{j,i,c,k}^C (\mathbf{I}_M + \mathbf{Q}_{c,k} \check{\mathbf{A}}_{j,i,c,k}^C)^{-1} - \check{\mathbf{A}}_{j,i,c,k}^D (\mathbf{I}_M + \mathbf{Q}_{c,k} \check{\mathbf{A}}_{j,i,c,k}^D)^{-1}]; \quad (8.27)$$

avec

$$\begin{aligned} \check{\mathbf{A}}_{j,i,c,k}^C &= \overline{\mathbf{H}}_{c,j,i}^H \check{\mathbf{R}}_{j,i,c,k}^{-1} \overline{\mathbf{H}}_{c,j,i} + \text{tr}\{\check{\mathbf{R}}_{j,i,c,k}^{-1}\} \Theta_{p,c,j,i} \\ \check{\mathbf{A}}_{j,i,c,k}^D &= \overline{\mathbf{H}}_{c,j,i}^H \check{\mathbf{R}}_{j,i,c,k}^{-1} \overline{\mathbf{H}}_{c,j,i} + \text{tr}\{\check{\mathbf{R}}_{j,i,c,k}^{-1}\} \Theta_{p,c,j,i}; \\ \check{\mathbf{R}}_{j,i,c,k} &= \sigma^2 \mathbf{I}_N + \overline{\mathbf{H}}_{j,i} \mathbf{Q}_{j,i,c,k} \overline{\mathbf{H}}_{j,i}^H + \text{tr}\{\mathbf{Q}_{j,i,c,k} \Theta_{p,j,i}\} \mathbf{I}_N; \\ \check{\mathbf{R}}_{j,i,c,k} &= \sigma^2 \mathbf{I}_N + \overline{\mathbf{H}}_{j,i} \mathbf{Q}_{c,k} \overline{\mathbf{H}}_{j,i}^H + \text{tr}\{\mathbf{Q}_{c,k} \Theta_{p,j,i}\} \mathbf{I}_N \end{aligned} \quad (8.28)$$

avec $\mathbf{Q}_{j,i,c,k} = \mathbf{Q} - \mathbf{I}_c \mathbf{Q}_{c,k} \mathbf{I}_c^H - \mathbf{I}_j \mathbf{Q}_{j,i} \mathbf{I}_j^H$. Une solution normalisée de \mathbf{G} est donné par:

$$\mathbf{G}'_{c,k} = \text{eigenmatrix}(\check{\mathbf{B}}_{c,k}, \check{\mathbf{A}}_{c,k} + \lambda_c \mathbf{I}_M) \quad (8.29)$$

Il ne reste qu'à ajuster les puissances par waterfilling.

Pour voir si notre approche est correcte, on fait des simulations. On compare notre approche avec ENAIVEKG et EWSMSE pour plusieurs configurations. D'après les figures 4.1, 4.2, 4.3, 4.4, 4.5, 4.6, on remarque que notre approche est toujours meilleure.

Comme pour WSMSE, on utilise la théorie matrices aléatoires pour dériver une expression déterministe du SINR. De même, on prouve que notre dérivation est correcte par simulations (Figure 4.11).

Dans ce qui suit, on vise à dériver des précodeur non linéaires pour le cas de connaissance partielle des canaux. Le précodeur non linéaire le plus connu est DPC. Mais DPC nécessite une connaissance parfaite des canaux. En plus, DPC n'est optimale que pour des scénarios monocellulaires. Ce qui n'est pas notre cas. Pour surmonter le problème de la connaissance des canaux, on propose d'utiliser une variante de DPC qui est LA.

Considérons un système IBC avec C cellules et un nombre total d'utilisateurs K users. On considère une numérotation des utilisateurs à l'échelle du système. k est servi par la BS b_k . Le signal de dimensions $N \times 1$ reçu par l'utilisateur k dans la cellule b_k est

$$\mathbf{y}_k = \underbrace{\mathbf{H}_{k,b_k} \mathbf{G}_k \mathbf{x}_k}_{\text{signal}} + \underbrace{\sum_{\substack{i \neq k \\ b_i = b_k}} \mathbf{H}_{k,b_k} \mathbf{G}_i \mathbf{x}_i}_{\text{interférence intracellulaire}} + \underbrace{\sum_{j \neq b_k} \sum_{i: b_i = j} \mathbf{H}_{k,j} \mathbf{G}_i \mathbf{x}_i}_{\text{interférence intercellulaire}} + \mathbf{v}_k \quad (8.30)$$

où \mathbf{x}_k est le signal de dimensions $d_k \times 1$, d_k est le nombre de flux, \mathbf{H}_{k,b_k} est le canal de dimensions $N \times M$ du BS b_k vers k . La BS b_k sert $K_{b_k} = \sum_{i:b_i=b_k} 1$ users. Le bruit est $\mathbf{v}_k \sim \mathcal{CN}(0, \sigma^2 \mathbf{I}_N)$. Le précodeur est une matrice de dimensions $M \times d_k$ nommée \mathbf{G}_k . On suppose que les utilisateurs $1, \dots, K_1$ appartiennent à la cellule-1; les utilisateurs $K_1 + 1, \dots, K_1 + K_2$ appartiennent à la cellule-2; ...; users $\sum_{c=1}^{C-1} K_c + 1, \dots, K$ appartiennent à la cellule- C . Dans chaque cellule b_k , LA est utilisée tel que l'utilisateur k ne reçoit pas d'interférence des utilisateurs $i > k : b_i = b_k$.

LA est caractérisée par une variable aléatoire \mathbf{u} de dimension $M \times 1$ avec une structure particulière:

$$\mathbf{u} = \mathbf{F}\mathbf{s} + \mathbf{x} \quad (8.31)$$

\mathbf{F} est la matrice d'assignement du LA et \mathbf{s} est l'interférence intracellulaire connue au Tx. Pour réaliser \mathbf{u} , il a été prouvé dans [49] que le maximum de débit est atteint en choisissant \mathbf{x} and \mathbf{s} Gaussiens et indépendant. Ainsi, quand le signal est transmis comme $\mathbf{x} = \mathbf{u} - \mathbf{F}\mathbf{s}$, le débit r_k de l'utilisateur k est atteignable, avec

$$r_k = \log_2 \det(\mathbf{Q}_k) - \mathbb{E}_H \{ \log_2 \det [\mathbf{C}_k - \mathbf{Y}_k \mathbf{H}_{k,b_k}^H (\mathbf{H}_{k,b_k} \mathbf{B}_k \mathbf{H}_{k,b_k}^H + \mathbf{R}_{\bar{k}})^{-1} \mathbf{H}_{k,b_k} \mathbf{Y}_k^H] \} \quad (8.32)$$

où

$$\mathbf{Q}_k = \mathbf{G}_k \mathbf{G}_k^H \quad (8.33)$$

$$\mathbf{Y}_k = \mathbf{F}_k \mathbf{S}_k + \mathbf{Q}_k \quad (8.34)$$

$$\mathbf{B}_k = \mathbf{S}_k + \mathbf{Q}_k \quad (8.35)$$

$$\mathbf{C}_k = \mathbf{F}_k \mathbf{S}_k \mathbf{F}_k^H + \mathbf{Q}_k$$

$$\mathbf{S}_k = \sum_{j:b_j=b_k; j>k+1} \mathbf{Q}_j. \quad (8.37)$$

$$\begin{aligned} \mathbf{R}_k &= \mathbf{H}_{k,b_k} \mathbf{Q}_k \mathbf{H}_{k,b_k}^H + \mathbf{R}_{\bar{k}}, \\ \mathbf{R}_{\bar{k}} &= \sum_{i \notin \{i:b_i=b_k, i \geq k\}} \mathbf{H}_{k,b_i} \mathbf{Q}_i \mathbf{H}_{k,b_i}^H + \sigma^2 \mathbf{I}_N. \end{aligned} \quad (8.38)$$

Contrairement aux études précédentes, on doit désormais optimiser par rapport à deux paramètres \mathbf{F} et \mathbf{G} . En optimisant par rapport à \mathbf{F} , on aura une

solution analytique de \mathbf{F} donnée par:

$$\begin{aligned} \mathbf{F}_k = & \mathbf{Q}_k \{ \mathbf{Q}_k + \sum_{j: b_j = b_k; j < k} \mathbf{Q}_j \\ & + [\bar{\mathbf{H}}_{k, b_k}^H (\mathbf{R}_{inter, k} + \sigma^2 \mathbf{I}_N)^{-1} \bar{\mathbf{H}}_{k, b_k} \\ & + \mathbf{C}_{p, k, b_k} \text{tr}((\mathbf{R}_{inter, k} + \sigma^2 \mathbf{I}_N)^{-1})]^{-1} \}^{-1} \end{aligned} \quad (8.39)$$

avec

$$\mathbf{R}_{inter, k} = \sum_{j: b_j \neq b_k} \mathbf{H}_{k, b_j} \mathbf{Q}_j \mathbf{H}_{k, b_j}^H \quad (8.40)$$

Il nous manque que de calculer \mathbf{Q}_k . Dans (8.32), on remplace \mathbf{F}_k par sa solution analytique (8.39), l'expression obtenue sera limitée par une limite supérieure qui correspond à une nouvelle fonction d'utilité:

$$\mathbf{E}_{\mathbf{H}} \sum_k u_k \log_2 \det(\mathbf{I}_M + \mathbf{H}_{k, b_k}^H \mathbf{R}_{\bar{k}}^{-1} \mathbf{H}_{k, b_k} \mathbf{Q}_k) \quad (8.41)$$

En d'autres termes, notre but est de réaliser conjointement les précodeurs qui maximisent l'espérance de la somme des débits en supposant l'IA. Le problème paraît être similaire au problème déjà résolu (EWSR), la seule différence qu'ici $\mathbf{R}_{\bar{k}}$ ne contient pas l'interférence de tous les utilisateurs de la même cellule. En fait, DPC ou LA encodent les signaux de telle manière à que les utilisateurs ne voient l'interférence de certaines utilisateurs de la même cellule. On sait résoudre (8.18) si on avait une seule cellule. Quand on a plusieurs cellules, il suffit de linéariser la somme des débits correspondant aux cellules différentes que celle où l'utilisateur qui nous intéresse se trouve. On aura une maximisation de la somme des débits d'utilisateurs dans une cellule d'intérêt moins une certaine pénalité qui représente physiquement l'interférence causée aux différentes cellules voisines. Pour résoudre ce problème, on résoud son duel qui correspond à une maximisation des précodeurs au niveau des utilisateurs pour l'UL.

$$\begin{aligned} \max_{\mathbf{D}} \sum_{i: b_i = b_k} \log_2 \det & \left(\frac{\mathbf{I}_N + \sum_{j: b_j = b_k; j \geq i} \tilde{\mathbf{H}}_{i, b_k}^H \mathbf{D}_j \tilde{\mathbf{H}}_{i, b_k}}{\mathbf{I}_N + \sum_{j: b_j = b_k; j > i} \tilde{\mathbf{H}}_{i, b_k}^H \mathbf{D}_j \tilde{\mathbf{H}}_{i, b_k}} \right) \\ & - \text{tr}\{\mathbf{D}_i\} \\ \text{subject to } \mathbf{D}_i & \geq 0 \quad \forall i \end{aligned} \quad (8.42)$$

\mathbf{D}_i étant la covariance du précodeur à l'utilisateur i . C'est un problème concave, donc c'est facile d'obtenir \mathbf{D}_i à partir de cela. Ensuite, il suffit de calculer \mathbf{Q}_i

à partir de \mathbf{D}_i en utilisant la dualité DL-UL. Enfin, on calcule les espérances des expressions obtenus.

Par simulation, on montre que notre précodeur nonlinéaire est mieux que le ESEI-WSR linéaire.

8.5 Partie III: Relaying with random matrix theory

Dans cette partie, on considère un relai (Figure 8.4) avec des BSs à antennes multiples et des utilisateurs à antennes multiples également. Le signal transmis

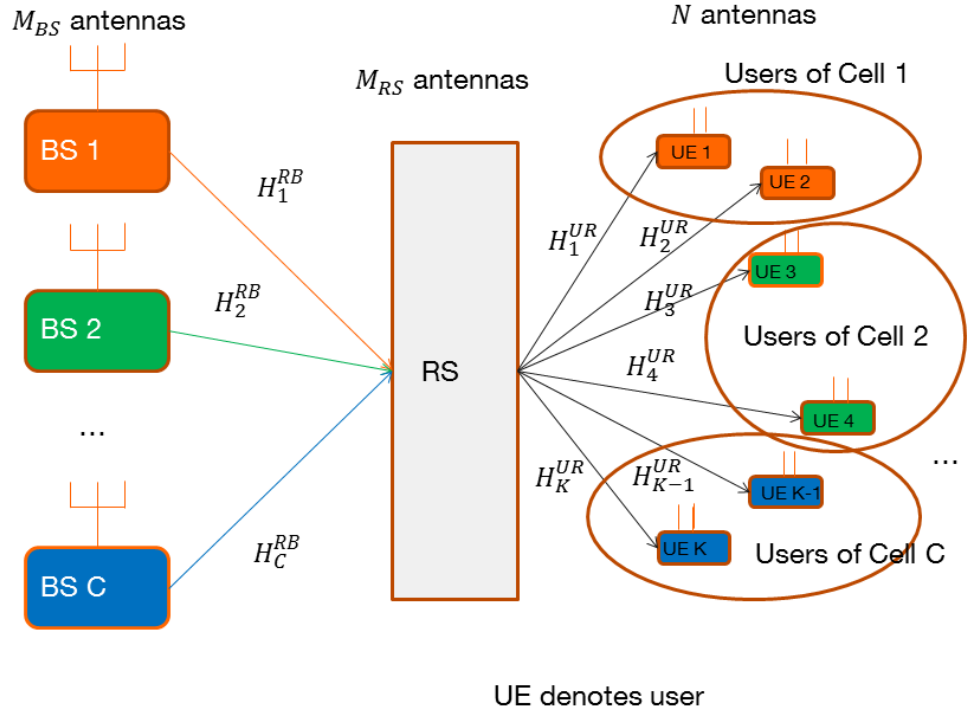


FIGURE 8.4: Scénario avec relais

à la BS c est donné par:

$$\mathbf{x}_c = \sum_{i: b_i=c} \mathbf{G}_i \mathbf{s}_i \quad (8.43)$$

avec $i : b_i = c$ veut dire les utilisateurs servis par BS c . $\mathbf{s}_i \in \mathbb{C}^{d_k \times 1}$ représente le signal de l'utilisateur i et est Gaussien. \mathbf{G}_i est le précodeur i de dimensions $M_{BS} \times d_i$ avec d_i étant le nombre de flux pour l'utilisateur i . Au relai, le signal

reçu:

$$\mathbf{Y}_{RS} = \sum_c \mathbf{H}_c^{RB} \mathbf{x}_c + \mathbf{n}_{RS} \quad (8.44)$$

avec $\mathbf{H}_c^{RB} \in \mathbb{C}^{M_{RS} \times M_{BS}}$ est le canal de la BS c vers le relai et $\mathbf{n}_{RS} \sim \mathcal{C}(0, \sigma_{RS}^2)$ est du bruit Gaussien d'espérance nulle et σ_{RS}^2 comme variance. La matrice de covariance \mathbf{R}_{RS} du signal reçu \mathbf{Y}_{RS} au relai est donné par:

$$\mathbf{R}_{RS} = \sum_j \mathbf{H}_j^{RB} \left(\sum_{i:b_i=j} \mathbf{G}_i \mathbf{G}_i^H \right) \mathbf{H}_j^{RB,H} + \sigma_{RS}^2 \mathbf{I}_{M_{RS}} \quad (8.45)$$

Le relai retransmet le signal après être multiplié par la matrice \mathbf{F} du relai de dimensions $M_{RS} \times M_{RS}$. Le signal reçu par l'utilisateur k est donné par:

$$\mathbf{Y}_k = \underbrace{\mathbf{H}_{k,b_k}^{UB} \mathbf{G}_k \mathbf{s}_k}_{\text{signal}} + \mathbf{Z}_k \quad (8.46)$$

avec

$$\mathbf{Z}_k = \underbrace{\sum_{\substack{i \neq k \\ b_i = b_k}} \mathbf{H}_{k,b_k}^{UB} \mathbf{G}_i \mathbf{s}_i}_{\text{interf. intracellulaire}} + \underbrace{\sum_{j \neq b_k} \sum_{i:b_i=j} \mathbf{H}_{k,j}^{UB} \mathbf{G}_i \mathbf{s}_i}_{\text{interf. intercellulaire}} + \underbrace{\mathbf{H}_k^{UR} \mathbf{F} \mathbf{n}_{RS} + \mathbf{n}_k}_{\text{bruit}}$$

avec $\mathbf{H}_k^{UR} \in \mathbb{C}^{N \times M_{RS}}$ est le canal du relai vers l'utilisateur k et $\mathbf{n}_k \sim \mathcal{C}(0, \sigma^2)$ et $\mathbf{H}_{k,b_k}^{UB} = \mathbf{H}_k^{UR} \mathbf{F} \mathbf{H}_k^{RB} \in \mathbb{C}^{N \times M_{BS}}$. Les signaux transmis par le relai et les stations de base sont soumis à des contraintes de puissance, comme suit:

$$\text{tr}(\mathbf{F} \mathbf{R}_{RS} \mathbf{F}^H) \leq P_{RS} \quad (8.47)$$

et

$$\text{tr} \mathbf{G}_c \mathbf{G}_c^H \leq P_c \text{ for } c \in \mathcal{C} \quad (8.48)$$

avec P_{RS} et P_c correspondant respectivement à la puissance maximale transmise par le RS et la BS c et \mathcal{C} est l'ensemble de toutes les BSs.

Notre fonction d'utilité est de maximiser la somme pondéré des débits:

$$\mathbf{G} = \arg \max_{\mathbf{G}} \sum_{c=1}^C \sum_k u_k r_k \quad (8.49)$$

subject to (8.47) and (8.48)

Le débit r_k est donné par:

$$r_k = \log \det(\mathbf{I}_N + \mathbf{\Gamma}_k) \quad (8.50)$$

$$\mathbf{\Gamma}_k = \mathbf{R}_{z_k}^{-1} \mathbf{H}_{k,b_k}^{\overline{UB}} \mathbf{Q}_k \mathbf{H}_{k,b_k}^{\overline{UB},H} \quad (8.51)$$

$\mathbf{\Gamma}_k$ est le SINR de l'utilisateur k et \mathbf{R}_{z_k} est la covariance de la matrice d'interférence plus bruit à l'utilisateur k :

$$\begin{aligned} \mathbf{R}_{z_k} = & \sum_{i \neq k: b_i = b_k} \mathbf{H}_{k,b_k}^{\overline{UB}} \mathbf{G}_i \mathbf{G}_i^H \mathbf{H}_{k,b_k}^{\overline{UB},H} + \\ & \sum_{j \neq b_k} \sum_{i: b_i = j} \mathbf{H}_{k,j}^{\overline{UB}} \mathbf{G}_i \mathbf{G}_i^H \mathbf{H}_{k,j}^{\overline{UB},H} + \sigma_{RS}^2 \mathbf{H}_k^{UR} \mathbf{F} \mathbf{F}^H \mathbf{H}_k^{UR,H} + \sigma^2 \mathbf{I}_N \end{aligned} \quad (8.52)$$

En plus, on défine \mathbf{R}_k , la matrice de covariance du signal total reçu à l'utilisateur k , comme suit:

$$\begin{aligned} \mathbf{R}_k = & \sum_j \sum_{i: b_i = j} \mathbf{H}_{k,j}^{\overline{UB}} \mathbf{G}_i \mathbf{G}_i^H \mathbf{H}_{k,j}^{\overline{UB},H} + \sigma_{nRS}^2 \mathbf{H}_k^{UR} \mathbf{F} \mathbf{F}^H \mathbf{H}_k^{UR,H} + \sigma^2 \mathbf{I}_N \\ = & \mathbf{R}_{z_k} + \mathbf{H}_{k,b_k}^{UR} \mathbf{G}_k \mathbf{G}_k^H \mathbf{H}_{k,b_k}^{UR,H} \end{aligned} \quad (8.53)$$

La solution est donné par un algorithme itératif, où à chaque itération, on calcule plusieurs variables:

$$\mathbf{W}_k = \mathbf{\Psi}_k^{-1} \quad (8.54)$$

$$\mathbf{D}_k = \mathbf{G}_k^H \mathbf{H}_{k,b_k}^{\overline{UB},H} (\mathbf{R}_k)^{-1} \quad (8.55)$$

$$\begin{aligned} \mathbf{F} = & \left(\sum_i \mathbf{H}_i^{UR,H} \mathbf{D}_i^H \mathbf{W}_i \mathbf{D}_i \mathbf{H}_i^{UR} + \lambda \mathbf{I}_{MRS} \right)^{-1} \\ & \times \left(\sum_j \sum_{l \neq b_k} \sum_{i: b_i = l} \mathbf{H}_j^{UR,H} \mathbf{D}_j \mathbf{W}_j \mathbf{D}_j^H \mathbf{H}_j^{UR} \mathbf{F} \mathbf{H}_l^{RB} \mathbf{G}_i \mathbf{G}_i^H \mathbf{H}_l^{RB,H} \right. \\ & \left. - \sum_i \mathbf{H}_i^{UR,H} \mathbf{D}_i \mathbf{W}_i \mathbf{G}_i^H \mathbf{H}_{b_i}^{RB,H} \right) \left(\sum_j \sum_{i: b_i = j} \mathbf{H}_j^{RB} \mathbf{G}_i \mathbf{G}_i^H \mathbf{H}_j^{RB,H} + \sigma_{RS}^2 \mathbf{I}_{MRS} \right)^{-1} \end{aligned} \quad (8.56)$$

$$\begin{aligned} \mathbf{G}_k = & \left(\sum_i \mathbf{H}_{i,b_k}^{\overline{UB},H} \mathbf{D}_i \mathbf{W}_i \mathbf{D}_i^H \mathbf{H}_{i,b_k}^{\overline{UB}} + \xi (\mu_{b_k} \mathbf{I}_{MBS} \right. \\ & \left. + \lambda \mathbf{E}_{b_k}^{RB,H} \mathbf{F}^H \mathbf{F} \mathbf{E}_{b_k}^{RB}) \right)^{-1} \mathbf{H}_{k,b_k}^{\overline{UB},H} \mathbf{D}_k \mathbf{W}_k \end{aligned} \quad (8.57)$$

Dans ce qui suit, on propose une variante pour calculer \mathbf{G}_k en utilisant DC: (8.49). On aura un nouveau problème dont le Lagrangien est donné par:

$$WSR(\mathbf{G}, \hat{\mathbf{G}}, \lambda) = \sum_{j=1}^C \mu_j P_c + \sum_{k=1}^K u_k \log \det(\mathbf{I}_{d_k} + \mathbf{G}_k^H \hat{\mathbf{B}}_k \mathbf{G}_k) - \text{tr}\{\mathbf{G}_k^H (\hat{\mathbf{A}}_k + \mu_{b_k} \mathbf{I}_M + \lambda \mathbf{H}_{b_k}^{RB,H} \mathbf{F}^H \mathbf{F} \mathbf{H}_{b_k}^{RB} \mathbf{G}_k)\} \quad (8.58)$$

avec
$$\hat{\mathbf{B}}_k = \mathbf{H}_{k,b_k}^{\overline{UB},H} \hat{\mathbf{R}}_{z_k}^{-1} \mathbf{H}_{k,b_k}^{\overline{UB}}. \quad (8.59)$$

Cela aboutit à une solution sous forme de matrices généralisées. On conclut par simulations (Figure 6.2) que cette approche hybride de calcul de \mathbf{G} tout en calculant \mathbf{F} via WSMSE est mieux que WSMSE pure.

La dernière contribution se base sur le fait de supposer que maintenant les BSs et les utilisateurs peuvent communiquer directement et via les relais. Deux techniques d'interférence sont en jeu: l'IA qui est le sujet de la majorité des contributions de cette thèse et la neutralisation des interférences (IN), où des chemins multiples artificiels sont créés et se recombinent au Rx pour annuler les interférences.

8.6 Conclusions

Les travaux de cette thèse s'inscrivent dans le cadre de deux projets Européens H2020 Fantastic5G et One5G. La thèse traite le problème de l'annulation des interférences et de la maximisation de la capacité dans les réseaux Massive MIMO 5G. L'étude se concentre sur le segment d'accès sans fil des communications cellulaires 5G et cible le problème clé de l'interférence qui est due à la réutilisation des fréquences. Cela a été une déficience de longue date dans les réseaux cellulaires de toutes les générations qui sera encore exacerbée dans les réseaux 5G, en raison du déploiement de cellules denses prévu. Dans ce contexte, la thèse propose de nouvelles alternatives de gestion des interférences pour le régime d'antennes MIMO Massive, en tenant compte également des défis pratiques des réseaux d'antennes Massive. Le chapitre 1 fournit la motivation et prépare le terrain pour les études de thèse. Il introduit également la notation clé et le modèle de système à étudier. Les principaux inconvénients et défis de la conception d'antennes et de systèmes lorsque le nombre d'antennes à la station de base évolue vers un grand nombre (tels que les dégradations RF

et la contamination des canaux) sont discutés, suivi d'une discussion sur le sujet important de contamination pilote et son élimination. Ceci est suivi d'une présentation des bandes de fréquences pour 5G et d'une motivation de la communication MmWaves / Massive MIMO combinés. Après la notation et la configuration du système, deux algorithmes de précodage (WSMSE et KG) sont présentés en détail, puisqu'ils constituent la base des techniques proposées par la thèse pour le régime MIMO massif. Ceci est suivi de la présentation DA et de l'estimation de canal pour cette configuration considérée. Une liste des principales contributions de la thèse est également incluse dans ce chapitre. Le chapitre 2 contient une analyse des performances de l'algorithme WSMSE dans un système large (antennes, utilisateurs) de réseaux MISO massifs multi-cellules multi-utilisateurs basée sur la théorie des matrices aléatoires. Le travail peut être vu comme une extension d'études antérieures qui reposent sur des expressions SINR équivalentes déterministes (puisque SINR est un paramètre de capacité clé pour les systèmes MISO). Cette approche est également adoptée ici et appliquée aux précodeurs WSMSE présentés au Chapitre 1, en supposant un CSI parfait et un précodage centralisé. Les expressions équivalentes déterministes dérivées sont ensuite validées numériquement, montrant un bon accord avec les débits réels pour le cas de 3 cellules, 30 antennes et de l'ordre de 10 utilisateurs par cellule. Les résultats sont ensuite étendus aux cas de flux unique MIMO, où l'approche déterministe équivalente SINR est de nouveau montrée d'être valide. Les expressions SINR équivalentes déterministes dérivées sont ensuite utilisées pour prouver un résultat d'échelle de capacité dans le cas des récepteurs multi-antennes. Le chapitre 3 considère le cas de CoBF décentralisée qui repose sur un échange lent d'informations d'évanouissement entre les stations de base. La grande approche d'analyse de système est à nouveau adoptée, en mettant l'accent sur la technique WSMSE et en ciblant des solutions optimales de formation de précodeur dans ce sens. L'approche repose sur l'échange d'informations via des liaisons terrestres fixes (parfaitement fiables). Comme en général cet échange peut être lourd et prendre de nombreuses itérations jusqu'à ce qu'il converge, l'initialisation des précodeurs est la clé tant en termes de vitesse de convergence que de la solution atteinte. Pour cela, la thèse propose une nouvelle initialisation asymptotiquement optimale dans le régime large (antenne infinie / utilisateurs infinis, avec rapport fixe entre eux) (Théorème 3.1), appelé 'LS-précodeur'. Trois variantes différentes de calcul et d'échange de fuites entre stations de base, allant du calcul de

l'interférence intracellulaire uniquement basée sur la connaissance des canaux locaux et le non-respect total des interférences intercellulaires au calcul de toutes les interférences intra et inter cellules mises à jour. Fait intéressant, même les deux variantes sous-optimales qui n'utilisent pas les interférences intercellulaires à jour, fonctionnent mieux que les techniques précédemment proposées et semblent en fait avoir des performances identiques entre elles et offrir un gain minimal sur l'initialisation du précodeur LS dans le cas non entièrement chargé. Ils convergent aussi très vite (en 2 à 3 itérations). Les résultats montrent également que les réseaux non entièrement chargés ($KC / M < 1$) fonctionnent nettement mieux que les réseaux entièrement chargés. Le chapitre se termine par quelques expressions analytiques du précodeur LS pour certaines hypothèses hautement idéalisées des matrices de covariance diagonale des canaux (qui peuvent se rapporter à des situations réelles dans des régimes asymptotiques à grande échelle). Le chapitre 4 change de direction en supposant une CSIT partielle (supposant toujours une connaissance des canaux aux récepteurs CSIR parfait) et en ciblant à nouveau des précodeurs optimaux pour le régime de système large. Le problème est formulé comme une optimisation de la fonction d'objectif EWSR. La technique proposée est appelée ESEI-WSR et repose sur le fait que dans le régime de système large (Massive), l'espérance de la somme pondérée des débits convergera vers le WSR réel et peut être écrite en fonction du WSR correspondant au canal estimé et un terme d'erreur qui repose sur la matrice de covariance d'erreur de canal. Le précodeur correspondant est optimal dans ce sens (ayant supposé, comme tout au long de la thèse, une matrice de covariance de canal d'identité à chaque récepteur). DA est à nouveau adopté afin de conduire la solution à un optimum global. L'ESEI-WSR ainsi obtenu est ensuite évalué numériquement pour des configurations petites / pratiques (2 cellules, 8 antennes et 4 utilisateurs par cellule) et montre de faibles gains par rapport aux précédentes approches sous-optimales dans le cas des récepteurs à antenne unique. Pour les récepteurs avec multi-antennes (2 ou 4), les approches sous-optimales montrent un plafonnement de leurs performances. Bien qu'optimale dans le sens ci-dessus, la technique ESEI-WSR est lourde en termes d'échange d'informations de canal entre les exigences des stations de base. Pour cela, une extension décentralisée pratique est dérivée, dans laquelle la CSIT instantané n'est utilisé que pour les récepteurs prévus, tandis que les récepteurs involontaires d'autres cellules sont uniquement captés via les matrices de covariance correspondantes (les

canaux intracellulaires sont supposés parfaitement connus via TDD, tandis que les canaux intercellulaires sont inconnus). L'algorithme est adapté à une implémentation distribuée (en raison du petit échange d'informations requis) et a une faible complexité et une convergence rapide. Ses performances sont évaluées numériquement pour un certain nombre de cas (canaux de rang inférieur corrélés et canaux non corrélés avec des covariances de canal d'identité). L'ESEI-WSR est ensuite formulé et simplifié dans le cas des canaux MISO massifs. Une approche sous-optimale alternative basée sur l'algorithme KG est ensuite proposée pour les antennes d'émission et de réception croissantes à l'infini avec un rapport fini, montrant des gains numériquement significatifs par rapport à l'approche naïve. Le chapitre 5 s'écarte du précodage linéaire et considère les schémas non linéaires. La configuration de l'IBC MIMO est formulée et l'approche poursuivie consiste en une combinaison de schémas non-linéaires par cellule et une gestion coopérative des interférences fuites des précodeurs de toutes les cellules afin d'optimiser conjointement le critère ESEI-WSR introduit au chapitre 4. En vue de la CSIT partielle, le précodage non linéaire choisi par cellule est LA au lieu de DPC, ce qui serait optimal dans le cas d'une CSIT parfaite. Après la formulation du problème IBC, les matrices d'affectation linéaire et de formation de précodeurs sont formulées, établissant la base pour la conception d'émission conjointe recherchée. Comme les deux ensembles de paramètres (matrices) dépendent les uns des autres, une approche d'optimisation alternative aurait du sens, mais nécessiterait une grande complexité. Pour éviter cela, une expression analytique est dérivée pour la matrice LA. Cela a réduit la recherche de la matrice optimale de formation de précodeur à un seul critère (ESWR), similaire à celui introduit au chapitre 1. Dans le cas de la CSIT parfaite, une approche précédemment dérivée par Nguyen et Le-Ngoc est adoptée. L'expansion en série de Taylor de la matrice de covariance, combinée à une annulation d'interférence successive pour le problème duel (MAC), conduit à un problème d'optimisation convexe séparable qui fournit successivement les solutions pour les décodeurs optimaux. Dans le cas de la CSIT partielle, la même approche est suivie, mais l'effet de la CSIT partielle est capturé en considérant les expressions asymptotiques de covariances de canal qui dans la limite d'antenne infinie égalent les valeurs déterministes correspondantes (même approche que dans la section 4.3). Les matrices de précodage sont obtenues itérativement en supposant une certaine propriété de diagonalisation des corrélations de canaux séparables. La solution obtenue

est évaluée numériquement pour les cas de 3 cellules, 3 utilisateurs par cellule, 8 antennes de station de base et 2 antennes par récepteur et comparée (et supérieure) à la solution robuste linéaire, ainsi qu'à d'autres cas particuliers et bornes. Enfin, le chapitre 6 considère le cas du canal de diffusion d'interférences avec utilisation de relais (appelé IRBC). Une configuration de relais à deux sauts est considérée et un relais AF est adopté, dans lequel les nœuds de relais effectuent une nouvelle combinaison linéaire avec les signaux reçus, sous réserve de nouvelles contraintes de puissance. Il est en outre supposé que les relais sont en FD (par opposition au relais semi-duplex conventionnel), afin de renforcer encore l'efficacité spectrale. Après l'introduction du modèle de signal IBRC, l'algorithme WSMSE de maximisation de la somme pondérée des débits sous réserve des contraintes de puissance est expliqué. Nous proposons ensuite une optimisation alternative, en utilisant la matrice de précodage WSMSE pour les stations relais et le précodeur KG pour les stations de base. Le chapitre conclut en considérant le cas où des liens directs entre les stations de base et les utilisateurs finaux existent également et en déduit des conditions et une solution qui impliquent le précodage à forçage zéro (IA) et la neutralité d'interférence.

Appendix A

Random Matrix Theory

We will recall lemmas and a theorem from Random Matrix Theory established by [28].

Lemma A.1 (Matrix Inversion Lemma):

Let \mathbf{U} be an $M \times M$ invertible matrix and $\mathbf{x} \in \mathbb{C}^M$, $c \in \mathbb{C}$ for which $\mathbf{U} + c\mathbf{x}\mathbf{x}^H$ is invertible. Then

$$\mathbf{x}^H(\mathbf{U} + c\mathbf{x}\mathbf{x}^H)^{-1} = \frac{\mathbf{x}^H\mathbf{U}^{-1}}{1 + c\mathbf{x}^H\mathbf{U}^{-1}\mathbf{x}}. \quad (\text{A.1})$$

Lemma A.2 (Resolvent Identity): Let \mathbf{U} and \mathbf{V} be two invertible complex matrices of size $M \times M$. Then

$$\mathbf{U}^{-1} - \mathbf{V}^{-1} = -\mathbf{U}^{-1}(\mathbf{U} - \mathbf{V})\mathbf{V}^{-1}. \quad (\text{A.2})$$

Lemma A.3 Let $\mathbf{A} \in \mathbb{C}^{M \times M}$ and $x, y \sim \mathcal{CM}(0, \frac{1}{M}\mathbf{I}_M)$. Assume that \mathbf{A} has uniformly bounded spectral norm (with respect to M) and that x and y are mutually independent and independent of \mathbf{A} . Then

$$x^H - \frac{1}{M}\text{tr}\mathbf{A} \xrightarrow{M \rightarrow \infty} 0 \quad (\text{A.3})$$

Lemma A.4 Let $\mathbf{A}_1, \mathbf{A}_2, \dots$, with $\mathbf{A}_M \in \mathbb{C}^{M \times M}$, be deterministic with uniformly bounded spectral norm and $\mathbf{B}_1, \mathbf{B}_2, \dots$ with $\mathbf{B}_M \in \mathbb{C}^{M \times M}$, be random hermitian, with eigenvalues $\lambda_1^{\mathbf{B}_M} \preceq \dots \preceq \lambda_M^{\mathbf{B}_M}$ such that, with probability 1, there exist $\epsilon > 0$ for which $\lambda_1^{\mathbf{B}_M} > \epsilon$ for all large M . Then for $v \in \mathbb{C}^M$

$$\frac{1}{M}\text{tr}\mathbf{A}_M\mathbf{B}_M^{-1} - \frac{1}{M}\text{tr}\mathbf{A}_M(\mathbf{B}_M + \mathbf{v}\mathbf{v}^H)^{-1} \xrightarrow{M \rightarrow \infty} 0 \quad (\text{A.4})$$

almost surely, where \mathbf{B}_M^{-1} and $(\mathbf{B}_M + \mathbf{v}\mathbf{v}^H)^{-1}$ exist with probability 1.

Theorem A.1 Let $\mathbf{B}_M = \mathbf{X}_M^H \mathbf{X}_M + \mathbf{S}_M$ with $\mathbf{S}_M \in \mathbb{C}^{M \times M}$ Hermitian non negative definite and $\mathbf{X}_M \in \mathbb{C}^{m \times M}$ random. The i th column \mathbf{x}_i of \mathbf{X}_M^H is $\mathbf{x}_i = \mathbf{\Psi}_i \mathbf{y}_i$, where the entries of $\mathbf{y}_i \in \mathbb{C}^{r_i}$ are i.i.d. of zero mean, variance $\frac{1}{M}$ and have eight-order moment of order $O(\frac{1}{M^4})$. The matrices $\mathbf{\Psi}_i \in \mathbb{C}^{M \times r_i}$ are deterministic. Furthermore, let $\mathbf{\Theta}_i = \mathbf{\Psi}_i \mathbf{\Psi}_i^H \in \mathbb{C}^{M \times M}$ and define $\mathbf{Q}_M \in \mathbb{C}^{M \times M}$ deterministic. Assume $\limsup_{M \rightarrow \infty} \sup_{1 \leq i \leq m} \|\mathbf{\Theta}_i\| \preceq \infty$ and let \mathbf{Q}_M have uniformly bounded spectral norm (with respect to M). Define

$$m_{\mathbf{B}_M, \mathbf{Q}_M}(z) = \frac{1}{M} \text{tr} \mathbf{Q}_M (\mathbf{B}_M - z \mathbf{I}_M)^{-1} \quad (\text{A.5})$$

Then, for $z \in \mathbb{R}^+$, as m, M grow large with ratios $\beta_{M,i} = \frac{M}{r_i}$ and $\beta_M = \frac{M}{m}$ such that $0 < \liminf_M \beta_M \preceq \limsup_M \beta_M < \infty$, we have that

$$m_{\mathbf{B}_M, \mathbf{Q}_M}(z) - \bar{m}_{\mathbf{B}_M, \mathbf{Q}_M}(z) \xrightarrow{M \rightarrow \infty} 0 \quad (\text{A.6})$$

with $\bar{m}_{\mathbf{B}_M, \mathbf{Q}_M}(z)$ given by

$$\bar{m}_{\mathbf{B}_M, \mathbf{Q}_M}(z) = \frac{1}{M} \text{tr} \mathbf{Q}_M \left(\frac{1}{M} \sum_{j=1}^m \frac{\mathbf{\Theta}_j}{1 + e_{M,j}(z)} + \mathbf{S}_M - z \mathbf{I}_M \right)^{-1} \quad (\text{A.7})$$

where the functions $e_{M,1}(z) \dots e_{M,m}(z)$ form the unique solution of

$$e_{M,i}(z) = \frac{1}{M} \text{tr} \mathbf{\Theta}_i \left(\frac{1}{M} \sum_{j=1}^m \frac{\mathbf{\Theta}_j}{1 + e_{M,j}(z)} + \mathbf{S}_M - z \mathbf{I}_M \right)^{-1} \quad (\text{A.8})$$

which is the Stieltjes transform of a non negative finite measure on \mathbb{R}^+ . Moreover, for $z < 0$, the scalars $e_{M,1}(z) \dots e_{M,m}(z)$ are the unique non negative solutions to (A.8).

Appendix B

Proof of an equivalent deterministic expression: Perfect CSIT

Lemmas A.1, A.2, A.3, A.4 and Theorem A.1 from Appendix A are used. Using Lemma A.2,

$$\mathbf{\Gamma}_m^{-1,(j)} = \mathbf{\Gamma}_{m,[c,k],[m,l]}^{-1,(j)} + (\mathbf{\Gamma}_m^{-1,(j)} - \mathbf{\Gamma}_{m,[c,k],[m,l]}^{-1,(j)}); \quad (\text{B.1})$$

$$(\mathbf{\Gamma}_m^{-1,(j)} - \mathbf{\Gamma}_{m,[c,k],[m,l]}^{-1,(j)}) = -\mathbf{\Gamma}_m^{-1,(j)} (\mathbf{\Gamma}_m^{(j)} - \mathbf{\Gamma}_{m,[c,k],[m,l]}^{(j)}) \mathbf{\Gamma}_{m,[c,k],[m,l]}^{-1,(j)}; \quad (\text{B.2})$$

$$\begin{aligned} (\mathbf{\Gamma}_m^{(j)} - \mathbf{\Gamma}_{m,[c,k],[m,l]}^{(j)}) &= \frac{1}{M} \mathbf{h}_{m,c,k} \bar{d}_{c,k}^{(j)} \mathbf{h}_{m,c,k}^H + \frac{1}{M} \mathbf{h}_{m,m,l} \bar{d}_{m,l}^{(j)} \mathbf{h}_{m,m,l}^H \\ &= \bar{\mathbf{\Theta}}_{m,c,k}^{\frac{1}{2},(j)} \mathbf{z}_{m,c,k} \mathbf{z}_{m,c,k}^H \bar{\mathbf{\Theta}}_{m,c,k}^{\frac{1}{2},(j)} + \bar{\mathbf{\Theta}}_{m,l}^{\frac{1}{2},(j)} \mathbf{z}_{m,m,l} \mathbf{z}_{m,m,l}^H \bar{\mathbf{\Theta}}_{m,l}^{\frac{1}{2},(j)}; \end{aligned} \quad (\text{B.3})$$

Denoting,

$$m_{m,l}^{(j)} = \mathbf{z}_{m,m,l}^H \bar{\mathbf{\Theta}}_{m,l}^{\frac{1}{2},(j)} \mathbf{\Gamma}_{m,[c,k],[m,l]}^{-1,(j)} \bar{\mathbf{\Theta}}_{m,l}^{\frac{1}{2},(j)} \mathbf{z}_{m,m,l}; \quad (\text{B.4})$$

$$m_{m,c,k}^{(j)} = \mathbf{z}_{m,c,k}^H \bar{\mathbf{\Theta}}_{m,c,k}^{\frac{1}{2},(j)} \mathbf{\Gamma}_{m,[c,k],[m,l]}^{-1,(j)} \bar{\mathbf{\Theta}}_{m,c,k}^{\frac{1}{2},(j)} \mathbf{z}_{m,c,k}; \quad (\text{B.5})$$

Using Lemmas A.1,A.3 and A.4 and (B.5),

$$\mathbf{z}_{m,c,k}^H \bar{\mathbf{\Theta}}_{m,c,k}^{\frac{1}{2},(j)} \mathbf{\Gamma}_m^{-1,(j)} \bar{\mathbf{\Theta}}_{m,c,k}^{\frac{1}{2},(j)} \mathbf{z}_{m,c,k} = \frac{m_{m,c,k}}{1 + m_{m,c,k}}; \quad (\text{B.6})$$

Using (B.1), (B.2), (B.3), (B.4), (B.5) and (B.6),

$$\begin{aligned}
& \mathbf{z}_{m,c,k}^H \bar{\Theta}_{m,c,k}^{\frac{1}{2},(j)} \mathbf{\Gamma}_{m,l}^{-1,(j)} \bar{\Theta}_{m,l}^{\frac{1}{2},(j)} \mathbf{z}_{m,m,l} \\
&= \mathbf{z}_{m,c,k}^H \bar{\Theta}_{m,c,k}^{\frac{1}{2},(j)} \mathbf{\Gamma}_{m,[c,k],[m,l]}^{-1,(j)} \bar{\Theta}_{m,l}^{\frac{1}{2},(j)} \mathbf{z}_{m,m,l} - \\
& \mathbf{z}_{m,c,k}^H \bar{\Theta}_{m,c,k}^{\frac{1}{2},(j)} \mathbf{\Gamma}_{m,l}^{-1,(j)} \bar{\Theta}_{m,c,k}^{\frac{1}{2},(j)} \mathbf{z}_{m,c,k} \mathbf{z}_{m,c,k}^H \bar{\Theta}_{m,c,k}^{\frac{1}{2},(j)} \mathbf{\Gamma}_{m,[c,k],[m,l]}^{-1,(j)} \bar{\Theta}_{m,l}^{\frac{1}{2},(j)} \mathbf{z}_{m,m,l} - \\
& \mathbf{z}_{m,c,k}^H \bar{\Theta}_{m,l}^{\frac{1}{2},(j)} \mathbf{\Gamma}_{m,l}^{-1,(j)} \bar{\Theta}_{m,l}^{\frac{1}{2},(j)} \mathbf{z}_{m,m,l} \mathbf{z}_{m,m,l}^H \bar{\Theta}_{m,l}^{\frac{1}{2},(j)} \mathbf{\Gamma}_{m,[c,k],[m,l]}^{-1,(j)} \bar{\Theta}_{m,l}^{\frac{1}{2},(j)} \mathbf{z}_{m,m,l} \\
&= \frac{1}{1+m_{m,l}^{(j)}} \frac{1}{1+m_{m,c,k}^{(j)}} \mathbf{z}_{m,c,k}^H \bar{\Theta}_{m,c,k}^{\frac{1}{2},(j)} \mathbf{\Gamma}_{m,[c,k],[m,l]}^{-1,(j)} \bar{\Theta}_{m,l}^{\frac{1}{2},(j)} \mathbf{z}_{m,m,l}; \\
&= L_{m,c,k,m,l}^{(j)} \mathbf{z}_{m,c,k}^H \bar{\Theta}_{m,c,k}^{\frac{1}{2},(j)} \mathbf{\Gamma}_{m,[c,k],[m,l]}^{-1,(j)} \bar{\Theta}_{m,l}^{\frac{1}{2},(j)} \mathbf{z}_{m,m,l};
\end{aligned}$$

with

$$L_{m,c,k,m,l}^{(j)} = \frac{1}{1+m_{m,l}^{(j)}} \frac{1}{1+m_{m,c,k}^{(j)}}. \quad (\text{B.7})$$

Thus,

$$\begin{aligned}
\Upsilon_{inter,c,k} &= \sum_{(m,l); m \neq c} \mathbf{h}_{m,c,k}^H \mathbf{g}_{m,l} \mathbf{g}_{m,l}^H \mathbf{h}_{m,c,k}; \\
& \frac{\mathbf{h}_{m,c,k}^H \mathbf{g}_{m,l} \mathbf{g}_{m,l}^H \mathbf{h}_{m,c,k} \times \bar{d}_{c,k}^{(j)}}{\xi_c^{2,(j)}} \\
&= \mathbf{z}_{m,c,k}^H \bar{\Theta}_{m,c,k}^{\frac{1}{2},(j)} \mathbf{\Gamma}_{m,c,k}^{-1,(j)} \bar{\Theta}_{m,l}^{\frac{1}{2},(j)} \mathbf{z}_{m,m,l} \mathbf{z}_{m,m,l}^H \bar{\Theta}_{m,l}^{\frac{1}{2},(j)} \mathbf{\Gamma}_{m,l}^{-1,(j)} \bar{\Theta}_{m,c,k}^{\frac{1}{2},(j)} \mathbf{z}_{m,c,k} \\
&= |L_{m,c,k,m,l}^{(j)} \mathbf{z}_{m,c,k}^H \bar{\Theta}_{m,c,k}^{\frac{1}{2},(j)} \mathbf{\Gamma}_{m,[c,k],[m,l]}^{-1,(j)} \bar{\Theta}_{m,l}^{\frac{1}{2},(j)} \mathbf{z}_{m,m,l}|^2 \\
&\stackrel{(a)}{\rightarrow} |L_{m,c,k,m,l}^{(j)}|^2 \times \frac{1}{M} |\mathbf{z}_{m,m,l}^H \bar{\Theta}_{m,l}^{\frac{1}{2},(j)} \mathbf{\Gamma}_{m,[c,k],[m,l]}^{-1,(j)} \bar{\Theta}_{m,c,k}^{\frac{1}{2},(j)}|^2 \\
&\stackrel{(b)}{\rightarrow} |L_{m,c,k,m,l}^{(j)}|^2 \times \frac{1}{M} |\text{tr} \bar{\Theta}_{m,c,k}^{(j)} \mathbf{\Gamma}_{m,[c,k],[m,l]}^{-1,(j)} \bar{\Theta}_{m,l}^{(j)} \mathbf{\Gamma}_{m,[c,k],[m,l]}^{-1,(j)}| \\
&= |L_{m,c,k,m,l}^{(j)}|^2 \times \frac{1}{M} |\text{tr} (\bar{\Theta}_{m,l}^{-\frac{1}{2},(j)} \bar{\Theta}_{m,c,k}^{(j)} \bar{\Theta}_{m,l}^{-\frac{1}{2},(j)} \bar{\Theta}_{m,l}^{\frac{1}{2},(j)}) \times \\
& \quad \mathbf{\Gamma}_{m,[c,k],[m,l]}^{-1,(j)} \bar{\Theta}_{m,l}^{\frac{1}{2},(j)} \bar{\Theta}_{m,l}^{\frac{1}{2},(j)} \mathbf{\Gamma}_{m,[c,k],[m,l]}^{-1,(j)} \bar{\Theta}_{m,l}^{\frac{1}{2},(j)}| \\
&= |L_{m,c,k,m,l}^{(j)}|^2 \times \frac{1}{M} |\text{tr} \{ (\bar{\Theta}_{m,l}^{-\frac{1}{2},(j)} \bar{\Theta}_{m,c,k}^{(j)} \bar{\Theta}_{m,l}^{-\frac{1}{2},(j)}) \\
& \quad \times (\bar{\Theta}_{m,l}^{\frac{1}{2},(j)} \mathbf{\Gamma}_{m,[c,k],[m,l]}^{(j)} \bar{\Theta}_{m,l}^{\frac{1}{2},(j)})^{-1} \times (\bar{\Theta}_{m,l}^{\frac{1}{2},(j)} \mathbf{\Gamma}_{m,[c,k],[m,l]}^{(j)} \bar{\Theta}_{m,l}^{\frac{1}{2},(j)})^{-1} \}| \\
&\stackrel{(c)}{\rightarrow} |L_{m,c,k,m,l}^{(j)}|^2 \times \frac{1}{M} \text{tr} \{ \\
& \quad \bar{\Theta}_{m,c,k}^{(j)} (\mathbf{F}_m + \bar{\alpha}^{(j)} \mathbf{I})^{-1} \times (\mathbf{F}_{m,m,l}' + \bar{\Theta}_{m,l}^{(j)}) \times (\mathbf{F}_m + \bar{\alpha}^{(j)} \mathbf{I})^{-1} \} \\
&= L_{m,c,k,m,l}^{(j),2} e_{m,c,k,m,l}'
\end{aligned}$$

Note that (a), (b) and (c) above correspond to "using Lemma A.3 and the fact that the matrices in a trace of a product can be switched", "using Lemma A.3 and the property of trace" and "using Theorem A.1" respectively. Now, the proof is completed.

Appendix C

Proof of an equivalent deterministic expression: Imperfect CSIT

The equation (4.10) can be reformulated as

$$\begin{aligned}
 \mathbf{A}_k &= \sum_{i \neq k}^K u_i [\mathbf{A}_{i,k}^A - \mathbf{A}_{i,k}^B]; \\
 \mathbf{A}_{i,k}^A &= \mathbf{H}_{i,b_k}^H \mathbf{R}_{\bar{i}}^{-1} \mathbf{H}_{i,b_k}; \mathbf{A}_{i,k}^B = \mathbf{H}_{i,b_k}^H \mathbf{R}_i^{-1} \mathbf{H}_{i,b_k} \\
 \mathbf{R}_{\bar{i}}^{-1} &= \mathbf{R}_{i,\bar{k}}^{-1} + (\mathbf{R}_{\bar{i}}^{-1} - \mathbf{R}_{i,\bar{k}}^{-1}) \text{ with} \\
 \mathbf{R}_{i,\bar{k}} &= \sum_{j \neq i, j \neq k} \mathbf{H}_{i,b_j} \mathbf{Q}_j \mathbf{H}_{i,b_j}^H + \sigma^2 \mathbf{I}_N
 \end{aligned} \tag{C.1}$$

Applying [Lemma A.2],

$$\begin{aligned}
 (\mathbf{R}_{\bar{i}}^{-1} - \mathbf{R}_{i,\bar{k}}^{-1}) &= -\mathbf{R}_{\bar{i}}^{-1} (\mathbf{R}_{\bar{i}} - \mathbf{R}_{i,\bar{k}}) \mathbf{R}_{i,\bar{k}}^{-1} \\
 &= -\mathbf{R}_{\bar{i}}^{-1} (\mathbf{H}_{i,b_k} \mathbf{Q}_k \mathbf{H}_{i,b_k}^H) \mathbf{R}_{i,\bar{k}}^{-1}; \\
 \mathbf{A}_{i,k}^A &= \mathbf{H}_{i,b_k}^H \mathbf{R}_{i,\bar{k}}^{-1} \mathbf{H}_{i,b_k} \\
 &\quad - \mathbf{H}_{i,b_k}^H \mathbf{R}_{\bar{i}}^{-1} (\mathbf{H}_{i,b_k} \mathbf{Q}_k \mathbf{H}_{i,b_k}^H) \mathbf{R}_{i,\bar{k}}^{-1} \mathbf{H}_{i,b_k}; \\
 \mathbf{A}_{i,k}^A &= \mathbf{A}_{i,k}^C - \mathbf{A}_{i,k}^A \mathbf{Q}_k \mathbf{A}_{i,k}^C \text{ with } \mathbf{A}_{i,k}^C = \mathbf{H}_{i,b_k}^H \mathbf{R}_{i,\bar{k}}^{-1} \mathbf{H}_{i,b_k}.
 \end{aligned}$$

Similarly,

$$\begin{aligned}\mathbf{A}_{i,k}^B &= \mathbf{A}_{i,k}^D - \mathbf{A}_{i,k}^B \mathbf{Q}_k \mathbf{A}_{i,k}^D \\ \text{with } \mathbf{A}_{i,k}^D &= \mathbf{H}_{i,b_k}^H \mathbf{R}_{i,\bar{k}}^{-1} \mathbf{H}_{i,b_k} \\ \text{and } \mathbf{R}_{i,\bar{k}} &= \sum_{j \neq k} \mathbf{H}_{i,b_j} \mathbf{Q}_j \mathbf{H}_{i,b_j}^H + \sigma^2 \mathbf{I}_N.\end{aligned}$$

Using the channel model in section 1.6,

$$\begin{aligned}\mathbf{A}_{i,k}^C &= \bar{\mathbf{H}}_{i,b_k}^H \mathbf{R}_{i,\bar{k}}^{-1} \bar{\mathbf{H}}_{i,b_k} \\ &+ \boldsymbol{\Theta}_{p,i,b_k}^{\frac{1}{2},H} \tilde{\mathbf{H}}_{p,i,b_k}^H \mathbf{C}_{r,i}^{\frac{1}{2},H} \mathbf{R}_{i,\bar{k}}^{-1} \mathbf{C}_{r,i}^{\frac{1}{2}} \tilde{\mathbf{H}}_{p,i,b_k} \boldsymbol{\Theta}_{p,i,b_k}^{\frac{1}{2}} \\ &- \boldsymbol{\Theta}_{p,i,b_k}^{\frac{1}{2},H} \tilde{\mathbf{H}}_{p,i,b_k}^H \mathbf{C}_{r,i}^{\frac{1}{2},H} \mathbf{R}_{i,\bar{k}}^{-1} \bar{\mathbf{H}}_{i,b_k} \\ &- \bar{\mathbf{H}}_{i,b_k}^H \mathbf{R}_{i,\bar{k}}^{-1} \mathbf{C}_{r,i}^{\frac{1}{2}} \tilde{\mathbf{H}}_{p,i,b_k} \boldsymbol{\Theta}_{p,i,b_k}^{\frac{1}{2}} \xrightarrow{(a)} \\ &\bar{\mathbf{H}}_{i,b_k}^H \check{\mathbf{R}}_{i,\bar{k}}^{-1} \bar{\mathbf{H}}_{i,b_k} + \text{tr}\{\check{\mathbf{R}}_{i,\bar{k}}^{-1} \mathbf{C}_{r,i}\} \boldsymbol{\Theta}_{p,i,b_k} = \check{\mathbf{A}}_{i,k}^C; \\ \mathbf{R}_{i,\bar{k}} &= \sigma^2 \mathbf{I}_{N_i} + \sum_{j \neq i, j \neq k}^K \bar{\mathbf{H}}_{i,b_j} \mathbf{Q}_j \bar{\mathbf{H}}_{i,b_j}^H \\ &+ \sum_{j \neq i, j \neq k}^K \mathbf{C}_{r,i}^{\frac{1}{2}} \tilde{\mathbf{H}}_{p,i,b_j} \boldsymbol{\Theta}_{p,i,b_j}^{\frac{1}{2}} \mathbf{Q}_j \boldsymbol{\Theta}_{p,i,b_j}^{\frac{1}{2},H} \tilde{\mathbf{H}}_{p,i,b_j}^H \mathbf{C}_{r,i}^{\frac{1}{2},H} \\ &- \sum_{j \neq i, j \neq k}^K [\mathbf{C}_{r,i}^{\frac{1}{2}} \tilde{\mathbf{H}}_{p,i,b_j} \boldsymbol{\Theta}_{p,i,b_j}^{\frac{1}{2}} \mathbf{Q}_j \bar{\mathbf{H}}_{i,b_j}^H \\ &\quad + \bar{\mathbf{H}}_{i,b_j} \mathbf{Q}_j \boldsymbol{\Theta}_{p,i,b_j}^{\frac{1}{2},H} \tilde{\mathbf{H}}_{p,i,b_j}^H \mathbf{C}_{r,i}^{\frac{1}{2},H}] \\ &\xrightarrow{(b)} \sum_{j \neq i, j \neq k}^K \bar{\mathbf{H}}_{i,b_j} \mathbf{Q}_j \bar{\mathbf{H}}_{i,b_j}^H + \text{tr}\{\mathbf{Q}_j \boldsymbol{\Theta}_{p,i,b_j}\} \mathbf{C}_{r,i} \\ &\quad + \sigma^2 \mathbf{I}_{N_i} = \check{\mathbf{R}}_{i,\bar{k}};\end{aligned} \tag{C.2}$$

Moreover,

$$\begin{aligned}\mathbf{A}_{i,k}^D &\xrightarrow{(c)} \bar{\mathbf{H}}_{i,b_k}^H \check{\mathbf{R}}_{i,\bar{k}}^{-1} \bar{\mathbf{H}}_{i,b_k} + \text{tr}\{\check{\mathbf{R}}_{i,\bar{k}}^{-1} \mathbf{C}_{r,i}\} \boldsymbol{\Theta}_{p,i,b_k} = \check{\mathbf{A}}_{i,k}^D; \\ \mathbf{R}_{i,\bar{k}} &\xrightarrow{(d)} \sum_{j \neq k}^K \bar{\mathbf{H}}_{i,b_j} \mathbf{Q}_j \bar{\mathbf{H}}_{i,b_j}^H + \text{tr}\{\mathbf{Q}_j \boldsymbol{\Theta}_{p,i,b_j}\} \mathbf{C}_{r,i} \\ &\quad + \sigma^2 \mathbf{I}_{N_i} = \check{\mathbf{R}}_{i,\bar{k}}.\end{aligned} \tag{C.3}$$

Note that (a) and (c) above correspond to "using the expected value of the matrix and (C.2)", and "using the expected value of the matrix and (C.3)" respectively, while (b) and (d) correspond both to "using the expected value of the matrix". Now, the proof is completed.

List of Publications and Bibliography

- 5G European Projects deliverables:
 1. Fantastic5G IR4.1, D4.1, IR4.2 and 4.2
 2. One5G IR4.1
- Patents owned by Orange Labs:
 1. Tabikh, Wassim; Yuan-Wu, Yi; Slock, Dirk, Beamforming design with combined channel estimate and covariance CSIT via random matrix theory, FR Patent FR 1659993, October, 2016.
- Journal Papers:
 1. Tabikh, Wassim; Yuan-Wu, Yi and Slock, Dirk; Massive MIMO beamforming design for multicell multiuser communications with imperfect channel knowledge, submitted to IEEE Transactions on Wireless Communications, 2018.
- Conference Papers:
 1. Christo Kurisummoottil Thomas; Wassim Tabikh; Dirk Slock; Yi Yuan-Wu, Noncoherent Multi-User MIMO Communications using Covariance CSIT, Asilomar 2017, October 29th - November 1st, 2017 Asilomar Hotel Conference Grounds, Pacific Grove, CA
 2. Tabikh, Wassim; Slock, Dirk TM; Yuan-Wu, Yi, MIMO IBC beamforming with combined channel estimate and covariance CSIT, ISIT 2017, IEEE International Symposium on Information Theory June 25-30, 2017, Aachen, Germany
 3. Tabikh, Wassim; Yuan-Wu, Yi; Slock, Dirk, Beamforming design with combined channel estimate and covariance CSIT via random matrix theory, ICC 2017, IEEE International Conference on Communications, IEEE ICC 2017 Wireless Communications Symposium, May 21-25, Paris, France
 4. Tabikh, Wassim; Slock, Dirk TM; Yuan-Wu, Yi, MaMISO IBC beamforming design with combined channel estimate and covariance CSIT: a large system analysis, ICC 2017, WS08-3rd International Workshop on Advanced PHY and MAC Technology for Super Dense Wireless Networks (CROWD-NET), May 21-25, Paris, France

5. Tabikh, Wassim; Slock, Dirk TM; Yuan-Wu, Yi, Relay aided coordinated beamforming and interference neutralization, ITA 2017, Information Theory and Applications Workshop, February 12-17, 2017, San Diego, USA
6. Tabikh, Wassim; Slock, Dirk; Yuan-Wu, Yi, A large system analysis of weighted sum rate maximization of single stream MIMO interference broadcast channels under linear precoding, ISWCS 2016, International Symposium on Wireless Communication Systems, 20-23 September 2016, Poznan, Poland
7. Tabikh, Wassim; Yuan-Wu, Yi; Slock, Dirk TM, Decentralizing multi-cell maximum weighted sum rate precoding via large system analysis, EUSIPCO 2016, 24th European Signal Processing Conference, 28 August-2 September 2016, Budapest, Hungary
8. Tabikh, Wassim; Slock, Dirk TM; Yuan-Wu, Yi, Weighted sum rate maximization of MISO interference broadcast channels via difference of convex functions programming: A large system analysis, SSP 2016, IEEE Workshop on Statistical Signal Processing, 26-29 June 2016, Palma de Mallorca, Spain
9. Tabikh, Wassim; Slock, Dirk TM; Yuan-Wu, Yi, Weighted sum rate maximization of correlated MISO interference broadcast channels under linear precoding: A large system analysis, VTC 2016-Spring, IEEE 83rd Vehicular Technology Conference, 15-18 May 2016, Nanjing, China
10. Tabikh, Wassim; Slock, Dirk TM; Yuan-Wu, Yi, Optimal beamforming with combined channel and path CSIT for multi-cell multi-user MIMO, ITA 2016, Information Theory and Applications Workshop, January 31-February 5, 2016, San Diego, USA
11. Tabikh, Wassim; Slock, Dirk; Yuan-Wu, Yi, Massive MIMO inspired 2-stage design of the multi-cell multi-user MIMO downlink, JNCW 2015, NEWCOM/COST Workshop on Wireless Communications, October 14-15, 2015, Barcelona, Spain
12. Tabikh, Wassim; Slock, Dirk TM; Yuan-Wu, Yi, The pathwise MIMO Interfering broadcast channel, SPAWC 2015, 16th IEEE International Workshop on Signal Processing Advances in Wireless Communications, June 28 2015-July 1 2015, Stockholm, Sweden

Bibliography

- [1] E. G. Larsson, O. Edfors, F. Tufvesson, and T. L. Marzetta. Massive MIMO for next generation wireless systems. *IEEE Communications magazine*, 2014.
- [2] S. Yang and L. Hanzo. Fifty years of MIMO detection: the road to large-scale MIMOs. *IEEE Communication surveys tutorials*, vol. 17, no. 4, fourth quarter, 2015.
- [3] E. Björnson, J. Hoydis, M. Kountouris, and M. Debbah. Massive MIMO systems with non-ideal hardware: energy efficiency, estimation and capacity limits. *IEEE Transactions on information theory*, Vol. 60, no. 11, 2014.
- [4] A. Hakkarainen, J. Werner, M. Renfors, K. R. Dandekar, and M. Valkama. Transceiver I/Q imbalance and widely-linear spatial processing in large antenna systems. *IEEE International symposium on wireless communication systems (ISWCS)*, 2015.
- [5] A. Pitarokoilis, E. Björnson, and E.G. Larsson. ML detection in phase noise impaired SIMO channels with uplink training. *IEEE Transactions on communications*, Vol. 64, no. 1, 2016.
- [6] T. L. Marzetta, G. Caire, M. Debbah, I. Chih-Lin, and S. K. Mohammed. Special issue on massive mimo. *Journal of communications and networks*, vol. 15, no. 4, August 2013.
- [7] H.Q. Ngo, E. G. Larsson, and T.L. Marzetta. Energy and spectral efficiency of very large multiuser mimo systems. *IEEE Trans. Commun.*, 2012.
- [8] Emil Björnson, L. Sanguinetti, J. Hoydis, and M. Debbah. Optimal design of energy-efficient multi-user MIMO systems: is Massive MIMO the answer? *IEEE Transactions on wireless communications*, Vol. 14, no. 6, 2015.
- [9] A. Alkhateeb, G. Leus, and R.W. Heath Jr. Multi-layer precoding: a potential solution for full-dimensional massive MIMO systems. *IEEE Transactions on wireless communications*, 2016.
- [10] J. Hoydis, S.T. Brink, and M. Debbah. Massive mimo in the ul/dl of cellular networks: How many antennas do we need? *IEEE Journal on selected areas in communications*, vol. 31, no. 2, February 2013.
- [11] D. Liu, W. Ma, S. Shao, Y. Shen, and Y. Tang. Performance analysis of TDD reciprocity calibration for Massive MU-MIMO systems with ZF

- beamforming. *IEEE Journal on selected areas in communications*, Vol. 32, no. 6, pp. 1230-1238, 2016.
- [12] H. Yin, D. Gesbert, M. Filippou, and Y. Liu. A coordinated approach to channel estimation in large-scale multiple-antenna systems. *IEEE journal on selected areas in communications*, Vol. 31, no. 2, 2013.
 - [13] T. E. Bogale and L. B. Le. Beamforming for multiuser massive MIMO systems: Digital versus hybrid analog-digital. *IEEE Global communications conference (GLOBECOM)*, 2014.
 - [14] A. Liu and V. Lau. Hierarchical interference mitigation for Massive MIMO cellular networks. *IEEE Transactions on signal processing*, vol. 62, issue 18, 2014.
 - [15] Y. Xu, G. Yue, N. Prasad, S. Rangarajan, and S. Mao. User grouping and scheduling for large scale MIMO systems with two-stage precoding. *IEEE International conference on communications (ICC)*, 2014.
 - [16] A.F. Molisch, V.V. Ratnam, S.Han, Z. Li, S.L.H. Nguyen, L. Li, and K. Haneda. Hybrid beamforming for Massive MIMO – a survey. *IEEE Communications magazine*, Vol. 55, Issue 9, 2017.
 - [17] H. Q. Ngo, H. A. Suraweera, M. Matthaiou, and E. G. Larsson. Multipair full-duplex relaying with massive arrays and linear processing. <https://arxiv.org/abs/1405.1063>, 2014.
 - [18] H. Prabhu, J. Rodrigues, O. Edfors, and Fredrik. Approximative matrix inverse computations for very-large MIMO and applications to linear precoding systems. *IEEE Wireless communications and networking conference (WCNC): PHY*, 2013.
 - [19] H.Q. Ngo, E. G. Larsson, and T.L. Marzetta. Massive mu-mimo downlink tdd systems with linear precoding and downlink pilots. *Fifty-first annual Allerton conference*, October 2013.
 - [20] H.Q. Ngo, E.G. Larsson, and T.L. Marzetta. Aspects of favorable propagation in massive mimo. <https://arxiv.org/abs/1403.3461>.
 - [21] H. Wymeersch N. Garcia and D. T. M. Slock. Optimal robust precoders for tracking the AoD and AoA of a mm-Wave path. <https://arxiv.org/abs/1703.10978>, 2017.
 - [22] Q. Shi, M. Razaviyayn, M.S. Boroujeni, Z.-Q. Luo, and C. He. An iteratively weighted mmse approach to distributed sum-utility maximization for a mimo interfering broadcast channel. *IEEE Trans. on signal processing*, vol. 59, no. 9, 2011.
 - [23] F. Negro, I. Ghauri, and D.T.M. Slock. Deterministic annealing design and analysis of the noisy mimo interference channel. *IEEE Information theory and applications (ITA) Workshop*, February 2011.
 - [24] S. Christensen, R. Agarwal, E. de Carvalho, and J. M. Cioffi. Weighted sum-rate maximization using weighted mmse for mimo-bc beamforming design. *IEEE Trans. wireless commun.*, vol. 7, no. 12, December 2008.
 - [25] S.-J. Kim and G. B. Giannakis. Optimal resource allocation for mimo ad hoc cognitive radio networks. *IEEE Trans on Inf. Theory*, vol. 57, No 5,

- May 2011.
- [26] H. Al-Shatri and T. Weber. Achieving the maximum sum rate using d.c. programming in cellular networks. *IEEE Trans on signal processing*, Vol. 60, No. 3, March 2012.
 - [27] S. Wagner and D. Slock. Weighted sum rate maximization of correlated miso broadcast channels under linear precoding: A large system analysis. *12th IEEE International workshop on signal processing advances in wireless communications*, June 2011.
 - [28] S. Wagner, R. Couillet, M. Debbah, and D.T.M. Slock. Large system analysis of linear precoding in correlated miso broadcast channels under linear feedback. *IEEE Trans. on inf. theory*, vol. 58, no. 7, July 2012.
 - [29] S. Wagner, R. Couillet, M. Debbah, and D.T.M. Slock. Deterministic equivalent for the sinr of regularized zero-forcing precoding in correlated miso broadcast channels with imperfect csit. *IEEE International conference on communications (ICC)*, 2011.
 - [30] S.Lagen, A.Agustin, and J. Vidal. Decentralized coordinated precoding for dense tdd small cell networks. *IEEE Trans. on wireless communications*, vol.14, no.8, 2015.
 - [31] A. Müller, R. Couillet, E. Björnson, S. Wagner, and M. Debbah. Interference-aware rzf precoding for multi cell downlink systems. *IEEE trans. on signal processing*, vol. 63, no. 15, August 2015.
 - [32] S. Lakshminarayana, M. Assaad, and M. Debbah. Coordinated multicell beamforming for massive mimo: a random matrix approach. *IEEE Trans. on information theory*, vol. 61, no. 6, 2015.
 - [33] H. Asgharimoghaddam, A. Tölili, and N. Rajatheva. Decentralizing the optimal multi-cell beamforming via large system analysis. *IEEE International conference on communications (ICC)*, 2014.
 - [34] H. Asgharimoghaddam, A. Tölili, and N. Rajatheva. Decentralizing multi-cell beamforming via large system analysis in correlated channels. *Proceedings of the 22nd European signal processing conference (EUSIPCO)*, 2015.
 - [35] Z. D. Bai and J. W. Silverstein. No eigenvalues outside the support of the limiting spectral distribution of large dimensional sample covariance matrices. *Annals of probability*, vol. 26, no. 1, pp. 316–345, 1998.
 - [36] P. Komulainen, A. Tölili, and Markku Juntti. Decentralized beam coordination via sum rate maximization in tdd multi-cell mimo systems. *IEEE 22nd International Symposium on Personal, Indoor and Mobile Radio Communications*, 2011.
 - [37] P. Komulainen, A. Tölili, and Markku Juntti. Effective csi signaling and decentralized beam coordination in tdd multi-cell mimo systems. *IEEE Trans. on signal processing*, vol. 61, no. 9, May 2013.
 - [38] J. Kaleva, A. Tölili, and Markku Juntti. Primal decomposition based decentralized weighted sum rate maximization with qos constraints for interfering broadcast channel. *IEEE 14th Workshop on signal processing*

advances in wireless communications (SPAWC), 2013.

- [39] A. Müller, R. Couillet, E. Björnson, S. Wagner, and M. Debbah. Interference-aware rzf precoding for multi cell downlink systems. *IEEE Trans. on signal processing*, vol. 63, no. 15, August 2015.
- [40] F. Negro, I. Ghauri, and D.T.M. Slock. Sum rate maximization in the noisy mimo interfering broadcast channel with partial csit via the expected weighted mse. *IEEE International symposium on wireless communication systems (ISWCS)*, March 2012.
- [41] H. Yin, D. Gesbert, and L. Cottatellucci. Dealing with interference in distributed large-scale mimo systems: a statistical approach. *IEEE Journal of selected topics in signal processing*, Vol. 8, No. 5, October 2014.
- [42] N. H. Mahmood, G. Berardinelli, K.I. Pedersen, and P. Mogensen. An interference-aware distributed transmission technique for dense small cell networks. *IEEE ICC - Workshop on small cell and 5G networks (SmallNets)*, October 2015.
- [43] S. Bazzi, G. Dietl, and W. Utschick. Large system analysis of interference alignment achievable rates for the MIMO interference channel. *IEEE Transactions on signal processing*, vol. 63, no. 6, 2015.
- [44] J. Dumont, W. Hachem, P. Loubaton S. Lasaulce, and J. Najim. On the Capacity achieving covariance matrix for rician MIMO channels: An asymptotic approach. *IEEE Trans. Info. Theory*, 2010.
- [45] G. Taricco. Asymptotic mutual information statistics of separately correlated Rician fading MIMO channels. *IEEE Trans. Info. Theory*, 2008.
- [46] W. Yu and J.M. Cioffi. Sum Capacity of Gaussian Vector Broadcast Channels. In *IEEE Transactions on Information Theory*, Vol. 50, No. 9, 2004.
- [47] D.H.N. Nguyen and T. Le-Ngoc. Sum-rate maximization in the multi-cell MIMO broadcast channel with interference coordination. In *IEEE Transactions on signal processing*, 2014.
- [48] I. Bergel, D. Yellin, and S. Shamai. Dirty paper coding with partial channel state information. In *Spawc*, 2014.
- [49] A. Bennatan and D.Burshtein. On the fading-paper achievable region of the fading MIMO broadcast channel. In *IEEE transactions on information theory*, Vol. 54, No. 1, 2008.
- [50] Y. Wu, S. Jin, X. Gao, M.R. McKay, and C.Xiao. Transmit designs for the MIMO broadcast channels with statistical CSI. In *IEEE Transactions on signal processing*, vol.62, no.17, 2014.
- [51] H. Harashima and H. Miyakawa. Matched-transmission technique for channels with intersymbol interference. In *IEEE Trans. Commun.*, vol. 20, no. 4, pp. 774–780, 1972.
- [52] C. B. Peel, B. M. Hochwald, and A. L. Swindlehurst. A vector-perturbation technique for near-capacity multiantenna multiuser communications—Part II: Perturbation. In *IEEE Trans. Commun.*, vol. 53, no. 3, 2005.

- [53] S. Vishwanath, N. Jindal, and A. Goldsmith. Duality, achievable Rates and sum-rate capacity of Gaussian MIMO broadcast channels. In *IEEE Transactions on information theory*, vol. 49, no. 10, 2003.
- [54] H. Choi, K.-J. Lee, C. Song, H. Song, and I. Lee. Weighted sum-rate maximization for multiuser multirelay MIMO systems. *IEEE Transactions on vehicular technology*, February 2013.
- [55] H. Choi, K.-J. Lee, C. Song, H. Song, H. Kim, and I. Lee. Weighted sum-rate maximization for multi-user multi-relay MIMO systems with direct links. *Vehicular technology conference (VTC)*, June 2013.
- [56] K.-J. Lee, H. Sung, E. Park, and I. Lee. Joint optimization for one and two-way MIMO AF multiple-relay systems. *IEEE Transactions on wireless communications*, December 2010.
- [57] C.-E. Chen and S.-K. Chou. A gradient-descent weighted sum MSE transceiver design for multi-user multi-relay downlink systems. *IEEE Transactions on vehicular technology*.
- [58] N. Lee and R.W. Heath Jr. Degrees of freedom for the two-Cell two-Hop MIMO interference channel: interference-free relay transmission and spectrally efficient relaying protocol. *IEEE Transactions on information theory*, May 2013.
- [59] N. Lee and R.W. Heath Jr. Joint beamforming and transmit design for the non-regenerative MIMO broadcast relay channel. *IEEE 8th Sensor array and multichannel Signal processing workshop (SAM)*, 2014.
- [60] G. Okeke, W.A. Krzymień, and Y. Jing. Beamforming in non-regenerative MIMO broadcast relay networks. *IEEE transactions on signal processing*, December 2012.
- [61] M. Zeng, R. Zhang, and S. Cui. On design of collaborative beamforming for two-way relay networks. *IEEE Transactions on signal processing*, May 2011.
- [62] M. Zeng, R. Zhang, and S. Cui. Distributed beamforming design for SINR balancing approach in cooperative two-way networks based on second-order statistics. *23rd Iranian conference on electrical engineering (ICEE)*, May 2015.
- [63] E. Chiu and V.K.N. Lau. Cellular multiuser two-way MIMO AF relaying via signal space alignment : minimum weighted SINR maximization. *IEEE Transactions on signal processing*, September 2012.
- [64] A. Aziz, C. Thron, and S. Cui. Joint optimization of source and relay for MIMO two-way relay networks using MSE duality. *IEEE communications letters*, July 2014.
- [65] Y. Rong. Joint source and relay optimization for two-way MIMO multi-relay networks. *IEEE Communications letters*, December 2011.
- [66] A. Aziz, C. Thron, and S. Cui. Linearized robust beamforming for two-way relay systems. *IEEE Signal processing letters*, August 2014.
- [67] J. Liu, F. Gao, and Z. Qiu. Robust transceiver design for downlink

- multiuser MIMO AF relay systems. *IEEE Transactions on wireless communications*, August 2015.
- [68] L. Shen, Y. Fu, C. Liu, and W.-P. Zhu. Joint relay and destination design for two-way MIMO AF multi-relay systems. *IEEE Communications letters*, 2014.
- [69] C.-C. Hu and Y.-F. Chou. Precoding design of MIMO AF two-way multiple-relay systems. *IEEE Signal processing letters*, June 2013.
- [70] Y. Rong. Simplified relay algorithm for two-way MIMO relay communications. *17th Asia-Pacific Conference on Communications (APCC)*, October 2011.
- [71] K.T. Truong, P. Sartori, and R.W. Heath Jr. Cooperative algorithms for MIMO amplify-and-forward relay networks. *IEEE Transactions on signal processing*, March 2013.
- [72] W.-C. Choi and D.-J. Park. Iterative beamformer design for multi-node MIMO two-way relay networks using duality. *IEEE Transactions on vehicular technology*, August 2016.
- [73] C. Zhao and B. Champagne. A unified approach to optimal Transceiver Design for non regenerative MIMO relaying. *IEEE Transactions on vehicular technology*, 2015.
- [74] C. Sun, E.A. Jorswieck, and Y.-X. Yuan. Sum rate maximization for non-regenerative MIMO relay networks. *IEEE Transactions on signal processing*, December 2016.
- [75] D. Nguyen, L.-N. Tran, and P. Pirinen. On the spectral efficiency of full-duplex small cell wireless systems. *IEEE Transactions on wireless communications*, September 2014.
- [76] D. Nguyen, L.-N. Tran, and P. Pirinen. Precoding for full duplex multiuser MIMO systems: spectral and energy efficiency maximization. *IEEE Transactions on signal processing*, 2013.
- [77] D. Nguyen, L.-N. Tran, and P. Pirinen. Transmission strategies for full duplex multiuser MIMO systems. *International workshop on small cell wireless networks*, 2012.
- [78] A.C. Cirik, R. Wang, Y. Hua, and M. Latva-aho. Weighted sum-rate maximization for full-duplex MIMO interference channels. *IEEE Transactions on communications*, March 2015.